ISSN 0021-9673

VOL. 370 NO. 3 DECEMBER 24, 1986
THIS ISSUE COMPLETES VOL. 370

JOURNAL OF CHROMATOGRAPHY

INTERNATIONAL JOURNAL ON CHROMATOGRAPHY, ELECTROPHORESIS AND RELATED METHODS

ELSEVIER

JOURNAL OF CHROMATOGRAPHY

Scope. The *Journal of Chromatography* publishes papers on all aspects of chromatography, electrophoresis and related methods. Contributions consist mainly of research papers dealing with chromatographic theory, instrumental development and their applications. The section *Biomedical Applications,* which is under separate editorship, deals with the following aspects: developments in and applications of chromatographic and electrophoretic techniques related to clinical diagnosis (including the publication of normal values); screening and profiling procedures with special reference to metabolic disorders; results from basic medical research with direct consequences in clinical practice; combinations of chromatographic and electrophoretic methods with other physicochemical techniques such as mass spectrometry. In *Chromatographic Reviews,* reviews on all aspects of chromatography, electrophoresis and related methods are published.

Submission of Papers. Papers in English, French and German may be submitted, in three copies. Manuscripts should be submitted to: The Editor of *Journal of Chromatography,* P.O. Box 681, 1000 AR Amsterdam, The Netherlands, or to: The Editor of *Journal of Chromatography, Biomedical Applications,* P.O. Box 681, 1000 AR Amsterdam, The Netherlands. Review articles are invited or proposed by letter to the Editors and will appear in *Chromatographic Reviews* or *Biomedical Applications.* An outline of the proposed review should first be forwarded to the Editors for preliminary discussion prior to preparation. Submission of an article is understood to imply that the article is original and unpublished and is not being considered for publication elsewhere. For copyright regulations, see below.

Subscription Orders. Subscription orders should be sent to: Elsevier Science Publishers B.V., P.O. Box 211, 1000 AE Amsterdam, The Netherlands. The *Journal of Chromatography* and the *Biomedical Applications* section can be subscribed to separately.

Publication. The *Journal of Chromatography* (incl. *Biomedical Applications, Chromatographic Reviews* and *Cumulative Author and Subject Indexes, Vols. 326–350*) has 38 volumes in 1986. The subscription prices for 1986 are:

J. Chromatogr. (incl. *Chromatogr. Rev.* and *Cum. Indexes, Vols. 326–350*) + *Biomed. Appl.* (Vols. 346–383): Dfl. 6080.00 plus Dfl. 912.00 (postage) (total *ca.* US$ 2742.00)

J. Chromatogr. (incl. *Chromatogr. Rev.* and *Cum. Indexes, Vols. 326–350*) only (Vols. 346–373): Dfl. 5040.00 plus Dfl. 672.00 (postage) (total *ca.* US$ 2240.00)

Biomed. Appl. only (Vols. 374–383): Dfl. 1850.00 plus Dfl. 240.00 (postage) (total *ca.* US$ 819.50).

Journals are automatically sent by airmail at no extra costs to Argentina, Australia, Brasil, Canada, China, Hong Kong, India, Israel, Japan, Malaysia, Mexico, New Zealand, Pakistan, Singapore, South Africa, South Korea, Taiwan, Thailand and the U.S.A. Back volumes of the *Journal of Chromatography* (Vols. 1 through 345) are available at Dfl. 219.00 (plus postage). Claims for issues not received should be made within three months of publication of the issue. If not, they cannot be honoured free of charge. Customers in the U.S.A. and Canada wishing information on this and other Elsevier journals, please contact Journal Information Center, Elsevier Science Publishing Co. Inc., 52 Vanderbilt Avenue, New York, NY 10017. Tel. (212) 916-1250.

Abstracts/Contents Lists published in Analytical Abstracts, ASCA, Biochemical Abstracts, Biological Abstracts, Chemical Abstracts, Chemical Titles, Current Contents/Physical, Chemical & Earth Sciences, Current Contents/Life Sciences, Deep-Sea Research/Part B: Oceanographic Literature Review, Excerpta Medica, Index Medicus, Mass Spectrometry Bulletin, PASCAL-CNRS, Referativnyi Zhurnal and Science Citation Index.

See page 3 of cover for Publication Schedule, Information for Authors and information on Advertisements.

0021-9673/86/$03.50

Printed in The Netherlands

CONTENTS

(Abstracts/Contents Lists published in Analytical Abstracts, ASCA, Biochemical Abstracts, Biological Abstracts, Chemical Abstracts, Chemical Titles, Current Contents/Physical, Chemical & Earth Sciences, Current Contents/Life Sciences, Deep-Sea Research/Part B: Oceanographic Literature Review, Excerpta Medica, Index Medicus, Mass Spectrometry Bulletin, PASCAL-CNRS, Referativnyi Zhurnal and Science Citation Index)

Retention studies of alkyl- and halogen-substituted aromatics on normal-phase silica and alumina columns. I. Alkylbenzenes and halogenoalkylbenzenes
by R. F. Rekker, G. de Vries and G. J. Bijloo (Amsterdam, The Netherlands) (Received August 26th, 1986) 355

Hydrophobic-dispersive partition coefficient in alkyl-bonded reversed-phase systems with water–methanol mobile phases
by R. N. Nikolov and M. M. Darzhalieva (Sofia, Bulgaria) (Received August 13th, 1986) 377

General reversed-phase high-performance liquid chromatographic method for the separation of drugs using triethylamine as a competing base
by R. W. Roos and C. A. Lau-Cam (New York, NY, U.S.A.) (Received August 26th, 1986) 403

Column poisoning by multivalent cations in ion chromatographic analysis for alkali metals
by D. R. Jenke (Morton Grove, IL, U.S.A.) (Received August, 14th, 1986) 419

Electrochemiluminescence as a detection technique for reversed-phase high-performance liquid chromatography. III. A high-performance flow cell
by E. Hill, E. Humphreys and D. J. Malcolme-Lawes (London, U.K.) (Received July 16th, 1986) 427

Metallic copper-containing post-column reactor for the detection of thiram and disulfiram in liquid chromatography
by H. Irth, G. J. de Jong, U. A. Th. Brinkman and R. W. Frei (Amsterdam, The Netherlands) (Received August 27th, 1986) 439

Headspace gas analysis. Quantitative trapping and thermal desorption of volatiles using fused-silica open tubular capillary traps
by B. V. Burger and Z. Munro (Stellenbosch, South Africa) (Received July 29th, 1986) . 449

Derivatization of phenolic acids for capillary gas chromatography with hydrogen flame ionization and electron-capture detection
by K. Lehtonen and M. Ketola (Turku, Finland) (Received August 18th, 1986) . . . 465

Direct analytical and preparative resolution of enantiomers using albumin adsorbed to silica as a stationary phase
by P. Erlandsson, L. Hansson and R. Isaksson (Lund, Sweden) (Received August 14th, 1986) 475

Thin-layer electrophoretic behaviour of oligo- and monosaccharides, uronic acids and polyhydroxy compounds obtained as biomass degradation products
by G. Bonn and M. Grünwald (Innsbruck, Austria), H. Scherz (Garching, F.R.G.) and O. Bobleter (Innsbruck, Austria) (Received August 19th, 1986) 485

Correlation of urokinase activity from biopotency and high-performance liquid chromatographic assays
by R. A. Cox, K. N. McFarland, P. Holt Sackett and M. T. Short (North Chicago, IL, U.S.A.) (Received August 13th, 1986) 495

(Continued overleaf)

Purification of copper-zinc-superoxide dismutase and catalase from human erythrocytes by copper-chelate affinity chromatography
by M. Miyata-Asano, K. Ito, H. Ikeda and S. Sekiguchi (Sapporo, Japan) and K. Arai and N. Taniguchi (Osaka, Japan) (Received August 23rd, 1986) 501

Notes

Simple device for high-performance liquid chromatographic separation on microbore columns
by A. S. Bhown, J. Wayland and J. C. Bennett (Birmingham, AL, U.S.A.) (Received August 5th, 1986) 508

One-step chromatographic isolation of collagen cross-links
by P. A. Ryan and P. F. Davis (Wellington, New Zealand) (Received August 5th, 1986) . 513

Chemische Unterscheidungsmerkmale der Samen von *Trifolium repens* L. und *Trifolium repens* L. var. *giganteum*
by J. Sachse (Zürich, Schweiz) (Eingegangen am 26. September 1986) 520

Author Index 528

Erratum 532

In articles with more than one author, the name of the author to whom correspondence should be addressed is indicated in the article heading by a 6-pointed asterisk (*)

Journal of Chromatography, 370 (1986) 355–376
Elsevier Science Publishers B.V., Amsterdam — Printed in The Netherlands

CHROM. 19 043

RETENTION STUDIES OF ALKYL- AND HALOGEN-SUBSTITUTED AROMATICS ON NORMAL-PHASE SILICA AND ALUMINA COLUMNS

I. ALKYLBENZENES AND HALOGENOALKYLBENZENES

ROELOF F. REKKER*
Department of Pharmacochemistry, Vrije Universiteit, De Boelelaan 1083, 1081 HV Amsterdam (The Netherlands)
GERRIT DE VRIES
Department of Analytical Chemistry, Vrije Universiteit, De Boelelaan 1083, 1081 HV Amsterdam (The Netherlands)
and
GREETJE J. BIJLOO
Department of Pharmacochemistry, Vrije Universiteit, De Boelelaan 1083, 1081 HV Amsterdam (The Netherlands)
(First received June 20th, 1986; revised manuscript received August 26th, 1986)

SUMMARY

Normal-phase liquid chromatography has been applied to alkylbenzenes and compounds with mixed halogen–alkyl substitution. Experiments were performed on both silica gel and alumina packed columns. With *n*-hexane as the mobile phase good peak differentiations were possible. Many of the derived log(capacity factors) could be correlated with structural features and predictions could be made. Substituent bulk and mesomeric effects are of major importance in regulating the transport of the investigated compounds. In addition, however, symmetry conditions seem to play a distinct role; group dipole moment values can therefore serve as suitable parameters in a number of instances.

INTRODUCTION

Several years ago some studies[1–5] were devoted to the chromatographic behaviour of over 200 compounds in the systems *n*-hexane–silica gel and *n*-hexane–alumina in order to obtain information on optimal separation techniques and the possible relationship between structure and retention. In addition to alkyl and halogenoalkyl aromatics, the series contained polychlorobiphenyls (PCBs), polybromobiphenyls (PBBs), polymethylbiphenyls (PMeBs), polychloronaphthalenes (PCNs) and polymethylnaphthalenes (PMeNs). The principle of the work described in this and forthcoming papers was to find parameters that describe effectively the transfer of the compounds. In a way, our studies link up with investigations performed by Snyder[6] on a number of similar structures on alumina columns, although Snyder's investi-

0021-9673/86/$03.50

gations were not intended to unravel the necessary parametrization of retention values. Also, the application of regression techniques was not in common use at the time.

EXPERIMENTAL

The compounds investigated were of several origins. All products were of sufficient purity with one main peak in the chromatogram.

n-Hexane (Baker, Deventer, The Netherlands)) was used throughout as the eluent, pre-treated with a suspension of sodium in solid paraffin[7], followed by drying over pre-heated molecular sieve 5A (200°C for at least 8 h[8]).

Retention times were determined on a Siemens high-performance liquid chromatographic (HPLC) apparatus, Type S 100, equipped with a Zeiss PM 2 UV absorbance detector, absorption was measured at 200–300 nm.

The silica gel column was packed with LiChrosorb Si 60, particle size 5 μm, column length 250 mm, I.D. 3.0 mm (Chrompack, Middelburg, The Netherlands). The alumina column was packed with LiChrosorb Alox T5, particle size 5 μm, column length 250 mm, I.D. 3.0 and 4.6 mm (Chrompack).

Sample concentrations were chosen so as to give a low but discernible signal from injection volumes of 10 μl.

Retention times are expressed in terms of log(capacity factors, k') using the equation

$$\log k' = \log(t_R - t_0)/t_0$$

where t_R is the retention time of the compound and t_0 the elution time of unretained *n*-hexane.

The flow-rate of the eluent was 2 ml/min for the silica gel column and 2 or 3.5 ml/min for the alumina column, depending on its diameter.

RESULTS AND DISCUSSION

Methylbenzenes on a silica gel column

The experimental log k' values are given in Table I for all methyl-substituted benzene derivatives and benzene.

Considering the general trend in the tabulated log k' values, we first tried to correlate log k' with the total number of methyl groups (n_{Me}), which resulted in the following equation (with 95% confidence intervals in parentheses):

$$\log k' = 0.088\ (\pm 0.010) n_{Me} + 0.378\ (\pm 0.035) \quad (1)$$

$$n = 13;\ r = 0.985;\ s = 0.027;\ F = 346$$

This equation accounts for 97% of the variances. Close inspection of the data points (Fig. 1) shows that seven out of the thirteen data points are slightly different from the others. They fit the following equation:

$$\log k' = 0.084\ (\pm 0.002) n_{Me} + 0.376\ (\pm 0.008) \quad (2)$$

$$n = 7;\ r = 0.9997;\ s = 0.004;\ F = 8280$$

These seven compounds (marked with asterisks in Fig. 1) will serve as a "backbone" for further improvement of the data correlation. The deviating behaviour of the six "non-asterisked" compounds in Fig. 1 seems to be connected with symmetry conditions in the methyl substitution pattern. For that reason, we decided to operate with n_{ortho} and n_{para} as additional parameters to n_{Me}. The two parameters denote the total number of methyl groups involved in *ortho* and *para* positions, respectively.

$$\log k' = 0.083\ (\pm 0.005)n_{Me} + 0.021\ (\pm 0.004)n_{ortho} - 0.020\ (\pm 0.003)n_{para} + 0.379\ (\pm 0.009) \quad (3)$$

$$n = 13;\ r = 0.9994;\ s = 0.006;\ F = 2840$$

Eqn. 3 has one drawback: it is slightly "under"-filled with data points (as a rule we recommend five data points for each independent parameter). The identity of the regressor values of n_{ortho} and n_{para} in eqn. 3 (with opposite algebraic sign), however, permits a parameter reduction by applying $n_{ortho} - n_{para}$ instead of n_{ortho} and n_{para} separately:

$$\log k' = 0.085\ (\pm 0.002)n_{Me} + 0.020\ (\pm 0.003)(n_{ortho} - n_{para}) + 0.377\ (\pm 0.007) \quad (4)$$

$$n = 13;\ r = 0.9994;\ s = 0.006;\ F = 4390$$

and this excellent result leaves no more than 0.2% of the variances unexplained.

Additional proof that symmetry conditions really are important and that the numerical difference in the *ortho* and *para* substitutions gives an adequate means of parametrizing this symmetry factor is demonstrated by eqn. 5 with the group dipole moment sum (μ) functioning as an additional parameter to n_{Me}:

$$\log k' = 0.088\ (\pm 0.005)n_{Me} + 0.083\ (\pm 0.029)\mu + 0.354\ (\pm 0.019) \quad (5)$$

$$n = 13;\ r = 0.997;\ s = 0.013;\ F = 785$$

Methylbenzenes on an alumina column

The experimental log k' values are given in Table II for all methyl-substituted benzene derivatives, including benzene. The following equation correlates log k' with the total number of methyl groups:

$$\log k' = 0.205\ (\pm 0.035)n_{Me} - 0.129\ (\pm 0.118) \quad (6)$$

$$n = 13;\ r = 0.969;\ s = 0.089;\ F = 169$$

The quality of this equation, which explains 94% of the variances, is significantly lower than that for the silica gel column (eqn. 1). Only five compounds are suitable to use as a "backbone" (Fig. 2) and are fitted by the equation

$$\log k' = 0.118\ (\pm 0.025)n_{Me} - 0.027\ (\pm 0.036) \quad (7)$$

$$n = 5;\ r = 0.994;\ s = 0.018;\ F = 230$$

TABLE I

CHROMATOGRAPHIC DATA FOR METHYLBENZENES ON A SILICA GEL COLUMN

n_{Me} = total number of methyl groups; the subscripts *o* and *p* denote *ortho* and *para*, respectively; μ = dipole moment in Debye units (calculated from that for a methyl group[8]).

No.	*Compound*	*Log* k'_{obs}	n_{Me}	n_o	n_p	$n_o - n_p$	μ	*Log* k'_{est}		
								Eqn. 3	*Eqn. 4*	*Eqn. 5*
1	Benzene	0.375	0	0	0	0	0	0.379	0.377	0.354
2	Toluene	0.461	1	0	0	0	0.37	0.462	0.462	0.472
3	1,2-Dimethylbenzene	0.585	2	2	0	2	0.64	0.587	0.587	0.583
4	1,3-Dimethylbenzene	0.548	2	0	0	0	0.37	0.545	0.546	0.560
5	1,4-Dimethylbenzene	0.512	2	0	2	−2	0	0.506	0.506	0.529
6	1,2,3-Trimethylbenzene	0.690	3	3	0	3	0.74	0.691	0.692	0.679
7	1,2,4-Trimethylbenzene	0.633	3	2	2	0	0.37	0.631	0.631	0.648
8	1,3,5-Trimethylbenzene	0.621	3	0	0	0	0	0.628	0.631	0.617
9	1,2,3,4-Tetramethylbenzene	0.767	4	4	2	2	0.64	0.756	0.756	0.758
10	1,2,3,5-Tetramethylbenzene	0.736	4	3	2	1	0.37	0.735	0.736	0.736
11	1,2,4,5-Tetramethylbenzene	0.716	4	4	4	0	0	0.717	0.716	0.705
12	Pentamethylbenzene	0.820	5	5	4	1	0.37	0.821	0.821	0.823
13	Hexamethylbenzene	0.881	6	6	6	0	0	0.886	0.885	0.881

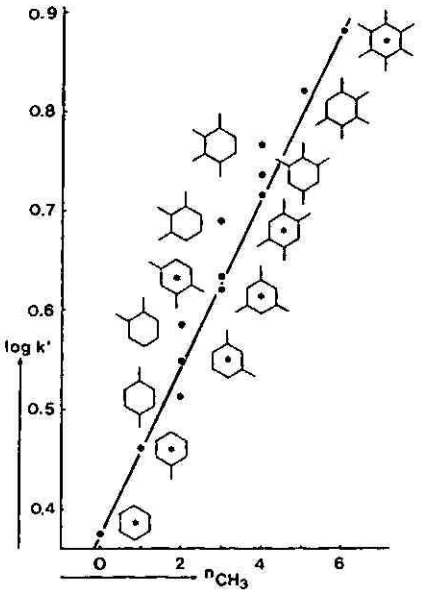

Fig. 1. Plot of log k' *versus* the number of methyl groups in methylbenzenes. Column: silica gel. The straight line correlates data obtained on the structures marked with asterisks; see eqn. 2.

Close inspection of Figs. 1 and 2, in particular the situation of the heavier methyl-substituted benzenes with regard to the two "backbones", suggests that symmetry conditions acting in the retention behaviour on an alumina column are different from those on a silica gel column. The non-equivalence of *para-* and *ortho-*

TABLE II

CHROMATOGRAPHIC DATA FOR METHYLBENZENES ON AN ALUMINA COLUMN

n_{ME} = Total number of methyl groups; the subscript o denotes *ortho*; n_{o-o} = number of ortho pairs.

No.	*Compound*	*Log* k'_{obs}	n_{Me}	n_o	n_{o-o}	*Log* k'_{est}*	
						Eqn. 8	*Eqn. 9*
1	Benzene	−0.032	0	0	0	*−0.035*	−0.004
2	Toluene	0.093	1	0	0	*0.083*	0.111
3	1,2-Dimethylbenzene	0.350	2	2	1	*0.351*	0.316
4	1,3-Dimethylbenzene	0.233	2	0	0	0.201	*0.226*
5	1,4-Dimethylbenzene	0.193	2	0	0	*0.201*	0.226
6	1,2,3-Trimethylbenzene	0.591	3	3	2	*0.545*	0.521
7	1,2,4-Trimethylbenzene	0.433	3	2	1	0.470	*0.432*
8	1,3,5-Trimethylbenzene	0.318	3	0	0	*0.319*	0.342
9	1,2,3,4-Tetramethylbenzene	0.778	4	4	3	*0.738*	0.727
10	1,2,3,5-Tetramethylbenzene	0.643	4	3	2	0.663	*0.637*
11	1,2,4,5-Tetramethylbenzene	0.625	4	4	2	0.738	*0.637*
12	Pentamethylbenzene	0.929	5	5	4	0.932	0.932
13	Hexamethylbenzene	1.176	6	6	6	1.125	1.227

* Estimates in italics indicate the best fitting of both values.

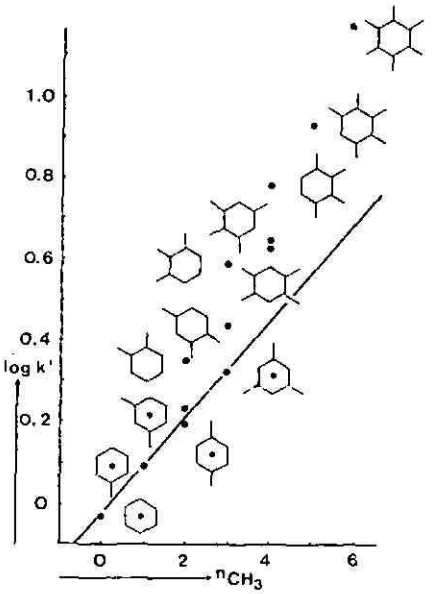

Fig. 2. Plot of log k' *versus* the number of methyl groups in methylbenzenes. Column: alumina. The straight line correlates data obtained on the structures marked with asterisks; see eqn. 7.

methyl substitution is especially evident. Compare, for instance, the location of hexamethylbenzene in Figs. 1 and 2. A good data fit could therefore be obtained by means of the exclusive use of n_{ortho} as additional parameter.

$$\log k' = 0.118\ (\pm 0.040)n_{Me} + 0.075\ (\pm 0.031)n_{ortho} - 0.035\ (\pm 0.073) \qquad (8)$$

$$n = 13;\ r = 0.992;\ s = 0.047;\ F = 320$$

A different parametrization of the *ortho*-effect is applied in eqn. 9. The parameter n_{o-o} denotes the number of *ortho* pairs present in the considered structure. The statistics of the new equation are slightly improved over those of eqn. 8. Comparison of the log k'_{est} values (Table II) shows that eqn. 8 seems to be more effective with restricted methyl substitution and eqn. 9 seems to be more effective when more extended methyl substitution is involved. Eqn. 9 accounts for 99% of the variances and eqn. 8 for 98% of the variances.

$$\log k' = 0.115\ (\pm 0.032)n_{Me} + 0.090\ (\pm 0.028)n_{o-o} - 0.004\ (\pm 0.063) \qquad (9)$$

$$n = 13;\ r = 0.995;\ s = 0.039;\ F = 500$$

The application of group dipole moments was not successful. This emphasizes that symmetry conditions are less important on alumina than on silica gel columns.

Alkylbenzenes on a silica gel column

Table III gives the experimentally derived log k' values of 38 alkylbenzenes. Comparison of these data shows that ethyl, propyl and higher alkyl substituents have a reducing effect on the capacity factor. In order to establish whether this effect could

be assigned a constant value, we correlated log k' with the total number of substituent carbons for toluene, ethylbenzene, isopropylbenzene and *n*-butylbenzene. This led to the following equation:

$$\log k' = -0.049\ (\pm 0.029)n_C + 0.508\ (\pm 0.079) \qquad (10)$$
$$n = 4;\ r = 0.982;\ s = 0.015;\ F = 52.8$$

The statistics are acceptable and the straight line is shown in Fig. 3b. The *tert.*-butyl-substituted compound had to be omitted from the regression on account of its bad fit ($\log k'_{obs} = 0.389$, $\log k'_{est} = 0.312$). The reason for this is discussed later.

Comparison of lines b and a in Fig. 3 (the latter represents the same line as that in Fig. 1) led to the choice of the following parametrization: n_1 is the total number of carbon atoms in the alkyl substituents, irrespective of branching or ring position, and n_2 is n_1 minus the total number of alkyl substituents. After removal of all non-fitting outliers, the following equation was obtained for eighteen (encircled) data points:

$$\log k' = 0.085\ (\pm 0.008)n_1 - 0.137\ (\pm 0.010)n_2 + 0.366\ (\pm 0.025) \qquad (11)$$
$$n = 18;\ r = 0.991;\ s = 0.022;\ F = 414$$

Included in this equation were the seven data points from eqn. 2. After completion of the regression analysis it appeared that four of the omitted data points might as well have been included in the equation. The total number of fitting structures is then 22. The residuals of the sixteen non-fitting compounds range from $+0.121$ to -0.238 and are at least partly connected with uncorrected symmetry conditions. Different from the transfer of eqn. 2 into eqn. 4 or 5, it is not simple to find an equation that includes all 38 compounds. This problem is as yet unsolved. The observed phenomenon may be attributed, partly, to the absence of adsorptivity of bulky alkyl groups on silica gel, resulting in an apparent lift of the adsorbed aromatic[9]. In the next section alumina is shown to behave in an identical manner. Similar suggestions were made by Snyder and Poppe[10] and by Popl *et al.*[11].

Alkylbenzenes on an alumina column

Table IV gives the experimentally derived log k' values of 38 alkylbenzenes. The regression study of the data was similar to that described above for the silica gel data. The analogues of eqns. 10 and 11 are the following equations, with identical parametrizations:

$$\log k' = -0.095\ (\pm 0.028)n_C + 0.180\ (\pm 0.076) \qquad (12)$$
$$n = 4;\ r = 0.995;\ s = 0.014;\ F = 217$$

and

$$\log k' = 0.117\ (\pm 0.011)n_1 - 0.214\ (\pm 0.015)n_2 - 0.027\ (\pm 0.021) \qquad (13)$$
$$n = 12;\ r = 0.996;\ s = 0.015;\ F = 555$$

TABLE III

CHROMATOGRAPHIC DATA FOR ALKYLBENZENES ON A SILICA GEL COLUMN

No.	*Compound*	*Log k'_{obs}*	n_1*	n_2**	*Log k'_{est} (eqn. 11)****	
					Fitting compounds	*Non-fitting compounds*
1	Benzene	0.375	0	0	0.366 (0.009)	
2	Methylbenzene	0.461	1	0	0.452 (0.009)	
3	1,2-Dimethylbenzene	0.585	2	0	*0.537* (0.048)	
4	1,3-Dimethylbenzene	0.548	2	0	0.537 (0.011)	
5	1,4-Dimethylbenzene	0.512	2	0	*0.537* (−0.025)	
6	1,2,3-Trimethylbenzene	0.690	3	0		0.623 (0.067)
7	1,2,4-Trimethylbenzene	0.633	3	0	0.623 (0.010)	
8	1,3,5-Trimethylbenzene	0.621	3	0	0.623 (−0.002)	
9	1,2,3,4-Tetramethylbenzene	0.767	4	0		0.708 (0.059)
10	1,2,3,5-Tetramethylbenzene	0.736	4	0	*0.708* (0.028)	
11	1,2,4,5-Tetramethylbenzene	0.716	4	0	0.708 (0.008)	
12	Pentamethylbenzene	0.820	5	0	*0.794* (0.026)	
13	Hexamethylbenzene	0.881	6	0	0.879 (0.002)	
14	1-Methyl-4-ethylbenzene	0.435	3	1	0.486 (−0.051)	
15	1,3-Dimethyl-5-isopropylbenzene	0.524	5	2	0.521 (0.003)	
16	1-Methyl-4-*tert.*-butylbenzene	0.407	5	3	0.384 (0.023)	
17	1,4-Dimethyl-2-*tert.*-butylbenzene	0.591	6	3		0.470 (0.121)
18	1,3-Dimethyl-5-*tert.*-butylbenzene	0.544	6	3		0.407 (0.074)
19	1,2,3-Trimethyl-5-*tert.*-butylbenzene	0.562	7	3	0.555 (0.007)	
20	1,2-Dimethyl-5-*tert.*-butylbenzene	0.462	6	3	0.470 (−0.008)	

21	1-Methyl-3,4-di-*tert.*-butylbenzene	0.334	9	6	0.317 (0.017)	
22	Ethylbenzene	0.398	2	1	0.401 (−0.003)	
23	1,3-Diethylbenzene	0.398	4	2	0.435 (−0.037)	
24	1,4-Diethylbenzene	0.326	4	2		0.435 (−0.109)
25	1,2,4-Triethylbenzene	0.386	6	3		0.470 (−0.084)
26	1,3,5-Triethylbenzene	0.332	6	3		0.470 (−0.138)
27	1-Ethyl-3,5-di-*tert.*-butylbenzene	0.137	10	7		0.266 (−0.129)
28	Isopropylbenzene	0.377	3	2	0.350 (0.027)	
29	1,3-Diisopropylbenzene	0.303	6	4	0.333 (−0.030)	
30	1,4-Diisopropylbenzene	0.176	6	4		0.333 (−0.157)
31	1,2,4-Triisopropylbenzene	0.086	9	6		0.317 (−0.231)
32	1,3,5-Triisopropylbenzene	0.079	9	6		0.317 (−0.238)
33	1,2,4,5-Tetraisopropylbenzene	0.079	12	8		0.300 (−0.221)
34	1-Isopropyl-3,5-di-*tert.*-butylbenzene	0.013	11	8		0.215 (−0.202)
35	*n*-Butylbenzene	0.305	4	3	0.299 (0.006)	
36	*tert.*-Butylbenzene	0.389	4	3		0.299 (0.090)
37	1,4-Di-*tert.*-butylbenzene	0.086	8	6		0.231 (−0.145)
38	1,3,5-Tri-*tert.*-butylbenzene	−0.027	12	9		0.164 (−0.191)

* n_1 = Total number of carbon atoms in alkyl substituents.

** $n_2 = n_1$ − number of alkyl substituents.

*** In parentheses: differences between observed and estimated log k' values; data in italics were not included in regression eqn. 11 as they did not fit eqn. 6 accurately; after all, there is no reason to exclude them from being ranged in the last column but one with compounds fitting eqn. 11.

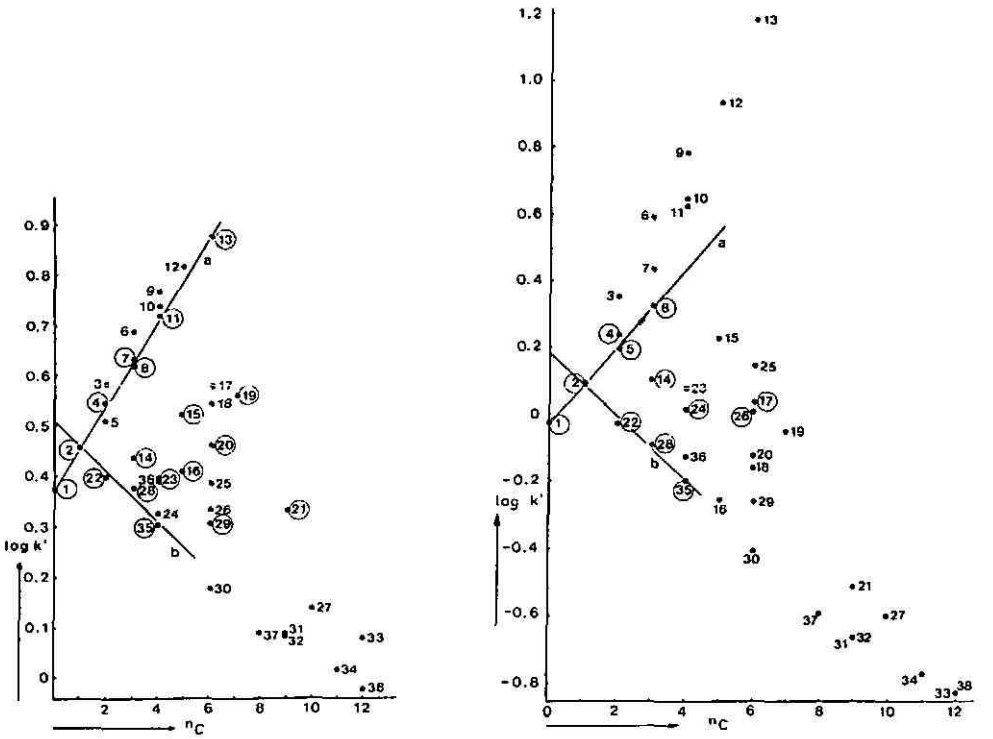

Fig. 3. Plot of log k' *versus* the number of alkyl carbon atoms (n_C) in alkylbenzenes. Column: silica gel. Numbering as in Table III. Straight line a comprises data points 1, 2, 4, 7, 8, 11 and 13 and corresponds with the straight line in Fig. 1 (see eqn. 2); straight line b comprises data points 2, 22, 28 and 35 (see eqn. 10); the encircled data points (1, 2, 4, 7, 8, 11, 13, 14, 15, 16, 19, 20, 21, 22, 23, 28, 29 and 35) can be included in regression eqn. 11.

Fig. 4. Plot of log k' *versus* the number of alkyl carbon atoms (n_C) in alkylbenzenes. Column: alumina. Numbering as in Table IV. Straight line a comprises data points 1, 2, 4, 5 and 8 and corresponds with the straight line drawn in Fig. 2 (see eqn. 7); straight line b comprises data points 2, 22, 28 and 35 (see eqn. 12); the encircled data points (1, 2, 4, 5, 8, 14, 17, 22, 24, 26, 28 and 35) can be included in regression eqn. 13.

The total number of fitting data points (encircled in Fig. 4) is strongly reduced with regard to the equation for silica gel data (eqn. 11). The total number of outliers is now 26 with residuals ranging from +0.504 to −0.480.

Comparison of eqns. 11 and 13, guided by the schematized line pattern given in Fig. 5, reveals the following trends for alkyl substitution, independent of whether the column packing is silica gel or alumina.

(1) Methyl-substitution increases log k' with a uniform pattern; independent of whether the methyl groups are introduced in benzene (toluene) or in ethylbenzene, propylbenzene, etc., the introduction of one methyl group is accompanied by a constant log k' increase of:

for silica gel columns: 0.084 (eqn. 2), 0.085 (eqn. 11);

for alumina columns: 0.118 (eqn. 7), 0.117 (eqn. 13).

There is a constant upward movement along the straight lines denoted by a'_0, a_2, a_3,..., in Fig. 5.

(2) Alkyl substitution decreases log k' along the straight lines b_0, b_1, b_2 in Fig. 5. These log k' decreases can easily be derived from eqns. 11 and 13 and are 0.052 for silica gel columns and 0.097 for alumina columns.

(3) Changes in the symmetry pattern cause large differences between the predicted and observed log k' values (see relevant columns in Tables III and IV). Attempts to make the necessary corrections as performed for methylbenzenes (eqns. 4, 5, 8 and 9) proved ineffectual.

(4) The effect of alkyl substitution on log k' seems to consist of two distinguishable factors, one being attributable to the substituent bulk and the other to mesomeric effects of the alkyl substituent on the phenyl nucleus. The following calculation enables some detailed information to be obtained:

	SiO_2	Al_2O_3
Toluene: log k'_{obs}	0.461	0.093
"CH_2 bulk" factor	−0.052	−0.097
Benzene: log k'_{pred}	0.513	0.190
Benzene: log k'_{obs}	0.375	−0.032
Δ =	0.138	0.222

The observed log k' values for benzene are 0.138 and 0.222, respectively, lower than predicted. These deviations can be attributed to the mesomeric impact of methyl and other alkyl groups on the benzene ring according to

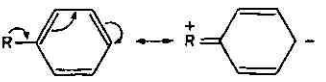

where R represents an aliphatic hydrocarbon residue. These mesomeric effects are fairly consistent, as follows from their Hammett σ-values (-0.152 ± 0.015 for an *n*-alkyl group[12]). An isopropyl group is not different ($\sigma = -0.15$) but a *tert.*-butyl group with $\sigma = -0.20$ has a significantly higher mesomeric effect on a benzene ring. This is probably the reason why an isopropyl group fits correctly the b-line equation, whereas the *tert.*-butyl group has a significantly increased log k' value*.

(5) The basic values for log k' moving along the a lines by a mesomeric effect and along the b lines by the introduction of bulk [see the values in paragraphs (1) and (4) above, respectively] permit predictions of log k' values. The following examples can be given for 1,3-diethylbenzene and 1-methyl-4-ethylbenzene.

1,3-Diethylbenzene: starting from log k' (benzene), two moves upwards along a_0 and two moves downwards along b_1 are required, resulting in the following calculations:

log $k'(SiO_2) = 0.375 + 2 \cdot 0.085 - 2 \cdot 0.052 = 0.441$ (fit eqn. 11, 0.435; obs., 0.398)
log $k'(Al_2O_3) = -0.032 + 2 \cdot 0.117 - 2 \cdot 0.097 = 0.008$ (fit eqn. 13, 0.010; obs., 0.083)

* A Hammett σ-value describes the total electronic substituent effect, but for an alkyl group it represents the proper mesomeric effect as the inductive counterpart of an alkyl mesomeric effect is zero, independent of length, branching or cyclization of the alkyl group[13].

TABLE IV

CHROMATOGRAPHIC DATA FOR ALKYLBENZENES ON AN ALUMINA COLUMN

No.	*Compound*	*Log k'_{obs}*	n_1*	n_2**	*Log k'_{est} (eqn. 13)****	
					Fitting compounds	*Non-fitting compounds*
1	Benzene	−0.032	0	0	−0.027 (−0.005)	
2	Methylbenzene	0.093	1	0	0.089 (0.004)	
3	1,2-Dimethylbenzene	0.350	2	0		0.206 (0.144)
4	1,3-Dimethylbenzene	0.233	2	0	0.206 (0.027)	
5	1,4-Dimethylbenzene	0.193	2	0	0.206 (−0.013)	
6	1,2,3-Trimethylbenzene	0.591	3	0		0.322 (0.269)
7	1,2,4-Trimethylbenzene	0.433	3	0		0.322 (0.111)
8	1,3,5-Trimethylbenzene	0.318	3	0	0.322 (−0.004)	
9	1,2,3,4-Tetramethylbenzene	0.778	4	0		0.439 (0.339)
10	1,2,3,5-Tetramethylbenzene	0.643	4	0		0.439 (0.204)
11	1,2,4,5-Tetramethylbenzene	0.625	4	0		0.439 (0.186)
12	Pentamethylbenzene	0.929	5	0		0.555 (0.374)
13	Hexamethylbenzene	1.176	6	0		0.672 (0.504)
14	1-Methyl-4-ethylbenzene	0.104	3	1	0.108 (−0.004)	
15	1,3-Dimethyl-5-isopropylbenzene	0.225	5	2		0.127 (0.098)
16	1-Methyl-4-*tert.*-butylbenzene	−0.252	5	3		−0.088 (−0.164)
17	1,4-Dimethyl-2-*tert.*-butylbenzene	0.037	6	3	0.029 (0.008)	
18	1,3-Dimethyl-5-*tert.*-butylbenzene	−0.161	6	3		0.029 (−0.180)
19	1,2,3-Trimethyl-5-*tert.*-butylbenzene	−0.051	7	3		0.146 (−0.197)
20	1,2-Dimethyl-5-*tert.*-butylbenzene	−0.119	6	3		0.029 (−0.148)

21	1-Methyl-3,4-di-*tert.*-butylbenzene	−0.509	9	6		−0.264 (−0.245)
22	Ethylbenzene	−0.027	2	1	−0.008 (−0.019)	
23	1,3-Diethylbenzene	0.083	4	2		0.010 (0.073)
24	1,4-Diethylbenzene	0.021	4	2	0.010 (0.011)	
25	1,2,4-Triethylbenzene	0.152	6	3		0.029 (0.123)
26	1,3,5-Triethylbenzene	0.013	6	3	0.029 (−0.016)	
27	1-Ethyl-3,5-di-*tert.*-butylbenzene	−0.602	10	7		−0.362 (−0.240)
28	Isopropylbenzene	−0.097	3	2	−0.106 (0.009)	
29	1,3-Diisopropylbenzene	−0.260	6	4		−0.185 (−0.075)
30	1,4-Diisopropylbenzene	−0.409	6	4		−0.185 (−0.224)
31	1,2,4-Triisopropylbenzene	−0.658	9	6		−0.264 (−0.394)
32	1,3,5-Triisopropylbenzene	−0.658	9	6		−0.264 (−0.394)
33	1,2,4,5-Tetraisopropylbenzene	−0.824	12	8		−0.344 (−0.480)
34	1-Isopropyl-3,5-di-*tert.*-butylbenzene	−0.770	11	8		−0.770 (−0.460)
35	*n*-Butylbenzene	−0.201	4	3	−0.204 (0.003)	
36	*tert.*-Butylbenzene	−0.125	4	3		−0.204 (0.079)
37	1,4-Di-*tert.*-butylbenzene	−0.585	8	6		−0.381 (−0.204)
38	1,3,5-Tri-*tert.*-butylbenzene	−0.824	12	9		−0.557 (−0.267)

* n_1 = total number of carbon atoms in alkyl substituents.

** n_2 = n_1 − number of alkyl substituents.

*** In parentheses: differences between observed and estimated log k' values.

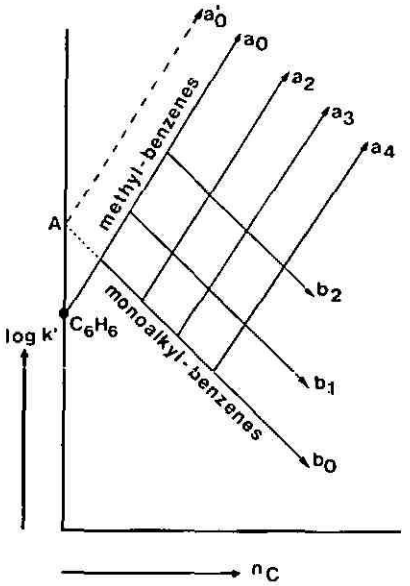

Fig. 5. Schematized log k' *versus* n_C plot for alkylbenzenes on silica gel or alumina columns. The a lines depict the effect of methyl substitution in a monoalkylbenzene, the subscripts denoting the number of carbon atoms in the alkyl group; a'_0 is the hypothetical a_0 line with exclusion of mesomeric methyl effects; A indicates the hypothetical location of benzene. The b lines depict the effect of alkyl substitution in a methylbenzene, the subscripts denoting the number of methyl groups.

1-Methyl-4-ethylbenzene: starting from log k' (benzene), two moves upwards along a_0 and one move downwards along b_1 are required, resulting in the following calculations:

$\log k'(SiO_2) = 0.375 + 2 \cdot 0.085 - 1 \cdot 0.052 = 0.493$ (fit eqn. 11, 0.486; obs., 0.435)
$\log k'(Al_2O_3) = -0.032 + 2 \cdot 0.117 - 1 \cdot 0.097 = 0.105$ (fit eqn. 13, 0.108; obs., 0.104)

(6) Lengthening of the aliphatic chain in an alkylbenzene will gradually decrease log k' on both silica gel and alumina columns. An aliphatic behavioural pattern will finally dominate, first on an alumina and then on a silica gel column.

It is interesting that the essential features of the relationships between log k' and the number of carbon atoms in an alkylbenzene as shown in Figs. 3–5 can also be found in the papers by Ageev *et al.*[14] and Kříž and co-workers[15,16]. Ageev *et al.* gave a line pattern corresponding to lines a and b in Fig. 3 for the retention of methylbenzenes (a) and monoalkylbenzenes on a silica gel column. Kříž *et al.* extend the plot to more and heavier substituted alkylbenzenes[15] and to alkylnaphthalenes[16]. Neither group used alumina packed columns and the scope of their work was restricted to qualitative considerations.

Silica gel versus alumina in alkylbenzene retention

Careful comparison of Tables III and IV reveals a close parallel between the observed retention values for at least some of the investigated alkylbenzenes. The

correlation of alumina data *versus* those obtained on silica gel for the complete data set is given by

$$\log k'(Al_2O_3) = 1.996\ (\pm 0.224)\log k'\ (SiO_2) - 0.847\ (\pm 0.107) \qquad (14)$$
$$n = 38;\ r = 0.949;\ s = 0.156;\ F = 324$$

The sensitivity for alkylbenzenes on an alumina column is twice that on a silica gel column. Eqn. 14 confirms our findings that retentions obtained on both silica gel and alumina are mainly regulated by bulk factors in the transported hydrocarbons (see eqns. 1, 6, 11 and 13) and that any specific factor on alkylbenzene retention originating from the applied column packing is of only secondary importance.

Straight line A in Fig. 6 clearly reflects the mutual relationships in the investigated series. It is of interest how all ethyl compounds (marked with asterisks in Fig. 6) are clustered on the left side of line A and that especially the higher methylated benzenes tend to follow a deviating pattern. This led us to check some non-linear fits. All thirteen methylbenzenes could be correctly fitted by a "pit" parabola:

$$\log k'(Al_2O_3) = 1.857\ (\pm 0.127)[\log k'(SiO_2)]^2 - 0.314\ (\pm 0.059) \qquad (15)$$
$$n = 13;\ r = 0.995;\ s = 0.037;\ F = 1020$$

The six ethylbenzenes could be fitted by this equation (details in Table V) and the complete methyl- and ethylbenzene set (thirteen data points) could be correlated as follows:

$$\log k'(Al_2O_3) = 3.152\ (\pm 0.918)[\log k'(SiO_2)]^2 -$$
$$1.728\ (\pm 1.078)\ \log k'(SiO_2) + 0.242\ (\pm 0.295) \qquad (16)$$
$$n = 19;\ r = 0.992;\ s = 0.048;\ F = 501$$

This equation is represented by curve B in Fig. 6 and it puts all alkylbenzenes higher than ethyl benzenes aside. Their retention values on alumina remain considerably lower than those obtained on silica gel and the effect depends to some extent on (a) the number and (b) the size of the alkyl groups.

Halogenomethylbenzenes on a silica gel column

Table VI gives the experimentally derived log k' values of a series of 28 halogenomethylbenzenes. Simple comparisons of analogous trios (1–10–25, 2–11–26, etc.) clearly indicate an effect of increasing halogen bulk on the capacity factor. We decided to account for this effect by the application of a suitable set of indicator values (dummy parameters). For chloro compounds $D_1 = 0$, $D_2 = 0$, for bromo compounds $D_1 = 1$ and $D_2 = 0$ and for iodo compounds $D_1 = 0$ and $D_2 = 1$. The simplest parametrization gives the following equation:

$$\log k' = 0.034\ (\pm 0.038)n_{Me} + 0.034\ (\pm 0.015)D_1 +$$
$$+ 0.057\ (\pm 0.051)D_2 + 0.037\ (\pm 0.076) \qquad (17)$$
$$n = 28;\ r = 0.747;\ s = 0.043;\ F = 11.6$$

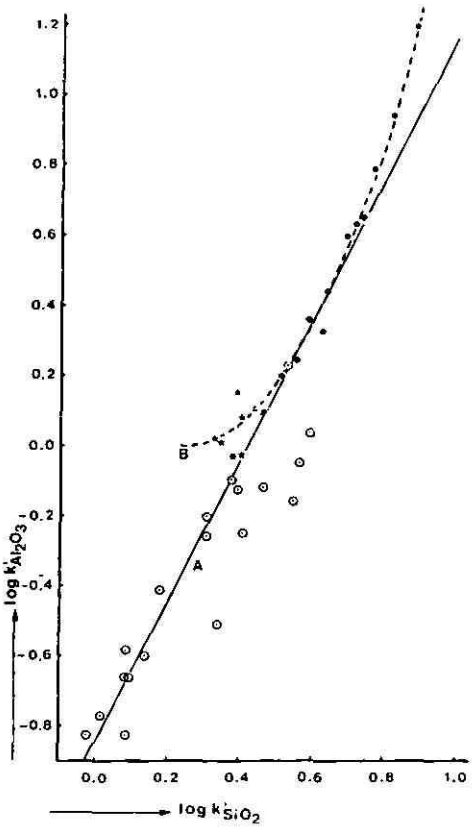

Fig. 6. Plot of log k' (alumina) *versus* log k' (silica gel) for 38 alkylbenzenes (data taken from Tables III and IV). Curve A, eqn. 14; curve B; eqn. 16. ●, Methylbenzenes; ★, ethylbenzenes; ⊙, higher alkylbenzenes.

This equation is far from significant. It can be improved by the replacement of n_{Me} by the parameters $n_{meta+para}$, n_{ortho} and n_{para}:

$$\log k' = 0.051\ (\pm 0.007)n_{meta+para} + 0.034\ (\pm 0.008)D_1 + 0.062\ (\pm 0.011)D_2 + \\ + 0.022\ (\pm 0.005)n_{ortho} - 0.013\ (\pm 0.004)n_{para} + 0.040\ (\pm 0.007) \quad (18)$$

$$n = 28;\ r = 0.990;\ s = 0.010;\ F = 245$$

There is a striking correspondence between the parametrizations of eqns. 3 and 18. The algebraic signs of the n_{ortho} and n_{para} regressors are the same, although their values are no longer statistically equal. It is therefore justified to try the introduction of a summed group dipole moment μ as an additional parameter to eqn. 17. For detailed information we refer to Table VI. The results of this calculation are given in eqn. 19.

TABLE V

CHROMATOGRAPHIC DATA FOR ETHYLBENZENES ON AN ALUMINA COLUMN

Benzene and toluene data have been added for comparison.

Compound	*Log* k'_{obs}	*Log* k'_{cal}					
		Eqn. 14	*Δ*	*Eqn. 15*	*Δ*	*Eqn. 16*	*Δ*
1-Methyl-4-ethylbenzene	0.104	0.021	0.083	0.037	0.067	0.086	0.018
Ethylbenzene	−0.027	−0.053	0.026	−0.021	−0.006	0.052	−0.079
1,3-Diethylbenzene	−0.083	−0.053	0.136	−0.021	−0.062	0.052	0.031
1,4-Diethylbenzene	0.021	−0.197	0.218	−0.117	0.138	0.013	0.008
1,2,4-Triethylbenzene	0.152	−0.077	0.229	−0.037	0.189	0.045	0.107
1,3,5-Triethylbenzene	0.013	−0.185	0.198	−0.110	0.123	0.015	−0.002
Benzene	−0.032	−0.099	0.067	−0.052	0.020	0.038	−0.070
Toluene	0.093	0.073	0.020	0.081	0.012	0.117	−0.024

$$\log k' = 0.030\ (\pm 0.007)n_{Me} + 0.055\ (\pm 0.019)D_1 + \\ + 0.068\ (\pm 0.025)D_2 + 0.141\ (\pm 0.033)\mu - 0.221\ (\pm 0.062) \quad (19)$$

$$n = 28;\ r = 0.947;\ s = 0.021;\ F = 55.8$$

in which the correlation coefficient r has increased significantly from 0.747 in eqn. 17 to 0.947.

Halogenomethylbenzenes on an alumina column

The experimentally derived log k' values are given in Table VI. A regression equation with a parametrization identical with that of eqn. 17 is

$$\log k' = 0.156\ (\pm 0.027)n_{Me} + 0.154\ (\pm 0.067)D_1 + \\ + 0.385\ (\pm 0.091)D_2 - 0.001\ (\pm 0.063) \quad (20)$$

$$n = 28;\ r = 0.950;\ s = 0.075;\ F = 81.1$$

In contrast with eqn. 17, the statistics of eqn. 20 are acceptable, although the addition of n_{para} and n_{o-o} as extra parameters gives a substantial improvement:

$$\log k' = 0.082\ (\pm 0.014)n_{Me} + 0.156\ (\pm 0.021)D_1 + 0.380\ (\pm 0.029)D_2 + \\ + 0.034\ (\pm 0.020)n_{para} + 0.112\ (\pm 0.016)n_{o-o} + 0.071\ (\pm 0.023) \quad (21)$$

$$n = 28;\ r = 0.995;\ s = 0.025;\ F = 526$$

The introduction of the sum group dipole moment in eqn. 20 was unsuccessful.

Comparison between methylbenzenes and halogenomethylbenzenes

From the preceding sections, it is obvious that the chromatographic behaviour of methylbenzenes and halogenomethylbenzenes on both silica gel and alumina has distinct points of concurrence. Close observation of the obtained regression equations (compare eqns. 3 and 4 with eqns. 18 and 8 and compare eqn. 9 with eqn. 20) reveals,

TABLE VI

CHROMATOGRAPHIC DATA FOR HALOGENOMETHYLBENZENES ON SILICA GEL AND ALUMINA COLUMNS

n_{Me} = total number of methyl groups; D_1 and D_2 = indicator values (dummy parameters); for chloro compounds $D_1 = D_2 = 0$, for bromo compounds $D_1 = 1$ and $D_2 = 0$ and for iodo compounds $D_1 = 0$ and $D_2 = 1$; the subscripts *m*, *p* and *o* denote *meta*, *para* and *ortho*, respectively; n_{o-o} = number of *ortho*-methyl pairs; μ = dipole moment in Debye units (calculated from group moments).

No.	*Compound*	*Log* k'_{obs}		n_{Me}	$n_{m,p}$	n_o	n_p	n_{o-o}	D_1	D_2	μ	*Log* k'_{est}			
		SiO_2	Al_2O_3									SiO_2 *(eqn. 15)*	Al_2O_3 *(eqn. 18)*	SiO_2 *(eqn. 16)*	Al_2O_3 *(eqn. 19)*
	Chlorobenzenes														
1	Unsubstituted	0.033	0.061	0	0	0	0	0	0	0	1.76	0.040	0.071	0.028	0.033
2	2-Methyl	0.045	0.143	1	0	0	0	0	0	0	1.61	0.040	0.152	0.037	0.109
3	3-Methyl	0.090	0.143	1	1	0	0	0	0	0	1.97	0.091	0.152	0.088	0.242
4	4-Methyl	0.086	0.176	1	1	0	0	0	0	0	2.13	0.091	0.186	0.110	0.161
5	2,3-Dimethyl	0.137	0.380	2	1	2	0	1	0	0	1.87	0.134	0.346	0.104	0.293
6	2,4-Dimethyl	0.090	0.283	2	1	0	0	0	0	0	1.97	0.091	0.268	0.118	0.242
7	2,6-Dimethyl	0.037	0.250	2	0	0	0	0	0	0	1.39	0.040	0.234	0.036	0.221
8	3,4-Dimethyl	0.188	0.384	2	2	2	0	1	0	0	2.34	0.185	0.380	0.170	0.370
9	2,5-Dimethyl	0.072	0.201	2	1	0	2	0	0	0	1.76	0.065	0.234	0.088	0.349
	Bromobenzenes														
10	Unsubstituted	0.079	0.243	0	0	0	0	0	1	0	1.64	0.074	0.226	0.065	0.208
11	2-Methyl	0.083	0.307	1	0	0	0	0	1	0	1.49	0.074	0.308	0.074	0.285
12	3-Methyl	0.127	0.297	1	1	0	0	0	1	0	1.85	0.125	0.308	0.125	0.418

13	4-Methyl	0.127	0.332	1	1	0	0	0	1	0	2.01	0.125	0.342	0.148	0.336
14	2,4-Dimethyl	0.127	0.436	2	1	0	0	0	1	0	1.85	0.125	0.424	0.125	0.418
15	3,5-Dimethyl	0.170	0.346	2	2	0	0	0	1	0	2.01	0.176	0.389	0.178	0.336
16	3,4-Dimethyl	0.223	0.526	2	2	2	0	1	1	0	2.22	0.219	0.536	0.208	0.546
17	2,3-Dimethyl	0.164	0.538	2	1	2	0	1	1	0	1.76	0.168	0.501	0.143	0.464
18	2,6-Dimethyl	0.079	0.410	2	0	0	0	0	1	0	1.27	0.074	0.389	0.074	0.397
19	2,5-Dimethyl	0.104	0.350	2	1	0	2	0	1	0	1.64	0.098	0.389	0.126	0.525
20	2,4,6-Trimethyl	0.114	0.528	3	1	0	0	0	1	0	1.64	0.125	0.505	0.156	0.525
21	2,3,6-Trimethyl	0.130	0.598	3	1	2	2	1	1	0	1.49	0.142	0.583	0.135	0.601
22	2,3,4,6-Tetramethyl	0.210	0.825	4	2	3	2	2	1	0	1.85	0.214	0.811	0.216	0.734
23	2,3,5,6-Tetramethyl	0.190	0.782	4	2	4	4	2	1	0	1.64	0.210	0.776	0.187	0.841
24	2,3,4,5,6-Pentamethyl	0.303	1.086	5	3	5	4	4	1	0	2.01	0.282	1.116	0.269	0.970
	Iodobenzenes														
25	Unsubstituted	0.097	0.465	0	0	0	0	0	0	1	1.71	0.103	0.450	0.088	0.417
26	2-Methyl	0.114	0.542	1	0	0	0	0	0	1	1.56	0.103	0.532	0.097	0.493
27	3-Methyl	0.146	0.516	1	1	0	0	0	0	1	1.92	0.153	0.532	0.148	0.626
28	2,4-Dimethyl	0.155	0.639	2	1	0	0	0	0	1	1.92	0.153	0.648	0.178	0.626

however, that mutual similarities are not such as to allow the incorporation of both series in one regression equation.

A comparison of both series, based on a replacement of one methyl group from a methylbenzene by a halogen atom, showed some striking parallels between the methylbenzene and halogenomethylbenzene series. These parallels are illustrated in Figs. 7 and 8. They also give the following set of equations:

(a) Bromomethylbenzenes with the bromine atom flanked by two methyl groups:

on silica gel columns:

$$\log k'_{\text{Br-Me}} = 1.152\ (\pm 0.316)\log k'_{\text{Me}} - 0.734\ (\pm 0.288) \qquad (22)$$

$n = 6$; $r = 0.975$; $s = 0.020$; $F = 76.4$

on alumina columns:

$$\log k'_{\text{Br-Me}} = 1.116\ (\pm 0.193)\log k'_{\text{Me}} - 0.234\ (\pm 0.167) \qquad (23)$$

$n = 6$; $r = 0.992$; $s = 0.034$; $F = 258$

(b) The whole bromomethylbenzene series were correlated by applying an extra parameter n_{ortho}, denoting the number of methyl groups in an *ortho* position with respect to bromine:

on silica gel columns:

$$\log k'_{\text{Br-Me}} = 0.932\ (\pm 0.205)\log k'_{\text{Me}} - 0.094\ (\pm 0.028)n_{ortho} - 0.374\ (\pm 0.114) \qquad (24)$$

$n = 15$; $r = 0.942$; $s = 0.023$; $F = 51.0$

on alumina columns:

$$\log k'_{\text{Br-Me}} = 1.047\ (\pm 0.159)\log k'_{\text{Me}} - 0.129\ (\pm 0.055)n_{ortho} + 0.077\ (\pm 0.053) \qquad (25)$$

$n = 15$; $r = 0.984$; $s = 0.045$; $F = 198$

(c) The integrated halogenomethylbenzene series coupled together by means of a set of dummy parameters, identical with the set presented in Table VI:

on silica gel columns:

$$\log k'_{\text{Hal-Me}} = 0.908\ (\pm 0.127)\log k'_{\text{Me}} - 0.093\ (\pm 0.016)n_{ortho} + 0.036\ (\pm 0.016)D_1 + 0.064\ (\pm 0.022)D_2 - 0.395\ (\pm 0.068) \qquad (26)$$

$n = 28$; $r = 0.958$; $s = 0.019$; $F = 72.6$

on alumina columns:

$$\log k'_{\text{Hal-Me}} = 1.033\ (\pm 0.118)\log k'_{\text{Me}} - 0.133\ (\pm 0.037)n_{ortho} + 0.161\ (\pm 0.037)D_1 + 0.392\ (\pm 0.050)D_2 - 0.071\ (\pm 0.039) \qquad (27)$$

$n = 28$; $r = 0.985$; $s = 0.043$; $F = 211$

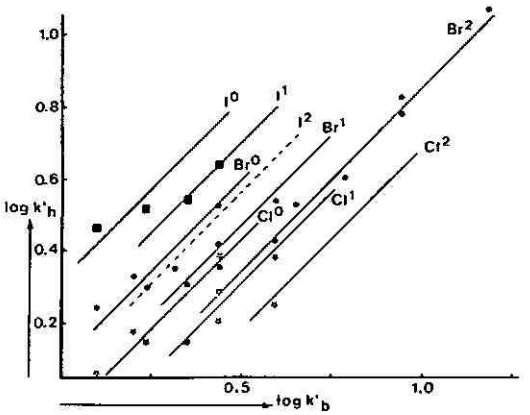

Fig. 7. Plot of log k' for halogenomethylbenzenes (log k'_h) on a silica gel column *versus* corresponding data for related methylbenzenes (log k'_b). ☆, Chloromethylbenzenes; ●, bromomethylbenzenes; ■, iodomethylbenzenes. The superscripts 0, 1 and 2 denote the number of methyl groups in an *ortho* position with respect to the halogen.

Eqns. 26 and 27 permit the nine parallel lines in Figs. 7 and 8 to be drawn. Each of these lines comprises the halogenomethylbenzenes indicated by Cl, Br and I; the superscripts 0, 1 and 2 denote the number of methyl groups in an *ortho* position with respect towards the halogen atom. The equivalence of both systems is surprisingly evident, especially if one considers the regressor values of the first right-hand terms in eqns. 26 and 27: they are not significantly differing from unity.

Owing to the difference between the weights of the halogen effects, as indicated by the computed dummy regressor values, part of the line pattern in Fig. 8 has moved compared with the pattern in Fig. 7, thus clearly demonstrating the difference between the two column packings.

CONCLUSION

Retention of methylbenzenes on silica (elution with *n*-hexane) is regulated by the number of methyl groups and to a lesser extent by symmetry conditions. This

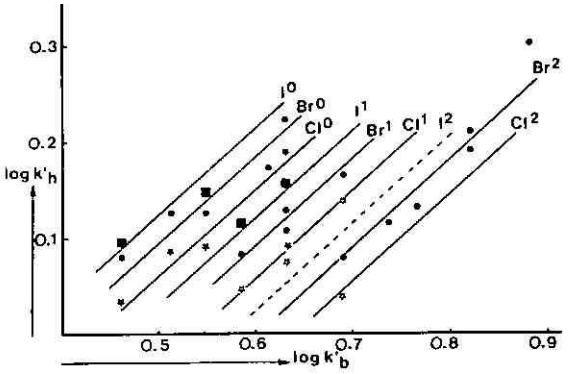

Fig. 8. Plot of log k' for halogenomethylbenzenes (log k'_h) on an alumina column *versus* corresponding data for related methylbenzenes (log k'_b). Symbols and superscripts as in Fig. 7.

can be correctly parametrized either by the $n_{ortho} - n_{para}$ number or by a summed group dipole moment. On alumina the number of methyl groups is equally important and, the additional parameter is the number of *ortho* pairs. Extension of a methyl group to a higher alkyl leads to a network plot of log k' *versus* the number of alkyl carbon atoms with an indication that larger alkyl groups give a "lift" to the adsorbed aromatics away from the packing material. Introduction of one halogen atom in the nucleus of methylbenzenes does not essentially change the features of retention, and indicated above for methylbenzenes, the observed retentions run largely parallel.

ACKNOWLEDGEMENT

The authors thank Prof. Dr. U. A. Th. Brinkman for commenting on the manuscript.

REFERENCES

1 U. A. Th. Brinkman, A. de Kok, G. de Vries and H. G. M. Reymer, *J. Chromatogr.*, 128 (1976) 101.
2 U. A. Th. Brinkman, A. de Kok, H. G. M. Reymer and G. de Vries, *J. Chromatogr.*, 129 (1976) 193.
3 J. J. de Kok, A. de Kok, U. A. Th. Brinkman and R. M. Kok, *J. Chromatogr.*, 142 (1977) 367.
4 U. A. Th. Brinkman and G. de Vries, *J. Chromatogr.*, 169 (1979) 167.
5 U. A. Th. Brinkman, J. W. F. L. Seetz and H. G. M. Reymer, *J. Chromatogr.*, 116 (1976) 353.
6 L. R. Snyder, *J. Chromatogr.*, 6 (1961) 22.
7 U. A. Th. Brinkman, P. M. Onel and G. de Vries, *J. Chromatogr.*, 171 (1979) 424.
8 V. I. Minkin, O. A. Osipov and Yu. A. Zhdanov, *Physical Methods in Organic Chemistry, Vol. I, Dipole Moments in Organic Chemistry*, Plenum Press, New York, London, 1970.
9 L. R. Snyder, *Principles of Adsorption Chromatography*, Marcel Dekker, New York, 1968.
10 L. R. Snyder and H. Poppe, *J. Chromatogr.*, 184 (1980) 363.
11 M. Popl, V. Dolanský and J. Mostecký, *J. Chromatogr.*, 91 (1974) 649.
12 M. Charton, *Prog. Phys. Org. Chem.*, 8 (1971) 235.
13 G. J. Bijloo and R. F. Rekker, *QSAR*, 2 (1983) 66.
14 A. N. Ageev, A. V. Kiselev and Ya. I. Yashin, *Chromatographia*, 13 (1980) 669.
15 J. Kříž, L. Vodička, J. Punčochářová and M. Kuraš, *J. Chromatogr.*, 219 (1981) 53.
16 J. Punčochářová, L. Vodička and J. Kříž, *J. Chromatogr.*, 267 (1983) 222.

Journal of Chromatography, 370 (1986) 377–402
Elsevier Science Publishers B.V., Amsterdam — Printed in The Netherlands

CHROM. 19 011

HYDROPHOBIC-DISPERSIVE PARTITION COEFFICIENT IN ALKYL-BONDED REVERSED-PHASE SYSTEMS WITH WATER–METHANOL MOBILE PHASES

R. N. NIKOLOV*
Higher Institute of Chemical Technology, Central Research Laboratory, BU-1156 Sofia (Bulgaria)
and
M. M. DARZHALIEVA
Higher Institute of Chemical Technology, Department of Organic Chemistry, BU-1156 Sofia (Bulgaria)
(First received November 11th, 1985; revised manuscript received August 13th, 1986)

SUMMARY

Based on a recently proposed model of monomeric alkyl-bonded silica, the hydrophobic-dispersive partition coefficient is considered as a complex function of the polarity of the solute and of its molecular geometry, of the eluent composition and of the amount of the alkyl ligates bonded. An equation for the coefficient is derived by following the thermodynamic approach and using the solubility parameter concept; it involves energy terms reflecting the solute interactions with the reversed-phase system. A variety of experimental data is used for evaluation of the enthalpy effects governing the retention of different solutes in RP-18–water–methanol systems. The results are correlated with changes in mobile phase composition and the amount of alkyl ligates in the packings. Conclusions are drawn concerning the rôle of hydrophobic bonding and its significance to the retention.

INTRODUCTION

Recently, a model for monomeric alkyl-bonded silica was proposed[1], accounting for the availability of unreacted surface silanols together with the anchored alkyl ligates. In binary aqueous–organic mobile phases the silanols appear to be hydrated, while the hydrocarbonaceous moieties are partially or fully solvated by molecules of the organic modifier. Generalizing the numerous studies discussed in refs. 1 and 2, it was suggested that the solute retention in an alkyl-bonded reversed-phase (RP) system is governed (in absence of solute dissociation) by mixed silanophilic (SPH) and hydrophobic-dispersive (HD) mechanisms. An appropriate retention equation was derived[2], written in the form

$$E = N_{AH}K_{SP} + W_{AL}K_{HD} \quad (1)$$

where E is the so-called integral retention effect, representing the net retention volume

0021-9673/86/$03.50

per gram of packing[3], K_{SP} and K_{HD} are the partial partition coefficients related to the SPH and HD mechanisms, respectively, N_{AH} is the number of moles of the accessible surface silanols and W_{AL} is the mass of the alkyl ligates, both N_{AH} and W_{AL} being expressed per gram of packing.

As already mentioned[2], the hydrophobic-dispersive partition coefficient, K_{HD}, is a complex function of a variety of factors such as the polarity and molecular geometry of the solute, the eluent composition and the amount of the bonded alkyl moieties. In the commonly used RP-18 systems, W_{AL} is large and varies within the range 0.1–0.25 g g^{-1}, corresponding to a carbon content of 9–20%. Because of the strong shielding effect of the alkyl chains on the silanols, W_{AL} is usually enough to prevent a contribution from the SPH mechanism. Then, the first term on the right-hand side of eqn. 1 can be cancelled and the behaviour of the experimentally observed capacity ratio, k, wil parallel that of K_{HD}.

A number of studies have dealt with the dependence of k (or ln k) on the eluent composition[4–10]. Linear[4,9] and quadratic[8,10] equations have been proposed to represent this dependence in the case of binary aqueous–organic eluents. Attention has been paid also to the stationary phase effects in RP systems, including the interactions of the solute with silanols, alkyl ligates and the solvating molecules[11,12]. However, the absence of comprehensive publications dealing with the rigorous interpretation of the dependence of k on the amount of ligates is quite surprising, especially when this dependence has been demonstrated experimentally[13–15].

In the present paper an attempt is made to derive an expression for K_{HD}, which encompasses all factors governing its complex character. Following a thermodynamic approach, an equation is obtained that combines the energy terms for the various interactions in the RP system with an appropriate function of W_{AL}. The possibility of an approximate evaluation of the HD interactions is considered.

THEORETICAL

Characteristic dependences relevant to the stationary phase

It is commonly accepted that the effect of a modifier on a stationary phase is mainly due to solvation of the alkyl ligates by oriented modifier molecules extracted from the aqueous–organic eluent. Recent studies by McCormick and Karger[16] and Yonker *et al.*[17,18] showed that the stationary phase is also mechanically associated with molecules of the eluent. However, it is arguable whether all the stagnant mobile phase components can be considered as stationary phase ingredients in an alkyl-bonded silica packing.

Following the above mentioned model[1,2], a stationary phase will be considered as a system consisting of modifier-solvated alkyl chains bonded to the silica surface, whose unreacted silanols are hydrated. Each alkyl ligate is surrounded by a limited space which is filled by solvating organic molecules, as well as by free (non-solvating) molecules of the eluent, providing the hydrating water molecules do not enter this "solvation space". Obviously, the volume and molecular capacity of this space are dependent on the length of the alkyl chain and its configuration, on the amount of ligates in the packing and on the mobile phase composition.

With pure organic modifier as the eluent, the solvation space has its maximum capacity. For example, in a RP-18–methanol system it is supposed that the methyl

groups of the solvating methanol molecules are oriented towards alkyl chains and from an approximate monolayer around them. The capacity of this layer can be expressed in terms of the number of solvating molecules that is equivalent to the ratio n_O/n_A, where n_O and n_A are the numbers of moles of the solvating molecules and the ligates, respectively, per gram of packing. Taking into account the molecular geometries of the C_{18} alkyl chain and methanol[19], it can be shown that the maximum solvation space capacity in pure methanol, *i.e.*, n_O/n_A, does not exceed 36 molecules. There is evidence that in pure acetonitrile or tetrahydrofuran the solvation space could be formed by more than one monolayer of solvating molecules[18]. Hence, this should be reflected in the different approaches to evaluating the maximum capacity of the solvation space.

As shown later, the present study involves characteristic dependences relevant to the stationary phase. Unfortunately, it was not possible to derive them rigorously, following any theoretical approach. They were determined by using the experimental data of Yonker *et al.*[17] concerning the stagnant amount of water–methanol mobile phase in a RP-18 packing. To obtain the important relationship between n_O/n_A and the eluent composition at a given W_{AL}, the initial volume of extracted methanol (data from ref. 17) was reduced at each mobile phase composition by the volume of the available non-solvating molecules. The latter was calculated by multiplying the volume of water present in the stagnant mobile phase with a factor equal to the methanol-to-water volume ratio of the corresponding eluent. Having the volume of the solvating molecules per gram of packing and the carbon content of the stationary phase (19.8% according to ref. 17), simple calculations allowed the data to be represented in n_O/n_A values, which were correlated with the water weight fraction, ψ, of the eluent. Assuming this dependence holds for a relatively large W_{AL} range, the following equation was proposed (see Appendix I)

$$n_O/n_A = \Psi A \cdot \exp(BW_{AL}^2 + CW_{AL}) \tag{2}$$

wherein

$$\Psi = (1 - \psi)/(1 + \psi) \tag{3}$$

The constants in eqn. 2; $A = 29.97$, $B = 21.35$ and $C = -10.02$, were estimated by using data for RP-18 packings of different W_{AL} prepared by Hennion *et al.*[15]. All calculations were performed by the method of rigorous least squares adjustment applicable to non-linear problems[20,21]. The good fitness of eqn. 2 to the recalculated data from ref. 17 is illustrated by curve 1 in Fig. 2 and will be discussed later. It is interesting that A represents the average miximum capacity of the ligate solvation space for a RP-18–methanol system. As seen, $A < 36$ and the difference, $(36 - A)$, can be referred to as the average number of the non-solvating methanol molecules present in this space.

The volume fraction of the solvating molecules, φ'_S, can be defined as

$$\varphi'_S = V^s_M/V^s \tag{4}$$

where V^s_M and V^s are the volumes of the solvating methanol molecules and the total

solvation space, respectively, both per gram of packing at constant ψ and W_{AL}. Obviously, to calculate φ'_S in the case of different ψ and W_{AL} values, it is essential to know V^s_M and V^s as functions of these quantities. While V^s_M can be expressed as

$$V^s_M = n_A \bar{V}_M \Psi A \cdot \exp(BW^2_{AL} + CW_{AL}) \quad (5)$$

where $\bar{V}_M$ is the molar volume of methanol, no explicit function is obtainable for V^s.

Assuming as a first approximation that the relationship between V^s and ψ at each W_{AL} parallels that between the total volume of stagnant mobile phase, V_{ES} (per gram of packing), and ψ. Then, an useful plot of V_{ES}/n_A *vs.* ψ can be obtained by recalculating the experimental data from ref. 17. Such a plot is presented in Fig. 2 and discussed later. Further, it can be written

$$V^s = V^s_{max}(V_{ES}/V^{max}_{ES}) \quad (6)$$

where V^s_{max} and V^{max}_{ES} are the corresponding maximum values of V^s and V_{ES} at $\psi = 0$. It is obvious that

$$V_{ES}/V^{max}_{ES} = (V_{ES}/n_A)/(V^{max}_{ES}/n_A)$$

where V_{ES}/n_A (at given ψ) and V^{max}_{ES}/n_A (at $\psi = 0$) are obtainable from the plot of V_{ES}/n_A *vs.* ψ. Moreover, according to eqn. 3, in pure methanol, $\Psi = 1$ and therefore V^s_{max} can be expressed as

$$V^s_{max} = n_A \bar{V}_M A' \cdot \exp(BW^2_{AL} + CW_{AL}) \quad (7)$$

where $A' = 36$. Then, the combination of eqns. 4–7 gives

$$\varphi'_S = \Psi (AV^{max}_{ES}/A'V_{ES}) \quad (8)$$

and hence the volume fraction of the solvating molecules can be approximated.

Thermodynamic considerations

The aqueous–organic mobile phase in a RP system typically represents a mixture of two liquids of non-limited mutual miscibility. By ascribing to the mixture the properties of a single liquid, we can consider it under chromatographic conditions as a solvent, in which the solute forms an infinitely diluted mobile phase solution. Then, the solute chemical potential in the eluent, μ_E, can be expressed as

$$\mu_E = \mu^0 + RT \cdot \ln \gamma_E X_E \quad (9)$$

where μ^0 is the bulk chemical potential of the pure solute, X_E is the solute mole fraction in the eluent, γ_E is the corresponding solute activity coefficient and R and T are the gas constant and the absolute temperature, respectively.

It is supposed that on partitioning the solute molecules enter the ligate solvation space, displacing preferentially the non-solvating free molecules of the eluent. As a result, no change in the mobile phase composition upon displacement is expected, and this has been confirmed experimentally by Scott and Kucera[22]. Once in

the solvation space, the solute molecules form a layer-like solution, whose surface-to-volume ratio appears to be large. This enables us to consider it as a superficial stationary phase solution, in which the solute chemical potential, μ_S, can be presented as

$$\mu_S = \mu_S^0 + RT \cdot \ln \gamma_S X_S \tag{10}$$

where μ_S^0 is the chemical potential of the pure solute as a layer and X_S and γ_S are the corresponding solute mole fraction and activity coefficient in the stationary phase.

Taking into account that the superficial stationary phase solution immediately comes into contact with the mobile phase solution and following the approach of Lucassen-Reynders[23,24], it can be shown that μ_S is related to μ_E by

$$\mu_E = \mu_S + \bar{A}(\sigma_E - \sigma_S) \tag{11}$$

where the term $\bar{A}(\sigma_E - \sigma_S)$ accounts for the excess surface energy change caused by the difference between the surface tensions of both the mobile phase (σ_E) and the stationary phase (σ_S) solutions. Here $\bar{A}$ represents the so-called partial molar area, *i.e.*, the interfacial surface area per mol of solute. Further, the combination of eqns. 9–11 leads to

$$RT \cdot \ln (X_S/X_E) = RT \cdot \ln(\gamma_E/\gamma_S) + (\mu^0 - \mu_S^0) - \bar{A}(\sigma_E - \sigma_S) \tag{12}$$

where $(\mu^0 - \mu_S^0)$ represents the difference between the chemical potentials of the pure solute in two different standard states, *i.e.*, the bulk and layer, respectively. In accordance with the common convention[25], the layer of the pure solute is considered to be extended to a surface area of value $\bar{A}$. Then

$$\mu^0 - \mu_S^0 = -\bar{A}\sigma \tag{13}$$

where σ is the solute surface tension and eqn. 12 can be rewritten in the form:

$$RT \cdot \ln(X_S/X_E) = RT \cdot \ln(\gamma_E/\gamma_S) - \bar{A}(\sigma_E - \sigma_S + \sigma) \tag{14}$$

Bearing in mind the nature of the HD interactions[9,25,26], the last term of eqn. 14 can be considered as an energy gain due to the hydrophobic bonding. Therefore, it will be designated further by ΔH_H and interpreted as a partial molar excess surface enthalpy effect[25], *i.e.*:

$$\Delta H_H = \bar{A}(\sigma_E - \sigma_S + \sigma) \tag{15}$$

After introducing ΔH_H into eqn. 14, the latter can be rearranged in the form:

$$\ln(X_S/X_E) = \ln(\gamma_E/\gamma_S) - \Delta H_H/RT \tag{16}$$

As follows from eqn. 1, K_{HD} is defined by:

$$K_{HD} = \frac{\text{number of moles of solute interacting with the stationary phase per gram of alkyl ligates}}{\text{number of moles of solute dissolved in unit volume of mobile phase}}$$

On the other hand

$$X_S/X_E = n_S^s n_E/(n_A + n_O)n_E^s \tag{17}$$

where n_S^s and n_E^s are the numbers of moles of solute present in the stationary and mobile phases, respectively, $(n_A + n_O)$ represents the number of moles of stationary phase (including those of the ligates, n_A, and of the solvating molecules, n_O) and n_E is the number of moles of eluent. By rearranging eqn. 17 and multiplying both its sides by $\bar{V}_E/M_A$, where $\bar{V}_E$ is the molar volume of the eluent and M_A is the molecular mass of the ligate, it can be shown that

$$\begin{aligned}(X_S V_E/X_E M_A)\,(1 + n_O/n_A) &= n_S^s(n_E V_E)/(n_A M_A)n_E^s \\ &= n_S^s V_E/W_A n_E^s \cong K_{HD}\end{aligned} \tag{18}$$

where V_E and W_A are the total volume of the eluent and the total mass of the ligates, respectively. Taking into account the previous discussion about the dependence of n_O/n_A on ψ and W_{AL}, eqn. 18 can be rewritten in the form

$$K_{HD} = (X_S\bar{V}_E/X_E M_A)\,[1 + f(\psi, W_{AL})] \tag{19}$$

where, in case of a water–methanol mobile phase, $f(\psi, W_{AL})$ is defined by eqns. 2 and 3. Further, a combination of eqns. 16 and 19 gives:

$$K_{HD} = (\bar{V}_E/M_A)\,[1 + f(\psi, W_{AL})]\,(\gamma_E/\gamma_S)\exp(-\Delta H_H/RT) \tag{20}$$

Eqn. 20 represents K_{HD} as a function of both ψ and W_{AL} in an incomplete form. As shown by Horváth *et al.*[27], the molar volume, $\bar{V}_E$, of a binary aqueous–organic eluent can be evaluated from the expression

$$\bar{V}_E = 1/[\psi/M_w + (1 - \psi)/M_o]\,\rho_E \tag{21}$$

where ρ_E is the eluent density and M_w and M_o are the corresponding molecular masses of water and organic modifier in the mobile phase. Thus, $\bar{V}_E$ depends on ψ. On the other hand, γ_E and γ_S are also functions of ψ, while ΔH_H appears to depend on both ψ and W_{AL}. Hence, to be practically employed, in eqn. 20 these quantities need to be either known or defined explicitly.

Unfortunately, it is difficult to find data for the above quantities as regards different solutes in actual RP systems. There are also not many approaches to define

them as explicit functions. An useful and simple approach is the regular solution theory developed by Hildebrand and Scott[28] on the basis of the so-called solubility parameter concept. The latter has been applied by some authors[10,29,30] to retention problems in RP systems, but contradictory conclusions have been drawn concerning its adaptability.

It must be mentioned, however, that in all cases of treating the retention by the solubility parameter concept, no attention has been paid to the following evidence: (i) the solute molecules form with the stationary phase a superficial rather than a bulk solution, in which the surface energy change plays an important rôle, and (ii) the solute concentration in the stationary phase solution is sufficiently high, that within the zone spreading the solution cannot be considered as infinitely diluted.

According to the regular solution theory[28,31], the solute activity coefficient in an infinitely diluted mobile phase solution is determined by

$$\gamma_E = \exp [\bar{V}(\delta - \delta_E)^2 \varphi_E^2/RT]$$

where $\bar{V}$ is the solute molar volume, δ and δ_E are the solubility parameters of the solute and the eluent, respectively, and φ_E is the volume fraction of the eluent in the mobile phase solution. In the case of infinite dilution, $\varphi_E \approx 1$, hence:

$$\gamma_E = \exp [\bar{V}(\delta - \delta_E)^2/RT] \tag{22}$$

For a binary eluent mixture

$$\delta_E = \varphi_o \delta_o + (1 - \varphi_o)\delta_w \tag{23}$$

where δ_o and δ_w are the solubility parameters of the organic modifier and water, respectively[31,32]; φ_o is the volume fraction of the organic modifier calculable from

$$\varphi_o = (1 - \psi)/[\psi/\rho_w + (1 - \psi)/\rho_o]\, \rho_o \tag{24}$$

where ρ_w and ρ_o are the densities of water and the organic modifier respectively.

Let us assume now that the solubility parameter concept is applicable to the superficial stationary phase solution[31]. It then follows that

$$\gamma_S = \exp [\bar{V}(\delta - \delta_S)^2 \varphi_S^2/RT] \tag{25}$$

where φ_S is the volume fraction of solvating molecules in the superficial solution, referred to the entire solvation space and δ_S represents the stationary phase solubility parameter defined as:

$$\delta_S = \varphi_S' \delta_o + (1 - \varphi_S')\delta_E \tag{26}$$

Note that φ_S and φ_S' must be distinguished. As stated above, φ_S' is the volume fraction of solvating molecules in the solvation space before the solute molecules enter it. In the case of a water–methanol mobile phase, φ_S' is calculable from eqn. 8.

Another problem is how to evaluate φ_S. This quantity depends not only on

both ψ and W_{AL}, but also on the molecular dimensions of the solute. Taking account of the steric hindrance, it can be shown (see Appendix II) that φ_S is related to φ'_S by

$$\varphi_S = \varphi'_S (1 - p) \tag{27}$$

where p is the probability of the solute molecule penetrating among the alkyl ligates. The simplest way of evaluating p is from the relationship

$$p = (\bar{d}_l - \bar{d}_m)/\bar{d}_l \tag{28}$$

where $\bar{d}_l$ is the average chain-to-chain distance determined as the square root of the mean accessible silica surface area around a ligate[2]. The parameter $\bar{d}_m$ represents an averaged linear dimension of the solute molecule. It is obtained from those molecular dimensions which are smaller than $\bar{d}_l$ and, hence, enable either the full or partial penetration of the solute molecule. Using available data[19], $\bar{d}_m$ can easily be evaluated. Thus, the combination of eqns. 27 and 28 leads to:

$$\varphi_S = \varphi'_S \bar{d}_m/\bar{d}_l \tag{29}$$

Thus, by combining eqns. 25–29, it is possible to evaluate γ_S. It must be mentioned, however, that eqn. 25 enables the determination of only a "fraction" of the activity coefficient in the superficial stationary phase solution. This fraction corresponds to that part of the solution consisting of both the solute and the solvating molecules. Hence, it is assumed that the non-solvating eluent molecules, present in the solution, do not play a significant rôle in the formation of the solution, although their influence upon the intermolecular interactions is taken into account by δ_S in enq. 26. Therefore, the γ_S value obtained by using eqn. 25 might be interpreted as "directly contributing" to the solute retention.

To proceed further, we introduce the right-hand sides of eqns. 22 and 25 into eqn. 20. Then the latter acquires the more common and complete form:

$$K_{HD} = \frac{\bar{V}_E}{M_A} [1 + f(\psi, W_{AL})] \exp \left\{ \frac{\bar{V}[(\delta - \delta_E)^2 - (\delta - \delta_S)^2 \varphi_S^2] - \Delta H_H}{RT} \right\} \tag{30}$$

As stated above, ΔH_H depends on both ψ and W_{AL} and it would be desirable to know this dependence. However, it is certainly difficult to define ΔH_H as an explicit function of these quantities, although eqn. 15 shows a probable way. Hence, eqn. 30 cannot serve for predicting K_{HD}. Nevertheless, insofar as it enables the evaluation of ΔH_H on the basis of experimentally obtained K_{HD} values, a rearrangement in the form

$$\Delta H_H = \bar{V}[(\delta - \delta_E)^2 - (\delta - \delta_S)^2 \varphi_S^2] - RT \cdot \ln \left\{ \frac{K_{HD} M_A}{[1 + f(\psi, W_{AL})] \bar{V}_E} \right\} \tag{31}$$

will be quite useful because, as shown below, $-\Delta H_H$ can also be conventionally interpreted as the energy of the HD interactions between the solute molecules and the alkyl ligates.

EXPERIMENTAL

Materials

LiChrosorb Si 100 of mean particle size 7 μm and octadecyltrichlorosilane (both from E. Merck, Darmstadt, F.R.G.) were used for preparing a RP-18 packing. Eluent mixtures were made up from LiChrosolv grade methanol (E. Merck) and twice distilled water. Additional solvents employed were tetrachloromethane and *n*-heptane (E. Merck), both of LiChrosolv grade.

Twelve solutes of well specified solubility parameters[31,33], benzene, toluene, ethylbenzene, *o*-xylene, *m*-xylene, 1-propanol, 1-butanol, 2-propanol, 2-butanol, 2-butanone, 3-pentanone and *m*-cresol, were selected for the chromatographic experiments. All were obtained from Poly Science (Niles, IL, U.S.A.) and were of minimum 99.5% purity. Deuterated water (E. Merck) was used as a non-retained species for determining the breakthrough time.

Apparatus

Experiments were performed with equipment assembled from a Series 2 liquid chromatograph, a Model LC-25 refractive index (RI) detector, a Model 2 calculating integrator (all from Perkin-Elmer, Norwalk, CT, U.S.A.) and a Servogor Model RE 512 recorder (Goerz Electro, Austria). A polished bore stainless-steel column blank of 250 mm × 4.6 mm I.D. obtained from Perkin-Elmer was used for preparing the column. Both the detector and the column were thermostatted at 25°C by circulating water.

Procedures

The RP-18 packing was prepared by using the procedure of Evans *et al.*[34], suitably modified in the laboratory to allow more complete silica derivatization at room temperature. A bonded phase containing 15.04% carbon was obtained, as compared to that obtained with the conventional method (4–6%). The column was packed via the balanced-density slurry method performed in a home-made device. To determine the packing mass, a combination of weight measurements and a chromatographic determination of the column dead volume in pure methanol was employed.

Eluent mixtures were prepared gravimetrically. Prior to mixing, both methanol and water were thoroughly degassed under vacuum. Portions of each liquid were weighed with an accuracy of ±0.01 g and mixed. During the experiments the eluents were thermostatted at 25°C and continuously stirred magnetically for additional degassing. At each composition the eluent density was measured at 25°C via the conventional picnometric method.

Before the flow-rate measurements, the column was equilibrated with approximately 200 ml of the corresponding eluent mixture. To avoid column contamination, the packing was washed in all cases prior to changing the mobile phase composition. This was performed by pumping solvents through the column in the order: methanol, tetrachloromethane, *n*-heptane, tetrachloromethane, methanol. Eluent flow-rates were measured by use of a precise burette thermostatted at 25°C. For determining the extra-column volume, five replicate injections of ^2H_2O were made into pure methanol with the column removed.

Samples were prepared by dissolving the selected solutes in methanol at typical concentrations of 1–3 μl ml^{-1}. Three to five successive injections of 3–5 μl from each sample were made to estimate the average solute retention time. In the case of asymmetrical peaks, the finite concentration technique developed by Conder[35] was used for determining the retention.

The solute integral retention effects, E (eqn. 1), were calculated and reduced by the corresponding silanophilic contributions, $E_{SP} = N_{AH}K_{SP}$, according to the procedure described in ref. 2. Only net hydrophobic-dispersive retention effects, $E_{HD} = W_{AL}K_{HD}$, were taken into account when evaluating the solute K_{HD} values.

RESULTS AND DISCUSSION

Stationary phase model and characteristic dependences

Fig. 1 represents an attempt to visualize the model of an alkyl-bonded RP system as discussed above. The mobile phase is a water–methanol mixture. Possible interactions of two different molecules, *n*-hexane and phenol, with the stationary phase are also illustrated.

Following eqn. 2, curve 1 in Fig. 2 demonstrates the dependence of n_O/n_A on ψ at constant W_{AL}. It is in good agreement with the recalculated experimental data[17]. The ratio V_{ES}/n_A is represented as a function of ψ by curve 2 in Fig. 2, and this dependence is employed to evaluate the volume fraction, φ'_S. For both curves 1 and 2, the points at $\psi = 0.241$ corresponding to water–methanol (20:80%, v/v) as mobile

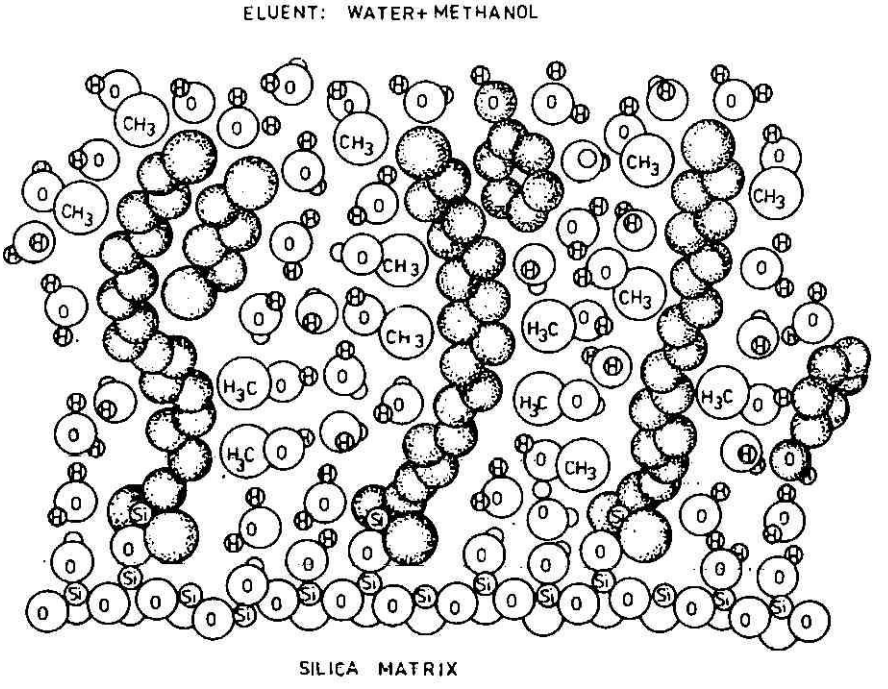

Fig. 1. Model of a C_{18} alkyl-bonded RP system. Alkyl ligates and solute molecules are depicted as shaded circles. Eluent: water–methanol mixture. Solutes: *n*-hexane and phenol.

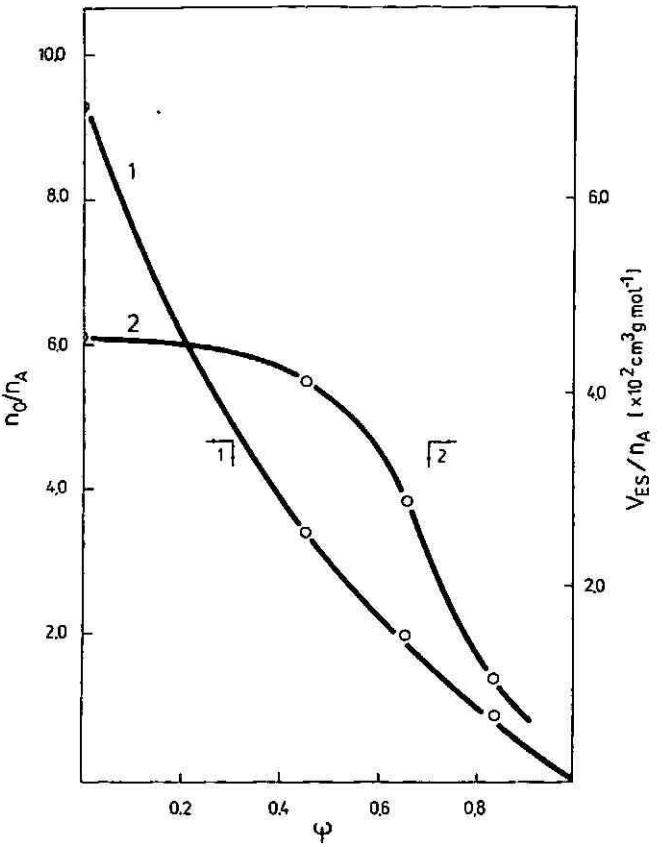

Fig. 2. Dependences of n_O/n_A (1) and V_{ES}/n_A (2) on ψ at W_{AL} = 0.233 g g^{-1}. The points were obtained by recalculating data from ref. 17 for a RP-18–water–methanol system.

phase[17] are omitted, their relatively large deviations probably being due to incorrect determination of V_{ES}. Both n_O/n_A and V_{ES}/n_A decrease at different rates with increasing ψ. However, this is readily explained in terms of the expected ligate shrinkage caused by the water enrichment of the mobile phase.

The dependence of n_O/n_A on W_{AL} (eqn. 2) is demonstrated in Fig. 3 by a family of curves for different ψ values. Each curve is drawn through a set of points calculated for the corresponding experimental values of W_{AL}[2,15,17]. It follows from eqns. 2 and 3, that at ψ = 1, n_O/n_A = 0 in the full range of W_{AL}. For each ψ, the ratio n_O/n_A decreases with increasing W_{AL} and tends to a minimum at W_{AL} = 0.234 g g^{-1}, which is nearly equal to the amount of ligates on the RP-18 packing used in ref. 17. With further increase in W_{AL} a slight increase in n_O/n_A is observed in accordance with eqn. 2. To explain this, it should be noted that a W_{AL} value of 0.268 g g^{-1} represents almost the maximum amount of ligates that can be bonded to the silica (carbon content 23%). The mean chain-to-chain distance in this case is 0.24 nm, which is approximately half the average diameter of methanol molecules. Although methanol molecule penetration among the ligates is strongly inhibited, solvation can occur around

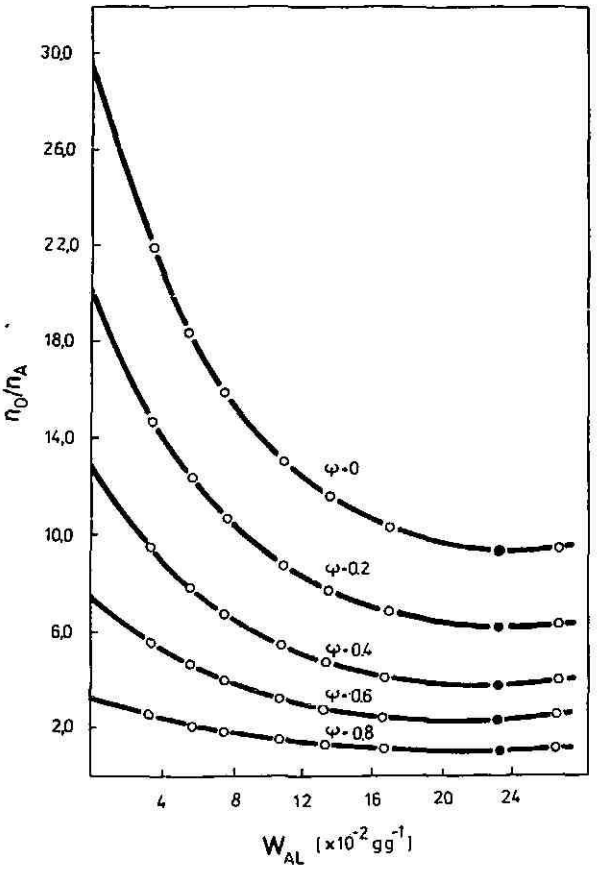

Fig. 3. Dependence of n_O/n_A on W_{AL} at different ψ values according to eqn. 2. All points correspond to RP-18 packings of various W_{AL}. ○, Data from refs. 2 and 15; ●, data from ref. 17. Eluents: water–methanol mixtures.

the end methyl groups of the chains, the latter being able to form a relatively compact layer-like structure. Thus, the existence of a complete solvating layer over this structure appears to be the reason for the slight increase in the n_O/n_A ratio.

Values of all quantities depending on ψ and characterizing both the mobile and the stationary phases of the RP-18 system studied are presented in Table I. As expected, the mobile phase molar volume, $\bar{V}_E$, decreases whereas the solubility parameter, δ_E, increases with increasing ψ. A similar behaviour of the stationary phase solubility parameter, δ_S is observed; however, the rate of increase is lower than that of δ_E in the ψ range of 0.1–0.9. In comparison with the moderately decreasing volume fraction, φ'_S, the ratio n_O/n_A decreases quickly with increasing ψ. This is compatible with the relatively large ligate content of the packing, W_{AL} = 0.1762 g g^{-1}, the average chain-to-chain distance, $\bar{d}_1$, varying within the range 0.2–0.5 nm.

TABLE I

CHARACTERISTICS OF A RP-18–WATER–METHANOL SYSTEM AS FUNCTIONS OF THE MOBILE PHASE COMPOSITION

Parent silica: Si 100; surface area 363 $m^2 g^{-1}$. RP-18 packing: carbon content, 15.04%; mass in the column, 1.9980 g; $W_{AL} = 0.1762$ g g^{-1}.

ψ	*Mobile phase characteristics*			*Stationary phase characteristics*			
	ρ_E* (*g cm* $^{-3}$)	V_E** (*cm*^{3} *mol*$^{-1}$)	δ_E*** (*cal cm*$^{-3}$)$^{\frac{1}{2}}$	n_0/n_A§	$\varphi_S^{\S\S}$	δ_S§§§ (*cal cm*$^{-3}$)$^{\frac{1}{2}}$	$\bar{d}_1$ (*nm*)
0.00	0.7865	40.74	14.50	9.949	0.833	14.50	0.494
0.10	0.8155	36.45	15.23	8.140	0.692	14.72	0.479
0.20	0.8415	32.95	15.99	6.633	0.570	15.14	0.461
0.30	0.8673	29.95	16.78	5.357	0.471	15.71	0.441
0.40	0.8907	27.43	17.61	4.264	0.395	16.38	0.418
0.50	0.9123	25.28	18.48	3.316	0.336	17.14	0.391
0.60	0.9310	23.46	19.39	2.487	0.297	17.94	0.359
0.70	0.9497	21.84	20.35	1.756	0.283	18.70	0.319
0.80	0.9660	20.44	21.36	1.105	0.281	19.43	0.267
0.90	0.9824	19.18	22.42	0.524	0.254	20.41	0.195
1.00	0.9971	18.07	23.53	0.000	0.242†	23.53	–

* Determined picnometrically at 25°C.
** Calculated from eqn. 21.
*** Calculated from eqn. 23.
§ Calculated from eqn. 2.
§§ Calculated from eqn. 8.
§§§ Calculated from eqn. 26.
† Extrapolated value corresponding to the volume fraction of water molecules present in the solvation space.

Energy terms governing retention

Let us rewrite eqn. 30 in the form

$$K_{HD} = \Phi \cdot \exp[(\Delta H_E - \Delta H_S - \Delta H_H)/RT] \quad (32)$$

where:

$$\Phi = (\bar{V}_E/M_A)[1 + f(\psi, W_{AL})]$$

According to the solubility parameter concept[32], $\Delta H_E = \bar{V}(\delta - \delta_E)^2$ and $\Delta H_S = \bar{V}(\delta - \delta_S)^2\varphi_S^2$ are the partial molar excess enthalpies of mixing in the mobile and the stationary phases, respectively. From eqn. 32, the solute retention is governed by three energy terms: ΔH_E, ΔH_S and ΔH_H. Their calculated values depending on ψ are presented in Table II together with the experimental values of K_{HD} for the selected solutes. The solutes are additionally characterized by the values of their molar volume, $\bar{V}$, solubility parameter, δ, and average molecular linear parameter, $\bar{d}_m$. Because of unfavourable retention, K_{HD} values are not listed for the aromatic hydrocarbons with $\psi > 0.5$; for the oxygen-containing solutes with $\psi = 0$, for 3-pentanone with $\psi = 1$ and for *m*-cresol with $\psi > 0.8$.

TABLE II

HYDROPHOBIC-DISPERSIVE PARTITION COEFFICIENT AND ENERGY TERMS FOR SELECTED SOLUTES AS FUNCTIONS OF THE MOBILE PHASE COMPOSITION

Dimensions of quantities: $\bar{V}$ (cm^3 mol^{-1}); δ (cal cm^{-3})$^{\frac{1}{2}}$; $\bar{d}_m$ (nm); K_{HD} (cm^3 g^{-1}); ΔH_E, ΔH_S and ΔH_H (kcal mol^{-1}).

Solute and its characteristics		*K_{HD} and energy terms*	*Water weight fraction of the mobile phase, ψ*										
			0.00	*0.10*	*0.20*	*0.30*	*0.40*	*0.50*	*0.60*	*0.70*	*0.80*	*0.90*	*1.00*
Benzene		K_{HD}	1.073	2.299	4.314	7.567	13.52	23.99					
$\bar{V}$	89.41	ΔH_E	2.55	3.29	4.17	5.19	6.38	7.77					
δ	9.16	ΔH_S	0.837	0.667	0.566	0.507	0.482	0.487					
$\bar{d}_m$*	0.340	ΔH_H	2.01	2.30	2.73	3.32	4.03	4.90					
Toluene		K_{HD}	1.533	3.264	6.545	12.16	23.58	46.60					
$\bar{V}$	106.84	ΔH_E	3.31	4.24	5.33	6.58	8.05	9.74					
δ	8.93	ΔH_S	1.29	1.02	0.863	0.768	0.726	0.729					
$\bar{d}_m$*	0.370	ΔH_H	2.11	2.68	3.34	4.17	5.12	6.24					
Ethylbenzene		K_{HD}	1.828	4.087	8.680	17.46	36.95	81.10					
$\bar{V}$	123.08	ΔH_E	3.94	5.03	6.29	7.76	9.47	11.4					
δ	8.84	ΔH_S	1.74	1.38	1.16	1.03	0.972	0.959					
$\bar{d}_m$*	0.394	ΔH_H	2.18	2.97	3.85	4.87	6.02	7.37					
o-Xylene		K_{HD}	2.083	4.479	9.327	18.16	37.70	80.85					
$\bar{V}$	121.21	ΔH_E	3.59	4.61	5.82	7.22	8.86	10.8					
δ	9.06	ΔH_S	1.39	1.11	0.939	0.838	0.796	0.801					
$\bar{d}_m$*	0.370	ΔH_H	2.09	2.78	3.56	4.50	5.58	6.85					
m-Xylene		K_{HD}	2.157	4.626	9.775	19.49	41.24	90.31					
$\bar{V}$	123.48	ΔH_E	3.90	4.98	6.24	7.71	9.41	11.4					
δ	8.88	ΔH_S	1.52	1.20	1.01	0.901	0.851	0.853					
$\bar{d}_m$*	0.370	ΔH_H	2.26	3.03	3.87	4.88	6.02	7.36					

1-Propanol		K_{HD}	0.454	0.985	1.601	2.180	3.065	4.201	6.012	8.468	13.27	32.02
$\mathcal{V}$	75.19	ΔH_E	0.699	1.09	1.59	2.22	2.98	3.91	5.02	6.34	7.88	9.69
δ	12.18	ΔH_S	0.203	0.202	0.208	0.207	0.209	0.220	0.255	0.311	0.329	0.567
$\bar{d}_m$*	0.448	ΔH_H	1.13	0.893	0.935	1.21	1.61	2.17	2.85	3.71	4.74	5.50
1-Butanol		K_{HD}	0.715	1.542	2.537	4.008	6.119	10.01	16.30	26.23	45.41	112.8
$\mathcal{V}$	91.99	ΔH_E	1.21	1.77	2.47	3.32	4.35	5.58	7.04	8.76	10.8	13.1
δ	11.60	ΔH_S	0.375	0.354	0.345	0.329	0.319	0.326	0.370	0.444	0.461	0.767
$\bar{d}_m$*	0.448	ΔH_H	1.20	1.16	1.40	1.84	2.46	3.22	4.17	5.33	6.77	7.96
2-Propanol		K_{HD}	0.449	0.883	1.470	2.004	2.526	3.525	4.939	6.773	10.72	27.01
$\mathcal{V}$	76.97	ΔH_E	1.11	1.59	2.19	2.93	3.81	4.86	6.11	7.57	9.30	11.3
δ	11.44	ΔH_S	0.397	0.343	0.312	0.294	0.283	0.287	0.324	0.387	0.400	0.659
$\bar{d}_m$*	0.490	ΔH_H	1.35	1.32	1.49	1.89	2.48	3.16	3.99	5.00	6.20	7.08
2-Butanol		K_{HD}	0.670	1.401	2.327	3.525	5.262	8.140	12.73	19.85	34.38	88.09
$\mathcal{V}$	92.39	ΔH_E	1.59	2.23	3.00	3.94	5.06	6.38	7.94	9.76	11.9	14.3
δ	11.08	ΔH_S	0.586	0.495	0.440	0.406	0.384	0.383	0.428	0.508	0.519	0.839
$\bar{d}_m$*	0.490	ΔH_H	1.40	1.53	1.89	2.45	3.19	4.09	5.15	6.44	7.99	9.27
2-Butanone		K_{HD}	0.630	1.182	1.868	2.628	3.667	5.495	8.674	14.27	28.29	105.6
$\mathcal{V}$	90.1	ΔH_E	3.17	4.03	5.04	6.22	7.59	9.17	11.0	13.1	15.5	18.2
δ	9.3	ΔH_S	1.25	0.999	0.823	0.706	0.626	0.593	0.636	0.728	0.717	1.07
$\bar{d}_m$*	0.475	ΔH_H	2.36	2.93	3.68	4.61	5.70	6.90	8.23	9.75	11.5	12.9
3-Pentanone		K_{HD}	0.931	1.775	2.912	4.570	6.988	11.68	20.22	37.29	80.49	
$\mathcal{V}$	106.41	ΔH_E	4.05	5.11	6.34	7.78	9.44	11.4	13.6	16.1	19.0	
δ	9.06	ΔH_S	1.61	1.28	1.05	0.891	0.786	0.740	0.790	0.902	0.884	
$\bar{d}_m$*	0.475	ΔH_H	2.65	3.49	4.49	5.65	7.01	8.49	10.1	12.0	14.2	
m-Cresol		K_{HD}	0.789	1.948	3.502	6.278	11.47	22.93	47.03	94.62		
$\mathcal{V}$	104.7	ΔH_E	2.65	3.51	4.53	5.75	7.18	8.84	10.8	13.0		
δ	10.2	ΔH_S	0.669	0.586	0.544	0.536	0.559	0.553	0.604	0.703		
$\bar{d}_m$*	0.387	ΔH_H	2.28	2.52	3.08	3.79	4.72	5.76	7.05	8.59		

* Evaluated at $\psi = 0$ in correspondence with the chain-to-chain distance, $\bar{d}_1$, of the RP-18 packing in Table I.

In terms of the solubility parameter concept, the greater the enthalpy of mixing in an infinitely diluted solution, the smaller is the solute solubility in the corresponding solvent. As this holds for the mobile phase solution in a RP system, the increase in ΔH_E with increasing ψ agrees well with the decreased solubility of the solutes in the water-enriched eluent mixtures. With a predominant methanol content of the mobile phase, ΔH_E for the alcohols is smaller than that for the aromatic hydrocarbons, thus reflecting the higher solubility of the former in methanol. Ketones exhibit ΔH_E values comparable with those for the hydrocarbons, while for *m*-cresol has ΔH_E values intermediate between those for alcohols and hydrocarbons.

As to the enthalpy of mixing in the superficial stationary phase solution, two important factors leading to lower values should be mentioned. First, the stationary phase solution is usually concentrated, which is a premise for higher solute solubility due to strong solute–solute interactions. Secondly, the presence of passive alkyl ligates (favouring steric hindrance) lowers the overall energy of the stationary phase solution and, hence, also the solute partial molar enthalpy of mixing, ΔH_S. This is the main factor responsible for the decrease in ΔH_S when ψ varies between 0 and 0.5. When $\psi > 0.5$, the low solute solubility in the water-enriched stationary phase layer becomes responsible for the gradual increase in ΔH_S.

As seen from Table II, for each solute the partial molar enthalpy, ΔH_H, increases with increasing ψ. This corresponds to the reinforcement of hydrophobic bonding upon water enrichment of the mobile phase. At constant eluent composition, both the polarity and the area of contact of the solute molecule with the ligates determine the extent of the hydrophobic effect. Usually, this effect is stronger for less polar molecules and for those having a large non-polar moiety. Since the solubility parameter, δ, is a measure of the solute polarity, a certain correlation between ΔH_H and δ is observed. The smaller the solubility parameter, the greater is the hydrophobic effect and *vice versa*. This correlation holds for most solutes within the full range of ψ values in our study. Deviations are observed for the solute pairs toluene–*o*-xylene, ethylbenzene–*m*-xylene and 1-butanol–2-propanol and a brief explanation of their behaviour is given below.

Toluene ($\delta = 8.93$) is insignificantly less polar than *o*-xylene ($\delta = 9.06$) and the enthalpy effects of solvophobic bonding for both solutes, *i.e.*, their ΔH_H values at $\psi = 0$, correlate well with the corresponding δ values, the difference being negligible. At $\psi \geq 0.1$ however, ΔH_H for *o*-xylene becomes greater than that for toluene. This is due probably to *o*-xylene exhibiting a greater surface area than that of toluene. As expected, with equal or slightly different solute polarities, the contact area plays an important rôle.

Analogously, because of the weaker steric hindrance, the more compact molecule of *m*-xylene ($\delta = 8.88$) exhibits a greater effective contact area in comparison with that of ethylbenzene ($\delta = 8.84$). This is especially evident, when molecules of approximately equal polarities are able to penetrate among the ligates, *i.e.*, when $\psi < 0.5$. With further increase in ψ, however, the penetration is avoided and then, in agreement with the correlation observed, ΔH_H for ethylbenzene tends to become greater than that for *m*-xylene.

An interesting subject of debate involves the variations of ΔH_H for both 1-butanol ($\delta = 11.60$) and 2-propanol ($\delta = 11.44$). With methanol-enriched eluent mixtures, ΔH_H for 2-propanol is greater than that for 1-butanol, thus obeying the

correlation with δ. When the water content of the mobile phase becomes noticeable ($\psi \geqslant 0.6$), an inversion occurs, so that the slightly more polar 1-butanol exhibits greater ΔH_H values in comparison with the less polar 2-propanol. To explain this behaviour, let us compare the $\bar{d}_m$ values of both solutes (Table II) with the chain-to-chain distances, $\bar{d}_i$, at ψ within the range of 0.1–0.5 (Table I). Even with methanol-enriched eluents, the full penetration of these molecules among the ligates is prevented. A partial penetration, however, seems possible, thus the difference between the effective contact areas of the molecules should be insignificant. Although, in comparison with 2-propanol, 1-butanol exhibits *a priori* a greater molecular area, at $\psi \leqslant 0.5$ the two solutes are subject to approximately equal steric conditions and, hence, the main factor responsible for their hydrophobic bonding appears to be the solute polarity. With water-enriched mobile phases, however, the molecules of both solutes interact under the conditions of a stationary phase layer. Then, in the absence of steric hindrance, the size of the area of effective contact becomes more substantial for the hydrophobic effect than the solute polarity.

Further, let us compare the variations of the hydrophobic-dispersive partition coefficient with those of the corresponding enthalpy effects for the solutes under the same chromatographic conditions. It is evident from Table II that there is no dominant dependence of K_{HD} on the any of the energy terms which would be capable of explaining the deviations observed. Obviously, K_{HD} is a characteristic quantity that incorporates the influence of the three ΔH terms, thus describing quantitatively the solute retention in a RP system. Comparing all ΔH values for a solute, it can be concluded that the strongest interactions arise in the mobile phase, in accord with accepted opinion[12,27]. However, it is of interest to discuss the rôle of the hydrophobic bonding and its significance to the retention.

It is well known that the hydrophobic effect is connected with the repulsive forces between a solute and the water molecules in a mobile phase. As a consequence, the solute molecules are constrained to associate with the alkyl ligates. The energy gain, ΔH_H, that accompanies this process can be considered to have "originated" from the mobile phase and to be "introduced" into the stationary phase. This enables us to interpret the hydrophobic bonding as a result of the so-called HD interactions between the solute molecules and the ligates[1,2]. Conventionally, we can ascribe a negative sign to the ΔH_H value, *i.e.*, $-\Delta H_H$, and consider it as a partial molar energy of the HD interaction. It should be borne in mind, however, that this "interaction energy" does not follow from the reduction of the internal energy of both the stationary and the mobile phases. Finally, it is apparent that the hydrophobic bonding "compensates" energetically the weak interactions associated with the stationary phase. In other words, it increases the solute concentration in the stationary phase, thus realizing the retention itself.

Dependence of retention and hydrophobic bonding on the amount of alkyl ligates

Experimental data of Hennion *et al.*[15] enabled us to study the retention behaviour as well as the hydrophobic bonding of the polyaromatic hydrocarbons and the hydroxy-aromatic compounds as a function of the amount of ligates. Solute K_{HD} values obtained with RP packings of different W_{AL} were taken from ref. 2. Two water–methanol eluent mixtures (30:70 and 60:40, v/v, respectively) have been used in the experiments. The values of all the mobile and stationary phase characteristics,

TABLE III

MOBILE AND STATIONARY PHASE CHARACTERISTICS DEPENDENT ON THE MOBILE PHASE COMPOSITION

Calculated according to the experimental conditions of Hennion *et al.*[15]

Eluent	ψ	*Mobile phase*			*Stationary phase*	
		$\bar{V}_E$ ($cm^3\ mol^{-1}$)	ρ_E ($g\ cm^{-3}$)	δ_E $(cal\ cm^{-3})^{\frac{1}{2}}$	φ'_S	δ_S $(cal\ cm^{-3})^{\frac{1}{2}}$
Water–methanol (30:70)	0.352	28.60	0.8793	17.21	0.415	16.09
Water–methanol (60:40)	0.655	22.53	0.9419	19.92	0.289	18.35

dependent only on ψ, are presented in Table III. Those stationary phase characteristics which depend on both ψ and W_{AL} are given in Table IV.

A serious problem connected with the calculation of the enthalpy effects in eqn. 32 was the absence of data for the solubility parameters. Usually, δ values are given for liquid compounds at 25°C[31,33]. Except for benzene, the solutes listed in Table V are solids under normal conditions and no data for their solubility parameters were available. To use the experimental information, we attempted to evaluate δ following the recommendations reviewed in ref. 33. The method of the so-called molar attraction constants[36] was employed in the case of polyaromatic hydrocarbons. As it is inapplicable to the hydroxy-aromatic compounds, their δ values were evaluated by using Hildebrand's empirical equation[28], mainly applied to liquids. Obviously, there is no guarantee of the reliability of the calculated values, however, they enabled us to estimate approximately the enthalpy effects and hence to shed some light on the dependence of both the retention and the hydrophobic bonding upon the amount of alkyl ligates.

All solutes listed in Table V are characterized by the values of $\bar{V}$, δ and $\bar{d}_m$. Since the hydrocarbons and the hydroxycompounds were eluted with different mobile

TABLE IV

STATIONARY PHASE CHARACTERISTICS DEPENDENT OF BOTH THE MOBILE PHASE COMPOSITION AND THE AMOUNT OF ALKYL LIGATES

Calculated according to the experimental conditions of Hennion *et al.*[15].

Amount of alkyl ligates, $W_{AL} \cdot 10^{-2}$ ($g\ g^{-1}$)	$\psi = 0.352$		$\psi = 0.655$	
	n_O/n_A	$\bar{d}_1$ (*nm*)	n_O/n_A	$\bar{d}_1$ (*nm*)
3.39	10.48	2.10	4.559	2.08
5.62	8.750	1.53	3.806	1.49
7.62	7.578	1.21	3.296	1.16
11.0	6.177	0.829	2.687	0.746
13.5	5.480	0.619	2.384	0.521
16.9	4.861	0.467	2.114	0.383
26.8	4.540	0.203	1.974	0.158

phases (ψ = 0.352 and 0.655, respectively), they are presented as two separate groups together with the corresponding data and the calculated results.

The dependence of K_{HD} on W_{AL} for the solutes studied is conveniently visualized in Figs. 4 and 5. For each compound there is an obvious tendency for K_{HD} to increase with increasing W_{AL} up to a definite value, beyond which K_{HD} decreases. As seen from Fig. 4, the maxima for hydrocarbons lie within a narrow W_{AL} range between 0.16 and 0.19 g g^{-1}. For the hydroxycompounds, however (Fig. 5), the maxima appear at different W_{AL} values. Hence, the observed phenomena seem well compatible with the solute molecular structure and dimensions, which to a large extent determine the possibility of penetration among the ligates.

As is evident from Table V, the solubility parameters of the polyaromatic hydrocarbons increase slightly with the number of rings. The rise in polarity is undoubtedly connected with the increased effect of conjugation in the molecules. Nevertheless, their δ values remain substantially lower than those of the hydroxy-aromatic compounds, whose polarity is determined by the presence of hydroxyl groups. Therefore, a difference is observed in the solubilities of both types of solutes in the mobile phase. With increasing δ, the enthalpy of mixing of the hydroxy-compounds with the eluent, ΔH_E, decreases, corresponding to a higher solubility. On the contrary, except for anthracene, increase in δ for the hydrocarbons leads to a greater ΔH_E value, in agreement with their lower solubility, as soon as the number of rings rises. Obviously, the different nature of the polarity is responsible for the observed phenomenon. In terms of the solubility parameter concept, this is due to the higher energy of cavity formation necessary for the large hydrocarbon molecules.

As expected, the enthalpy of mixing with the stationary phase, ΔH_S, is small

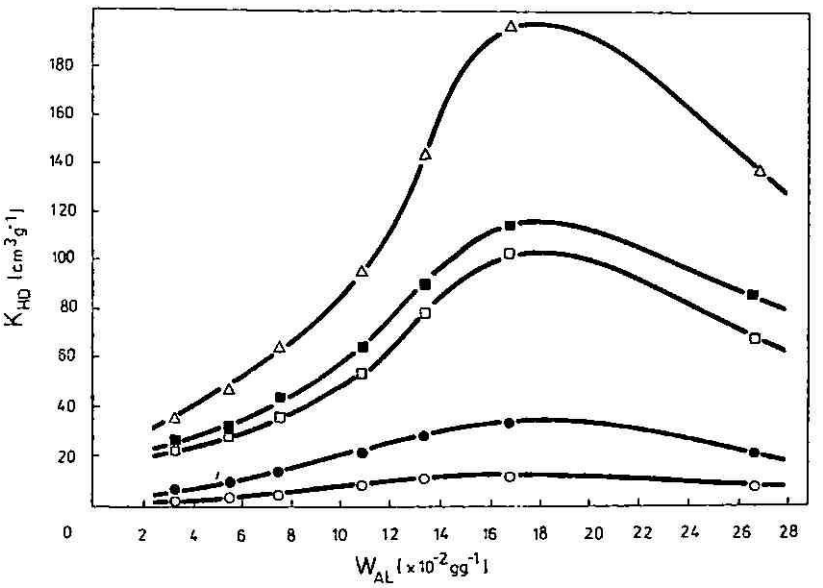

Fig. 4. Dependence of K_{HD} on W_{AL} for polyaromatic hydrocarbons under the experimental conditions of Hennion *et al.*[15]: RP-18 packings; eluent mixture, water–methanol, ψ = 0.352. ○, Benzene; ●, naphthalene; □, phenanthrene; ■, anthracene; △, pyrene.

TABLE V

ENERGY TERMS FOR POLYAROMATIC HYDROCARBONS AND HYDROXY-AROMATIC COMPOUNDS AS FUNCTIONS OF THE AMOUNT OF ALKYL LIGATES

Calculated according to the experimental conditions of Hennion *et al.*[15]. Dimensions of quantities as in Table II.

ψ	*Solute*	*Solute characteristics*			*Energy terms*		*Amount of alkyl ligates,* $W_{AL} \cdot 10^{-2}$ *(g g*$^{-1}$*)*						
		V	δ	$\bar{d}_m$*	ΔH_E**		*3.39*	*5.62*	*7.62*	*11.0*	*13.5*	*16.9*	*26.8*
0.352	Benzene***	89.41	9.16	0.538	5.79	ΔH_S	0.048	0.091	0.146	0.312	0.558	0.738	0.738
						ΔH_H	5.54	5.18	4.82	4.13	3.65	3.35	3.66
	Naphthalene	111.50	9.38	0.662	6.84	ΔH_S	0.086	0.162	0.258	0.551	0.863	0.863	0.863
						ΔH_H	5.82	5.39	5.03	4.36	3.83	3.65	3.93
	Phenanthrene	152.34	9.56	0.761	8.92	ΔH_S	0.147	0.276	0.442	0.941	1.12	1.12	1.12
						ΔH_H	7.04	6.71	6.34	5.53	5.05	4.82	5.03
	Anthracene	143.40	9.66	0.743	8.17	ΔH_S	0.128	0.240	0.384	0.819	1.02	1.02	1.02
						ΔH_H	6.25	5.92	5.53	4.77	4.25	4.11	4.25
	Pyrene	163.11	9.70	0.801	9.20	ΔH_S	0.167	0.314	0.502	1.07	1.15	1.15	1.15
						ΔH_H	7.08	6.66	6.21	5.31	4.94	4.69	4.87
0.655	Hydroquinone	83.42	13.8	0.596	3.12	ΔH_S	0.012	0.023	0.038	0.092	0.144	0.144	0.144
						ΔH_H	1.44	1.16	0.975	0.885	0.875	0.951	1.25
	Resorcinol	87.40	13.3	0.539	3.83	ΔH_S	0.013	0.024	0.040	0.097	0.186	0.186	0.186
						ΔH_H	1.80	1.58	1.41	1.22	1.16	1.23	1.53
	5-Methylresorcinol	97.88	12.8	0.569	4.96	ΔH_S	0.019	0.037	0.061	0.146	0.252	0.252	0.252
						ΔH_H	2.67	2.39	2.19	1.94	1.81	1.85	2.21
	Phenol	89.38	11.3	0.519	6.64	ΔH_S	0.023	0.045	0.074	0.180	0.368	0.371	0.371
						ΔH_H	3.72	3.47	3.21	2.84	2.50	2.48	2.84

* Evaluated at ψ values corresponding to the chain-to-chain distance, $\bar{d}_1$, of the RP-18 packing having $W_{AL} = 3.39 \cdot 10^{-2}$ g g^{-1}.

** Not dependent on the amount of alkyl ligates.

*** Employed as a reference compound when considering the influence of condensed rings.

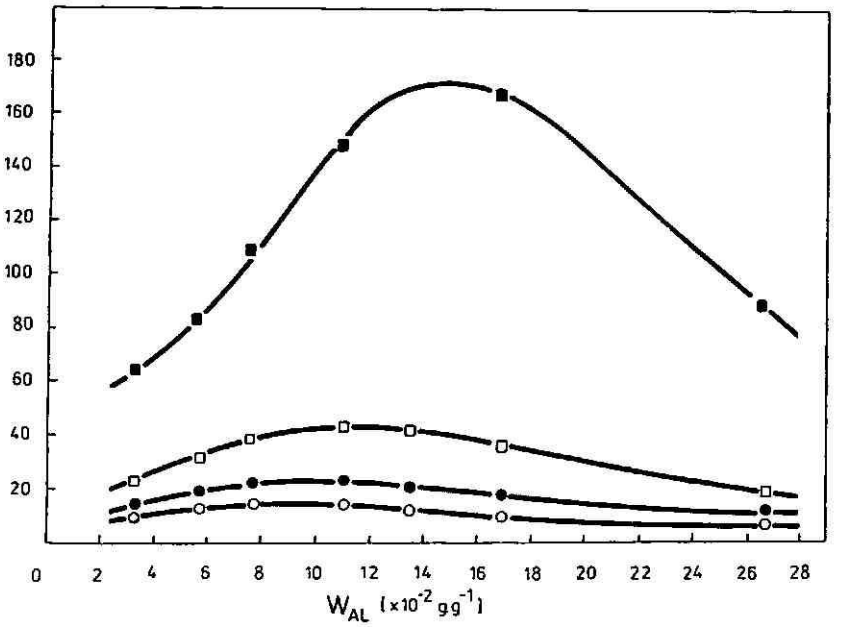

Fig. 5. Dependence of K_{HD} on W_{AL} for hydroxy-aromatic compounds under the experimental conditions of Hennion *et al.*[15]: RP-18 packings; eluent mixture, water–methanol, $\psi = 0.655$. ○, Hydroquinone; ●, resorcinol; □, 5-methylresorcinol; ■, phenol.

for all the solutes. It tends to increase slightly as W_{AL} increases to a definite value. Obviously, the restricted penetration of the solute molecules among the ligates leads to a lowering their solubility in the stationary phase. As soon as full penetration of the molecules becomes impossible, their interactions with the stationary phase layer remain invariable, corresponding to the constant ΔH_S values obtained with large amount of ligates.

Comparing the enthalpy effects of hydrophobic bonding for the polyaromatic hydrocarbons, it is seen that ΔH_H generally increases with the number of rings, in spite of the increased polarity. This is due to the enlargement of the molecular surface area capable for contact with the ligates. Since the molecules of phenanthrene and anthracene exhibit equal areas, their hydrophobic bonding is governed by the polarity. Therefore, the ΔH_H values for anthracene ($\delta = 9.66$) always remain lower than those for phenanthrene ($\delta = 9.56$).

An interesting exception is the large molecule of pyrene ($\delta = 9.70$). Contrary to initial expectations, its ΔH_H values are generally lower than those for phenanthrene. However, one should not forget that the hydrophobic effect is favoured by the contact area between the solute molecule and the ligate, rather than by the whole solute molecular surface area. It may well be that the fourth ring contributes negligibly to the extent of the contact area realized with a molecule having three rings. Moreover, the penetration of pyrene into the stationary phase appears to be sterically more hindered than that of phenanthrene. Therefore, we consider the ΔH_H values obtained as quite reasonable.

As for the hydroxy compounds, their ΔH_H values correlate well with the corresponding solubility parameters. The more polar the solute, the weaker is the effect of hydrophobic bonding. Nevertheless, in comparison with the hydrocarbons, these solutes have been eluted with a more polar mobile phase, and their ΔH_H values are smaller. Hence, this is also evidence of the importance of both the polarity and the contact area for the hydrophobic effect.

As is seen from Table V, the molar enthalpy of hydrophobic bonding decreases for all the solutes with an initial increase in the amount of ligates. This is in agreement with the decreased concentration of the free eluent molecules in the ligate solvation space and especially that of water. As soon as the solute penetration becomes impossible at a definite value of W_{AL}, the molecules start to associate with the end methyl groups of the chains. Then, further increase in W_{AL} leads to a more compact ligate layer structure, thus increasing the probability for a better contact with the solute molecules. As a result, ΔH_H also starts to increase in correspondence with the conditions favourable for hydrophobic bonding.

The behaviour of ΔH_H is illustrated in Fig. 6. For hydrocarbons the minimum ΔH_H value conforms to the maximum of the hydrophobic-dispersive partition coefficient, K_{HD}. An analogous situation is observed for the hydroxy compounds. However, comparing Figs. 5 and 6, it is seen that for the different solutes the ΔH_H minimum generally appears at a slightly higher W_{AL} value than the corresponding maximum of K_{HD}. A probable explanation of this discrepancy could be looked for in the inaccuracy of the calculated solubility parameters, especially since Hildebrand's equation tends to give increased values for δ.

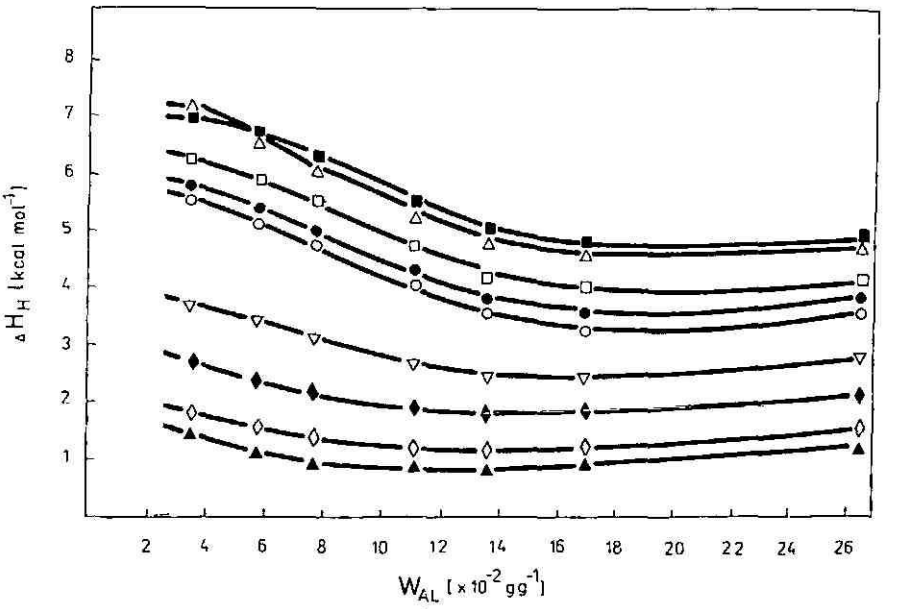

Fig. 6. Dependence of ΔH_H on W_{AL} for solutes chromatographed under the experimental conditions of Hennion *et al.*[15]. Polyaromatic hydrocarbons: ○, benzene; ●, naphthalene; □, anthracene; ■, phenanthrene; △, pyrene. Hydroxy-aromatic compounds: ▲, hydroquinone; ◇, resorcinol; ◆, 5-methylresorcinol; ▽, phenol.

In conclusion, it must be emphasized that the retention of even non-dissociated solutes in an alkyl-bonded RP system is an extraordinarily complex phenomenon governed by a variety of factors. The most important of them are:

(1) The nature of the solute expressed in terms of its molecular structure and dimensions, polarity, solubility in both the mobile and the stationary phases

(2) The mobile phase composition including the type of organic modifier and the water content

(3) The stationary phase formation determined by the structure, dimensions and amount of ligates causing the steric hindrance, as well as the composition of the extracted solvent filling the ligate solvation space.

The combined influence of all these factors determines the solute interactions with the RP system as a whole and, hence, the magnitude of the corresponding energy terms reflecting the solute behaviour in the system. If the so-called "side effects" occur, *e.g.*, equilibria connected with solute dissociation, then additional investigations are required in order to obtain insight into the nature of retention.

ACKNOWLEDGEMENTS

The authors gratefully acknowledge fruitful discussions with Assoc. Professor Dr. E. Sokolova, Department of Physical Chemistry and with Assoc. Professor Dr. Y. Dimitriev, Department of Silicate Technology, both from the Higher Institute of Chemical Technology, Sofia.

APPENDIX I

The correlation between n_O/n_A and ψ at W_{AL} = const. can be approximated by the function

$$n_O/n_A = \Psi L(W_{AL}) \tag{A1}$$

where

$$\Psi = (1 - \psi)/(1 + \psi)$$

and $L(W_{AL})$ is a parameter dependent on W_{AL}. At W_{AL} = const., $L(W_{AL})$ must also be constant, as confirmed on the basis of data in ref. 17. The relative deviations of the calculated L values from the average L value were within $\pm 1\%$.

Further, it was assumed that eqn. A1 holds for a relatively large W_{AL} range. An adequate approximation for $L(W_{AL})$ was achieved as follows.

(1) Since n_O is obviously dependent on both Ψ and n_A (where $n_A = W_{AL}/M_A$ and M_A is the molecular mass of the alkyl ligates), then, at Ψ = const., n_O will be a function only of W_{AL}. Hence:

$$n_O(W_{AL})/W_{AL} = (\Psi/M_A)L(W_{AL}) \qquad (\Psi = \text{const.}) \tag{A2}$$

Rearranging eqn. A2 in the form

$$L(W_{AL}) = (Q/W_{AL})n_O(W_{AL}) \tag{A3}$$

where $Q = M_A/\Psi$ is a constant, it becomes evident that $L(W_{AL})$ can be represented as a product of two functions: Q/W_{AL} and $n_O(W_{AL})$. The first one is an hyperbolic dependence, which tends to decrease, always remaining positive when W_{AL} increases. According to the accepted stationary phase model, $n_O(W_{AL})$ is expected to the positive and will increase with increasing W_{AL}. However, $n_O(W_{AL})$ cannot be linearly dependent on W_{AL}, because an increase in the surface ligate concentration will lead to a rapid decrease in the solvation space and, hence, to a non-proportional increase in n_O.

(2) On the other hand, at $W_{AL} = 0$, *i.e.*, $n_A = 0$, it follows that $n_O(W_{AL}) = 0$ (or $n_O = 0$), therefore $L(W_{AL})$ is undefined for $W_{AL} = 0$. However, for W_{AL} values very close to zero, the ratio n_O/n_A must be a real positive number, less but nearly equal to the maximum capacity of the solvation space at a given Ψ.

Summarizing the above considerations, the following conclusions can be made about the character of the $L(W_{AL})$ function at each Ψ = const.: (i) as a product of two positive functions, the first of which rapidly decreases while the second slowly increases with increasing W_{AL}, $L(W_{AL})$ will be a positive decreasing function, having a minimum; (ii) when W_{AL} tends to zero, $L(W_{AL})$ approaches its greatest value; (iii) with increasing W_{AL}, $L(W_{AL})$ decreases nearly in inverse proportion to W_{AL}, thus reaching its minimum at a definite W_{AL} value. Hence, a plot of $L(W_{AL})$ *vs.* W_{AL} is expected to show a nearly parabolic dependence, which can be approximated either by a second-degree polynomial or by an exponential function of the type $A \cdot \exp(BW_{AL}^2 + CW_{AL})$. Since the exponential function offers some advantages, it was preferred over the polynomial.

(3) It follows from eqn. A1 that n_O/n_A depends linearly on Ψ at each W_{AL}. Considering this dependence in a three-dimensional coordinate system (n_O/n_A *vs.* Ψ *vs.* W_{AL}) and using ordinary trigonometric rearrangements, it can be shown that at a reasonable constant n_O/n_A value, a definite value of Ψ corresponds to each W_{AL}. The Ψ value can be determined by solving a transcendental equation of the type $\Psi = f[n_O/n_A, W_{AL}, \cos^2\text{arctg}\,\lambda\,(\Psi, W_{AL})]$, employing the conventional Newton iterative procedure. Thus, for a set of RP-18 packings of different W_{AL}[15], the corresponding Ψ values were calculated and a system of equations was obtained on the basis of

$$n_O/n_A = \Psi A \cdot \exp(BW_{AL}^2 + CW_{AL}) \qquad \text{(A4)}$$

holding n_O/n_A the same as when determining the Ψ values. Further, the constants A, B and C were specified by using the method of rigorous least squares adjustment, applicable to non-linear problems[20,21].

APPENDIX II

In the case of a very low ligate concentration on the silica surface, we can consider the solute partitioning not to be sterically hindered. Then, it might be expected that the solute molecules are able to occupy the entire ligate solvation space, the solute volume fraction being equal to unity. Therefore, the following equation will hold

$$\lambda(1 - \varphi_E) = 1 \qquad \text{(A5)}$$

remembering that $(1 - \varphi_E)$ is the solute volume fraction in the mobile phase solution, while λ is a proportionality parameter.

As far as eqn. A5 is valid for the entire solvation space, it must also be valid for that part of this space initially occupied only by the solvating molecules, φ'_S. Then:

$$\varphi'_S = \lambda(1 - \varphi_E)\,\varphi'_S \tag{A6}$$

In other words, eqn. A6 reflects the fact that the volume fraction of the solute, which has displaced the solvating molecules, remains equal to their initial volume fraction, φ'_S.

In a real RP system the surface ligate concentration is usually sufficiently high to cause steric hindrance to the solute partitioning. Under these conditions, the superficial stationary phase solution is formed by both the solvating and the solute molecules, their volume fractions being φ_S and φ, respectively. Since the latter are referred to the solvation space, we may write

$$\varphi_S + \varphi = \varphi'_S$$

or

$$\varphi_S = \varphi'_S - \varphi \tag{A7}$$

Hence, in the case of steric hindrance, instead of eqn. A6 we have

$$\varphi = \lambda(1 - \varphi_E)\varphi'_S p \tag{A8}$$

where p is the probability of the solute molecules penetrating among the ligates. A combination of eqns. A5 and A8 yields

$$\varphi = \varphi'_S p$$

which, when introduced into eqn. A7, leads finally to eqn. 27, *e.g.*:

$$\varphi_S = \varphi'_S\,(1 - p)$$

REFERENCES

1 R. N. Nikolov, *Izv. Khim.*, 15 (1982) 36.
2 R. N. Nikolov, *J. Chromatogr.*, 286 (1984) 147.
3 R. N. Nikolov, in E. Kovàts (Editor), *Column Chromatography (Proceedings of Symposium, Lausanne, October 7–10, 1969)*, Swiss Chemists' Association, 1970, p. 156.
4 W. R. Melander, B.-K. Chen and Cs. Horváth, *J. Chromatogr.*, 185 (1979) 99.
5 W. R. Melander, A. Nahum and Cs. Horváth, *J. Chromatogr.*, 185 (1979) 129.
6 P. J. Schoenmakers, H. A. H. Billiet and L. de Galan, *J. Chromatogr.*, 218 (1981) 261.
7 E. Grushka, H. Colin and G. Guiochon, *J. Chromatogr.*, 248 (1982) 325.
8 P. J. Schoenmakers, H. A. H. Billiet and L. de Galan, *J. Chromatogr.*, 282 (1983) 107.
9 A. Nahum and Cs. Horváth, *J. Chromatogr.*, 203 (1981) 53.
10 P. J. Schoenmakers, H. A. H. Billiet, R. Tijssen and L. de Galan, *J. Chromatogr.*, 149 (1978) 519.
11 W. Melander, J. Stoveken and Cs. Horváth, *J. Chromatogr.*, 199 (1980) 35.

12 H. Colin, A. Krstulović, G. Guiochon and Z. Yun, *J. Chromatogr.*, 255 (1983) 295.
13 H. Hemetsberger, P. Behrensmeyer, G. Henning and H. Ricken, *Chromatographia*, 12 (1979) 71.
14 R. Roumeliotis and K. K. Unger, *J. Chromatogr.*, 149 (1978) 211.
15 M. C. Hennion, C. Picard and M. Caude, *J. Chromatogr.*, 166 (1978) 21.
16 R. M. McCormick and B. L. Karger, *Anal. Chem.*, 52 (1980) 2249.
17 C. R. Yonker, T. A. Zwier and M. F. Burke, *J. Chromatogr.*, 241 (1982) 257.
18 C. R. Yonker, T. A. Zwier and M. F. Burke, *J. Chromatogr.*, 241 (1982) 269.
19 *Tables of Interatomic Distances and Configuration in Molecules and Ions*, Special Publication No. 11, Chemical Society, London, 1958.
20 W. E. Wentworth, *J. Chem. Educ.*, 42 (1965) 96.
21 W. E. Wentworth, *J. Chem. Educ.*, 42 (1965) 162.
22 R. P. W. Scott and P. Kucera, *J. Chromatogr.*, 142 (1977) 213.
23 E. H. Lucassen-Reynders, *J. Colloid Interface Sci.*, 41 (1972) 156.
24 E. H. Lucassen-Reynders, *J. Colloid Interface Sci.*, 42 (1973) 554.
25 A. W. Adamson, *Physical Chemistry of Surfaces*, Wiley-Interscience, New York, 1976, pp. 146, 321.
26 R. B. Hermann, *J. Phys. Chem.*, 75 (1971) 363.
27 Cs. Horváth, W. Melander and I. Molnár, *J. Chromatogr.*, 125 (1976) 129.
28 J. H. Hildebrand and R. L. Scott, *The Solubility of Non-electrolytes*, Dover Publications, New York, 1964.
29 P. J. Schoenmakers, H. A. H. Billiet and L. de Galan, *Chromatographia*, 15 (1982) 205.
30 T. L. Hafkenscheid and E. Tomlinson, *J. Chromatogr.*, 264 (1983) 47.
31 W. E. Acree, Jr., *Thermodynamic Properties of Non-electrolyte Solutions*, Academic Press, London, 1984, p. 82.
32 B. L. Karger, L. R. Snyder and Cs. Horváth (Editors), *An Introduction to Separation Science*, Wiley-Interscience, New York, 1973, p. 55.
33 A. F. M. Barton, *Chem. Rev.*, 75 (1975) 731.
34 M. B. Evans, A. D. Dale and C. J. Little, *Chromatographia*, 13 (1980) 5.
35 J. R. Conder, *J. Chromatogr.*, 39 (1969) 273.
36 P. A. Small, *J. Appl. Chem.*, 3 (1953) 71.

Journal of Chromatography, 370 (1986) 403–418
Elsevier Science Publishers B.V., Amsterdam — Printed in The Netherlands

CHROM. 19 036

GENERAL REVERSED-PHASE HIGH-PERFORMANCE LIQUID CHROMATOGRAPHIC METHOD FOR THE SEPARATION OF DRUGS USING TRIETHYLAMINE AS A COMPETING BASE

ROBERT W. ROOS* and CESAR A. LAU-CAM
Food and Drug Administration, Department of Health and Human Services, New York Regional Laboratory, 850 Third Avenue, New York, NY 11232 (U.S.A.)
(First received May 28th, 1986; revised manuscript received August 26th, 1986)

SUMMARY

Triethylamine (TEA) was evaluated as a competing base for the retention control and peak shape improvement in the reversed-phase high-performance liquid chromatographic (RP-HPLC) analysis of selected acidic, basic, and neutral drugs. The effects of this amine on the capacity factor and theoretical plate number values of ephedrine, phenol, and sulfamerazine were examined on three unmodified commercial octadecylsilane chromatographic columns. Based on these results, a general RP-HPLC elution scheme using a μBondapak C_{18} 10-μm column, methanol–acetic acid–TEA–water mobile phases, and an ultraviolet detector was developed for more than 150 drugs of pharmaceutical interest. The proposed method was applied to the separation of groups of chemically or pharmacologically related drugs that included sympathomimetic amines, anthihistamines, phenothiazines, local anesthetics, Cinchona and tropane alkaloids, xanthines, sulfonamides, and steroids. In addition, paired-ion drugs such as physostigmine salicylate and combinations of ascorbic acid, benzoic acid, salicylic acid, pamoic acid, and 8-chlorotheophylline with various basic moieties were readily and effectively resolved into their ionic components using almost identical RP-HPLC conditions.

INTRODUCTION

This laboratory is currently working on the development of uniform and straightforward approaches to the analysis of drugs of pharmaceutical interest by reversed-phase high-performance liquid chromatography (RP-HPLC). Only a few such procedures have been described in the literature. For example, Lurie and Demchuk[1,2] described RP ion-pair HPLC conditions for the separation of a wide range of drugs of forensic importance that included ergot and opium alkaloids, phenylethylamine, local anesthetics, and barbiturates. Likewise, Hoogewijs and Massart[3], Detaevernier *et al.*[4], and De Smet *et al.*[5] reported standardized analytical strategies for analyzing basic drugs in pharmaceutical dosage forms by HPLC on bonded phases with polar and non-polar mobile phases. More recently, and at variance with the

0021-9673/86/$03.50

RP-HPLC modality, Jane *et al.*[6] have described HPLC conditions for the analysis of more than 450 basic drugs on unmodified silica columns with non-aqueous ionic eluents using photometric, fluorescence, and electrochemical oxidation detections.

In RP-HPLC, mobile phase additives represent the first form of *in situ* column modification for effecting selectivity changes as well as remediating peak asymmetry[7]. Many substances have been used to alter selectivity but alkylamines and alkylsulfonate ion-pairing reagents are the most common ones. Alkylamines act primarily by hydrogen bonding to non-derivatized silanol sites, thereby reducing adsorption and/or ion-exchange effects[8]. The addition of an alkylamine to a mobile phase can dramatically improve peak shapes with little loss of retention. In addition to their ability to reduce peak tailing, alkylamines are also useful as selectivity-enhancing agents.

A number of publications have dealt with the inclusion of amines in the eluent to control peak retention and to improve column efficiency. Eggers and Saint-Joly[9] studied the effects of amine modifiers on the RP chromatographic behavior of salbutamol. Hung *et al.*[10] investigated the effects of various organic amines on the ion-pair chromatographic analysis of tricyclic antidepressant drugs. Pennington and Schmidt[11] added tetraethylammonium ions to the mobile phase for the quantitative determination of mixtures of atropine, hyoscyamine, and scopolamine in pharmaceutical products. Cooke and Olsen[12] discussed the effect of a hydrophilic amine such as nonyl amine on the RP chromatographic behavior of a number of phenothiazines. The suitability of amines as silanol-masking agents and their effect on the retention characteristics of a variety of phenylethylamines[13], dibenzo-crown ethers and peptides[14], and tricyclic antidepressants[15], has also been considered.

This paper describes the use of triethylamine (TEA) as a mobile phase modifier for the RP-HPLC separation of acidic, basic, and neutral drugs; and examines the behavior of prototype drugs in terms of retentions and column efficiencies on three brands of unmodified octadecylsilane (ODS) columns. The positive influence of TEA on the resolving efficiency of methanol–acetic acid–TEA–water mobile phases was demonstrated by achieving the separation of mixtures of structurally related drugs and of several of their paired-ion combinations.

EXPERIMENTAL

Equipment and experimental conditions

The liquid chromatograph consisted of a Model 3500B solvent delivery system, a Model 770 variable-wavelength detector, a sampling valve fitted with a 10-μl sample loop (Spectra-Physics, Mountain View, CA, U.S.A.), and a Model 3380A recording integrator (Hewlett-Packard, Avondale, PA, U.S.A.). The chromatographic columns were a 10 μm μBondapak C_{18}, 300 × 3.9 mm I.D. (Waters Assoc., Milford, MA, U.S.A.), a 5 μm Zorbax ODS, 250 × 4.6 mm I.D. (DuPont, Wilmington, DE, U.S.A.), and a 5 μm Ultrasphere ODS, 250 × 4.6 mm I.D. (Beckman Instruments, Berkeley, CA, U.S.A.). All analyses were performed at ambient temperature with the mobile phase delivered at a flow-rate of 1.5 ml/min.

Chemicals

The test compounds used throughout the study were of reagent grade or better,

and were obtained from commercial sources. Mobile phases were prepared using HPLC-grade methanol (J. T. Baker, Phillipsburg, NJ, U.S.A.), reagent grade glacial acetic acid (Fisher Scientific, Fair Lawn, NJ, U.S.A.), reagent grade TEA (J. T. Baker), and water that had been double-distilled in glass.

Chromatographic solutions

Capacity factor (k') and theoretical plate number (N) values of model drugs were determined using solutions that contained 1 mg/ml of ephedrine, 0.1 mg/ml of phenol, and 0.05 mg/ml of sulfamerazine in methanol–acetic acid–water (22.5:1.5:76.0). To study chromatographic mobility behaviors as a function of the concentration of methanol in the mobile phase, test compounds were individually dissolved in methanol–water (1:1) to contain 0.5 mg/ml. Solutions of mixed sympathomimetic amines and tropane alkaloids were prepared in methanol–water (1:1) to contain 1 mg/ml of each component. Solutions of antihistamines, phenothiazines, local anesthetics, steroids, Cinchona alkaloids, sulfonamides, and xanthines were also prepared in methanol–water (1:1) to contain 0.25 mg/ml of each component. The prednisolone peak appearing during the separation of the steroids represents an impurity of prednisolone succinate. Solutions of the paired-ion drugs hydroxyzine pamoate, pyrantol pamoate, pyrvinium pamoate, and physostigmine salicylate were individually prepared in methanol–water (1:1) to contain 0.25 mg/ml of each sample. The paired-ion combinations of 8-chlorotheophylline and quinine were prepared by dissolving equal amounts of the corresponding moieties in methanol–water (1:1) to obtain solutions containing 0.25 mg/ml of each component.

RESULTS AND DISCUSSION

Normalization of the retention behavior of a solute can be achieved by incorporating TEA in the eluent to serve as a competing base for masking accessible surface silanol groups and for providing heterogeneity on the RP bonded surface. Kiel *et al.*[8] and Bij *et al.*[14] have previously shown that retention is practically independent of sample load if an amine is present in the eluent, and that short chain tertiary amine modifiers like TEA are highly effective in reducing or eliminating

TABLE I

EFFECTS OF TEA ON PEAK RETENTION AND COLUMN EFFICIENCY

k' and N values for ephedrine, phenol, and sulfamerazine on μBondapak C_{18} (A), Zorbax ODS (B), and Ultrasphere ODS (C) columns as a function of the concentration of TEA in the mobile phase. Mobile phases were mixtures of methanol–acetic acid–TEA–water [22.5:1.5:(0 or 1):(76 or 75)].

Drug	k'						N					
	0% TEA			*1% TEA*			*0% TEA*			*1% TEA*		
	A	*B*	*C*	*A*	*B*	*C*	*A*	*B*	*C*	*A*	*B*	*C*
Ephedrine	0.60	22.79	20.10	0.97	1.73	2.26	494	75	20	2784	2880	4900
Phenol	2.65	5.23	6.25	2.44	5.90	6.48	4018	10 076	14 604	3836	9423	13 395
Sulfamerazine	1.75	3.26	2.43	1.73	3.20	2.46	2832	4239	4746	2750	3823	5150

silanophilic interactions. Similar effects have been described for other amines[12,16,17].

The effects of TEA on k', a measure of retention, and on N, a measure of efficiency, were investigated on three model drugs by using mobile phases that only differed in the concentration of TEA present, and three brands of ODS RP columns. In this study k' is defined as $(t_R/t_0) - 1$, where t_R and t_0 are the retention times of the compound under investigation and a non-retained compound, respectively, and where t_0 was measured as the first distortion of the base line following the injection of water. Of the several methods of measuring column plate count, the peak width at half height method, *i.e.* $N = 5.54\ (t_R/W_{0.5})^2$, was found the most convenient.

As shown in Table I, although the concentration of amine in the eluent played little or no role in determining the k' and N values of the relatively neutral phenol and acidic sulfamerazine, irrespective of the column used, it however greatly influenced the values of the weak base ephedrine. Interestingly, in the case of ephedrine a sharp reduction in k' values occurred on the Zorbax ODS and Ultrasphere ODS columns, whereas the N values increased on all three columns used.

Plots of k' and N values against the concentration of TEA in the eluent revealed further relationships between the concentration of modifying amine and the chromatographic behavior. As illustrated with ephedrine (Fig. 1), these plots demonstrated that although on all three columns the same concentration of alkylamine, *i.e.*

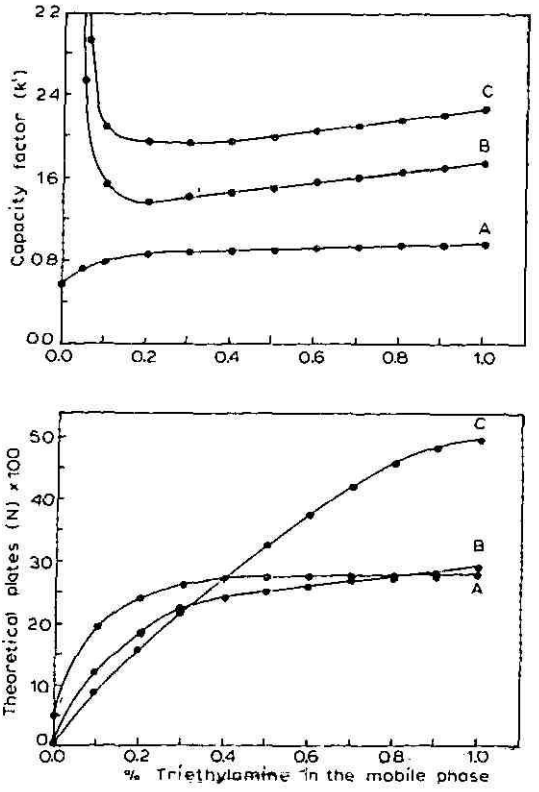

Fig. 1. Effect of the concentration of TEA in the mobile phase on k' and N values of ephedrine. See Table I for columns and mobile phases.

TABLE II

k' VALUES AS A FUNCTION OF THE CONCENTRATION OF METHANOL IN THE MOBILE PHASE

k' = capacity factor = $(t_R/t_0) - 1$, where t_0 = 2.5 min, were measured with a methanol–acetic acid–TEA–water (variable:1.5:0.5:variable, to yield 100 parts by volume) mobile phase.

Drug	*Parts of methanol per 100 parts of mobile phase*									
	0	*10*	*20*	*30*	*40*	*50*	*60*	*70*	*80*	*90*
Acetanilide	–	–	4.61	2.52	1.46	0.85	0.41	0.19	–	–
Acetophenazine	–	–	–	–	–	7.13	2.42	0.79	0.22	–
Acetyl sulfisoxazole	–	–	–	8.47	2.86	1.01	0.39	–	–	–
Aminopromazine	–	–	–	–	–	–	2.79	0.89	0.26	–
Amitriptyline	–	–	–	–	–	6.85	2.54	0.95	0.25	–
Amodiaquin	–	–	–	–	–	2.55	1.28	0.31	0.02	–
Amphetamine	–	2.33	1.63	0.85	–	0.32	–	–	–	–
Antazoline	–	–	–	–	3.20	1.50	0.48	0.08	–	–
Antipyrine	–	–	6.45	2.60	1.24	0.69	0.50	0.15	–	–
Atropine	–	12.12	4.26	1.09	0.75	0.36	0.18	–	–	–
Atropine methyl	–	9.18	3.19	0.89	0.63	0.31	0.16	–	–	–
Benzocaine	–	–	–	6.38	2.78	1.40	0.97	0.24	–	–
Benztropine	–	–	–	–	–	–	2.10	0.95	–	–
Bromodiphenhydramine	–	–	–	–	14.88	5.70	3.48	0.59	0.24	–
Brompheniramine	–	–	–	13.60	5.52	2.51	1.63	0.45	0.21	–
Bupivacaine	–	–	–	6.13	2.84	1.37	–	–	–	–
Butacaine	–	–	–	5.34	1.95	0.81	–	–	–	–
Butaperazine	–	–	–	–	–	33.04	9.04	2.57	0.80	0.21
Caffeine	–	–	4.11	1.48	0.74	0.46	0.31	0.10	–	–
Carbinoxamine	–	–	–	10.50	4.24	1.98	1.35	0.34	–	–
Chlorcyclizine	–	–	–	–	15.33	5.83	3.59	0.77	0.21	–
Chloroprocaine	–	–	–	0.92	0.44	0.22	–	–	–	–
Chloroquine	–	–	–	0.99	0.31	0.11	–	–	–	–
8-Chlorotheophylline	–	–	–	2.03	1.07	0.75	0.42	0.06	–	–
Chlorothiazide	–	–	–	0.31	0.23	0.09	–	–	–	–
Chlorpheniramine	–	–	–	10.05	4.51	2.11	1.35	0.34	0.12	–

(*Continued on p. 408*)

TABLE II (*continued*)

Drug	*Parts of methanol per 100 parts of mobile phase*									
	0	*10*	*20*	*30*	*40*	*50*	*60*	*70*	*80*	*90*
Chlorpromazine	–	–	–	–	–	11.28	3.86	1.20	0.41	0.05
Cinchonidine	–	–	–	–	2.93	1.23	–	–	–	–
Cinchonine	–	–	–	–	2.60	1.11	–	–	–	–
Clemizole	–	–	–	–	–	4.01	2.05	0.86	–	–
Cortisone acetate	–	–	–	–	–	–	2.19	0.84	0.18	–
Cyclizine	–	–	–	5.71	2.47	1.67	0.42	0.16	–	–
Cyclothiazide	–	–	–	–	2.51	0.75	0.24	–	–	–
Cycrimine	–	–	–	5.42	2.46	1.72	0.39	–	–	–
Desipramine	–	–	–	–	5.68	2.16	0.81	0.18	–	–
Dextromethorphan	–	–	–	4.61	2.14	1.55	0.40	0.18	–	–
Dibucaine	–	–	–	–	6.70	2.75	–	–	–	–
Dienestrol	–	–	–	–	16.44	4.70	1.43	0.32	–	–
Dietylstilbestrol	–	–	–	–	16.92	4.68	1.42	0.32	–	–
Dihydrocinchonidine	–	–	–	–	4.09	1.64	–	–	–	–
Dihydrocinchonine	–	–	–	–	3.64	1.48	–	–	–	–
Dihydroergocornine	–	–	–	–	4.26	1.36	0.41	–	–	–
Dihydroergocristine	–	–	–	–	8.22	2.36	0.67	–	–	–
Dihydroergocryptine	–	–	–	–	7.55	2.19	0.64	–	–	–
Dihydroquinidine	–	–	–	–	5.88	2.16	–	–	–	–
Dihydroquinine	–	–	–	–	7.91	2.64	–	–	–	–
Diphenhydramine	–	–	–	4.49	2.02	1.37	0.30	–	–	–
Diphenylpyraline	–	–	18.69	–	2.84	–	–	–	–	–
Doxylamine	–	–	4.24	2.03	1.04	0.71	0.16	–	–	–
Dyphylline	–	–	1.50	0.70	0.22	–	–	–	–	–
Ephedrine	2.72	1.70	1.04	0.55	–	–	–	–	–	–
Ergonovine	–	–	2.69	0.70	0.45	0.17	–	–	–	–
Ergotamine	–	–	–	–	–	4.82	1.55	0.45	–	–
Estradiol	–	–	–	–	–	–	4.67	1.59	0.41	–
Estradiol benzoate	–	–	–	–	–	–	–	–	3.53	0.68
Estradiol cypionate	–	–	–	–	–	–	–	–	7.45	1.32
Estradiol valerate	–	–	–	–	–	–	–	–	3.49	0.66
Estriol	–	–	–	–	–	–	0.99	0.35	0.02	–
Estrone	–	–	–	–	–	–	4.06	1.43	0.38	–

Ethinyl estradiol	–	–	–	–	–	–	4.12	1.45	0.32	–
Fluphenazine	–	–	–	–	–	–	6.99	1.93	0.53	0.03
Fluphenazine decanoate	–	–	–	–	–	–	–	–	3.49	1.12
Fluphenazine enanthate	–	–	–	–	–	–	–	–	2.49	0.50
Homatropine	–	4.66	1.69	0.50	0.34	0.20	0.09	–	–	–
Homatropine methyl	–	3.13	1.14	0.40	0.29	0.17	–	–	–	–
Hydrochlorothiazide	–	2.64	1.05	0.49	0.24	0.10	–	–	–	–
Hydroflumethazide	–	5.43	2.13	0.92	0.44	0.19	–	–	–	–
Hydrocortisone	–	–	–	–	–	–	1.27	0.56	0.11	–
Hydrocortisone acetate	–	–	–	–	–	–	2.25	0.91	0.21	–
Hydroxyamphetamine	1.25	0.90	0.50	–	–	0.09	–	–	–	–
Hydroxyzine	–	–	–	–	–	–	2.35	0.60	–	–
Hyoscyamine	–	12.82	4.76	1.09	0.75	0.36	0.18	–	–	–
Imipramine	–	–	–	–	–	5.25	2.14	0.84	0.21	–
Isoproterenol	0.71	0.34	0.18	–	–	–	–	–	–	–
Lidocaine	–	–	2.83	1.23	0.76	0.43	–	–	–	
Meclizine	–	–	–	–	–	–	–	–	1.94	0.48
Medroxyprogesterone acetate	–	–	–	–	–	–	–	3.12	0.77	–
Mephentermine	–	6.45	3.29	1.40	–	–	0.23	–	–	–
Mesoridazine	–	–	–	–	–	3.11	1.14	0.35	0.10	–
Mestranol	–	–	–	–	–	–	–	–	1.51	0.27
Methamphetamine	–	3.42	1.91	0.95	–	–	0.24	–	–	–
Methapyriline	–	–	–	5.24	2.14	1.08	0.73	0.18	–	–
Methotrimeprazine	–	–	–	–	–	–	2.41	0.58	0.21	–
Methoxyamphetamine	–	–	–	1.86	0.92	0.65	0.48	0.07	–	–
Methoxypromazine	–	–	–	–	–	–	2.17	0.54	0.14	–
Methyldopate	–	5.49	1.98	–	–	–	–	–	–	–
Methylparaben	–	–	–	–	–	1.44	0.74	0.27	–	–
Methyltestosterone	–	–	–	–	–	–	6.05	2.27	0.66	–
Naphazoline	–	–	–	2.52	1.23	0.66	0.47	0.09	–	–
Norethindrone	–	–	–	–	–	–	3.60	1.32	0.34	–
Norethindrone acetate	–	–	–	–	–	–	9.77	2.91	0.71	–
Nortriptyline	–	–	–	–	–	7.31	2.60	0.94	0.21	–
Oxyphencylcimine	–	–	–	–	11.63	4.78	2.79	0.67	0.21	–
Perchlorperazine	–	–	–	–	–	21.12	6.75	2.14	0.72	0.20
Perphenazine	–	–	–	–	–	–	5.12	1.59	0.50	0.06
Phenacetin	–	–	–	6.03	2.90	1.45	0.66	0.31	–	–

(*Continued on p. 410*)

TABLE II (*continued*)

Drug	*Parts of methanol per 100 parts of mobile phase*									
	0	*10*	*20*	*30*	*40*	*50*	*60*	*70*	*80*	*90*
Phenindamine	–	–	–	–	6.44	2.66	–	–	–	–
Pheniramine	–	–	–	3.40	1.62	0.84	0.65	0.17	–	–
Phenothiazine	–	–	–	–	–	–	5.51	1.56	0.47	–
Phenoxybenzamine	–	–	–	–	6.57	2.57	1.78	0.46	0.20	–
Phentermine	–	5.35	2.91	1.40	–	–	0.32	–	–	–
Phentolamine	–	–	–	6.87	2.41	1.50	1.05	0.13	–	–
Phenylpropanolamine	1.48	1.15	0.79	0.45	–	–	–	–	–	–
Phenylephrine	0.38	0.25	–	–	–	–	–	–	–	–
Phenyltoloxamine	–	–	–	–	7.63	3.03	2.00	0.41	0.14	–
Phthalylsulfathiazole	–	–	13.79	3.93	1.32	0.47	0.19	–	–	–
Physostigmine	–	–	–	1.60	0.57	–	–	–	–	–
Prednisolone	–	–	–	–	–	–	1.23	0.52	0.10	–
Prednisolone acetate	–	–	–	–	–	–	2.23	0.86	0.20	–
Prednisolone tebutate	–	–	–	–	–	–	14.73	4.00	0.86	–
Prednisone	–	–	–	–	–	–	0.85	0.36	0.04	–
Procaine	–	–	1.15	–	0.23	0.16	–	–	–	–
Prochlorperazine	–	–	–	–	21.12	6.75	3.57	2.14	0.72	–
Progesterone	–	–	–	–	–	–	10.36	3.39	0.91	–
Promazine	–	–	–	–	–	5.04	1.92	0.64	0.24	–
Promethazine	–	–	–	–	–	4.40	1.75	0.60	0.22	–
Protrophyline	–	–	–	–	–	5.76	2.03	0.73	0.13	–
Pseudoephedrine	3.52	1.96	1.07	0.55	–	–	–	–	–	–
Pyrantel	–	–	–	–	–	0.60	0.20	–	–	–
Pyrilamine	–	–	–	8.74	3.40	1.60	1.08	0.29	–	–
Pyrvinium	–	–	–	–	–	–	13.64	3.24	–	–
Quinidine	–	–	–	–	4.21	1.63	–	–	–	–
Quinine	–	–	–	–	5.49	1.89	–	–	–	–
Salicylamide	–	–	4.23	2.19	0.84	0.66	0.28	0.11	–	–
Salicylic acid	–	–	–	–	1.30	0.50	–	–	–	–
Scopolamine	–	3.98	1.63	0.55	0.40	0.21	0.11	–	–	–

Scopolamine aminoxide	–	3.32	1.40	0.48	0.34	0.21	0.10	–	–	–
Scopolamine methyl	–	5.46	2.12	0.65	0.47	0.26	0.12	–	–	–
Spironolactone	–	–	–	–	–	11.66	3.42	1.13	0.27	–
Succinylsulfathiazole	–	–	5.16	1.43	0.52	0.20	0.04	–	–	–
Sulfabenzamide	–	–	–	3.09	1.34	0.57	0.23	–	–	–
Sulfachlorpyridazine	–	–	8.45	2.01	0.93	0.43	0.20	–	–	–
Sulfadiazine	–	3.52	1.42	0.68	0.36	0.16	0.06	–	–	–
Sulfadimethoxine	–	–	–	6.90	2.56	1.00	0.42	0.09	–	–
Sulfamerazine	–	6.85	2.49	1.13	0.55	0.26	0.11	–	–	–
Sulfamethazine	–	–	4.06	1.72	0.80	0.38	0.17	–	–	–
Sulfamethizole	–	4.85	1.71	0.71	0.34	0.14	0.06	–	–	–
Sulfamethoxazole	–	–	5.46	2.21	0.97	0.41	0.20	–	–	–
Sulfamethoxypyridazine	–	–	4.35	1.79	0.80	0.36	0.16	–	–	–
Sulfanilamide	–	0.58	0.32	0.19	0.11	–	–	–	–	–
Sulfanilic acid	0.26	0.13	0.06	–	–	–	–	–	–	–
Sulfaphenazole	–	–	–	4.76	1.81	0.68	0.30	–	–	–
Sulfapyridine	–	5.49	1.98	0.89	0.45	0.21	0.11	–	–	–
Sulfathiazole	–	4.85	1.71	0.71	0.34	0.14	–	–	–	–
Sulfisomidine	–	4.07	1.61	0.65	0.34	0.17	0.07	–	–	–
Sulfisoxazole	–	–	6.57	2.54	1.04	0.43	0.17	–	–	–
Testosterone	–	–	–	–	–	–	4.48	1.75	0.52	–
Testosterone cypionate	–	–	–	–	–	–	–	–	8.07	1.48
Testosterone enanthate	–	–	–	–	–	–	–	–	7.12	1.33
Testosterone propionate	–	–	–	–	–	–	–	–	1.95	0.41
Tetracaine	–	–	–	12.16	4.55	2.06	1.33	0.33	–	–
Theobromine	–	–	1.23	–	0.29	0.19	–	–	–	–
Theophylline	–	–	2.08	0.87	0.48	0.31	–	–	–	–
Thioridazine	–	–	–	–	–	–	5.66	1.59	0.51	0.06
Thozylamine	–	–	–	5.31	2.22	1.10	0.75	0.19	–	–
Trichlormethiazole	–	–	7.47	2.89	1.26	0.56	0.21	–	–	–
Tiethylperazine	–	–	–	–	–	–	10.45	3.04	0.96	0.27
Triflupromazine	–	–	–	–	–	–	5.12	1.47	0.43	0.02
Trimeprazine	–	–	–	–	–	–	2.07	0.70	0.21	–
Tripelennamine	–	–	–	7.45	3.22	1.53	1.02	0.26	–	–
Triprolidine	–	–	–	15.90	5.74	2.40	1.52	0.35	–	–
Tropic acid	–	6.47	3.32	1.26	0.93	0.52	0.26	–	–	–

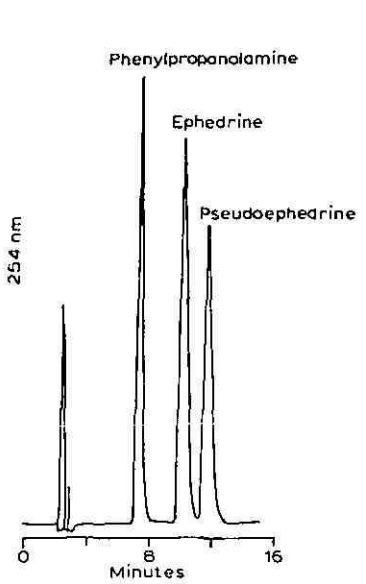

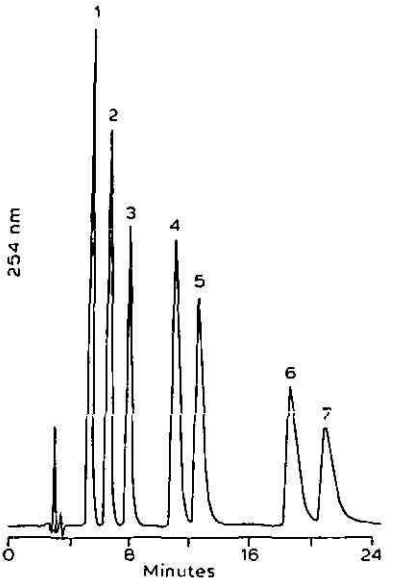

Fig. 2. Chromatographic separation of phenylpropanolamine and the diastereoisomers ephedrine and pseudoephedrine. Column, μBondapak C_{18}; mobile phase, methanol–acetic acid–TEA–water (5.0:1.5:0.5:93.0); detector sensitivity, 0.16 a.u.f.s.

Fig. 3. Chromatographic separation of sympathomimetic amines. Column, μBondapak C_{18}; mobile phase, methanol–acetic acid–TEA–water (15.0:1.5:0.5:83.0); detector sensitivity, 0.16 a.u.f.s. 1 = Hydroxyamphetamine; 2 = phenylpropanolamine; 3 = ephedrine; 4 = amphetamine; 5 = methamphetamine; 6 = phentermine; 7 = mephentermine.

0.2%, provided retention control, the same is not true of the peak shapes, as evidenced by the increase in N values with increasing amine in the eluent. Hence, control of N will require an amount of TEA that is dictated by the brand of column used. For example, whereas 0.5% of TEA was adequate for controlling the retention and peak shape of ephedrine on the μBondapak C_{18} and Zorbax ODS columns, a 1% concentration was needed on the Ultrasphere column. In any event, the same concentration (1.5%) of acetic acid in the mobile phase was sufficient to render the pH below 4.5, even at the maximum (1%) concentration of TEA added. Under these conditions weak bases will become ionized and weak acids will remain non-ionized.

Methanol–acetic acid–water mobile phases that contained 0.5% TEA, together with an arbitrarily selected RP-HPLC column (μBondapak C_{18}), were used to determine the chromatographic behavior of a large number of pharmaceutically important drugs, many of which are currently listed in the United States Pharmacopeia[18]. Table II gives the k' values for 166 compounds as a function of the concentration of methanol in the mobile phase. The data show that as the concentration of methanol increases the retention decreases, as would be expected in RP-HPLC[13]. From the compilation of k' values for a range of methanol concentrations in the mobile phase the most appropriate elution system may be selected for a given compound, whether this compound occurs singly or in combination with other listed compounds.

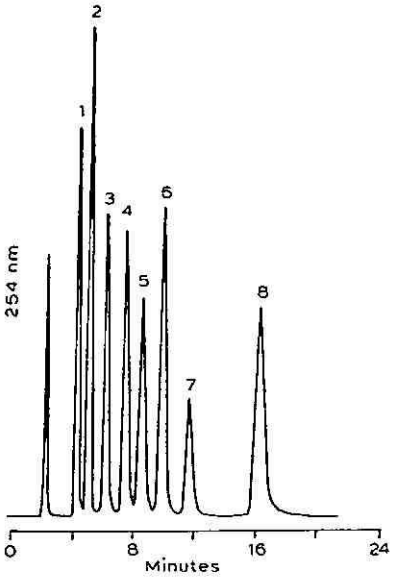

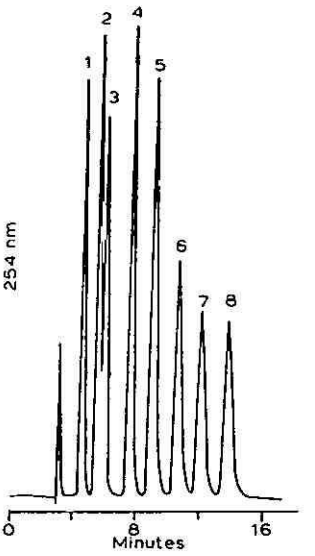

Fig. 4. Chromatographic separation of antihistamines. Column, μBondapak C_{18}; mobile phase, methanol–acetic acid–TEA–water (50.0:1.5:0.5:48.0); detector sensitivity, 0.16 a.u.f.s. 1 = Pheniramine; 2 = thozylamine; 3 = tripelennamine; 4 = chlorpheniramine; 5 = brompheniramine; 6 = phenindamine; 7 = phenyltoxamine; 8 = clemizole.

Fig. 5. Chromatographic separation of phenothiazines. Column, μBondapak C_{18}; mobile phase, methanol–acetic acid–TEA–water (70.0:1.5:0.5:28.0); detector sensitivity, 0.32 a.u.f.s. 1 = Mesoridazine; 2 = promethazine; 3 = acetophenazine; 4 = chlorpromazine; 5 = thioridazine; 6 = prochlorperazine; 7 = butaperazine; 8 = thiethylperazine.

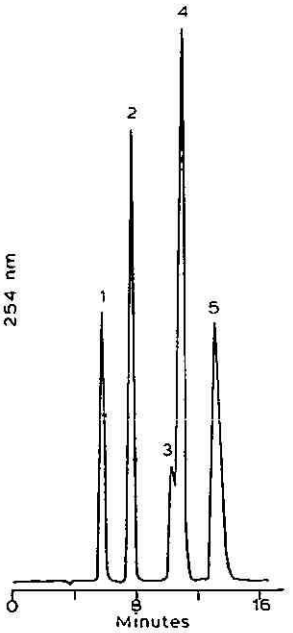

Fig. 6. Chromatographic separation of local anesthetics. Column, μBondapak C_{18}; mobile phase, methanol–acetic acid–TEA–water (50.0:1.5:0.5:48.0); detector sensitivity, 0.16 a.u.f.s. 1 = Lidocaine; 2 = butacaine; 3 = bupivacaine; 4 = benzocaine; 5 = tetracaine.

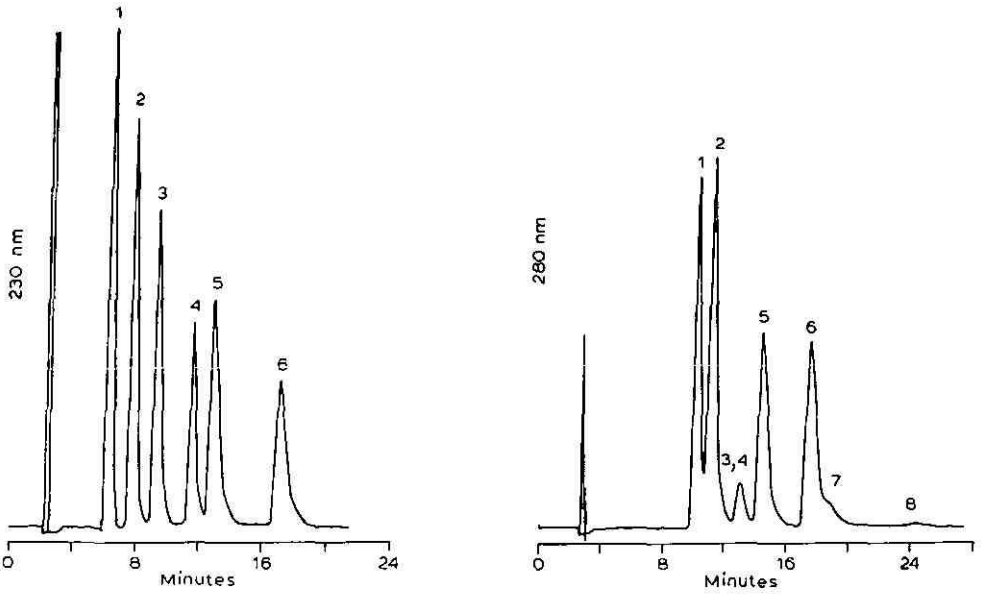

Fig. 7. Chromatographic separation of tropane alkaloids. Column, μBondapak C_{18}; mobile phase, methanol–acetic acid–TEA–water (15.0:1.5:0.5:83.0); detector sensitivity, 0.08 a.u.f.s. 1 = Homatropine; 2 = scopolamine; 3 = methscopolamine; 4 = tropic acid; 5 = atropine methyl; 6 = atropine.

Fig. 8. Chromatographic separation of Cinchona alkaloids. Column, μBondapak C_{18}; mobile phase, methanol–acetic acid–TEA–water (40.0:1.5:0.5:58.0); detector sensitivity, 0.64 a.u.f.s. 1 = Cinchonidine; 2 = cinchonine; 3 = dihydrocinchonine; 4 = dihydrocinchonidine; 5 = quinidine; 6 = quinine; 7 = dihydroquinidine; 8 = dihydroquinine.

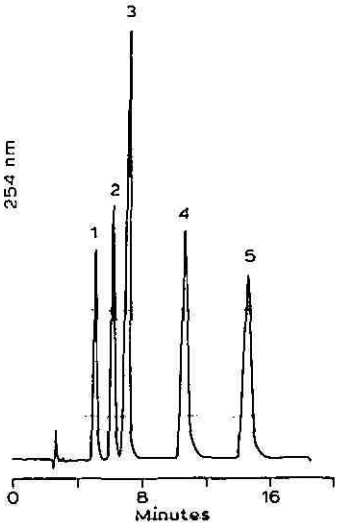

Fig. 9. Chromatographic separation of xanthines. Column, μBondapak C_{18}; mobile phase, methanol–acetic acid–TEA–water (25.0:1.5:0.5:73.0); detector sensitivity, 0.16 a.u.f.s. 1 = Theobromine; 2 = dyphylline; 3 = theophylline; 4 = caffeine; 5 = 8-chlorotheophylline.

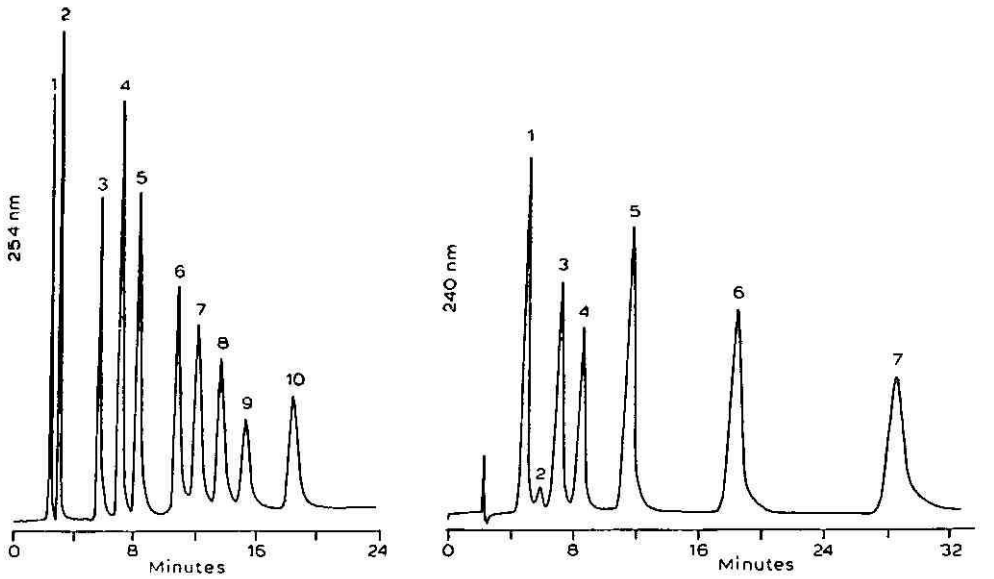

Fig. 10. Chromatographic separation of sulfonamides. Column, μBondapak C_{18}; mobile phase, methanol–acetic acid–TEA–water (20.0:1.5:0.5:78.0); detector sensitivity, 0.32 a.u.f.s. 1 = Sulfanilic acid; 2 = sulfanilamide; 3 = sulfadiazine; 4 = sulfapyridine; 5 = sulfamerazine; 6 = sulfamethizole; 7 = sulfamethazine; 8 = sulfamethoxazole; 9 = sulfisoxazole; 10 = sulfachlorpyridizine.

Fig. 11. Chromatographic separation of steroids. Column, μBondapak C_{18}; mobile phase, methanol–acetic acid–TEA–water (60.0:1.5:0.5:38.0); detector sensitivity, 0.32 a.u.f.s. 1 = Prednisone; 2 = prednisolone; 3 = prednisolone succinate; 4 = hydrocortisone acetate; 5 = norethindrone; 6 = methyltestosterone; 7 = progesterone.

From a qualitative point of view, a few structure–chromatographic behavior correlations become evident from the data in Table II. Among halogen-containing compounds, the halogenated derivatives consistently eluted after the corresponding parent compounds, as found for the pairs pheniramine and chlorpheniramine, cyclizine and chlorcyclizine, procaine and chlorprocaine, and theophylline and 8-chlortheophylline. Among phenolic compounds, hydroxylated ones eluted ahead of the parent compounds, as for hydroxyamphetamine and amphetamine. Compounds exhibiting multiple hydroxyl groups in the aromatic ring, like the catecholamines, were not retained by the ODS columns. An exception, however, was the catecholamine methyldopate, whose k' values are given in the same table.

The resolving efficiency of the proposed TEA-containing mobile phase systems for the RP-HPLC separation of groups of structurally or therapeutically related important drugs is illustrated in Figs. 2–11. Shown are chromatographic separations of sympathomimetic amines (Figs. 2 and 3), antihistamines (Fig. 4), phenothiazines (Fig. 5), local anesthetics (Fig. 6), tropane (Fig. 7) and Cinchona (Fig. 8) alkaloids, xanthines (Fig. 9), sulfonamides (Fig. 10), and steroids (Fig. 11). Whereas most of these separations entailed weakly basic drugs (Figs. 2–8), two included weakly acidic drugs (Figs. 9 and 10), and one included neutral steroids (Fig. 11). In general, excellent resolutions were obtained with a mobile phase containing 1.5% acetic acid, 0.5% TEA, and various ratios of a methanol–water mixture.

TABLE III

PAIRED-ION DRUGS ANALYZED BY RP-HPLC USING MOBILE PHASES CONTAINING TEA AS A MODIFIER

Drug	*Components*		*Main therapeutic use*
	Base	*Acid*	
Physostigmine salicylate	Physostigmine	Salicylic acid	Miotic, Belladonna alkaloids antidote
Hydroxyzine pamoate	Hydroxyzine	Pamoic acid	Tranquilizer, sedative
Pyrantel pamoate	Pyrantel	Pamoic acid	Anthelmintic
Pyrvinium pamoate	Pyrvinium	Pamoic acid	Anthelmintic
Dimenhydrinate	Diphenhydramine	8-Chlorotheophylline	Antihistaminic, antiemetic
Piprinhydrinate	Diphenylpyraline	8-Chlorotheophylline	Antihistaminic, antiemetic, sedative
Promethazine teoclate	Promethazine	8-Chlorotheophylline	Antihistaminic, antiemetic
Quinine ascorbate	Quinine	Ascorbic acid	Smoking deterrent
Quinine benzoate	Quinine	Benzoic acid	Antimalarial, analgesic
Quinine salicylate	Quinine	Salicylic acid	Antimalarial, analgesic

Based on the foregoing results, the same RP-HPLC system was applied to the resolution of a number of paired-ion drugs into their molecular components. Table III lists ten paired-ion drugs along with their chemical compositions and main therapeutic uses. Since without exceptions all the ionic components absorbed ultraviolet light above 230 nm, the proposed HPLC system will readily detect them in the

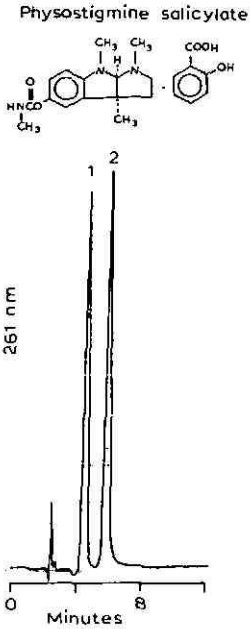

Fig. 12. Chromatographic separation of the components of physostigmine salicylate. Column, μBondapak C_{18}; mobile phase, methanol–acetic acid–TEA–water (35.0:1.5:0.5:63.0); detector sensitivity, 0.32 a.u.f.s. 1 = Physostigmine; 2 = salicylic acid.

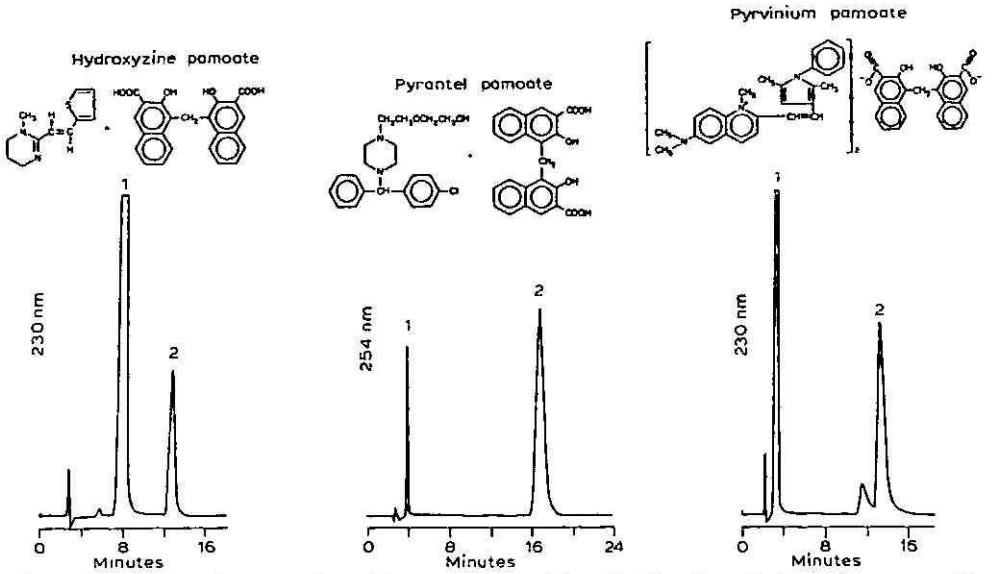

Fig. 13. Chromatographic separation of the components of the paired-ion drugs hydroxyzine pamoate (1 = pamoic acid; 2 = hydroxyzine), pyrantel pamoate (1 = pyrantel; 2 = pamoic acid), and pyrvinium pamoate (1 = pamoic acid; 2 = pyrvinium). Column, μBondapak C_{18}; mobile phases, methanol–acetic–TEA–water (58.0:1.5:0,.5:40.0) hydroxyzine pamoate; (50.0:1.5:0.5:48.0) pyrantel pamoate; and (67.0:1.5:0.5:31.0) pyrvinium pamoate.

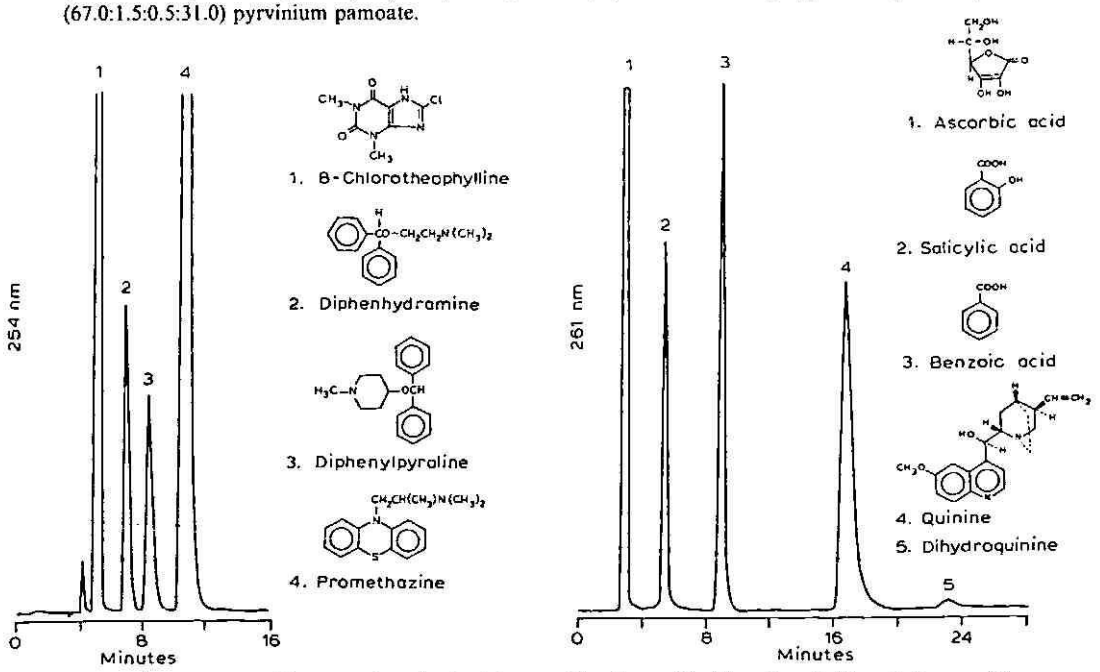

Fig. 14. Chromatographic separation of paired-ion combinations of 8-chlorotheophylline. Column, μBondapak C_{18}; mobile phase, methanol–acetic acid–TEA–water (60.0:1.5:0.5:38.0); detector sensitivity, 0.32 a.u.f.s.

Fig. 15 Chromatographic separation of paired-ion combinations of quinine. Column, μBondapak C_{18}; mobile phase, methanol–acetic acid–TEA–water (40.0:1.5:0.5:58.0); detector sensitivity, 0.64 a.u.f.s.

230–260 nm wavelength range. Chromatographic separations were achieved for the components of physostigmine salicylate (Fig. 12), pamoic acid combinations with hydroxyzine, pyrantel, and pyrvinium (Fig. 13), 8-chlorotheophylline pairs with diphenhydramine, diphenylpyraline, and promethazine (Fig. 14), and paired-ions of quinine with ascorbic, benzoic, and salicylic acids (Fig. 15).

In light of the results presented here, it is evident that the simultaneous addition of TEA and an organic acid such as acetic acid to a methanol–water mobile phase can provide both effective ion suppression of acidic drugs and ionization of basic ones, with the eventual improvement of column efficiency and peak shapes. A salient advantage to be gained from this type of mobile phase is the possibility of simultaneously analyzing a wide variety of weakly basic and acidic drugs and their paired-ion combinations using the same ODS column and ratio variations of the components of the quaternary mobile phase.

REFERENCES

1 I. S. Lurie and S. M. Demchuk, *J. Liq. Chromatogr.*, 4 (1981) 337.
2 I. S. Lurie and S. M. Demchuk, *J. Liq. Chromatogr.*, 4 (1981) 357.
3 G. Hoogewijs and D. L. Massart, *J. Pharm. Biomed. Anal.*, 1 (1983) 321.
4 M. R. Detaevernier, G. Hoogewijs and D. L. Massart, *J. Pharm. Biomed. Anal.*, 1 (1983) 331.
5 M. De Smet, G. Hoogewijs, M. Puttemans and D. L. Massart, *Anal. Chem.*, 56 (1984) 2662.
6 I. Jane, A. McKinnon and R. J. Flanagan, *J. Chromatogr.*, 323 (1985) 191.
7 B. A. Bidlingmeyer, *J. Chromatogr. Sci.*, 18 (1980) 525.
8 J. S. Kiel, S. L. Morgan and R. K. Abramson, *J. Chromatogr.*, 320 (1985) 313.
9 N. J. Eggers and C. M. Saint-Joly, *J. Liq. Chromatogr.*, 11 (1983) 1955.
10 C. T. Hung, R. B. Taylor and N. Paterson, *J. Chromatogr.*, 240 (1982) 61.
11 L. J. Pennington and W. F. Schmidt, *J. Pharm. Sci.*, 71 (1982) 951.
12 N. H. C. Cooks and K. Olsen, *J. Chromatogr. Sci.*, 18 (1982) 1.
13 R. Gill, S. P. Alexander and A. C. Moffat, *J. Chromatogr.*, 218 (1981) 639.
14 K. E. Bij, Cs. Horváth, W. R. Melander and A. Nahum, *J. Chromatogr.*, 203 (1981) 65.
15 A. Sokolowski and K.-G. Wahlund, *J. Chromatogr.*, 189 (1980) 299.
16 R. Gill, R. W. Abbott and A. C. Moffat, *J. Chromatogr.*, 301 (1984) 155.
17 Cs. Horváth, W. Melander and I. Molnár, *J. Chromatogr.*, 125 (1976) 129.
18 *The United States Pharmacopeia*, United States Pharmacopeial Convention, Inc., Rockville, MD, 21st rev., 1985.

Journal of Chromatography, 370 (1986) 419–426
Elsevier Science Publishers B.V., Amsterdam — Printed in The Netherlands

CHROM. 19 018

COLUMN POISONING BY MULTIVALENT CATIONS IN ION CHROMATOGRAPHIC ANALYSIS FOR ALKALI METALS

DENNIS R. JENKE
Travenol Laboratories, Inc., 6301 Lincoln Ave, Morton Grove, IL 60053 (U.S.A.)
(Received August 14th, 1986)

SUMMARY

Multivalent cations from the mobile phase, stainless-steel components of the chromatographic system and analyzed samples are not eluted from the analytical column under normal elution conditions used for alkali metal determinations by ion chromatography. Thus the analytical column becomes poisoned during use with the net result that performance degrades with time. Systems properties affected include retention time, resolution, plate count and peak heights while peak areas are unaffected by changing capacity until resolution is compromised. While various methods are proposed for counteracting or preventing the poisoning effect, a technique which couples a protective precolumn to scavenge mobilized metals from steel system components with systematic injection of a flush solution to remove other interfering cations represents the most cost effective option.

INTRODUCTION

Monovalent cations (Na^+, K^+, NH_4^+, organic species) are separated and quantitated by ion chromatography with columns containing low capacity resins and weak acid eluents[1–4]. The elution conditions are such that under these conditions multivalent cations are irreversably bound to the column (regardless of manufacturer or type). Thus multivalent cations present in the chromatographic system will then poison the analytical column. The net result of this column poisoning is degrading chromatographic performance as manifested in decreasing retention, efficiency and resolution but an apparent increase in peak height sensitivity. Primary sources of these multivalent species include: (1) impurities/contaminants in the mobile phase, (2) noninert components of the chromatographic system and (3) components of the sample themselves. The first source is readily circumvented through the use of high-purity reagents for mobile phase preparation. While the second source of column contaminants would readily be eliminated through the use of chemcially inert (*e.g.* Tygon, plastic) pumps, injectors, valves and tubing, such components are relatively uncommon in operating laboratories and are available from a limited number of vendors. Although stainless-steel components of chromatographic systems can potentially be passivated by exposure to more concentrated acids, it is this authors experience that such treatments are not completely effective in eliminating metal leaching during operation.

0021-9673/86/$03.50

Since the multivalent species which commonly cause the column poisoning can be re-mobilized with either stronger acid or complexing flush solutions, column regeneration is relatively easy to accomplish. However, if column poisoning occurs relatively quickly or only small changes in performance can be tolerated in a particular application, complete regeneration of the column must be performed relatively often and becomes cost and time ineffective. It is the purpose of this study to evaluate the magnitude of the column poisoning effect and to explore methods for its elimination/alleviation.

EXPERIMENTAL

Chromatographic system

The system employed included a Perkin Elmer Series 3B pump, a Perkin Elmer LC600 autosampler, a Bio-Rad conductivity monitor, a Linear stripchart recorder, a Dionex CFS-1 fiber suppressor and a Hewlett-Packard 3357 LAS computer integrator. The columns used were all Wescan type 269-024 high-speed cation separators. Automation equipment used for column/solvent switching included Autochrom Model 201 solenoid interface and Model 401 valve module and a Linberg Enterprises Model CD4SN ChronTrol® timer/controller. The mobile phase was 5 m*M* nitric acid supplied at a flow-rate of 2 ml/min. Depending upon application, connecting tubing and sample injector loops were either 316 stainless steel or Tygon.

Chromatographic studies

While exact experimental conditions varied in terms of analyte concentration, sample size and experimental design, the general process involved continuous injection of samples into a specific apparatus; analyte retention time, peak characteristics, peak areas and height were continuously monitored. Chromatographic columns were regenerated at the beginning and end of each analysis set by flushing with 0.1 *M* nitric acid for a period of 30 min followed by re-equilibration with the mobile phase. Both sodium and potassium were used to monitor chromatographic performance; calcium was used as a model to intentionally produce column poisoning. Both nitric acid and EDTA were evaluated in terms of their ability to act as regenerants for the columns.

Reagents

Samples were prepared by several dilutions of stocks prepared from the chloride salts of Na^+, K^+ and Ca^{2+}. Acids used for mobile phase–regenerant preparation were Ultrex® grade. All salts used were reagent grade. Deionized, distilled water was obtained from a Millipore Milli-Q® cartridge system.

RESULTS AND DISCUSSION

As noted previously, the two contributors to the capacity loss mechanism include multivalent cations either leached from the stainless-steel components of the chromatographic system or contained in the samples being characterized. In order to demonstrate the magnitude of these effects, the two processes were isolated and evaluated independently. Considering the latter process, it is common for samples

analyzed for alkali metals at Travenol to contain approximately 10 μg Ca^{2+}/Mg^{2+} per injection. As shown in Fig. 1, the continued injection of a sample containing this amount of Ca^{2+} causes a five-fold increase in the rate at which Na^{+} retention time degrades as compared to a water matrix containing no Ca^{2+}. The small loss of retention which occurs with the water matrix is attributed to leaching of transition metals from the stainless-steel components of the chromatographic system. While this effect was minimized by making all component connections with Tygon tubing, the pump and injector were still steel and thus prone to leaching. It is observed in passing that knowledge of the concentration of Ca^{2+} injected and the absolute loss of retention caused as a result of the injection allows one to estimate the total capacity of the column(s) being used.

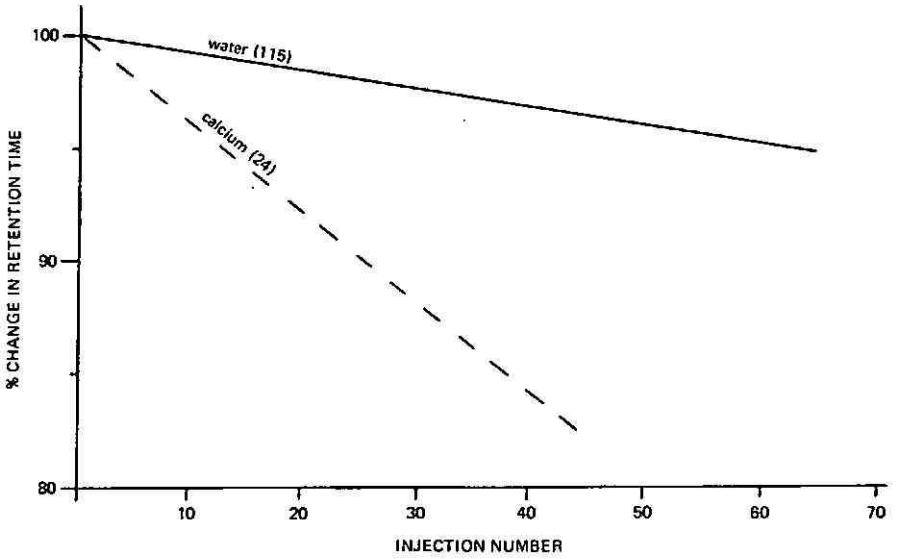

Fig. 1. Effect of sample composition on the rate of retention loss due to column poisoning. Data is for a sample using 60 ppm Na^{+} (the species being followed) in either a water matrix or one containing 40 ppm Ca^{2+}. A chromatographic system with inert tubing was used in this study. The number in brackets indicates the number of injections which produces a 10% loss in retention time.

Since a truly inert chromatographic system was not available to this research to provide a true baseline, it was impossible to assess experimentally the true magnitude of column poisoning by leaching of metals from a typical stainless-steel chromatographic system. However, it was possible to demonstrate the effect of stainless-steel connecting tubing (*versus* inert Tygon). As shown in Fig. 2, the presence of a minimum length of steel tubing increases the rate of column poisoning by nearly a factor of two. The column degradation observed was linearly related to mobile phase flow-rate, did not change in magnitude over the duration of the experiment (indicating no long term passivation is occuring) and was reproducible from column to column.

At this point in the discussion it is appropriate to note that neither type of

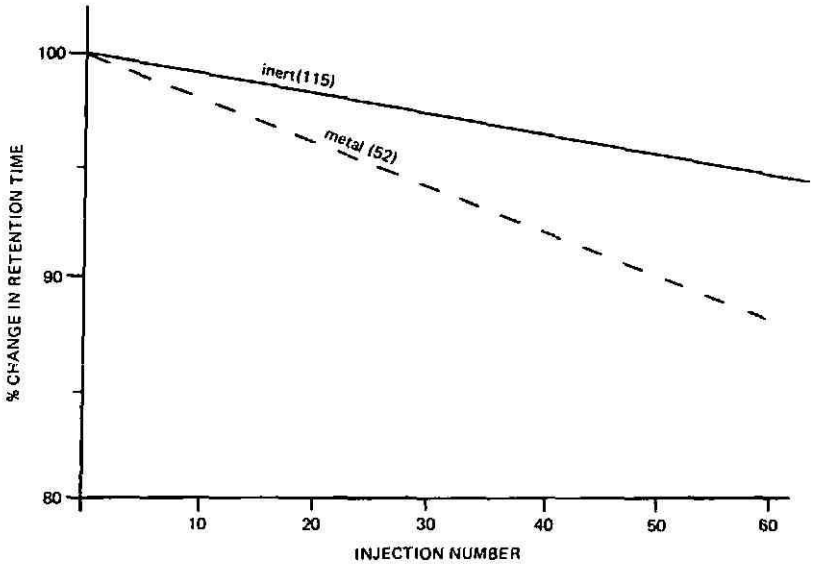

Fig. 2. Effect of the composition of connecting tubing on the rate of retention time loss due to column poisoning. Sample is 60 ppm Na^+ in water. Numbers in brackets indicate the number of injections which produces a 10% loss in retention time.

poisoning is truly irreversible in that both alkaline earth and transition metals can be removed from the column by use of a "stronger" eluent (flush). Appropriate flush solutions might include higher concentration acid (*e.g.* 0.1 *M* nitric acid) or a complexing mobile phase (*e.g.* EDTA). In some applications, the simplest way to deal with the retention loss is to ignore it (since the absolute change per sample is relatively small) and regenerate the column after a given number of injections has been made. Regeneration is accomplised by rinsing the column with one of the flush solutions mentioned above. This approach is appropriate if resolution is not critical, if only a small number of samples are to be analyzed or if peak areas are to be used for quantitation. Most pharmaceutical applications do not conform to these criteria and therefore alternative methods of eliminating/alleviating the problem were examined.

Considering the two loss mechanism separately, it is clear that three ways are potentially applicable for eliminating retention loss caused by multivalent species present in the sample. One approach would be to pretreat the sample prior to analysis (for example by selective extraction and/or precipitation). However, this approach is not time and cost effective and one must be concerned with quantitativeness as well. The latter two approaches fall under the category of column cleaning and differ with respect to quantitation of the column poisoning agent. In one scenario, the column is flushed with a higher concentration mobile phase for the sole purpose of metal removal while in the other (gradient elution) the change in mobile phase composition is such that the poisoning species can be quantitated along with the analyte(s). While in concept both approaches are sound, in practice their need for specialized equipement (gradient controllers, detectors which do not respond to the changing mobile phase) and increased per sample analysis time severly limits their utility.

Focusing on the other source of poisoning, clearly the most effective way to prevent leaching of contaminants from the chromatographic system is for the system to be completely inert. While such a system is now commerically available, it is not currently in exclusive use in cation chromatography. Thus a pertinent question raised in this research is how can one make a conventional stainless-steel system appear to be inert. Obviously, the use of PTFE or plastic connecting tubing represents an important step in this direction; however, as documented earlier, stainless-steel pump and injector components still contribute to column degradation. It is particularly difficult to isolate contaminants from the injector since to do so would require intervention after sample introduction. The intervention must be such that analytical performance is not adversely affected; an appropriate mechanism to accomplish this could not be identified by this researcher. Two aproaches which were examined both deal with pump related effects but differ in their ability to control the injector problem. In one approach, shown in Fig. 3, a pre-column containing a high-capacity cation exchange resin is placed between the pump and injector and serves to scavenge metals leached from the pump. In this study, the column contained a Dowex resin which had been hand-packed into an inert shell. Such a configuration contributes little or no back pressure to the system, cannot effect chromatographic performance, and is capable of effective column protection for long periods of use. This approach has the additional advantages of low cost and instrumental simplicty. The second approach, shown in Fig. 4, also utilizes a pre-column but in this case the column and sample injector can be switched either in or out of the analytical system. For "normal" operation, the pre-column is switched in-line and effectively protects the analytical column as the sample is being chromatographed. During sample introduction, the injector is switched in-line with the net result that the column is essentially unprotected. However, since the introduction process is only a small fraction (0.5% or less) of the total analysis time, column poisoning is minimized. While both these approaches result in a system which is virtually immune from metal poisoning (Fig. 5), the latter approach is instrumentally more complex and is not suggested for routine applications.

From this discussion, it is apparent that in order to deal effectively with both sources of column poisoning one would need to adopt a methodology that uses both protection and sequential flushing. An optimally protected system would thus include inert connecting tubing, a scavenging pre-column between the pump and injector and

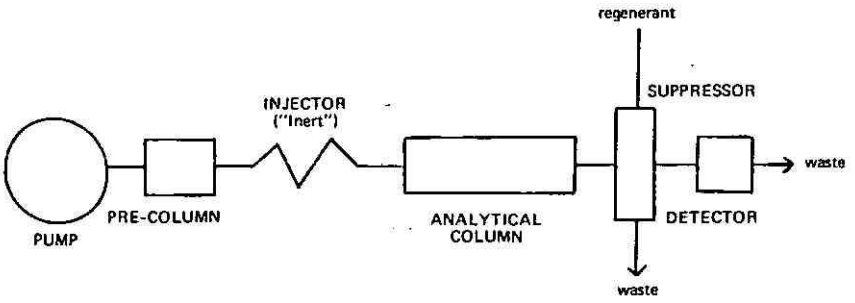

Fig. 3. Schematic diagram of the chromatographic system in which inertness is achieved by use of a scavenging pre-column.

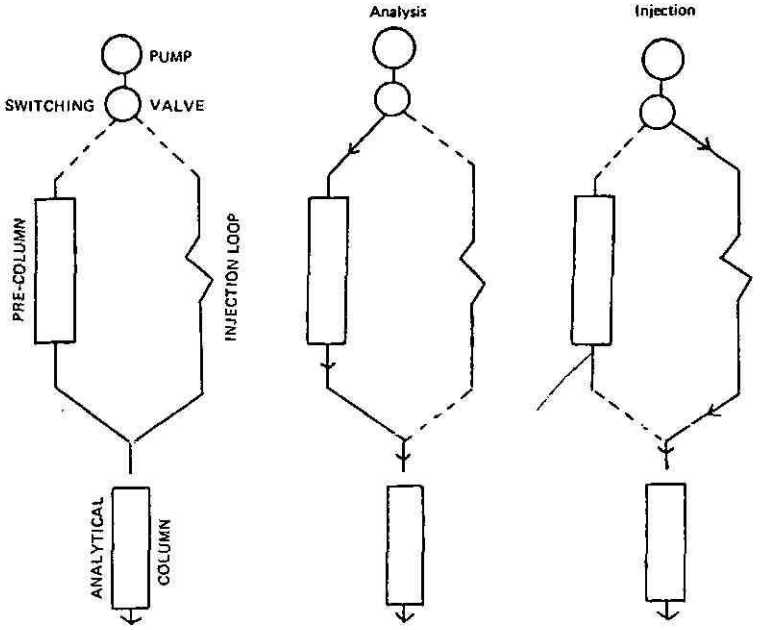

Fig. 4. Schematic diagram showing the approximation of an inert system obtained by switching between a pre-column scavenger and a sample injector.

injection of a flush solution (*e.g.* 0.1 *N* EDTA) at various points during the analytical run (say after every 30 injections of a sample). Thus one can envision a scenario in which the analyst performs a series of sequences which involves 30 sample injections

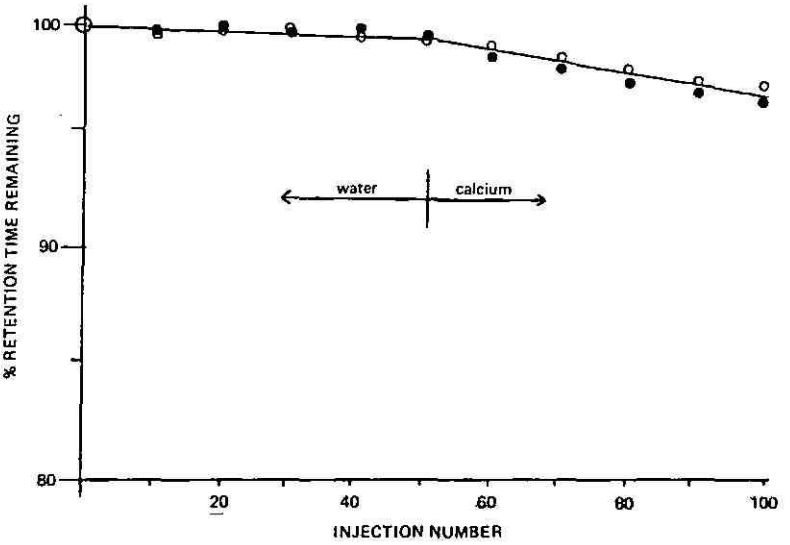

Fig. 5. Performance of both chromatographic systems shown in Figs. 3 and 4. Samples injected contained 200 ppm Na^+ (the species followed) and either water or 40 ppm Ca^{2+} as the matrix. ○ = data from system in Fig. 3; ● = data from system in Fig. 4.

TABLE I

LONG TERM STABILITY OF THE CHROMATOGRAPHIC SYSTEM: ACCURACY

Concentration injected (ppm)	*Actual concentration (ppm)*				
	Flush sequence				
	1	*2*	*3*	*4*	*5*
Sodium					
30	29.5	29.1	30.0	29.5	29.6
70	69.3	69.3	70.5	70.6	69.9
100	98.6	100.7	99.3	100.1	99.6
Potassium					
30	29.1	30.6	30.5	30.0	29.9
70	70.2	70.8	71.3	71.3	70.8
100	101.1	101.9	101.8	101.6	101.5

followed by a duplicate injection of the flush solution and a single injection of mobile phase (to allow total elution of the Na^+ from the EDTA flush) and then repeats this process as often as is necessary to complete his job. In order for this to be an effective strategy, an extremely small change in retention characteristics should be observed over the course of the run, no significant change in response should occur and no intra-sequence bias should exist. In an attempt to address these issues, samples containing 30–100 ppm Na^+ and K^+ in a matrix which was water (standards) or 20 ppm Ca^{2+} (simulated product) were repetitivily analyzed in an extended run which lasted over 27 h and involved 5 flush sequences. Results of the quantitation of samples against standards for each of the five flush sequences are shown in Table I; results obtained in every sequence are statistically equivalent at the 95% confidence level. As shown in Table II, the net change in retention observed over the course of the experiment, which consisted of over 150 injections, was extremely small. Both Na^+ and K^+ retention times changed at a rate of -0.12% per hour. While the peak height response change observed over the course of the experiment was relatively large at nearly 4%, peak area response was statistically equivalent over the entire course of the run and no trend in response was observed.

TABLE II

LONG TERM STABILITY OF THE CHROMATOGRAPHIC SYSTEM: RETENTION

Elapsed time (h:min)	*Retention time (min)*	
	Sodium	*Potassium*
0:00	4.19	8.96
7:05	4.12	8.83
15:08	4.19	9.08
24:03	4.07	8.69
27:10	4.06	8.65

CONCLUSION

Under conditions used to quantitate alkali metals, ion chromatography columns can be poisoned by multivalent cations contained in the samples themselves or leached from the stainless-steel components of conventional chromatographic systems. Utilization of a scavenging pre-column containing a high-capacity cation exchanger placed between the pump and injector coupled with sequential column flushes by injection of EDTA-containing solutions represents an effective solution to the long term degradation in column performance which results from the poisoning process.

REFERENCES

1 C. A. Pohl and E. L. Johnson, *J. Chromatogr. Sci.*, 18 (1980) 442.
2 J. S. Fritz, *LC, Liq. Chromatogr. HPLC Mag.*, 2 (1984) 446.
3 J. R. Benson, *Am. Lab. (Fairfield, Conn.)*, 17 (6) (1985) 30.
4 R. A. Wetzel, C. A. Pohl, J. M. Riviello and J. C. Mac Donald, *Chem. Anal. (N.Y.)*, 78 (1985) 355.

Journal of Chromatography, 370 (1986) 427–437
Elsevier Science Publishers B.V., Amsterdam — Printed in The Netherlands

CHROM. 19 037

ELECTROCHEMILUMINESCENCE AS A DETECTION TECHNIQUE FOR REVERSED-PHASE HIGH-PERFORMANCE LIQUID CHROMATOGRAPHY

III. A HIGH-PERFORMANCE FLOW CELL*

ELIZABETH HILL*, ELIZABETH HUMPHREYS and DAVID J. MALCOLME-LAWES
Centre for Research in Analytical Chemistry and Instrumentation, King's College London, Strand, London WC2R 2LS (U.K.)
(Received July 16th, 1986)

SUMMARY

A new flow cell has been designed and tested for continuous, medium-term use in an electrochemiluminescence detector. It is found that the cell efficiency may be maintained over periods of weeks by careful control of the excitation potential and by incorporating a cleaning agent within the eluent. A number of example chromatograms obtained in the presence of tetrabutyl ammonium chloride as a cleaning agent are reported.

INTRODUCTION

Electrochemiluminescence (ECL) is light emitted during the electrolysis of solutions of (usually) organic compounds. ECL was first observed[1] in 1927, although was not investigated in any detail[2,3] until 1964. There was much interest in the phenomenon throughout the late sixties, with particular emphasis on studies related to the mechanisms involved. During the 1970's the mechanisms were elucidated as the species involved became identified with the aid of electron spin resonance and magnetic field effects. Progress during this period has been thoroughly reviewed and the mechanistic processes summarised[4–6]. In recent years attempts have been made to enhance the ECL intensity observed from dilute solutions, generally to investigate the potential of ECL measurement as an analytical technique. The approaches adopted invariably reflect the requirements of the annihilation mechanism in that the emphasis has been on encouraging the interaction of the anion and cation formed during electrolysis, and on rigorously excluding species such as oxygen and water which are known to quench ECL emissions. ECL has been used as a detection technique for normal-phase liquid chromatography (LC), using a thin cell with tin oxide

* For Part II, see ref. 10.

0021-9673/86/$03.50

transparent electrodes[7,8]. However, the lifetime of the electrodes was said to be limited, and became very short in the presence of water.

We have been investigating the use of ECL as a detection technique for reversed-phase LC using relatively simple electrode assemblies which both avoid the complexity of moving electrodes and have much greater durability than tin oxide electrodes. We reported earlier[9] that a modest sensitivity could be achieved with a relatively simple two-electrode cell arrangement and non-deoxygenated eluents involving 10–20% water. Our initial experiments were carried out with a d.c. electrolysis current and involved flowing liquids through cells in which the electrodes were up to 2 cm apart. The major proportion of the emitted light was found to originate from the vicinity of the anode, even when the anode was upstream of the cathode. The light emission intensity from a given sample was found to be proportional to the total cell current, even at applied voltages up to 100 V d.c. We subsequently reported[10] on the improvement in sensitivity obtained through the use of an a.c. electrolysis potential, and more recently have detailed results obtained from lumograph studies[11], *i.e.* the variations of emission intensity as a function of electrolysis potential and frequency.

Our earlier experiments demonstrated that ECL offered some attractions as a detection technique for reversed phase high-performance liquid chromatography (HPLC), in that many classes of compounds appeared to emit light during electrolysis and the sensitivities for detection in a relatively crude cell were reasonable. However, potential problem areas were observed once the apparatus had been in use for any length of time. The two main problems we have observed are: (1) lack of reproducibility; on some occasions highly reproducible chromatograms could be obtained daily for several days, whereas at other times successive chromatograms differed both in terms of absolute peak height and even in relative peak heights for a multicomponent test sample. (2) Fouling of the flow cell; the first flow cells were glass tubes with pairs of platinum wires passed through the wall. The wires were small (requiring a magnifier for examination) and the electrolysis currents used routinely were small (typically < 1 mA). When we fabricated more substantial cells and operated with higher electrolysis currents and potentials, we found that the electrodes became covered with a brown deposit which, quite apart from lowering the light output, eventually blocked the cell.

Furthermore both problems became progressively worse over a period of about a year. It became clear that the more care we exercised in cleaning electrodes and purifying the components of the eluent, the more rapidly the problems returned. The present work was undertaken in an attempt to overcome these difficulties. We report below on a new flow cell design which allows operation at substantially higher currents than previously, and on new electronic and chemical approaches we have adopted to permit an ECL detector to operate reproducibly for long periods.

EXPERIMENTAL

Fig. 1 shows a block diagram of the elements of the ECL detector used. The major elements are the flow cell, the excitation supply, and the light detection system, and these are described in detail below. The other equipment used consisted of an HPLC pump (Biotech Instruments), a sample loading system (a Rheodyne valve,

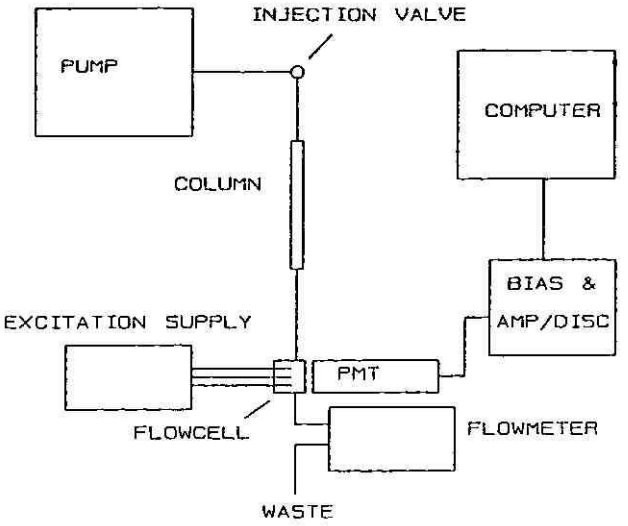

Fig. 1. Block diagram of ECL chromatography system.

Model 7125, fitted with a 20-μl loop), a 25-cm Spherisorb ODS (10 μm) column (Phase Separations), and a digital flow meter (Phase Separations) which monitored the flow-rate post cells. The chromatography was performed using the eluents described for each of the sample chromatograms reported below.

The flow cell design adopted is shown in Fig. 2, and was chosen to provide a large electrode surface area and a constant path length for current flow. The cell body was made from Kel-F, and tapped to accept standard Altex fittings to carry the eluent through 1/16 in. PTFE tubing. The electrodes were prepared from a disk of platinum 1 mm thick and approximately 10 mm in diameter. The disk was cut into two Ds and platinum wire conductors spot welded to each. The electrodes fitted into a circular recess in the cell body, and the conductors passed through narrow holes to the rear of the cell. The face of the cell (*i.e.* the part protruding beyond the recess holding the electrodes) was polished to accept a quartz window, held in position by a securing ring bolted to the cell body. The result was a narrow corridor between the two Ds of platinum, sealed at the rear by the Kel-F body, and at the front by the quartz window. Eluent entered this corridor via a hole drilled at one end of the corridor through to the rear of the cell, although to minimise dead volume we allowed the inlet PTFE tubing to pass through this hole and reach the bottom of the corridor. Eluent left the corridor via a (larger) hole drilled at the other end of the corridor. The dimensions of the corridor were approximately 10 × 1 × 1 mm, giving a cell volume of approximately 10 μl.

The cell was subsequently modified to allow a third electrode to be introduced as close to the corridor region as possible. In this work the third electrode has been a fine platinum wire passed, via an additional Altex connector, into the eluent outlet hole. In practice we position the end of this wire as close to the cell's corridor as possible. This electrode is used to provide a reference level for the control of the working electrode level. While a platinum wire is not normally considered to be

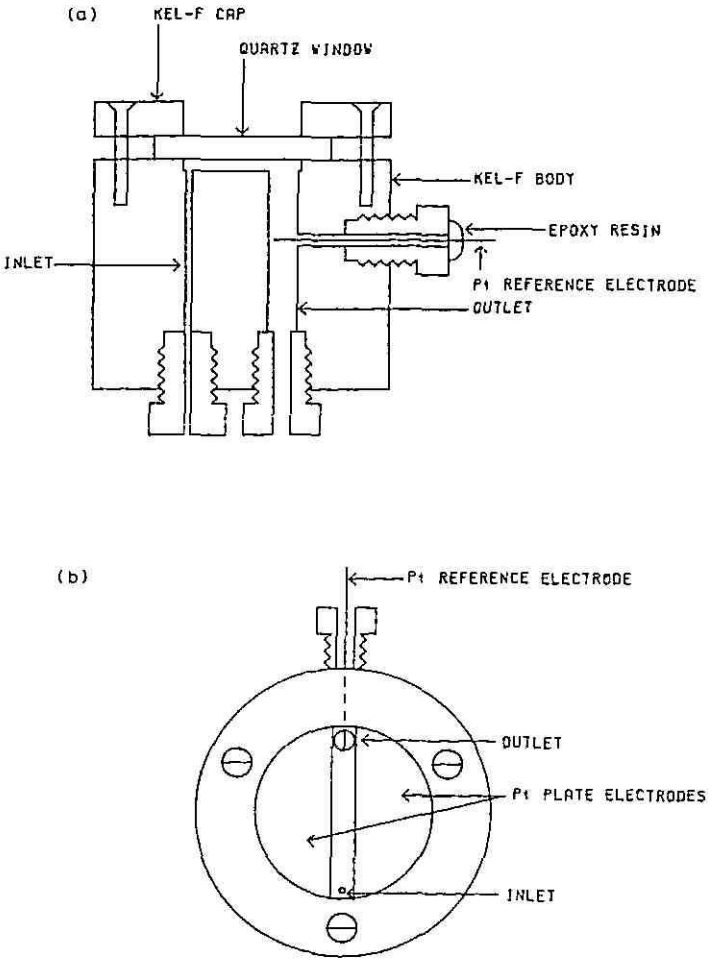

Fig. 2. Diagram of the ECL flow cell used, showing the cautela view (a) and the photomultiplier's view of the electrodes (b). The active volume of the cell is the channel between the electrodes, which in this work had a volume of approximately 10 μl.

adequate as a reference electrode for electrochemical measurements, it does offer the advantage of simplicity and small size, and was found to be useful under the conditions of the present experiments.

The excitation supply system is shown schematically in Fig. 3. The unit maintains one of the electrolysis electrodes at ground potential and sets the potential of the other to a level which causes the potential of the reference electrode to equal a predetermined level. The circuit compares the buffered potential difference between the reference electrode and ground with a level input from a potential divider (adjustable between 0 and 5 V), using the difference to drive one of the two 759 power amplifiers. The amplifier driven, and so the electrode which operates as a cathode, is selected by a 4066 CMOS switch which operates at a frequency determined by an

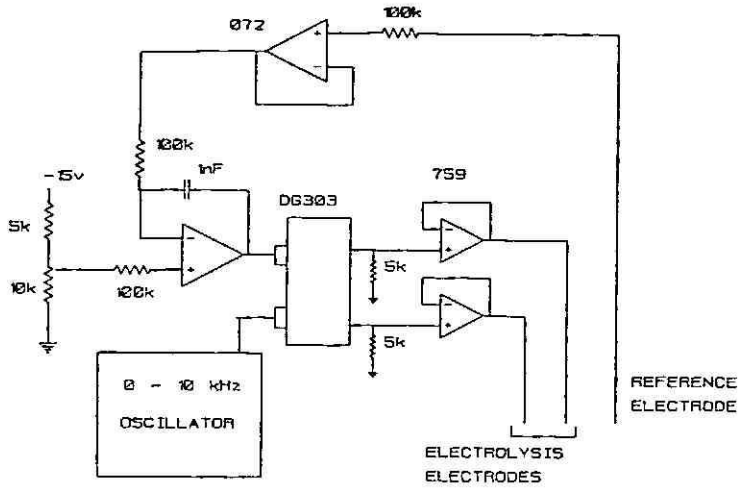

Fig. 3. The electrolysis supply circuit which maintains a constant amplitude for the potential between the electrolysis anode and the reference electrode. The electrolysis electrode acting as anode changes every half cycle. (k = kΩ).

external TTL oscillator, the two switched channels opening and closing alternately. The amplifier which is not driven through the switch has its input pulled to ground through the 10 kΩ resistor, thus ensuring that the appropriate electrolysis electrode (the anode) is operating at ground potential.

The light measurement system is shown in Fig. 4. It consists of a photomultiplier tube (Thorn EMI type 9789QB) together with a low-power bias supply (operated at approximately 1000 V), a preamplifier/discriminator which converts those anode pulses exceeding a preset threshold into TTL compatible logic pulses, and a low-cost microcomputer (Commodore 64) which counts the logic pulses and calculates the pulse rate. Details of the operation of this simple photon counting system have been reported[12].

Errors

The instruments used in recording potentials, current and light levels were calibrated and unlikely to provide significant sources of error for either d.c. elec-

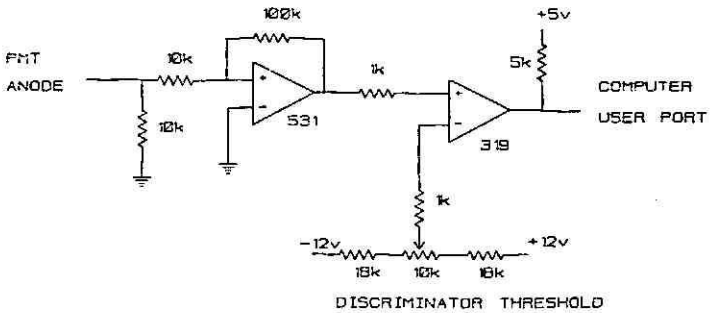

Fig. 4. The ECL intensity measuring system.

trolysis or for square wave electrolysis above 10 Hz. For low-frequency electrolysis the current measurements do fluctuate as the sampling frequency of the multimeter is of the same order as the electrolysis frequency. However, we have taken the maximum values recorded for the purposes of this work. (An alternative technique has been developed for recording currents during lumograph studies, and these will be reported in due course.) For the present we assign error limits of 10% to current reading below 10 Hz. The chromatograms recorded below were reproducible to within 5% from a given set of samples and eluent. Over a period of time and using different batches of eluent and samples, the reproducibility was found to be within 10%.

Materials

The sample materials, purity and manufacturer used in this work are: anthracene, naphthalene, Analar (Fisons); acenaphthylene, chrysene 95% (Aldrich); fluoranthene, 98% (Aldrich); pyrene, perylene, >99% (Aldrich); di-butylphthalate, dihexylphthalate, di-octylphthalate, >98% (Phase Separations Qual-kit). Pesticide samples (courtesy of the Laboratory of the Government Chemist; no detailed purity information available): 1-naphthyl methylcarbamate (carbaryl), 4-chloro-2-butynyl-3-chlorophenylcarbamate (Barban), 1,1,1-trichloro,2,2-bis(4-methoxyphenyl)ethane (methoxychlor), 2,2-bis(4-chlorophenyl)-1,1-dichloroethylene (*p,p'*-DDE), 1,1-bis(4-chlorophenyl)-2,2,2-trichloroethane (*p,p'*-DDT).

All test compounds were used without further purification. Tetrabutylammonium perchlorate (TBAP) was prepared by neutralising a concentrated solution of tetrabutylammonium hydroxide (Aldrich) with AR perchloric acid (Fisons) and was purified by two recrystallisations from ethylacetate–pentane. HPLC-grade acetonitrile (Rathburn Chemicals) was found to have a water content of about 700 ppm. Dry acetonitrile was prepared from HPLC-grade acetonitrile, either by distillation from phosphorus pentoxide or by standing over 3 Å molecular sieve (BDH Chemicals) as discussed in an earlier paper[11]. Distilled water was further purified using a Water-1 purification unit (Gelman Sciences) and filtered through a 0.45-μm, Millipore filter.

RESULTS AND DISCUSSION

We have determined that the formation of the deposit on the platinum electrodes could be prevented by maintaining a concentration of chloride ions in the carrier electrolyte. (A similar effect is produced by bromide ions.) Fig. 5 shows the variation of the signal-to-noise ratio (*i.e.* peak height to r.m.s. noise ratio) for the chromatographic peak produced from 100 ng of naphthalene eluted at 2 ml min^{-1} using an eluent of acetonitrile–water (95:5), with the concentration of added chloride, in the form of tetrabutylammonium chloride. (Electrolysis electrode–reference electrode potential difference 7 V and electrolysis frequency 5 Hz.) The ratio was determined from the average of six successive sample injections over a fixed period of 1 h. Thus variations in peak height (and we have found that reductions in the peak heights of successive peaks are a reliable indication that deposit is forming) show up as a reduction in the signal-to-noise ratio. The results indicate that a concentration of tetrabutyl ammonium chloride of less than $5 \cdot 10^{-4}$ *M* is insufficient to prevent

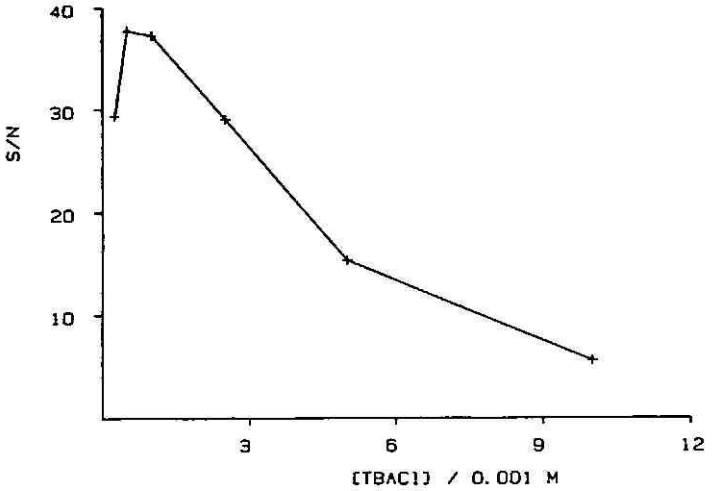

Fig. 5. Variation of the signal-to-noise ratio (S/N) recorded from 100 ng samples of naphthalene as a function of tetrabutylammonium chloride (TBACl) concentration in an acetonitrile–water (95:5) eluent. See text for chromatographic and ECL details.

the formation of deposit, and that much higher concentrations, while preventing the formation of deposit, also reduce the intensity of ECL emission from the sample. Similar results have been obtained using other sample materials. From these results we selected $5 \cdot 10^{-4}$ *M* as the optimum concentration of tetrabutylammonium chloride for this particular eluent.

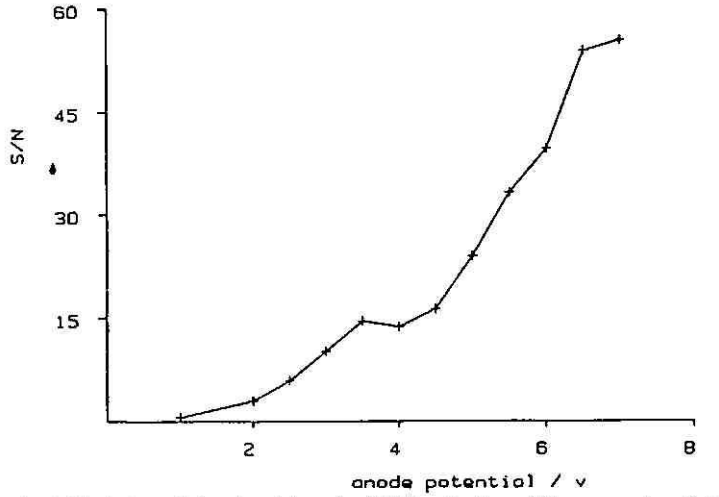

Fig. 6. Variation of the signal-to-noise (S/N) ratio from 100 ng samples of naphthalene as as function of the electrolysis anode–reference electrode potential difference at an electrolysis frequency of 5 Hz. See text for eluent details.

The variation of the signal-to-noise ratio recorded from the same sample and an eluent of acetonitrile–water (95:5), made $5 \cdot 10^{-3}$ *M* in tetrabutylammonium perchlorate and $5 \cdot 10^{-4}$ *M* in tetrabutylammonium chloride, as a function of the amplitude of the electrolysis electrode–reference electrode potential difference is shown in Fig. 6. Again the eluent flow-rate was 2.0 ml min^{-1} and the electrolysis frequency was 5 Hz. The maximum potential difference which can be generated by our present a.c. potentiostat is 7 V (corresponding to an electrolysis voltage of about 10 V), and the results of Fig. 6 indicate that it may be desirable to go to somewhat

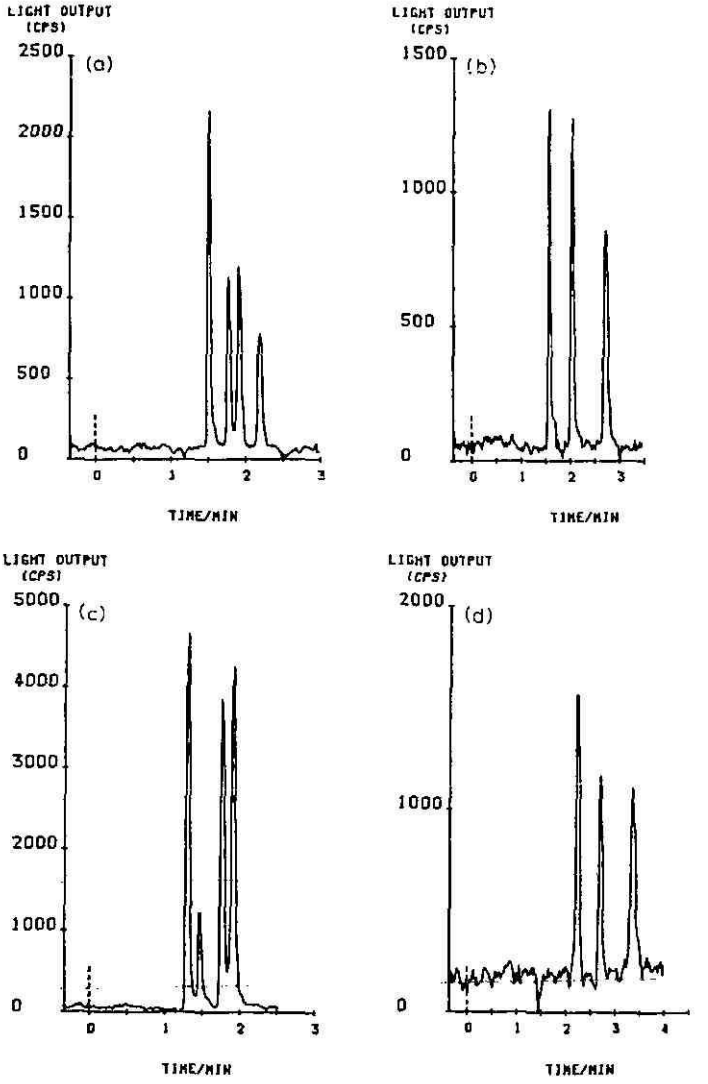

Fig. 7. Typical chromatograms recorded using the ECL flow cell of Fig. 2 in the presence of chloride. (a) *ca.* 27 ng each of naphthalene, anthracene, fluoranthene and chrysene; (b) *ca.* 14 ng each of acenaphthylene, pyrene and perylene; (c) carbaryl (96 ng), methoxychlor (150 ng), DDT (295 ng) and DDE (54 ng); (d) *ca.* 500 ng each of di-butyl, di-hexyl and di-octyl phthalates.

higher potentials. The chromatograms reported below were obtained with an electrolysis electrode-reference electrode potential difference of 7 V.

Some typical ECL chromatograms obtained using the eluent and potential described above are shown in Fig. 7, and serve to illustrate a selection of the materials which may be detected by ECL. Fig. 7a shows a chromatogram obtained from a sample of polynuclear aromatic hydrocarbons, consisting of (in order of elution), naphthalene (26.9 ng), anthracene (29.5 ng), fluoranthene (26.8 ng) and chrysene (28.4 ng). Fig. 7b shows the separation of acenaphthylene (13.6 ng), pyrene (14.8 ng) and perylene (13.4 ng). Fig. 7c shows a chromatograms from a sample of pesticides, consisting of carbaryl (96 ng), methoxychlor (150 ng), *p,p'*-DDT (295 ng) and *p,p'*-DDE (54 ng), eluted using the same conditions. Fig. 7d shows the separation of a series of phthalate esters, di-butyl (507 ng), di-hexyl (542 ng) and di-octyl (720 ng), recorded using an eluent of acetonitrile made $5 \cdot 10^{-3}$ *M* in tetrabutylammonium perchlorate and $5 \cdot 10^{-4}$ *M* in tetrabutylammonium chloride, with an electrolysis electrode–reference electrode potential difference of 7 V and an electrolysis frequency of 60 Hz.

Although we are still seeking improvements in sensitivity, we are encouraged by the reproducibility of chromatograms. Fig. 8 shows a pair of chromatograms recorded from the same sample solution four weeks apart (the system was in virtually full time use in between). This result is typical of many others and indicates that the electrodes may be maintained in a relatively constant condition by the use of chloride ion in the eluent during electrolysis. An important consequence of the improvement in the consistency of the condition of the electrodes is that the linearity of response as a function of sample size has also improved considerably. Fig. 9 shows how the integrated peak area (*i.e.* the total number of photons detected, corrected for back-

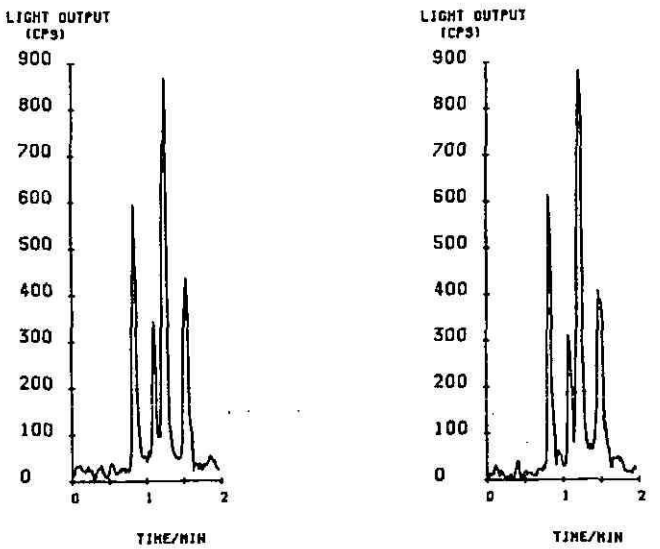

Fig. 8. Two ECL chromatograms recorded from a mixture of naphthalene, anthracene, fluoranthene and chrysene four weeks apart, illustrating the medium term reproducibility of the system when used with chloride containing electrolyte.

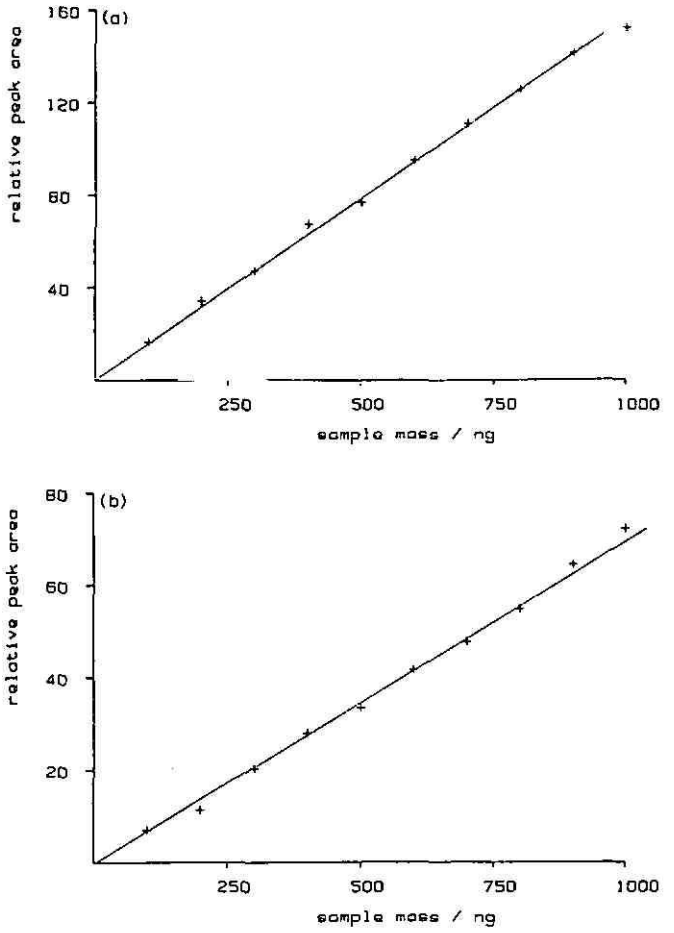

Fig. 9. Variation of peak area as as function of sample size for samples of (a) naphthalene and (b) Barban. Elution conditions as in Fig. 7.

ground) varies with the mass of sample injected for an aromatic hydrocarbon (naphthalene, Fig. 9a) and a pesticide (Barban, Fig. 9b), over the range 10–1000 ng.

ACKNOWLEDGEMENTS

This work was supported by the Science and Engineering Research Council and BP Sunbury Research Centre. DJM-L is a Royal Society Research Fellow in the Physical Sciences. The authors thank Johnson Matthey Ltd. for the loan of platinum metal for the fabrication of electrodes, and the Laboratory of the Government Chemist for the provision of some sample materials.

REFERENCES

1 R. T. Dufford, D. Nitingale and L. W. Gaddum, *J. Am. Chem. Soc.*, 49 (1927) 1858.
2 D. M. Hercules, *Science (Washington, D.C.)*, 145 (1964) 808.
3 R. E. Visco and E. A. Chandross, *J. Am. Chem. Soc.*, 86 (1964) 5350.
4 A. J. Bard, C. P. Keszthelyi, H. Tachikawa and N. E. Tokel, in M. J. Cormier, D. M. Hercules and J. Lee (Editors), *Chemiluminescence and Bioluminescence*, Plenum Press, New York, 1973.
5 L. R. Faulkner and A. J. Bard, *Electroanal. Chem.*, 10 (1977) 1.
6 S.-M. Park and D. A. Tryk, *Rev. Chem. Intermed.*, 4 (1981) 43.
7 H. Schaper, *J. Electroanal. Chem.*, 129 (1981) 335.
8 H. Schaper and E. Schnedler, *J. Phys. Chem.*, 86 (1982) 4380.
9 C. Blatchford and D. J. Malcolme-Lawes, *J. Chromatogr.*, 321 (1985) 227.
10 C. Blatchford, E. Humphreys and D. J. Malcolme-Lawes, *J. Chromatogr.*, 329 (1985) 281.
11 C. Blatchford and D. J. Malcolme-Lawes, *J. Chem. Soc., Faraday Trans. 2*, 82 (1986) 423.
12 E. Humphreys and D. J. Malcolme-Lawes, *Laboratory Microcomputer*, 5 (1986) 56.

Journal of Chromatography, 370 (1986) 439–447
Elsevier Science Publishers B.V., Amsterdam — Printed in The Netherlands

CHROM. 19 039

METALLIC COPPER-CONTAINING POST-COLUMN REACTOR FOR THE DETECTION OF THIRAM AND DISULFIRAM IN LIQUID CHROMATOGRAPHY

H. IRTH*, G. J. DE JONG, U. A. Th. BRINKMAN and R. W. FREI
Free University of Amsterdam, Department of Analytical Chemistry, De Boelelaan 1083, 1081 HV Amsterdam (The Netherlands)
(Received August 27th, 1986)

SUMMARY

A reaction detector has been developed for the selective detection of thiram and disulfiram. The detection is based on the post-column complexation of these analytes on a solid-state reactor packed with finely divided metallic copper to form a coloured copper complex, copper(II) N,N-dimethyldithiocarbamate, with an absorption maximum at 435 nm. The method is combined with a pre-concentration and clean-up step on a pre-column to permit the sub-ppb determination of, *e.g.*, thiram in surface water samples or disulfiram in urine. Separation is achieved by reversed-phase liquid chromatography.

INTRODUCTION

A major portion of the world fungicide use is represented by dithiocarbamates and their derivatives, the so-called thiuram disulphides[1]. Compounds such as thiram, ferbam and ziram (Fig. 1) are widely used as protective fungicides in agriculture. Other uses of dithiocarbamates are as accelerators in rubber vulcanization and, specifically, of disulfiram as a drug against alcohol abuse[2].

A review of the chemistry of this important group of compounds has been given by Thorn and Ludwig[2]. One characteristic property of the dithiocarbamates is their ability to form strong metal complexes with a wide variety of metal ions[3,4].

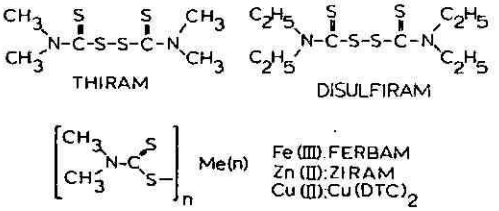

Fig. 1. Structures of the most important dithiocarbamate fungicides.

0021-9673/86/$03.50

Hence, they are widely applied in heavy metal analysis[5,6]. On the other hand, some photometric methods for the determination of dithiocarbamates and thiuram disulphides are based on their complexation reaction with metal ions such as copper(II). The intensely yellow coloured copper(II) dithiocarbamate has an analytically useful absorption maximum at 435 nm[2,7].

Gas chromatographic methods for the determination of dithiocarbamates are mostly based on the determination of carbon disulphide, which is produced by acidic digestion of the dithiocarbamates[7]. In recent years, several high-performance liquid chromatographic (HPLC) methods have been developed. Kirkbright and Mullins[8] used cetyltrimethylammonium bromide (cetrimide) in the mobile phase to achieve the separation of sodium dimethyl- and diethyldithiocarbamate and thiuram disulphides. Smith *et al.*[9] separated dithiocarbamates and thiuram disulphides as their nickel(II) and cobalt(II) complexes. Brandšteterová and co-workers[10,11] determined dithiocarbamate fungicides by normal- and reversed-phase chromatography with UV detection. Gustafsson and Thompson[12] determined thiram in food by HPLC with UV detection at 272 nm after extraction with chloroform and clean-up on a silica gel column.

Generally, the methods described are rather non-selective. UV detection, which was employed in all HPLC methods, requires several clean-up steps such as purification on silica gel, if contaminated samples are to be analysed. The aim of this work was to develop a selective analytical method for the most widely used fungicide of this group, thiram, in order to allow its determination in environmental or biological matrices without complicated sample pre-treatment. The method is based on the liquid chromatographic separation and the post-column derivatization of thiram with metallic copper. Furthermore, investigations were carried out on the pre-concentration of thiram on C_{18}-bonded silica and its stabilization in water samples to avoid losses due to complexation reactions with metal ions. In addition, some preliminary investigations were carried out to demonstrate the feasibility of this method for the determination of disulfiram in urine.

EXPERIMENTAL

Chemicals

Thiram (tetramethylthiuram disulphide) and disulfiram (tetraethylthiuram disulphide) were purchased from Fluka (Buchs, Switzerland) and were of 98% purity. Sodium N,N-dimethyldithiocarbamate [Na(DTC)] and EDTA were supplied by EGA Chemie (Steinheim, F.R.G.). All other organic chemicals were of analytical-reagent grade (Baker, Deventer, The Netherlands). Copper(II) sulphate, copper(I) chloride, calcium chloride and potassium citrate were Baker Analyzed Reagents. Sodium borohydride was of 99% purity (Baker).

Copper(II) N,N-dimethyldithiocarbamate [$Cu(DTC)_2$] was prepared by adding a 1 m*M* solution of copper(II) sulphate to a 2 m*M* aqueous solution of Na(DTC) in 10 m*M* phosphate buffer (pH 6.8). After the reaction, an aqueous 10 m*M* solution of EDTA and potassium citrate was added to avoid the formation of $Cu(DTC)^+$ due to the reaction of $Cu(DTC)_2$ with excess of Cu^{2+} ions. This positively charged 1:1 complex could not be chromatographed in a reversed-phase HPLC system. Injections of the poorly soluble $Cu(DTC)_2$ were made from fresh solutions to avoid precipi-

tation. Solutions of copper(I) chloride (10 m*M*) were made in 0.1 *M* acetate buffer (pH 4.5) containing 0.1 *M* calcium chloride [which was added to increase the solubility of copper(I) chloride] and used directly after preparation.

Instrumentation

The HPLC system (Fig. 2) consisted of a Hewlett-Packard (Waldbronn, F.R.G.) 1090 liquid chromatograph and a 200 × 2.1 mm I.D. stainless-steel column packed with 5 μm Hypersil ODS (Shandon Southern, Cheshire, U.K.). A Zeiss (Oberkochen, F.R.G.) PM2 DLC spectrophotometer or a Hewlett-Packard 1040 diode array detector was used as the detector at a detection wavelength of 435 nm. The pre-concentration pump was an Orlita (Giessen, F.R.G.) pump used at a flow-rate of 1.0 ml/min. Enrichment was carried out on laboratory-made[13] 4.0 × 2.1 mm I.D. pre-columns, which were hand-packed with a slurry of 5 μm LiChrosorb RP-18 (E. Merck, Darmstadt, F.R.G.) in methanol using a syringe. For the post-column reactor the same type of pre-columns of length 2.0 and 4.0 mm and I.D. 2.1 mm were used. In the pre-column derivatization mode, injections of the derivatization reagent were made with a 500-μl loop connected to a laboratory-made six-port injection valve. Acetonitrile–aqueous acetate buffer (10 m*M*, pH 5.0) (65–75:25–35) was used as the HPLC mobile phase.

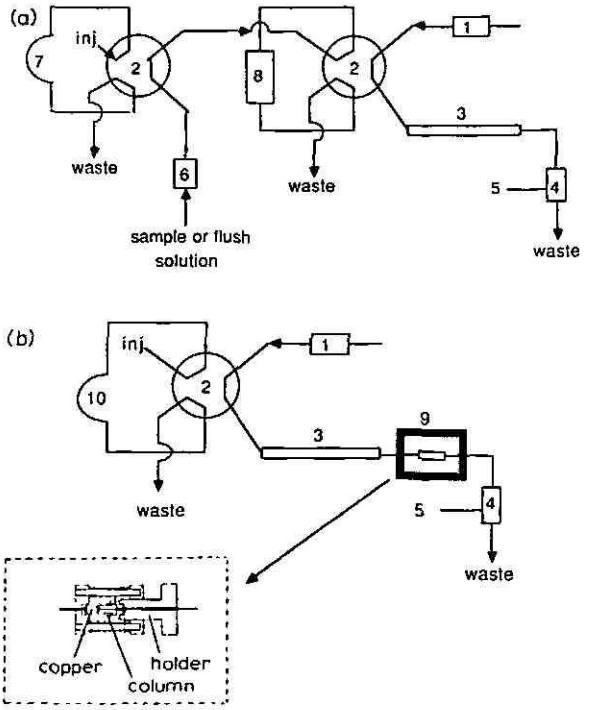

Fig. 2. Schematic diagram of the apparatus. 1 = HPLC pump; 2 = six-port injection valve; 3 = analytical column; 4 = detector; 5 = recorder/integrator. (a) Pre-column derivatization: 6 = pump; 7 = 500-μl loop; 8 = pre-column packed with C_{18}-bonded silica. (b) Post-column derivatization: 9 = copper post-column reactor; 10 = 10-μl injection loop.

Procedure for the pre-column derivatization system (Fig. 2a)

As a first step, thiram was pre-concentrated on a pre-column packed with C_{18}-bonded silica. Subsequently, 500 μl of 10 m*M* copper(I) chloride solution were injected on to the pre-column to form $Cu(DTC)_2$. After flushing the system with 10 m*M* EDTA to remove excess of copper(I) chloride, the $Cu(DTC)_2$ was eluted on-line to the chromatographic system.

Procedure for the post-column derivatization system (Fig. 2b)

Derivatization was carried out using a solid-state reactor filled with metallic copper prepared by reduction of copper(I) chloride. The reactor consisted of 2.0 or 4.0 mm long columns, which are conventionally used as pre-concentration columns. The metallic copper was prepared by carefully adding 1 g of solid copper(I) chloride to a solution of 2 g of sodium borohydride in 20 ml of doubly distilled water. The resulting (black) copper modification was washed twice with doubly distilled water and methanol to remove remaining borohydride and borate. It was suspended in methanol and treated in an ultrasonic bath to give fine particles. The slurry was then dried on tissue paper and pressed as densely as possible into the column with a micro-spatula. The post-column reactor was used immediately after preparation in order to avoid inactivation of the reactive reduced copper due to oxidation to copper(II) oxide.

RESULTS AND DISCUSSION

Derivatization principle

Fig. 3 shows the main reactions of the thiuram disulphides with copper compounds. Fredga[14] described the reaction of disulfiram with copper bronze (reaction 1), which yields $Cu(DTC)_2$. With longer reaction times and in the presence of an excess of copper bronze, Cu(DTC) was formed (reaction 2)[15,16]. This again reacts rapidly with thiuram disulphides to form $Cu(DTC)_2$ (reaction 3)[16]. The same product was obtained if copper(I) compounds such as copper(I) iodide were used instead of copper bronze (reaction 4)[16].

The copper(II) dithiocarbamate complex that is formed in this reaction has an absorption maximum at 435 nm with $\varepsilon = 13000$ in CCl_4 (see spectra in Fig. 4).

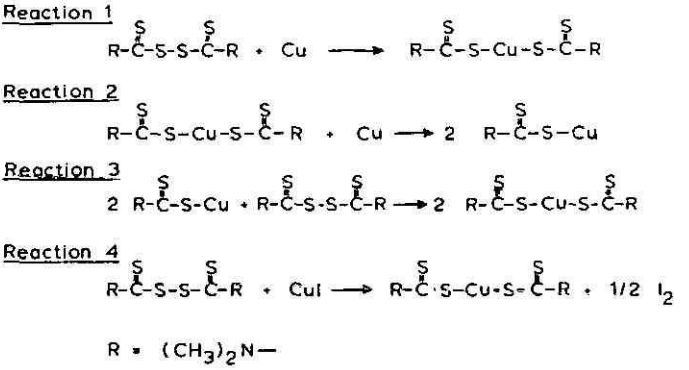

Fig. 3. Main reactions of thiuram disulphides with copper compounds.

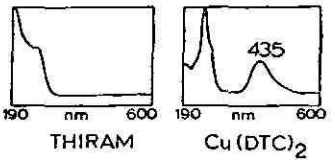

Fig. 4. UV–VIS absorption spectra of thiram and copper(II) dimethyldithiocarbamate.

Hence the transformation of the colourless thiuram disulphides into coloured derivatives offers an elegant possibility of enhancing the selectivity of the method, with almost the same sensitivity as UV detection at 254 nm.

Pre-column derivatization

Initially, copper(I) chloride was used as a derivatization reagent, as batch experiments had shown that thiram reacts rapidly and quantitatively with this compound. The formation of $Cu(DTC)_2$ was confirmed by comparison of the absorption spectrum of the reaction product with that of a standard $Cu(DTC)_2$ solution.

The above reaction was shown to be suitable for the on-pre-column derivatization of thiram (Fig. 2a). After pre-concentrating the non-polar thiram on C_{18}-bonded silica, $Cu(DTC)_2$ was easily formed by rinsing the pre-column with a small volume of a copper(I) chloride solution. Because of its low polarity, $Cu(DTC)_2$ was readily adsorbed on the pre-column; it was eluted to the chromatographic system after flushing the pre-column with 2 ml of 10 m*M* EDTA solution to remove excess of copper(I) chloride. With this method a mean recovery of 93.5% with a relative standard deviation (R.S.D.) of 9.5% ($n = 5$) was obtained. In addition to the poor reproducibility and the relatively complex instrumentation required, the pre-column derivatization has the disadvantage that no distinction can be made between thiram and other possible fungicidal metal dithiocarbamates such as ferbam or ziram, which also react with copper(I) chloride to form $Cu(DTC)_2$. In order to overcome these drawbacks, a post-column derivatization system based on a solide-state reactor was developed.

Post-column derivatization

Attempts to use copper(I) chloride mixed with C_{18}-bonded silica as a solid derivatization reagent were unsuccessful owing to the instability of copper(I) chloride towards the HPLC eluent. Further, it was found that red metallic copper reacted only slowly with thiram and therefore was not suitable in a post-column derivatization system. The reaction rate could be increased considerably, however, if the post-column reactor was packed with metallic copper prepared by the reduction of copper(I) salts with sodium borohydride. The instantaneous and quantitative formation of $Cu(DTC)_2$ using this reduced copper as a derivatization reagent was confirmed by recording the absorption spectra of the $Cu(DTC)_2$ peak using the diode array detector.

Optimization of the reactor performance

Influence of reactor bed length and eluent conditions. The reactor bed length and the pH of the eluent are the most important factors influencing the response of

the post-column reactor. Optimal results were obtained with 2.0–4.0 mm long columns (2.1 mm I.D.) and eluent flow-rates between 0.2 and 0.4 ml/min. A column longer than 4.0 mm resulted in a decreased response, possibly owing to catalytical degradation of $Cu(DTC)_2$. Flow-rates higher than 0.4 ml/min led to pressure drops greater than 300 bar for the total system and were therefore not suitable for the described chromatographic system.

The optimal pH of the eluent was between 4.5 and 6.0, under which conditions the thiram response remained almost constant. The response increased slightly if the pH was decreased; however, dithiocarbamates and thiuram disulphides are less stable at low pH[3]. pH values higher than 7.0 caused deactivation of the copper reactor, probably owing to (hydr)oxide formation. The same effect was observed when a phosphate buffer was present in the eluent [formation of copper(II) phosphate]. Acetonitrile was the only organic modifier that was used. A methanol-containing eluent led to a decreased column efficiency and to deactivation of the reduced copper. With an eluent consisting of acetonitrile and aqueous acetate buffer (10 m*M*, pH 5.0), optimal reactor performance was obtained.

Band broadening and stability of the reactor. The use of the post-column reactor did not cause substantial additional band broadening, as no retention takes place and only a small residence time is required. The increase in the peak width at half-height was 10% (with $\sigma_{reactor}$ = 2.1 s). In addition, the demands on column efficiency are not too high owing to the high inherent selectivity of the detection method. If the post-column reactor is used for several days, the asymmetry factor increases from 1.3 to 2.5 or more; it can therefore be used to monitor the gradual depletion of reduced copper in the reactor. The useful lifetime of the post-column reactor is determined by the amount of thiuram disulphides injected and by the presence of oxygen, which causes passivation. Typically, with a 2.0 mm long post-column reactor that contains about 8 mg of reduced copper, more than 200 injections of nanogram amounts can be made.

Stabilization of thiram samples against complexation reactions

A problem in the determination of dithiocarbamates is their instability in aqueous solutions in the presence of metal ions[3]. In environmental samples and particularly in surface water, the reaction with metal ions such as Cu^{2+} can lead to a considerable reduction in the free dithiocarbamate concentration within a short time. Our experiments have shown that the addition of 0.1 m*M* copper(II) sulphate to a solution containing 35 ppm of thiram resulted in a 50% decrease in the thiram concentration after 20 min. As dithiocarbamates and, to a lesser extent, thiuram disulphides possess a high affinity to many metal ions[3], the presence of these ions will generally lead to a rapid decrease in the free thiram concentration. Owing to the high complex stability constants of the metal dithiocarbamates and, especially, $Cu(DTC)_2$[3,17], complexing reagents such as EDTA, tartrate or citrate cannot compete against this complexation reaction. However, it was found that a 1:1 mixture of 10 m*M* EDTA and 10 m*M* potassium citrate was able to prevent the complexation reaction of thiram with Cu^{2+}. If a thiram sample was stabilized with this mixture, no significant losses were observed, even if the sample was stored for 16 h. Water samples were thus routinely stabilized with 10 m*M* EDTA–citrate (1:1) prior to analysis.

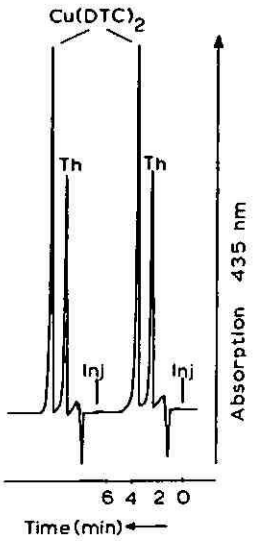

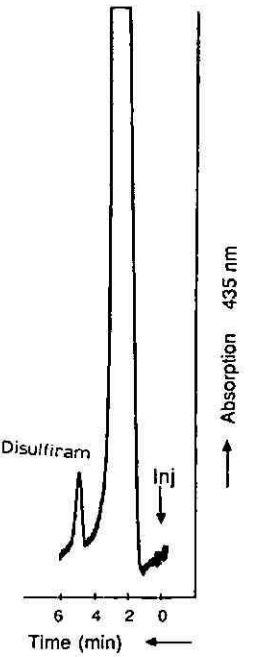

Fig. 5. Chromatogram of the duplicate injection of surface water spiked with 10 ppm of thiram and 20 ppm of $Cu(DTC)_2$. HPLC conditions: analytical column, 200 × 2.1 mm I.D. packed with 5 μm Hypersil ODS; copper reactor, 2.0 × 2.1 mm; eluent, acetonitrile–aqueous acetate buffer (10 m*M*, pH 5.0) (70:30); flow-rate, 0.3 ml/min; injection volume, 20 μl; detection wavelength, 435 nm.

Fig. 6. Determination of disulfiram in urine. HPLC conditions: analytical column, 200 × 2.1 mm I.D. packed with 5 μm Hypersil ODS; pre-column, 4.0 × 2.1 mm I.D. packed with 5 μm LiChrosorb RP-18; copper reactor, 2.0 × 2.1 mm; eluent, acetonitrile–aqueous acetate buffer (10 m*M*, pH 5.0) (65:35); flow-rate, 0.4 ml/min; detection wavelength, 435 nm (0.02 a.u.f.s.). Pre-concentration of 1.0 ml of urine spiked with 87 ppb of disulfiram (sample stabilized with 10 m*M* EDTA–citrate).

Analysis and pre-concentration of thiram samples

The calibration graph obtained using a 2.0 mm long copper-containing post-column reactor showed good linearity over almost three orders of magnitude with $r = 0.9992$. An absolute detection limit of 3.0 ng (signal-to-noise ratio = 3; 10 μl injection) was obtained. The mean R.S.D. was generally less than 2% ($n = 5$) at concentrations between 1 and 200 ppm. Fig. 5 shows the analysis of surface water spiked with 10 ppm of thiram and 20 ppm of $Cu(DTC)_2$. $Cu(DTC)_2$ is one of the main degradation products of thiram if Cu^{2+} is present. Using the copper-containing post-column reactor both compounds can be separated and detected at 435 nm.

In order to decrease the detection limit for thiram, the possibility of its pre-concentration on hydrophobic materials was investigated. As thiram is fairly non-polar, high enrichment factors can be obtained. A breakthrough volume for a 4.0 × 2.1 mm I.D. pre-column packed with 5 μm C_{18}-bonded silica of more than 50 ml was measured with a standard solution. This means that an enrichment factor of at least 5000 can be obtained compared with 10-μl injections. That is, thiram concentrations at the sub-ppb level can easily be determined. Pre-concentration of 40 ml of

a 5 ppb thiram solution resulted in a mean recovery of 93.4% with an R.S.D. of 5.0% ($n = 5$).

Determination of disulfiram in urine

The applicability of the proposed method for the determination of thiuram disulphides in urine was also studied. With the use of the copper-containing post-column reactor no complicated sample pre-treatment was required. Filtered urine was spiked with 87 ppb of disulfiram and stabilized with 10 m*M* EDTA–citrate. A 1-ml volume of the undiluted sample was pre-concentrated on a 4.0 mm long pre-column packed with C_{18}-bonded silica and then eluted to the chromatographic system with acetonitrile–aqueous 10 m*M* acetate buffer (65:35). With UV detection at 254 nm only one large band could be seen without the possibility of isolating the analyte signal. In contrast, the use of the copper-containing post-column reactor and detection at 435 nm allowed sufficient separation of the disulfiram peak for correct quantification (Fig. 6). Further work on the optimization of the method is in progress.

CONCLUSION

A post-column reactor packed with metallic copper offers the possibility of determining thiuram disulphides such as thiram and disulfiram selectively in complex samples. The conversion of thiram and disulfiram into the corresponding $Cu(DTC)_2$ is instantaneous and complete. A detection limit of 3 ng was obtained for thiram at 435 nm with a relatively old detector. Use of a modern detector will easily yield about 10-fold lower detection limits. The long lifetime of the post-column reactor allows the analysis of a large number of samples before a new reactor column is required. Owing to the selectivity of the detection wavelength, only short analysis times are required (3–5 min).

Trace enrichment of aqueous samples coupled to this detection mode can be powerful. The relatively low polarity of thiuram disulphides permits sample volumes larger than 50 ml to be pre-concentrated on 4-mm bed lengths of reversed-phase materials, yielding trace enrichment factors of over 5000. In addition, the method can be automated and, thus, permits the fast work-up of large series of samples in routine screening. The reaction principle can conceivably be used for many other chelate-forming analytes with fast reaction kinetics and favourable detection characteristics of the resulting complexes.

ACKNOWLEDGEMENT

The loan of the HPLC equipment and a diode array detector from Hewlett-Packard is gratefully acknowledged.

REFERENCES

1 N. R. McFarlane, *Herbicides and Fungicides*, Chemical Society, London, 1977.
2 G. Thorn and R. A. Ludwig, *The Dithiocarbamates and Related Compounds*, Elsevier, Amsterdam, 1962.
3 A. Hulanicki, *Talanta*, 14 (1967) 1371.
4 D. D. Perrin, *Stability Constants of Metal-Ion Complexes*, Pergamon Press, Oxford, 2nd ed., 1978.

5 G. Schwedt, *Chromatographia*, 12 (1979) 289.
6 A. M. Bond and G. G. Wallace, *Anal. Chem.*, 56 (1984) 2085.
7 J. H. Karchmer, *The Analytical Chemistry of Sulfur and its Compounds, Part II*, Wiley, New York, 1971.
8 G. F. Kirkbright and F. G. P. Mullins, *Anal. Chim. Acta*, 156 (1984) 279.
9 R. M. Smith, R. L. Moraji and W. G. Salt, *Analyst (London)*, 106 (1984) 129.
10 E. Brandšteterová, J. Lehotay, O. Liška, J. J. Garaj and I. Zacsik, *J. Chromatogr.*, 286 (1984) 339.
11 E. Brandšteterová, J. Lehotay, O. Liška and J. J. Garaj, *J. Chromatogr.*, 291 (1984) 439.
12 K. H. Gustafsson and R. A. Thompson, *J. Agric. Food Chem.*, 29 (1981) 729.
13 C. E. Goewie, M. W. F. Nielen, R. W. Frei and U. A. Th. Brinkman, *J. Chromatogr.*, 301 (1984) 325.
14 A. Fredga, *Recl. Trav. Chim. Pays-Bas*, 69 (1950) 417.
15 S. Akerstrom, *Acta Chim. Scand.*, 10 (1956) 699.
16 S. Akerstrom and P. E. B. Lindahl, *Acta Chim. Scand.*, 16 (1962) 1206.
17 M. J. Janssen, *Recl. Trav. Chim. Pays-Bas*, 75 (1957) 827.

Journal of Chromatography, 370 (1986) 449–464
Elsevier Science Publishers B.V., Amsterdam — Printed in The Netherlands

CHROM. 19 029

HEADSPACE GAS ANALYSIS

QUANTITATIVE TRAPPING AND THERMAL DESORPTION OF VOLATILES USING FUSED-SILICA OPEN TUBULAR CAPILLARY TRAPS

B. V. BURGER* and ZENDA MUNRO
Laboratory for Ecological Chemistry, University of Stellenbosch, Stellenbosch 7600 (South Africa)
(Received July 29th, 1986)

SUMMARY

A system has been devised with which volatiles can be effectively trapped from headspace gas samples at relatively high flow-rates. Material is trapped in fused-silica capillary traps, 1 m in length, and coated with either an immobilized SE-30 layer, or a suitable adsorbent such as activated carbon or a powdered porous organic polymer supported on immobilized SE-30. These fused-silica traps are installed and used in stainless-steel tubes (desorption tubes) through which an electrical current is passed to effect on-line thermal desorption of the trapped volatiles. Thermal conversion of labile compounds such as α-pinene and γ-terpinene can be avoided by temperature-programmed or -controlled desorption in conjunction with cold trapping of the desorbed volatiles on the capillary column. The capacity of different traps was compared for a number of compound types and their versatility demonstrated by carrying out headspace gas determinations on, for instance, wine, urine and an imitation fruit drink.

INTRODUCTION

The compounds employed by insects and mammals in semiochemical communication are normally isolated and identified by extraction of the secretion-producing glands with a suitable solvent and subjecting the extract to the conventional methods of separation, bioassay and identification of the biologically active constituents. If the interest in the active material is merely of a qualitative nature, the rate at which it is released into the surrounding atmosphere, may be considered to be of lesser importance. In recent years, however, it has transpired that semiochemical communication is largely an extremely complex process[1] and that several compounds often have to be present in a specific quantitative ratio to elicit the expected response in the insect or animal[2]. Since semiochemicals are mostly released into the atmosphere in minute quantities, the qualitative and quantitative determination of these air-borne volatiles is essentially a headspace-analytical problem and the techniques developed for the gas chromatographic determination of the headspace volatiles of

0021-9673/86/$03.50

food, beverages, plastics, etc., could therefore, with certain limitations, also be applied to semiochemical research.

The techniques employed in headspace gas analysis have recently been reviewed by Núñez *et al.*[3], and several books and monographs have appeared on this subject[4,5]. However, as Grob and Habich[6] have pointed out, these techniques have been developed for packed column gas chromatography and, when applied to capillary analysis, have given unsatisfactory results, the most serious problem being incomplete transfer of the sample from the trap onto the capillary column. This is due to the difference in the flow-rate required for complete and rapid desorption from, for example, a packed 3-mm I.D. concentration trap and the flow-rate through a capillary column. Grob and Habich[6] approached this problem by using capillary traps with approximately the same diameter as the capillary column, whereby the linear flow-rate through the trap is increased to facilitate rapid sample desorption. Two trap types, a charcoal-coated open tubular trap (COT) and a trap coated with a thick layer of immobilized PS-255 (FT), were used with excellent results.

In our work on the exocrine secretions of the male African sugarcane borer *Eldana saccharina*, extracts of the wing gland and abdominal hair pencil secretions of this moth were found to contain more than 30 compounds ranging from 4-hydroxy-4-methyl-2-pentanone to several unidentified C_{22} compounds[7]. However, *trans*-3,7-dimethyl-6-octen-4-olide (eldanolide), one of the major constituents of the male wing gland secretion, was the only compound eluted from the active charcoal filter when the volatiles were trapped under closed-loop stripping conditions, from air flowing over calling males[8]. The trapped material did not contain any of the other prominent constituents of the exocrine secretions of the male, such as vanillin, which is produced in such quantities that it can be detected by the human nose at a considerable distance from sugarcane plantations infested with this insect. Obviously, the γ-lactone, eldanolide, was adsorbed preferentially on the active charcoal with the exclusion of all the other air-borne volatiles. Although this problem can be eliminated by using several activated carbon filters in series, the coated open tubular traps developed by Grob and Habich[6] presented an alternative approach to the trapping of the semiochemicals emitted by insects.

Any method employed for this purpose must meet requirements imposed by the fact that the volatiles to be determined originate not simply from a large volume of liquid serving as a replenishing reservoir, but from a living organism which, depending on circumstances, will produce varying amounts of material and which will, furthermore, only produce these compounds if natural conditions can be imitated sufficiently accurately to induce calling behaviour in the insect. One possibility is to trap all the volatiles from a brisk stream of air flowing over the calling insect, thus restricting adsorption of the semiochemicals on glass surfaces or on the insect itself. Although some of the compounds secreted by *E. saccharina* were trapped quantitatively on short FTs, almost immediate break-through of vanillin was observed, already at a relatively low flow-rate of 30 ml/min. This flow-rate appears to be too high for this particular compound and the break-through of vanillin is therefore most likely due to its slow dissolution in SE-30 and not to saturation of the trap with this compound.

The composition of this secretion illustrates a situation that is often encountered in semiochemical work where compounds such as acetaldehyde and hexyl hexa-

noate[9] or formic acid and pentacosyl formate[10], *i.e.* compounds with widely different volatilities and polarities may be present in the same secretion and have to be determined in widely different concentrations. Rather than reverting to packed-trap concentration techniques for this type of problem, the feasibility of using longer capillary traps for the trapping of volatiles at reasonably high flow-rates, was investigated. A system which would meet the following requirements, was devised: (1) off-line trapping with on-line desorption of volatiles onto the analytical capillary column, (2) temperature-programmed or at least temperature-controlled thermal desorption of the trapped material, (3) traps in which, depending on prevailing circumstances, the properties and advantages of film- and charcoal-coated open tubular traps can be utilized, and (4) traps which would, as far as possible, give quantitative retention of volatiles at reasonably high flow-rates.

In this paper the preparation of fused-silica traps, 1 m in length and coated with SE-30 or with SE-30 plus an adsorbent, the thermal desorption of volatiles trapped on the capillary traps and experiments carried out to establish the capacity of these traps for a number of reference compounds are described. In addition, several headspace determinations were carried out to demonstrate the applicability of this system to the headspace gas analysis of biological samples, beverages, etc.

EXPERIMENTAL

Gas chromatographic analyses were carried out with a Carlo Erba Fractovap 4160 gas chromatograph (Carlo Erba, Milan, Italy) equipped with a flame ionization detector, using helium as carrier gas. Fused-silica capillary columns (40 m × 0.32 mm I.D. and 28 m × 0.32 mm I.D.) coated with SE-30 (film thickness 0.84 μm) were used for analytical separations. Gas samples were made up with nitrogen which was purified through a column (200 mm × 30 mm) of activated charcoal. Gas samples were injected onto the traps at specific flow-rates using gas-tight syringes (10 ml or 50 ml) installed in an infusion pump (Sage Instruments, White Plains, NY, U.S.A.).

Preparation of fused-silica capillary traps

Film open tubular traps (FOTTs). Lengths of deactivated[11] fused-silica capillary tubing (*ca.* 1.12 m × 0.32 mm I.D.) were statically coated with SE-30. The stationary phase was thoroughly removed from both end sections of the capillary with *n*-pentane, leaving the coating in the central 1-m section of the capillary intact, whereafter it was immobilized by subjecting the traps to γ-radiation (7.5 MRad) from a ^{60}Co source[12]. The traps were not rinsed with a solvent, but were conditioned at 230°C with a carrier gas flow of 20 ml/min before use. Traps with film thicknesses of 3 μm (FOTT-3) and 12 μm (FOTT-12) were prepared.

Film–activated carbon open tubular traps (FACOTTs). Film traps were coated with SE-30 (3 μm) and the stationary phase removed from the end sections as described above, whereafter the stationary phase in the central section of the traps was coated with a uniform layer of activated carbon by sucking the adsorbent into the traps. The particle size of the charcoal was determined by electron microscopy. Particles of carbon remaining in the end sections of the traps were carefully removed with dichloromethane. The stationary phase layer with imbedded activated carbon was immobilized by γ-radiation as before. Two trap types, FACOTT-10 and

FACOTT-80, were prepared using 1–10 μm and 10–80 μm activated carbon respectively.

Film–organic polymer open tubular traps (FOPOTTs). Traps with particles of Porapak Q imbedded in a layer of SE-30 were prepared using pulverized Porapak Q (1–10 μm) instead of activated carbon. The supporting SE-30 film was also immobilized by γ-radiation (7.5 MRad).

Combination film and film–activated carbon open tubular trap (FOTT/FACOTT). Using the methods described above, a trap was prepared in which one half of the middle 1-m section of a 1.12-m fused silica tube was coated with activated carbon (1–10 μm) supported on SE-30 (3 μm), and the other half with SE-30 (12 μm). This was accomplished by first coating *ca.* 500 mm of the tube with SE-30 and activated carbon, removing all activated carbon particles from the rest of the tube, and then coating the second 500-mm length of the tube with SE-30 from its other end. A short section remained uncoated between the coated sections of this FOTT-12/FACOTT-10 combination trap.

Thermal desorption tube

A stainless-steel tube (1 m × 1.0 mm O.D. × 0.65 mm I.D., 1.2 Ω/m) was silver soldered to a Carlo Erba ferrule-supporting conical washer as shown in Fig. 1. The stainless-steel tube was electrically insulated with PTFE tubing (1.5 mm I.D.). Using crocodile clips and contacts soldered to the desorption tube, the two ends of this tube were connected to the output terminals of a 12-V, 20-A transformer (Osborne Electric Co.) which was in turn plugged into a 2.5-kVA powerstat voltage regulator (Superior Electric Co., Bristol, CT, U.S.A.) as shown in Fig. 1. This arrangement allowed manual control of the temperature of the desorption tube by regulating the current flowing through the tube. For safety it is imperative that a secondary step-down transformer be used in series with the voltage regulator as no more than 10 V should ever be delivered to the desorption tube or its exposed tips. To calibrate this desorption device, a number of slits were made lengthwise in the PTFE insulating sheath, through which crystals of various organic compounds such as, for example, benzoic acid and *p*-nitrobenzoic acid, could be inserted and brought into contact with the desorption tube. By using the melting points of these compounds a calibration curve of the temperature of the desorption tube *vs.* the voltage regulator setting was obtained. Although this calibration procedure was complicated, to some extent, by the sublimation of the crystals near their melting points, sufficiently accurate results for the purpose for which the desorption tube was to be used, were obtained.

Several identical desorption tubes were manufactured. Fused-silica capillary traps were inserted into these desorption tubes as required for various headspace gas determinations.

Manipulation

A series of experiments were carried out to determine the capacity of the different traps for various compounds and compound types.

Break-through curves were recorded for a number of reference compounds by connecting one end of a trap to the needle of one of the gas-tight syringes, using a butt connector, and the other end to the flame ionization detector of the gas chro-

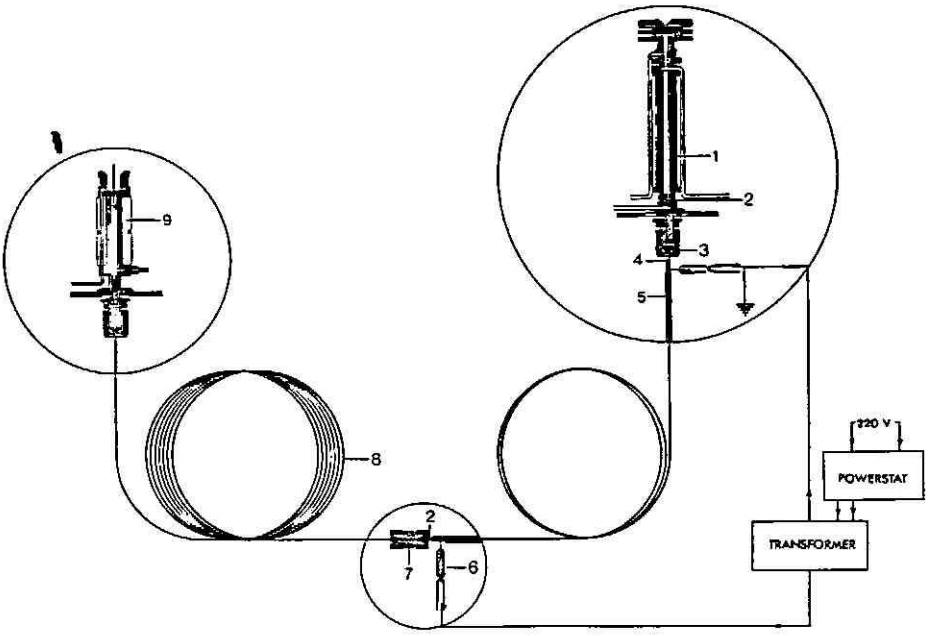

Fig. 1. Installation of a fused-silica open tubular trap in a Carlo Erba gas chromatograph: 1 = injector, 2 = fused-silica trap, 3 = ferrule-supporting conical washer, 4 = stainless-steel desorption tube soldered to conical washer, 5 = PTFE insulating sheath, 6 = crocodile clip attached to contact which is silver-soldered to the desorption tube, 7 = butt connector, 8 = analytical glass or fused-silica column, 9 = detector.

matograph. Gas samples were prepared by adding 1-μl quantities of methanol, chloroform, toluene, *n*-pentane and *n*-octane, respectively, to 5 l of purified nitrogen in 5-l flasks. A gas sample containing propane was similarly prepared by adding 1 ml of propane gas to 5 l of nitrogen. The gas mixtures were pushed through the traps at a steady pre-selected flow-rate using a syringe-type of infusion pump. The detector response was recorded *vs.* the volume of gas passing through the trap. Due to the compressibility of gases, the volume of the gas flowing through a trap lags behind the volume displaced by the plunger of the infusion pump syringe, resulting in a discrepancy which increases with increasing flow-rates. The flow-rate through a trap was, therefore, calibrated at different infusion pump settings by using a bubble flow meter connected to the outlet end of the trap.

The results obtained from these break-through curve determinations were verified for a number of reference compounds on different traps by determination of the percentage break-through at different sample sizes by employing two traps in series.

Applications

Headspace gas analyses using a FOTT-12, FACOTT-10 and FOPOTT-10 were carried out on a gas sample containing limonene, γ-terpinene and α-pinene (1 μl each on some glass wool in 100 ml of nitrogen) to determine the influence of thermal desorption parameters on thermally labile compounds. For comparison, a sample

containing these three terpenes, dissolved in dichloromethane, was injected onto the same capillary column, using split injection. The versatility of the fused-silica open tubular traps was further demonstrated by carrying out headspace gas analyses on citrus peel, a commercial cool drink, wine and a canine urine sample. For these determinations headspace gas samples were transferred from a 100-ml screw-capped bottle onto the traps with either helium from the detector of the gas chromatograph or with purified nitrogen. Sampling was carried out at room temperature (25°C) and sample sizes were measured at the outlet end of the traps using a bubble flow meter. For these determinations all glass-ware and the PTFE-lined gaskets used in the screw-capped bottles, were heated before use in a well ventilated oven at 100°C for 12 h.

RESULTS AND DISCUSSION

Since it is impossible to produce a fused-silica trap coated with activated carbon by the method described by Grob and Habich[6], attempts were made at producing a uniform layer of activated carbon on an inert material such as polyimide resin (Alltech, Deerfield, IL, U.S.A.). Fused-silica capillaries were dynamically coated with the resin, whereafter pulverized activated carbon was sucked into the coated capillaries and the resin cured at elevated temperatures. Although this procedure was found to be feasible for short traps, the carbon particles moving through the capillary, gradually removed the resin from the capillary wall. The front sections of longer traps were thus left uncoated, while the carbon in the rest of the traps was partially covered in resin. The resulting traps were expected to have low capacities and this approach was abandoned. Far superior results were obtained with a gum phase such as SE-30 as supporting layer. Such FACOTTs have the added advantage that they will retain headspace volatiles by dissolution as well as adsorption, thus extending the capacity and efficiency of the traps.

Initially the activated carbon was applied by forcing air-borne particles of the material from a small glass bottle into the capillary with a brisk stream of nitrogen, but as the capillary soon became clogged, the flow had to be regularly reversed to remove the excess of carbon from its front end. Better results were obtained by sucking the activated carbon into the capillary. Since a stationary phase film is expected to support an essentially mono-particulate layer of the adsorbent on the film, the capacity of the trap will depend on the particle size of the adsorbent, larger particles producing layers with a higher capacity. On the other hand, larger particle sizes would result in incomplete and slower desorption, with accompanying unacceptable catalytic effects. This aspect was not investigated in detail, but activated carbon with particle sizes below 1 μm was found to produce traps with such a thin layer of carbon that they remained almost transparent, whereas material with a particle size of 1–10 μm gave a satisfactory uniformly black layer of carbon. When these traps were coupled to the detector of the gas chromatograph for the recording of break-through curves, particles of carbon were transported into the detector resulting in an almost constant production of spikes. The carbon particles, therefore, appeared to adhere rather loosely to the stationary phase. The activated carbon layer could, however, be stabilized and the production of spikes totally eliminated by subjecting the traps to γ-radiation.

The capacity of a trap for a certain compound or headspace sample is usually

determined by using a second trap in series with the first one to trap any material not retained by the first trap. From the relative peak sizes obtained by gas chromatographic analysis of the material desorbed from the two traps, the percentage break-through can then be calculated. The determination of the efficiency with which material is retained on a trap at different sample sizes, usually requires a series of determinations, the results of which can be used to plot a break-through curve of amount of break-through *vs.* sample volume. Similar information can, however, also be obtained by using the flame ionization detector of the gas chromatograph instead of a second trap to detect break-through. Although this method does not give the percentage break-through at a specific sample volume, it can be employed to determine the volume range over which the trap may be safely used with total sample retention. Examples of such break-through curves are given in Fig. 2A–D. In these figures increasing detector response indicates break-through which increases until a situation is reached where the activated carbon is saturated or where the material, transported through the film-coated tube by normal chromatographic processes, reaches the outlet end, whereafter the trap merely acts as a tube conducting the gas sample to the flame ionization detector. The observed fluctuation of the detector response as this stage of the determination is approached, is due to the irregular movement of the syringe plunger.

In using this method a few precautions have to be taken into consideration. Serious errors may result from the fact that, due to the compressibility of the gas sample, the volume of sample actually flowing through the trap will lag behind the volume displaced by the infusion pump syringe plunger. The resulting discrepancy will increase with increasing flow-rates. Thus, before carrying out a break-through curve determination, a calibration curve has to be set up by plotting the volume flowing through the trap, as measured with a bubble flow meter connected to its outlet end, *vs.* the volume indicated on the infusion pump syringe at the flow-rate to be used in the break-through curve determinations. Corrected volumes are used in the presentation of the results in Fig. 2 A–D and in Table I.

The presence of volatile impurities in the sample under investigation or in the

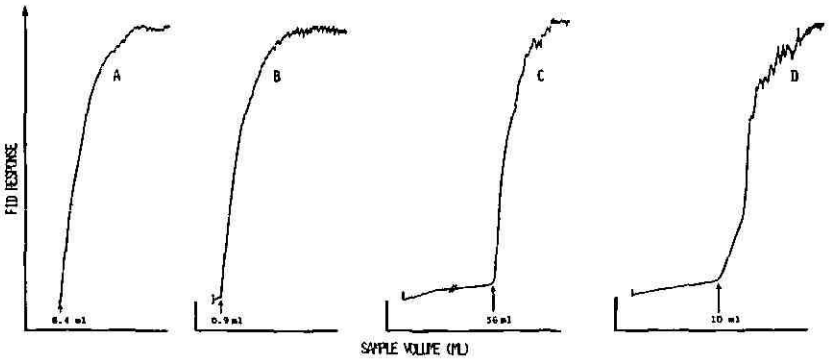

Fig. 2. Break-through curves for 0.2 ppm *n*-pentane in nitrogen determined at 24°C by using the flame ionization detector (attenuation, × 32) to detect break-through. (A) FOTT-3, flow-rate 1 ml/min; (B) FOTT-12, flow-rate 1 ml/min; (C) FACOTT-10, flow-rate 10 ml/min; (D) FOPOTT-10, flow-rate 5 ml/min.

gas which is used in the preparation of gas samples may also result in confusing results as the response of the detector to such volatile impurities may be interpreted as sample break-through. It is therefore essential that the gas used in the determination of break-through curves be purified, for example by passing it through an activated carbon filter. To guard against misinterpretation of results, it is furthermore advisable to desorb and identify the material which had accumulated on the trap when break-through is observed by, for example, retention time comparison. Removal of gas samples from the 5-l flasks in which the gas mixtures were made up, results in the dilution of the material in these flasks. More reliable information would therefore have been obtained by using gas sampling bags. Glass-ware was nevertheless preferred, since contaminants originally present in some bags and the high price of other types precluded their use in this investigation. To keep the dilution of the material in the flasks within limits, a freshly prepared mixture was used when more than 200 ml of the mixture had been removed from such a container.

Examples of break-through curves obtained for *n*-pentane on the FOTT-3, FOTT-12, FACOTT-10 and FOPOTT-10 at a flow-rate of 10 ml/min are given in Fig. 2 A–D. Whereas almost immediate break-through was observed on the FOTT-3, and the FOTT-12 has an only slightly higher capacity for *n*-pentane, the FOPOTT-10 and especially the FACOTT-10 have high capacities for this compound.

Parameters such as film thickness, activity and particle size of the activated carbon, exact length of the coated section of a trap and the temperature at which material is collected on the trap, will influence the capacity of a trap. Break-through curves should therefore only be used to obtain information as to the sample volume range over which the trap may be used without the risk of break-through occuring. This information should be checked regularly. Since information obtained from the break-through curves of gas samples containing single reference compounds are not applicable to the headspace determination of complex samples, it is essential to carry out break-through curve determinations at least for every type of sample under investigation. The break-through curves of simple reference gas mixtures may nevertheless be used to obtain information on the long-term behaviour of a trap or to compare the capacity of different traps and trap types, and is preferred to the time consuming determination of break-through with two traps used in series. In the present investigation the results obtained by break-through curve determinations were nevertheless verified for some traps and gas samples by carrying out percentage-break-through determinations at sample volumes at which, according to the break-through curves, break-through is expected to set in. The results of these determinations are included in Table I.

Whereas reasonably consistent results were obtained when determinations were repeated with FOTTs having the same film thickness, results varied with the FACOTTs, since it is obviously impossible to apply the activated carbon in an absolutely reproducible manner. With *n*-pentane, for example, break-through volumes varying from 40 to 500 ml were obtained with different FACOTT-10s. The increased particle size of the activated carbon used in the FACOTT-80 increased the capacity of this type of trap for *n*-pentane to almost 1.5 l. A break-through volume for propane of 46 ml indicates that this trap should also trap other volatiles quite effectively. On the other hand, however, it may retain thermally labile compounds so effectively that it may not be suitable for general purpose applications. This aspect was not pursued any further in the present investigation.

TABLE I

BREAK-THROUGH VOLUMES OBTAINED WITH DIFFERENT FUSED-SILICA OPEN-TUBULAR TRAPS

Gas samples were prepared by adding 1 μl of the respective compounds to 5 l of purified N_2 in a 5-l flask. The propane sample was prepared similarly by adding 1 ml of propane gas to 5 l of N_2.

Compound	*Trap*	*Flow-rate (ml/min)*	*Break-through volume (ml)*	*Percentage break-through at volume specified (ml)*
Propane	FOTT-12	1	0.2	2.7 (0.2)
	FOPOTT-10	1	0.8	4 (1.0)
	FACOTT-80	10	46	0.1 (47)
n-Pentane	FOTT-3	1	0.4	–
	FOTT-12	1	0.9	12 (1.1)
	FOPOTT-10	5	10	–
		25	10	4 (10)
	FACOTT-10	10	56	–
		100	55	–
	FACOTT-80	10	1480	1 (1510)
n-Octane	FOTT-3	10	7.5	2 (8.5)
	FOTT-12	10	26	–
		25	29	–
		100	28	–
	FOPOTT-10	20	340	–
	FACOTT-10	10	500	0.3 (550)
Toluene	FOTT-12	1	13	6 (13.8)
	FOPOTT-10	10	133	1 (138)
	FACOTT-80	10	> 1000	–
Chloroform	FOTT-12	1	3.5	2 (3.7)
	FOPOTT-10	10	40	4 (41)
	FACOTT-80	10	> 1000	–
Methanol	FOTT-12	1	0.4	5 (0.8)
	FOPOTT-10	1	4.0	1.3 (4.6)
	FACOTT-10	10	32	–
	FACOTT-80	10	233	0.1 (238)

As far as the FACOTTs are concerned, the following observations emerge from a consideration of the data in Table I. The same general trend found in Fig. 2 A–C, *viz.* that the FOTTs have relatively low capacities and that the FACOTT-10 has a much higher capacity, was also observed for other volatile compounds such as propane, methanol, chloroform, and toluene. As expected, chloroform was trapped more efficiently on non-polar FOTTs than methanol, which gave almost immediate break-through on both FOTTs. The high break-through volume of methanol on the FACOTT is therefore almost exclusively due to the contribution of the activated carbon layer. Methanol should be a useful reference compound for the determination

of the adsorptive capacity of a trap or for the comparison of traps containing different types or grades of adsorbent.

At extremely high flow-rates, traps could be expected to exhibit, to a certain extent at least, lower break-through volumes. This was, however, not found to be the case at the flow-rates between 1 and 100 ml/min which had been used in the present investigation. Since the infusion pump motor was not powerful enough to maintain constant plunger motion at high flow-rates, most of the break-through-curve determinations were carried out at a flow-rate of 10 ml/min. Some of the results obtained from successful determinations at higher flow-rates are nevertheless included in Table I.

A strong argument against using activated carbon in headspace traps is the production of artifacts from labile compounds when trapped material is thermally desorbed. However, the high capacity of the FACOTT made this type of trap so attractive for the quantitative headspace gas determination of the complex type of samples often encountered in biological work, that it was decided to investigate possible methods by which material could be desorbed without accompanying thermolysis or rearrangement of thermally labile compounds. Temperature programming of the trap by manually increasing the current flowing through the desorption tube and increasing the flow of the carrier gas through the trap during this step were possible techniques to achieve this goal.

Previous experience in our laboratory has shown that high injector temperatures tended to induce the production of artifacts from γ-terpinene and α-pinene and it was therefore decided to use a gas mixture containing these two terpenes as well as the thermally more stable limonene as test compounds. The results obtained by thermal desorption of these compounds are given in Fig. 3. Desorption of the terpenes from the FOTT-12 and FOPOTT-10 at 150°C for 3 min, the capillary column being kept at 25°C for the same period before starting the temperature programme, did not result in any appreciable production of artifacts. In the resulting gas chromatograms shown in Fig. 3B and C, respectively, the terpenes produced peaks almost as sharp as those obtained by a conventional analysis of a solution of the terpenes in dichloromethane (Fig. 3A). Considerable artifact formation was observed with the FACOTT-10, even when the desorption tube was temperature programmed from 70 to 150°C at 11°C/min (Fig. 3D). Increasing the carrier gas flow during the desorption step from a normal 1.7 ml/min to 3.4 ml/min and programming the trap from 70 to 130°C at 8.5°C/min suppressed, but did not totally eliminate artifact formation (Fig. 3E). However, as is illustrated in Fig. 3F, thermal conversion of the terpene mixture was almost totally eliminated by using a carrier gas flow-rate of 3.4 ml/min and temperature programming the trap from 80 to 120°C at 5°C/min.

The possibility of eliminating the conversion of thermally labile compounds by careful selection of desorption parameters adapted to the compound or sample under investigation, increases the attractiveness of the FACOTT type of trap for work with headspace samples of unknown composition which could possibly contain highly volatile components. The advantages offered by the FACOTT are illustrated by headspace analyses carried out on an imitation fruit drink and fresh citrus peel. In these and all further headspace gas determinations temperature-programmed desorption of the trapped volatiles was employed.

The results of headspace determinations, carried out with the FOTT-12 and

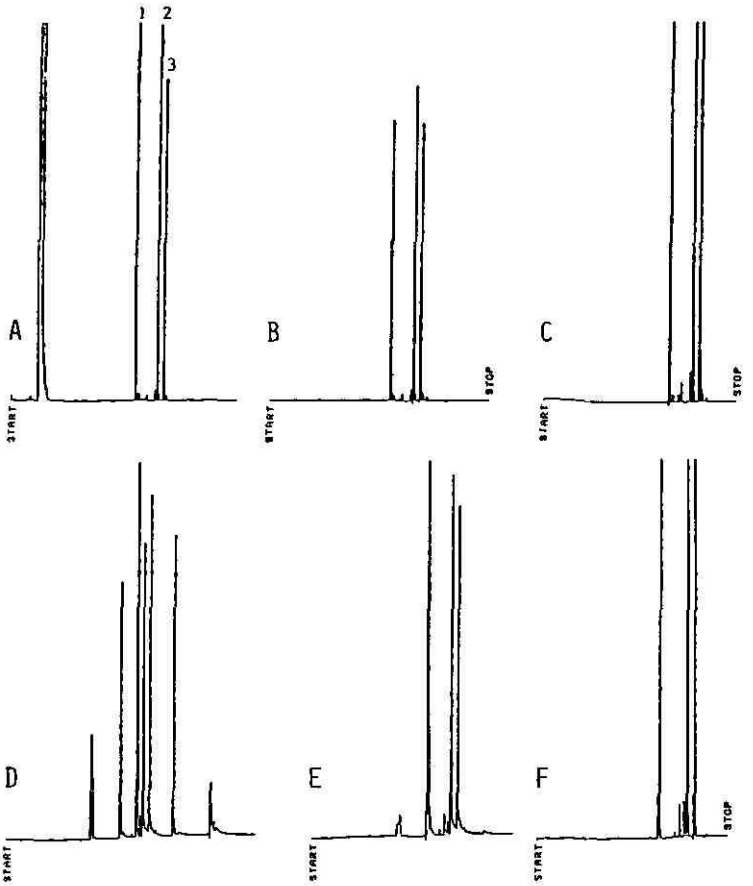

Fig. 3. Analysis of the headspace gas of thermally labile terpenes. Column, 40 m × 0.32 mm I.D. fused silica, 0.84 μm SE-30; temperature programme, from 25 to 180°C at 5°C/min; carrier gas, helium at 28.6 cm/s. (A) Split injection of the mixture of terpenes dissolved in dichloromethane. Injector, 80°C; detector, 220°C. Peaks: 1 = α-pinene, 2 = limonene, 3 = γ-terpinene. Headspace analyses were carried out by trapping 1 ml of a headspace gas sample containing these three terpenes on different traps to determine which desorption parameters would allow desorption without thermal conversion of the compounds. (B) FOTT-12, desorption temperature, 150°C (3 min); flow-rate through trap during desorption step, 1.7 ml/min; on-line desorption and analysis using a butt connector. (C) FOPOTT-10, desorption temperature, 150°C (3 min); flow-rate through trap, 1.7 ml/min; on-line desorption and analysis using a shrink-PTFE connection. (D) FACOTT-10, desorption temperature increased from 70 to 150°C at 11°C/min; flow-rate through trap during desorption, 1.7 ml/min; on-line desorption and analysis using a butt connector. (E) FACOTT-10, desorption temperature increased from 70 to 130°C at 8.5°C/min; flow-rate through trap during desorption, 3.4 ml/min; on-line desorption and analysis using a butt connector. (F) FACOTT-10, desorption temperature increased from 80 to 120°C at 5°C/min; flow-rate through trap during desorption, 3.4 ml/min; on-line desorption and analysis using a shrink-PTFE connection. Material was cold-trapped (25°C) on the capillary column during the slow desorption from the traps.

the FACOTT-10 on equal volumes of the headspace gas of an imitation passion-fruit cool drink, are compared in Fig. 4 and clearly show the much higher capacity of the FACOTT-10, especially for the more volatile constituents of the sample. The quantitative differences between the two analyses as far as the less volatile constituents

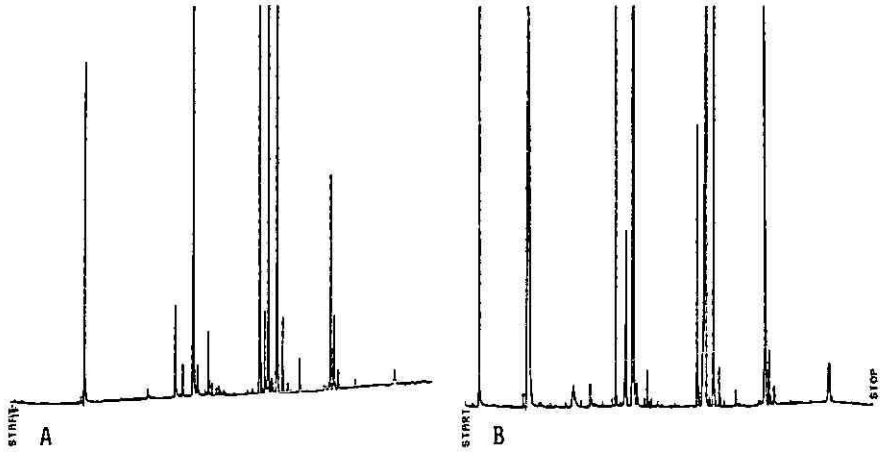

Fig. 4. Analysis of imitation passion-fruit cool drink headspace gas. Column, 40 m × 0.32 mm I.D. fused silica, 0.84 μm SE-30; carrier gas, helium at 28.6 cm/s; temperature programme, 25 to 160°C at 3°C/min; attenuation, × 16; 5 ml of headspace gas; desorption, 70 to 130°C at 12°C/min; on-line desorption and analysis using a butt connector. (A) FOTT-12 (B) FACOTT-10.

are concerned, could be due to the fact that the cool drink sample was not thermostatted and some time elapsed between the two analyses. Similar conclusions can be drawn from the results of the determination of the headspace gas of a 1 × 1 cm piece of citrus (kumquat) peel shown in Fig. 5.

A further number of headspace gas determinations were carried out on more complex samples such as urine and wine. Different trap types were used to collect the volatiles and a second trap was used in series with these traps to determine the

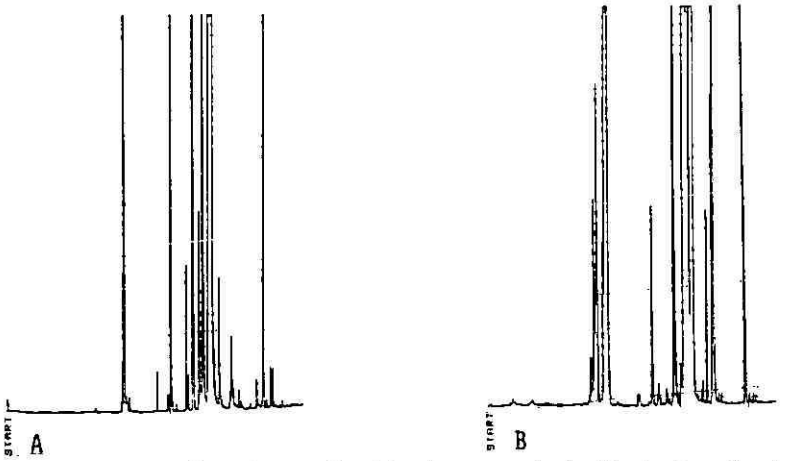

Fig. 5. Analysis of citrus (kumquat) peel headspace gas obtained by leaving a 1 × 1 cm piece of kumquat peel in a 100-ml screw-capped bottle for 2 h. Column, 40 m × 0.32 mm I.D. fused silica, 0.84 μm SE-30; carrier gas, helium at 28.6 cm/s; temperature programme, 25 to 160°C at 3°C/min; attenuation, × 16; 5 ml headspace gas; desorption, 70 to 130°C at 12°C/min; on-line desorption and analysis using a butt connector. (A) FOTT-12 (B) FACOTT-10.

amount of break-through, if any. In order to obtain the best possible gas chromatographic separations of the volatiles on the capillary column, the material desorbed from the traps were focussed on the capillary column by cold trapping using solid carbon dioxide as coolant. In these determinations the traps were removed before the analyses were started and the column connected directly to the injector (on-line desorption, off-line analysis).

In the first of these analyses, 35 ml of headspace gas of a sample of urine of the female red jackal, *Canis mesomelas*, was passed through a FACOTT-10 as first trap and a FOTT-12 as second trap. The results presented in Fig. 6 show almost total retention on the FACOTT, only traces of one of the major, apparently very polar compounds, breaking through to the FOTT. In the next set of analyses, the results of which are given in Fig. 7A, the headspace gas of a white wine (Gewürztraminer) was trapped with the FACOTT-10 as first and the FOTT-12 as second trap. The analysis was then repeated with the FOTT-12 as first and the FACOTT-10 as second trap (Fig. 7B). In the first of these analyses only ethanol and small quantities of one or two other volatile components broke through the FACOTT to be collected on the FOTT, whereas, with the FOTT-12 as first trap, major break-through of a large number of volatile compounds was found. The efficiency of the separations on the analytical column and the sharpness of the peaks in the gas chromatograms were found to be quite satisfactory.

A similar analysis was carried out using the FOPOTT-10 as first and the FACOTT-10 as second trap. In this analysis considerable break-through of a number of compounds, subsequently identified as alcohols, was observed. This type of trap could possibly be used to advantage in wine headspace analysis since, as was pointed out earlier, it does not have the strong catalytic activity of activated carbon towards thermally labile compounds and furthermore, it could be used to concentrate com-

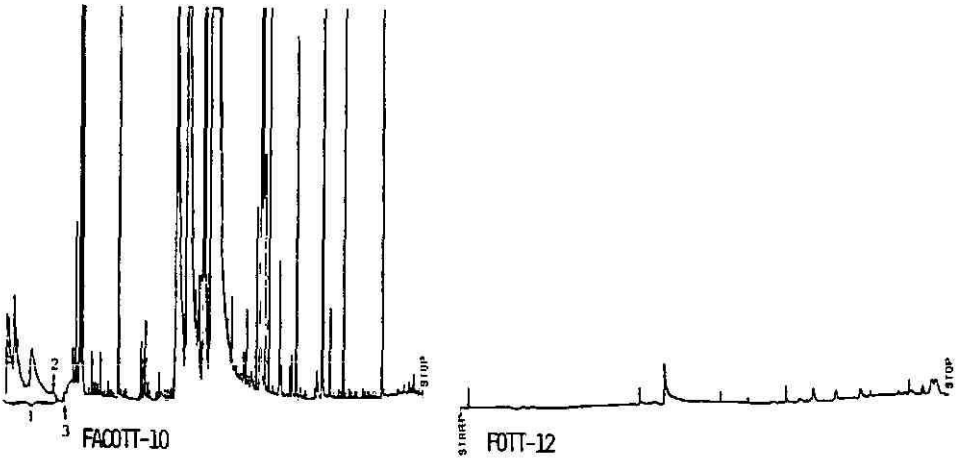

Fig. 6. Analysis of the headspace gas of the urine of a female red jackal (*Canis mesomelas*). Column, 40 m × 0.32 mm I.D. fused silica, 0.84 μm SE-30; carrier gas, helium at 28.6 cm/s; temperature programme, 25 to 180°C at 3°C/min; attenuation, ×8; 35 ml headspace gas; desorption, 70 to 160°C at 13°C/min; peaks: 1 = desorption and cold trapping of the desorbed material on the capillary column with solid carbon dioxide, 2 = shrink-PTFE connection and trap removed, 3 = programme started. FACOTT-10 as first trap and FOTT-12 as second trap.

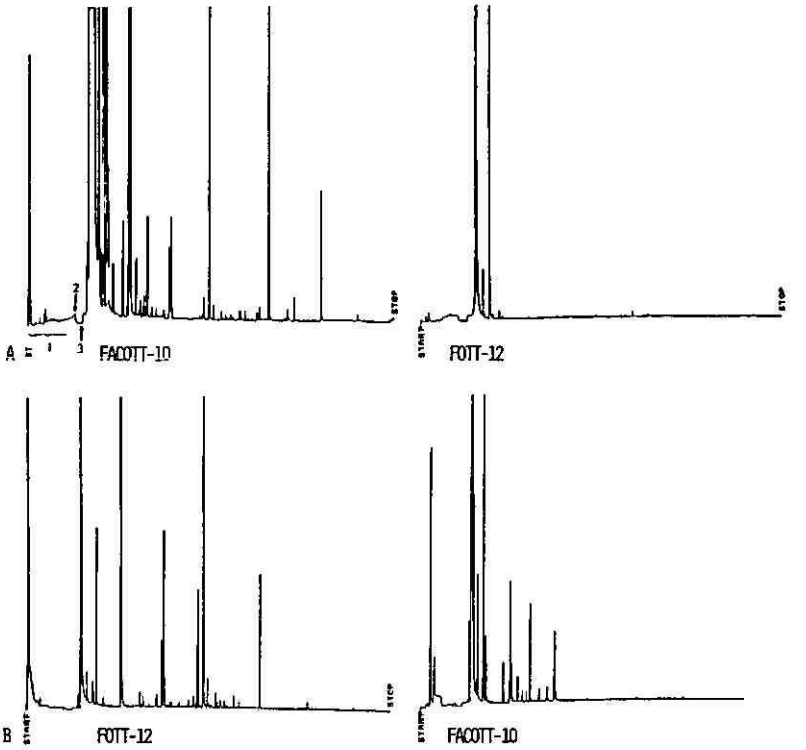

Fig. 7. Analysis of the headspace gas of a white wine (Gewürztraminer). Column, 28 m × 0.32 mm I.D. fused silica, 0.84 μm SE-30; carrier gas, helium at 28.6 cm/s; temperature programme, 25 to 180°C at 3°C/min; attenuation, × 16; 5 ml headspace gas; desorption, 70 to 140°C at 15°C/min; peaks: 1 = desorption and cold trapping of the desorbed material on the capillary column with solid carbon dioxide, 2 = butt connector and trap removed, 3 = programme started. (A) FACOTT-10 as first trap and FOTT-12 as second trap. (B) FOTT-12 as first trap and FACOTT-10 as second trap.

ponents other than the short-chain alcohols, thereby eliminating one of the annoying problems in wine flavour analysis.

Instead of using different traps in series, different phases and adsorbents can be used in different sections of the same fused-silica trap. To illustrate this, a combination FOTT-12/FACOTT-10 trap, having one half of its length coated with SE-30 and the other half with activated carbon supported on SE-30, was prepared. This trap was used with headspace gas flowing through it from the FOTT towards the FACOTT section. Only the most volatile components are thus expected to reach the FACOTT section and to be retained there. Since desorption was carried out with reversed flow, thermally labile compounds will come into contact with the activated carbon layer only if they are also highly volatile, and then only to the extent to which they are not retained by the FOTT section of the trap.

If, in addition, the desorption tube temperature is also carefully increased (manually programmed) it should be possible to restrict the thermal production of artifacts to an absolute minimum by using a combination type of trap. An analysis of the headspace gas of a white wine (Crouchen blanc), using a FOTT-12/FACOTT-10 combination trap, is shown in Fig. 8.

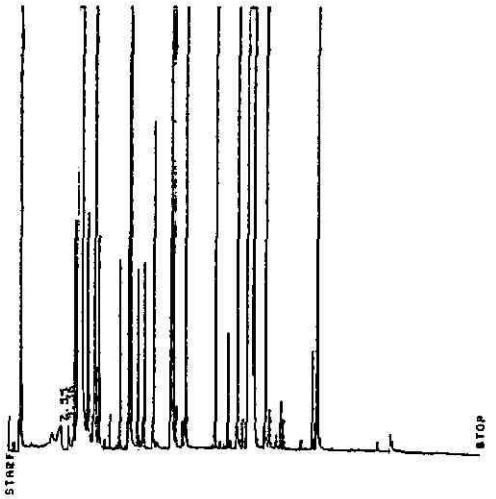

Fig. 8. Analysis of the headspace gas of a white wine (Crouchen blanc) using a FOTT-12/FACOTT-10 combination trap in such a manner that the FOTT section acts as first trap and the FACOTT section as guard trap. Desorption was carried out with carrier gas flowing in the opposite direction and with the trap temperature programmed at 11°C/min from 70 to 140°C. Gas chromatographic conditions as in Fig. 7; attenuation, ×4.

CONCLUSIONS

The present investigation can be seen as an extension of the work of Grob and Habich[6] on the development of open tubular traps for headspace gas analysis. The finger-printing of the volatile secretions produced by insects and other animals requires quantitative trapping of all the compounds in such exudates, which in turn requires traps with a high capacity for a wide range of compound types. In order to remove volatiles quantitatively from the atmosphere surrounding such a secreting organism, traps must preferably also allow quantitative trapping at relatively high flow-rates. A system was devised in which material is trapped on fused-silica open tubular traps coated with a suitable stationary phase or with an adsorbent supported on a film of immobilized SE-30. Trapped material is desorbed by installing the trap in a coiled stainless-steel tube which is heated electrically by passing an electric current through it. Connecting the traps directly to the flame ionization detector of a gas chromatograph when trapping volatile compounds from gas samples containing individual reference compounds, and recording the detector response *vs.* the volume of the gas sample introduced into the trap, proved to be a simple but rigorous test for break-through. From the results obtained with various volatile compounds, a trap coated with activated carbon on an immobilized film of SE-30 is clearly to be preferred to traps coated with the stationary phase only, as some volatiles are lost almost completely from the latter type of trap. Increasing the flow-rate at which a headspace sample is pushed through the traps up to 100 ml/min did not have an appreciable effect on the effectivity with which headspace volatiles are trapped. This is in agreement with the results obtained by Grob and Habich[6].

When using a trap containing activated carbon, thermal conversion of material

during the desorption step can be avoided by gradually increasing the temperature of the trap during this step and using cold trapping to focus the material on the analytical column, instead of employing isothermal desorption at high temperatures to obtain sharp bands of the desorbed material on the capillary column. As expected, increased carrier gas flow-rates facilitated desorption at lower temperatures. In those cases where thermal conversion on activated carbon is expected to take place in spite of programmed desorption at a high flow-rate, artifact formation could possibly be avoided by using a FOPOTT instead of a FACOTT, or otherwise by using a combination FOTT/FACOTT in such a way that the headspace gas volatiles will hit the FOTT section of the trap first. Only the most volatile components will then reach the FACOTT section and if desorption is carried out in the reverse direction, thermally unstable compounds with a lower volatility may not come into contact with the activated carbon at all. The relative lengths of the sections could also be adapted to the type of sample that has to be trapped.

Trapping the headspace volatiles from a number of samples of the type that are often encountered in headspace-analytical work, such as wine, urine, etc., produced such promising results that we believe that using this type of trap could prove to be a valuable addition to the already excellent traps introduced by Grob and Habich, especially in those cases where quantitative trapping of highly volatile constituents is essential in order to obtain an exact aromagram of the headspace sample.

Since the application of these traps to the determination of the material secreted by living organisms introduces further problems peculiar to research on insects and animals, the results of these determinations wil be published elsewhere.

ACKNOWLEDGEMENTS

The support of this work by the Foundation for Research Development, Pretoria, and the University of Stellenbosch is gratefully acknowledged. We thank Prof. K. Grob, ETH, Zürich, and Dr. I. M. Moodie, Medical Research Council, Cape Town, for reading the manuscript.

REFERENCES

1 J. H. Law and F. E. Regnier, *Ann. Rev. Biochem.*, 40 (1971) 533.
2 E. S. Albone, *Mammalian Semiochemistry*, Wiley, Chichester, 1984.
3 A. J. Núñez, L. F. González and J. Janák, *J. Chromatogr.*, 300 (1984) 127.
4 G. Charalambous (Editor), *Analysis of Food and Beverages, Headspace Techniques*, Academic Press, New York, 1978.
5 B. Kolb (Editor), *Applied Headspace Gas Chromatography*, Heyden, London, 1980.
6 K. Grob and A. Habich, *J. Chromatogr.*, 321 (1985) 45.
7 B. V. Burger, W. M. Mackenroth, D. Smit, H. S. C. Spies and P. R. Atkinson, *Z. Naturforsch.*, 40c (1985) 847.
8 B. V. Burger, W. M. Mackenroth, D. Smit and P. R. Atkinson, unpublished results.
9 B. V. Burger, Z. Munro, M. Röth, H. Geertsema and A. Habich, *Insect Biochem.*, 16 (1986) 687.
10 B. V. Burger, M. le Roux, H. S. C. Spies, V. Truter, R. C. Bigalke and P. A. Novellie, *Z. Naturforsch.*, 36c (1981) 344.
11 L. Blomberg, J. Buijten, K. Markides and T. Wännman, *J. Chromatogr.*, 239 (1982) 51.
12 G. Schomburg, H. Husmann, S. Ruthe and M. Herraiz, *Chromatographia*, 15 (1982) 599.

Journal of Chromatography, 370 (1986) 465–473
Elsevier Science Publishers B.V., Amsterdam — Printed in The Netherlands

CHROM. 19 021

DERIVATIZATION OF PHENOLIC ACIDS FOR CAPILLARY GAS CHROMATOGRAPHY WITH HYDROGEN FLAME IONIZATION AND ELECTRON-CAPTURE DETECTION

KEIJO LEHTONEN and MARTTI KETOLA*
Department of Chemistry, University of Turku, SF-20500 Turku (Finland)
(First received June 23rd, 1986; revised manuscript received August 18th, 1986)

SUMMARY

Ten methods of derivatization of phenolic acids and the suitability of the derivatives so obtained for non-polar (SE-30, OV-1) capillary gas chromatographic (GC) quantitation with the flame ionization detection (FID) and electron-capture detection (ECD) have been studied. The phenolic acids included three benzoic and three *trans*-cinnamic acids, both series consisting of 4-hydroxy, 4-hydroxy-3-methoxy and 4-hydroxy-3,5-dimethoxy derivatives. The trimethylsilyl (TMS) ethers of the phenolic acid methyl esters, the TMS ethers of the phenolic acid TMS esters and the heptafluorobutyrates of the phenolic acid methyl esters were found to be suitable for quantitation with FID and the first mentioned derivatives are preferred. For quantitation with ECD, the perfluorobutyrates of the phenolic acid methyl esters were the best derivatives. The quantitation of phenolic acids by GC–FID is suitable for samples with concentrations in the range of 0.01–10 μg per injection. The concentrations applicable to GC–ECD quantitation are much lower, 0.05–1 ng per injection.

INTRODUCTION

Derivatization is a common praxis when analyzing relatively non-volatile compounds and polar molecules including various functional groups by gas and liquid chromatography. There are also many specific reasons for the use of derivatives, *e.g.*, (i) to improve the resolution of closely related compounds, (ii) to increase the detector response for trace components and (iii) to utilize selective detection such as electron-capture detection (ECD) and nitrogen-phosphorus detection (NPD), which allow the analysis of complex mixtures without prior separation from the matrix. Numerous examples of applications of various derivatization reactions have been described[1–3].

Extracts from soils contain small amounts of phenolic acids which occur together with humic substances[4]. Extractable matter from Finnish peat was found to contain phenolic acids although at a very low concentration[5,6]. Phenolic acids must be modified prior to their gas chromatography (GC) and numerous derivatization methods have been presented[1,3]. The present paper describes the derivatization of simple phenolic acids with various reagents to test their analytical usefulness for GC

0021-9673/86/$03.50

quantitation with flame ionization detection (FID) and ECD. The model compounds include various benzoic and cinnamic acids with one free phenolic hydroxyl group, one carboxyl group and 0, 1 or 2 methoxy groups.

EXPERIMENTAL

Reagents and solvents

The following phenolic acids (purities 97–99%) were obtained from EGA-Chemie (Steinheim, F.R.G.): 4-hydroxy-, 4-hydroxy-3-methoxy- and 4-hydroxy-3,5-dimethoxybenzoic acids, and *trans*-4-hydroxy-, *trans*-4-hydroxy-3-methoxy- and *trans*-4-hydroxy-3,5-dimethoxycinnamic acids. 3-Hydroxy-4-methoxybenzoic acid (99%, EGA-Chemie) was used as an internal standard.

The derivatization reagents were: N,O-bis(trimethylsilyl)trifluoroacetamide (BSTFA) containing 1% trimethylchlorosilane (TMCS) (purum; Fluka, Buchs, Switzerland), pentafluorobenzoyl chloride (PFBC) (98%, EGA-Chemie), bromoacetyl chloride (BAC) (Sigma, St. Louis, MO, U.S.A.), chloroacetic anhydride (CAA) (Sigma), iodoacetic anhydride (IAA) (Sigma), trifluoroacetic anhydride (TFAA) (99%, EGA-Chemie), heptafluorobutyric anhydride (HFBA) (EGA-Chemie), pyridine (silylation grade; Chrompack, Middelburg, The Netherlands), Diazald (N-methyl-N-nitroso-*p*-toluenesulphonamide) (99%, EGA-Chemie), potassium hydroxide (purum; EKA, Surte, Sweden). Diethyl ether, ethyl acetate, methanol (all of analytical grade) and toluene (LiChrosolv) were supplied by E. Merck (Darmstadt, F.R.G.). Ethanol (Aa, 99.5 wt. %) was obtained from Oy Alko Ab (Helsinki, Finland). All reagents and solvents were used as received.

Gas chromatography

All the products formed in the reactions between the reagents and phenolic acids in the model compound mixture were analyzed on a Micromat HRGC 412 gas chromatograph (Orion Analytica, Finland) equipped with both flame ionization and electron-capture detectors. The two-channel instrument was adapted with two similar wall-coated open tubular (WCOT) fused-silica capillary columns (25 m × 0.32 mm I.D.) coated with SE-30 silicone polymer at a film thickness of 0.25 μm (Oriola Prolab, Finland), or with one WCOT fused-silica capillary column (50 m × 0.20 mm I.D.) with chemically bonded OV-1 stationary phase at a film thickness of 0.10 μm (Oriola Prolab) (connected to the operating channel). Hydrogen was used as the carrier gas at flow-rates of 2.7 ml/min (0.50 bar) for the SE-30 columns and 0.6 ml/min (1.30 bar) for the OV-1 column (at 120°C). The make-up gases for FID were hydrogen (0.30 bar) and air (1.00 bar). The optimum standing current for ^{63}Ni-ECD was adjusted with the make-up gas (argon–methane, 95:5), 0.70–1.00 bar, and the compensation current, 180–255 units. The splitting ratio was adjusted to about 30:1, and the injection volume was 0.7 μl for the SE-30 columns and 0.2–0.3 μl for the OV-1 column. The temperature was raised from 120 to 270°C at 8°C/min (SE-30) or from 100 to 250°C at 4°C/min (OV-1). The injector and detector temperatures were maintained at 300°C. The peak areas were integrated with the built-in microcomputer and the chromatograms and data were printed with a Micromat printer-plotter.

Ultrasonication

An ordinary laboratory ultrasound cleaner with a capacity of 2.7 l was used (USF Finnsonic W 181, Oy Ultra sonic finland, Finland).

Derivatization procedures

Separate stock solutions were prepared for benzoic and cinnamic acids by dissolving them in ethyl acetate (Table I). The derivatization reactions were carried out in 3-ml test-tubes with PTFE cup liners. Samples for derivatization were made by mixing 50 μl of each stock solution (Table I) and adding 50 μl of the internal standard solution (17.22 mg of 3-hydroxy-4-methoxybenzoic acid in 50 ml of ethyl acetate). 3-Hydroxy-4-methoxybenzoic acid, a phenolic acid found naturally in negligible amounts if at all, was chosen as an internal standard to illustrate isomer resolution of the various derivatives produced (the samples contain 4-hydroxy-3-methoxybenzoic acid, 2, an isomer of the internal standard). Samples of the derivatization products were introduced into the gas chromatograph by a 10-μl Hamilton syringe.

TABLE I

STOCK SOLUTIONS OF PHENOLIC ACIDS IN ETHYL ACETATE

		Weighed amount (mg)	*Purity* (%)*	*Concentration (mmol/50 ml)*
Mixture of benzoic acids				
4-Hydroxy-	(1)	14.32	99	0.103
4-Hydroxy-3-methoxy-	(2)	18.32	97	0.106
4-Hydroxy-3,5-dimethoxy-	(3)	20.82	97	0.102
Mixture of cinnamic acids				
trans-4-Hydroxy-	(4)	17.11	98	0.102
trans-4-Hydroxy-3-methoxy-	(5)	20.10	98	0.101
trans-4-Hydroxy-3,5-dimethoxy-	(6)	24.90	98	0.109

* According to the supplier.

All of the six phenolic acids (Table I) contain one free carboxyl group and one free phenolic hydroxyl group together with 0, 1 or 2 methoxy groups. In one of the ten derivatization procedures (A, Table II) the phenolic hydroxyl group was left free. All the other derivatization procedures (B to J, Table II) are capable of transforming both free carboxyl and phenolic hydroxyl groups into less polar groups. In all cases the aromatic carboxylic acids were esterified by diazomethane to methyl esters, except in procedure D which gave trimethylsilyl (TMS) esters. After esterification the free phenolic hydroxyl group was chemically modified in different ways. All ten procedures A to J are outlined in Table II and described below in more detail.

(A) *Methyl ester derivatives.* The phenolic acids were transformed into their methyl esters by diazomethane which was freshly prepared from Diazald and potassium hydroxide. After evaporating the solvent from the prepared model compound mixture under a stream of nitrogen, the residue was dissolved in 0.3 ml of diethyl

TABLE II

DERIVATIVES OF PHENOLIC ACIDS

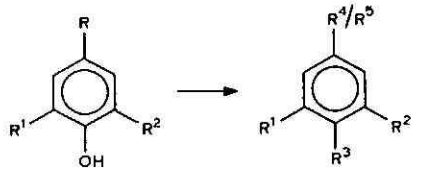

	R	R^1	R^2
1	$-CO_2H$	H	H
2	$-CO_2H$	H	$-OCH_3$
3	$-CO_2H$	$-OCH_3$	$-OCH_3$
4	$-CH=CHCO_2H$	H	H
5	$-CH=CHCO_2H$	H	$-OCH_3$
6	$-CH=CHCO_2H$	$-OCH_3$	$-OCH_3$

Procedure	*Temp. (°C)*	*Time*	*Reagent*	*Derivatives**		
				R^3	*A* R^4	*B* R^5
A	−15	0.5 min	CH_2N_2	HO–	CH_3OOC–	$CH_3OOCCH=CH$–
B	55	24 h	CH_2N_2	CH_3O–	CH_3OOC–	$CH_3OOCCH=CH$–
C	−15	0.5 min	CH_2N_2 +	TMSO–	CH_3OOC–	$CH_3OOCCH=CH$–
	80	30 min	BSTFA/TMCS			
D	80	30 min	BSTFA/TMCS	TMSO–	TMSOOC–	TMSOOCCH=CH–
E	−15	0.5 min	CH_2N_2 +	C_6F_5COO	CH_3OOC–	$CH_3OOCCH=CH$–
	20	9 min	PFBC			
F	−15	0.5 min	CH_2N_2 +	$BrCH_2COO$	CH_3OOC–	$CH_3OOCCH=CH$–
	20	9 min	BAC			
G	90	72 h	CAA +	$ClCH_2COO$	CH_3OOC–	$CH_3OOCCH=CH$–
	−15	0.5 min	CH_2N_2			
H	90	24 h	IAA +	ICH_2COO	CH_3OOC–	$CH_3OOCCH=CH$–
	−15	0.5 min	CH_2N_2			
I	−15	0.5 min	CH_2N_2 +	CF_3COO	CH_3OOC–	$CH_3OOCCH=CH$–
	20	1 h	TFAA			
J	−15	0.5 min	CH_2N_2 +	$CF_3(CF_2)_2COO$	CH_3OOC–	$CH_3OOCCH=CH$–
	80	1 h	HFBA			

* R^1, R^2 as in the starting compounds. A = Benzoic acid esters; B = cinnamic acid esters.

ether–methanol (9:1, v/v). After cooling at −15°C for 5 min, dilute diazomethane in diethyl ether solution (−15°C) was added until a slight yellow colour persisted. In order to prevent the reaction of phenolic hydroxyl groups, the diazomethane was removed within 30 s at −15°C under a stream of nitrogen, whereafter the solvent was evaporated. The residue was dissolved in toluene (100 µl) and an aliquot was analyzed by GC.

(B) *Methyl ester–methyl ether derivatives.* After evaporating the solvent under nitrogen, the phenolic acid residue was dissolved in diethyl ether–methanol (9:1, v/v) and an excess of the ethereal diazomethane (0.5 ml) was added. After keeping the mixture at 55°C for 6 h, an additional amount (1 ml) of diazomethane solution was added and the mixture was kept at the same temperature for 18 h. After evaporating the excess of diazomethane and the solvent, the residue was dissolved in toluene (100 µl) prior to GC analysis.

(C) *Methyl ester–TMS ether derivatives.* The carboxyl groups were methylated by procedure A. After evaporating the solvent under nitrogen, the residue was dissolved in 70 µl of pyridine and 30 µl of BSTFA containing 1% of TMCS were added.

After heating at 80°C for 30 min, the mixture was analyzed by GC.

(D) *TMS ester–TMS ether derivatives.* To trimethylsilylate both the carboxyl and hydroxyl groups of phenolic acids simultaneously, method C was used except that the methyl esterification step was excluded. The derivatives obtained were found to decompose partly within a few hours.

(E) *Methyl ester–pentafluorobenzoate derivatives.* The carboxyl groups of the phenolic acids were carefully methylated by diazomethane as described in procedure A. After evaporating to dryness under nitrogen, the sample was dissolved in 0.2 ml of pyridine, and 10 μl (16 mg, 0.069 mmol) pentafluorobenzoyl chloride (PFBC) were added. The mixture was shaken occasionally for 5 min at room temperature and the reaction was completed by ultrasonication for 4 min. Then 2 ml of diethyl ether and 0.5 ml of 0.1 *M* hydrochloric acid were added and the mixture was shaken vigorously. After separation of two phases, the ether layer was isolated, taken up and washed three times with 0.5 ml of distilled water. The ether solution was dried over anhydrous sodium sulphate overnight. After evaporation of the solvent, the residue was dissolved in toluene (100 μl) and analyzed by GC.

(F) *Methyl ester–bromoacetate derivatives.* To prepare these derivatives the method was essentially the same as E but 10 μl (20 mg, 0.077 mmol) of bromoacetyl chloride (BAC) were used instead of PFBC.

(G) *Methyl ester–chloroacetate derivatives.* To a solution of the phenolic acid mixture in 0.2 ml of ethyl acetate were added 20 mg (0.117 mmol) of chloroacetic anhydride (CAA). Then the mixture was heated in a sealed test-tube at 90°C for 72 h. The solvent and the excess of reagent were evaporated under nitrogen at 60°C in a water-bath. The residue was dissolved in 0.3 ml of diethyl ether–methanol (9:1, v/v) and the carboxyl groups were esterified by diazomethane according to procedure A. The resulting methyl ester–chloroacetate derivatives were then dissolved in 100 μl of toluene prior to GC analysis.

(H) *Methyl ester–iodoacetate derivatives.* This procedure was similar to that of G with two exceptions: (i) 20 mg (0.057 mmol) of iodoacetic anhydride (IAA) were used instead of CAA, and (ii) the reaction time was 24 h at 90°C which, however, was found to be insufficient to complete the reaction.

(I) *Methyl ester–trifluoroacetate derivatives.* The carboxyl groups of the phenolic acids were esterified by diazomethane according to procedure A. After evaporating the solvent under nitrogen, the residue was dissolved in 50 μl of ethyl acetate and 50 μl (75 mg, 0.355 mmol) of trifluoroacetic anhydride (TFAA) were added. The mixture was then kept at room temperature. Within 1 h the reaction went to completion. Then the excess of reagent and the solvent were evaporated at room temperature and the residue was dissolved in 100 μl of toluene prior to GC analysis.

(J) *Methyl ester–heptafluorobutyrate derivatives.* This procedure was similar to I except that 50 μl (83.5 mg, 0.204 mmol) of heptafluorobutyric anhydride (HFBA) were used instead of TFAA and the reaction was carried out in a water-bath at 80°C for 1 h, which led to completion of the reaction. The reaction was quantitative but a longer reaction time (6 h) was found to result in a partial decomposition of the cinnamic acid derivatives.

RESULTS AND DISCUSSION

Methylation

Methylation of both carboxyl and phenolic hydroxyl groups occurs in diethyl ether–methanol solution (9:1, v/v) by ethereal diazomethane. In procedure A the esterification was carried out at −15°C with a dilute diazomethane-solution and the slight excess of diazomethane was removed immediately after reaction under stream of nitrogen to prevent ether formation. The methyl esters of the phenolic acids thus obtained contain a free phenolic hydroxyl group, which causes peak tailing on non-polar columns (and with slightly polar columns, too) and thus these derivatives are not very suitable for GC quantitation. The derivatization of the phenolic hydroxyl group with different reagents gives, however, as we shall see, very valuable derivatives and thus the carboxyl group methylation will be very meaningful.

For methyl ether formation, an elevated temperature (55°C), longer reaction time (24 h) and an excess of diazomethane were required (procedure B). The benzoic acids reacted quantitatively in 6 h, but no adequate reaction conditions were found for the cinnamic acids. Under the reaction conditions applied here some side products were formed from cinnamic acids when diazomethane reacted with the double bond activated by the adjacent aromatic ring (ref. 3, pp. 523–524):

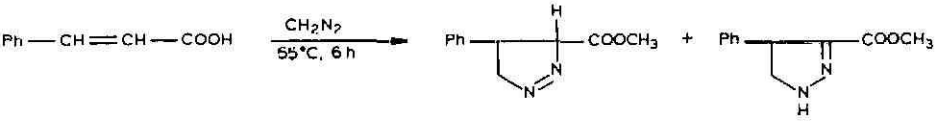

Thus the simultaneous methylation of carboxyl and hydroxyl groups was found to be unsatisfactory for quantifying phenolic acids containing cinnamic acids or structurally related compounds. The procedure is unsuitable also for quantitation of hydroxybenzoic acids, if the sample contains corresponding methoxybenzoic acids.

Trimethylsilylation

The reagent BSTFA containing 1% TMCS is a very powerful silylating agent particularly for compounds with an acidic hydrogen atom, *e.g.*, carboxylic acids and phenols. The two-stage procedure C which includes methyl esterification of the carboxyl group and trimethylsilylation of the phenolic hydroxyl group is useful for quantitation of phenolic acids with FID. All phenolic acids in the model compound mixture were found to react quantitatively and the reaction products were stable for several days. Thus the trimethylsilyl ethers of the phenolic acid methyl esters are very suitable for the GC–FID analysis. Appropriate concentrations are 0.01–10 μg of phenolic acid per injection. When ECD was applied the responses for the cinnamic acid derivatives were much greater than those of the benzoic acid analogues. This is probably due to the conjugated electron-rich system comprised of a carboxyl group, a double bond in the side chain, a benzene ring and a phenolic hydroxyl group[7]. So these derivatives are useful also in cinnamic acid trace analysis when ECD is used. The gas chromatograms of the trimethylsilyl ethers of the phenolic acid methyl esters using FID and ECD are illustrated in Fig. 1.

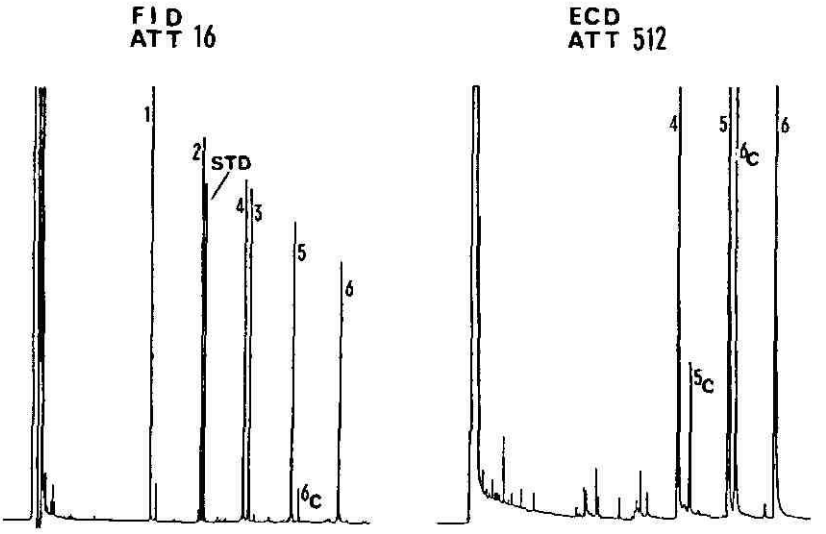

Fig. 1. Capillary gas chromatograms of the TMS ethers of phenolic acid methyl esters using FID and ECD. Peaks: 1 = 4-hydroxybenzoic acid; 2 = 4-hydroxy-3-methoxybenzoic acid; 3 = 4-hydroxy-3,5-dimethoxybenzoic acid; 4 = *trans*-4-hydroxycinnamic acid; 5 = *trans*-4-hydroxy-3-methoxycinnamic acid; 5C = *cis*-4-hydroxy-3-methoxycinnamic acid; 6 = *trans*-4-hydroxy-3,5-dimethoxycinnamic acid; 6C = *cis*-4-hydroxy-3,5-dimethoxycinnamic acid. STD = 3-hydroxy-4-methoxybenzoic acid as an internal standard. GC conditions: WCOT fused-silica capillary column (50 m × 0.20 mm I.D.) coated with chemically bonded OV-1, film thickness 0.10 μm; 1.3 bar hydrogen as the carrier gas; splitting ratio 30:1; attenuation (ATT) 16 for FID, 512 for ECD; column temperature raised from 100 to 250°C at 4°C/min.

The trimethylsilylation reactions both of carboxyl and hydroxyl groups were also found to proceed rapidly and quantitatively when procedure D was applied. These trimethylsilyl ethers of phenolic acid trimethylsilyl esters were also suitable for GC–FID analysis and cinnamic acid trace analysis when ECD was used. The resolution of the isomers 4-hydroxy-3-methoxybenzoic acid and 3-hydroxy-4-methoxybenzoic acid (internal standard) was, however, unsatisfactory when compared to the trimethylsilyl ether–methyl ester derivatives. The quantitation of these derivatives by GC should also be made immediately after derivatization because of the partial decomposition which was found to occur within a few hours.

Derivatization of phenolic hydroxyl group

The free hydroxyl groups in phenolic acid methyl esters were treated by six different derivatization reactions presented in Table II. Procedures E to J resulted in pentafluorobenzoates, various halogenoacetates and heptafluorobutyrates. Four procedures, namely E (reagent PFBC), G (CAA), I (TFAA) and J (HFBA) gave reaction products which were suitable for quantitation, but procedures F (BAC) and H (IAA) failed in this respect. In procedure F a decomposition of the reagent resulted in bromine which may react further with, *e.g.*, the double bonds of the cinnamic acid esters. In procedure H, 24 h at 90°C was insufficient for complete reaction. Some extraneous reaction products were also formed. Pentafluorobenzoates (procedure E) were formed quantitatively and they have high ECD responses, as do the other halo-

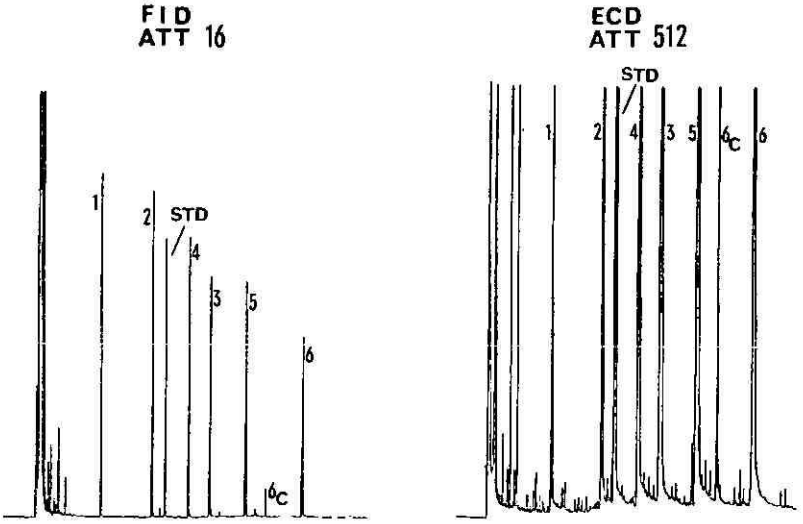

Fig. 2. Capillary gas chromatograms of the heptafluorobutyrates of phenolic acid methyl esters using FID and ECD. For peak identification and GC conditions, see Fig. 1.

genated derivatives. The derivatization was, however, complicated and troublesome. Chloroacetates which were obtained quantitatively by procedure G were useful derivatives for ECD. The drawback of this method is the long reaction time (72 h at 90°C). The trifluoroacetates (procedure I) and heptafluorobutyrates (procedure J) were also applicable to ECD and were prepared in 1 h which is short enough for practical work. The latter derivatives of cinnamic acid esters were found partly to decompose when longer reaction times and higher temperatures were applied. In the case of trifluoroacetates the acidification of the reaction mixture through the formation of trifluoroacetic acid may also promote decomposition of cinnamic acids. Newby *et al.*[8] have reported that hydroxycinnamic acids rapidly decompose in acidic and hot solution, whereas *p*-hydroxybenzoic acids are stable under the same conditions. The heptafluorobutyrates and the trifluoroacetates of phenolic acid methyl esters will, however, be the most useful derivatives in quantitation with ECD. The heptafluorobutyrated derivatives are preferred because of their higher stability and greater detector response. They are very suitable for quantiation by FID, too. The gas chromatograms of the heptafluorobutyrates of the phenolic acid methyl esters using both FID and ECD are illustrated in Fig. 2. In general, in our study a slight isomerization of cinnamic acids from *trans* to *cis* during their derivatization reactions could be observed.

CONCLUSIONS

The suitability of the different derivatives of phenolic acids prepared for GC quantitation with FID and ECD and the feasibility of various derivatization procedures can be summarized as follows:

1. The trimethylsilyl ethers of the phenolic acid methyl esters are the most

suitable derivatives for the GC quantitation with FID. In the first step of the derivatization procedure the carboxyl group is methylated with dilute ethereal diazomethane at −15°C and then in the second step the phenolic hydroxyl group is trimethylsilylated with BSTFA at 80°C for 30 min. The procedure is simple, rapid and quantitative. Resolution of isomers is adequate and the products are stable for several days. The GC quantitation is suitable for samples with relatively high concentrations of phenolic acids (0.01–10 μg per injection). Total trimethylsilylation of phenolic acids will also give suitable derivatives for GC–FID, but the resolution of isomers is not satisfactory. The reaction products are also unstable, partly decomposing within a few hours. The EC detection sensitive derivatives, heptafluorobutyrates of phenolic acid methyl esters will also be suitable for GC–FID quantitation, too, but the procedure J includes an additional step (evaporation–dissolution) and the detector responses are lower when compared to the trimethylsilylated phenolic acid methyl esters.

2. The best derivatives for quantitation with ECD are the heptafluorobutyrates of phenolic acid methyl esters. The derivatization (procedure J) is simple and quantitative. The possible decomposition of cinnamic acids can be prevented if the reaction time does not exceed 1 h at 80°C. The concentration for quantitation can vary in the range 0.05–1 ng of phenolic acid per injection.

ACKNOWLEDGEMENTS

We would like to thank Professor K. Pihlaja for his critical reading and comments on the manuscript. This study was partly supported by the Academy of Finland.

REFERENCES

1 A. E. Pierce, *Silylation of Organic Compounds*, Pierce Chemical Co., Rockford, IL, 1968.
2 J. F. Lawrence and R. W. Frei, *Chemical Derivatization in Liquid Chromatography*, Elsevier, Amsterdam, 1976.
3 D. R. Knapp, *Handbook of Analytical Derivatization Reactions*, Wiley, New York, Chichester, Brisbane, Toronto, 1979.
4 G. Eglinton and M. T. J. Murphy (Editors), *Organic Geochemistry*, Springer, Berlin, Heidelberg, New York, 1969, pp. 558–575.
5 K. Lehtonen and M. Ketola, *VTT Symposium 65. Turve- ja humussymposiumi (Peat and humus symposium), Turku, September 2–3, 1985*, (Finnish; Summary in English) Technical Research Centre of Finland, Espoo, 1986, pp. 178–183.
6 K. Hänninen, O. Lehto and P. Mälkönen, in C. H. Fuchsman (Editor), *Proc. 1981 Int. Peat Symposium, Bemidji, MN, October 21–23, 1981*, Bemidji State University, Bemidji, 1981, pp. 117–155.
7 C. F. Poole, *J. High Resolut. Chromatogr. Chromatogr. Commun.*, 5 (1982) 454–471.
8 V. Newby, R.-M. Sablon, R. Synge, K. Casteele and C. Van Sumere, *Phytochemistry*, 19 (1980) 651–657.

Journal of Chromatography, 370 (1986) 475–483
Elsevier Science Publishers B.V., Amsterdam — Printed in The Netherlands

CHROM. 19 019

DIRECT ANALYTICAL AND PREPARATIVE RESOLUTION OF ENANTIOMERS USING ALBUMIN ADSORBED TO SILICA AS A STATIONARY PHASE

PER ERLANDSSON*
Department of Technical Analytical Chemistry, Chemical Center, University of Lund, P.O. Box 124, S-221 00 Lund (Sweden)
LENNART HANSSON
Pierce Sweden AB, Sölvegatan 41, S-223 70 Lund (Sweden)
and
ROLAND ISAKSSON
Division of Organic Chemistry 3, Chemical Center, University of Lund, P.O. Box 124, S-221 00 Lund (Sweden)
(Received August 14th, 1986)

SUMMARY

A rapid and simple method for the preparation of high-performance liquid chromatography columns for chiral separations is described. The stationary phase is prepared by adsorbing bovine serum albumin on silica. Both analytical and preparative applications are described. A polarimeter was used as a detector to determine the enantiomer elution orders.

INTRODUCTION

During the last decade, interest in the determination of enantiomeric composition has increased dramatically, especially for pharmaceutical applications. A number of stationary phases for direct chiral separation by liquid chromatography, *i.e.*, resolution of enantiomers without prior derivatization, have been developed[1]. These have been based on, *e.g.*, naturally occurring chiral polymeric materials such as cellulose[2], starch, α_1-acid glycoprotein[3] and albumin[4].

In 1973, Stewart and Doherty[5] immobilized bovine serum albumin (BSA) on succinoylaminoethyl-Sepharose and completely resolved DL-tryptophan. Later, Allenmark *et al.*[4] covalently immobilized BSA on 10-μm silica in order to increase the column efficiency. This column has successfully been used to resolve various polar aromatic compounds, such as N-aroylamino acids and aromatic sulphoxides[1]. To the best of our knowledge, the immobilization technique used by Allenmark *et al.*[4] has not been described in the literature. BSA has also been used as a chiral additive in the mobile phase by, *e.g.*, Pettersson *et al.*[6].

The purpose of this work was to prepare analytical and preparative columns

0021-9673/86/$03.50

by irreversible adsorption of BSA to silica and secondly to compare the efficiency and selectivity of these columns with covalently bonded BSA columns.

EXPERIMENTAL

Materials

Bovine serum albumin (BSA) (Art. A-7030) was obtained from Sigma (St. Louis, MO, U.S.A.), D-tryptophan from United States Biochemical Corp. (Cleveland, OH, U.S.A.), DL-tryptophan and L-tryptophan from Merck (Darmstadt, F.R.G.) and DL-benzoin from BDH Chemicals, (Poole, U.K.). DL-Warfarin was a gift from AB Ferrosan (Malmö, Sweden), as were DL-Oxazepam from KabiVitrum (Stockholm, Sweden) and DL-Omeprazol from AB Hässle (Mölndal, Sweden).

Chromatography

Analytical columns were prepared by packing Vydac silica (5 μm, 300 Å, 100 m^2/g) (The Separations Group, Hesperion, CA, U.S.A.) or Nucleosil (5 μm, 300 Å, 120 m^2/g) (Macherey-Nagel, Düren, F.R.G.) into stainless-steel 200 mm × 4.6 mm Li-Chroma tubing (Skandinaviska GeneTec AB, Kungsbacka, Sweden) with an ascending slurry-packing technique[7]. A 3-g amount of silica was suspended in chloroform–methanol (2:1) and poured into a 75-ml packing bomb. The slurry was packed into the column at 400 bar using methanol as displacing medium.

For the preparative column, Matrex silica (20–45 μm, 500 Å) (Amicon-Grace, Helsingborg, Sweden) was packed into a 500 mm × 22 mm Valco stainless-steel column (Skandinaviska GeneTec AB) by a descending sedimentation technique. A 1120 mm × 22 mm glass tube was connected to the top of the open steel column with a plastic tube and the assembly was filled with a slurry of BSA–silica in 0.05 *M* phosphate buffer at pH 5.0. A water aspirator was connected to the bottom of the steel column and operated at the maximum available reduced pressure. During the sedimentation of the silica, more phosphate buffer was added until the bed had completely settled.

Potassium phosphate buffer mobile phases were prepared in MilliQ grade water obtained by purifying demineralized water in a MilliQ filtration system (Millipore, Bedford, MA, U.S.A.). In some cases, 1-propanol was used as the organic modifier. All mobile phases were degassed and filtered through a 0.45-μm Millipore filter prior to use. A standard chromatographic set-up was used comprising an LDC Constametric III pump or an Altex 110A pump with a preparative head (maximum flow-rate 28 ml/min). UV detection was performed with an LDC Spectromonitor III variable wavelength UV detector connected to a W+W 1200 dual-channel potentiometric recorder. The samples were injected with a Rheodyne 7120 injector with a 10-μl loop, or for preparative experiments with a 2-ml loop.

Specific rotation was monitored with a Perkin-Elmer 241 MC polarimeter using a 1 ml/l dm flow-cell to establish the elution order between the enantiomers[6].

Determination of BSA adsorption

To optimize the conditions for adsorption of BSA to silica, the influences of the phosphate concentration and pH were investigated. To 10 mg of 5-μm, 300-Å silica in a 10-ml glass test-tube were added 5 ml of a BSA–phosphate solution. The

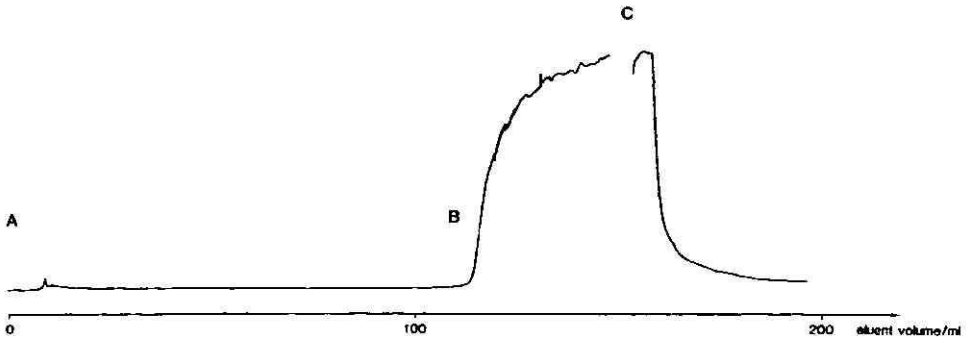

Fig. 1. Breakthrough of the eluting liquid from a 100 mm × 4.6 mm silica column during *in situ* adsorption of BSA on silica. UV detection at 280 nm. At A, a solution of 1 mg BSA/ml in 0.05 *M* phosphate, pH 5.0, is pumped into the column and at B, the breakthrough point is reached. At C, the column is washed with 0.05 *M* phosphate, pH 5.0.

tube was placed in an ultrasonic bath for 1 min and then on a vortex mixer for 10 s. The pH was measured and the contents of the tube were then centrifuged in a bench-top centrifuge to sediment the silica. The change in absorbance at 280 nm of the supernatant was monitored with an Hitachi Perkin-Elmer 124 spectrophotometer and the amount of adsorbed BSA per mg silica was calculated.

In situ immobilization of BSA by adsorption

The prepacked silica column was washed with approximately 50 column volumes of water and equilibrated with the same volume of 0.05 *M* phosphate buffer, pH 5.0. A solution of 1 mg BSA/ml in 0.05 *M* phosphate buffer pH 5.0 was pumped through the column until breakthrough of BSA was detected at 280 nm (see Fig. 1). From the breakthrough point the amount of BSA immobilized on the column was calculated. The column was then equilibrated with the same buffer but without BSA until a stable UV baseline was obtained. The leakage of BSA into the eluent was checked with Pierce BCA-protein assay reagent (Pierce Chemical Co., Rockford, IL, U.S.A.). The void volumes used for calculating k' and α were determined by injection of sodium nitrite, water or by observing the first baseline disturbance. Plate numbers, N, were calculated from the band widths at half-height[8].

RESULTS AND DISCUSSION

The amount of BSA adsorbed to silica is strongly dependent on the pH of the phosphate buffer (see Fig. 2), but the ionic strength has only a minor effect (see Fig. 3). The isoelectric point of BSA is located at pH 4.9[9], which is also the point of maximum adsorption. The maximum amount of BSA adsorbed is approximately 0.1 g per 100 m^2 silica (1 g). The surface area values employed were those stated by the supplier.

BSA has been described as a 140 Å × 40 Å prolate ellipsoid[10]. Assuming that, with a molecular weight of 66 500, it occupies an area of 140 × 40 $Å^2$ on silica, this will give a surface coverage of 60%. The surface area of silica that is accessible to the large BSA molecule is lower than the specific surface, 100 m^2/g, as measured by

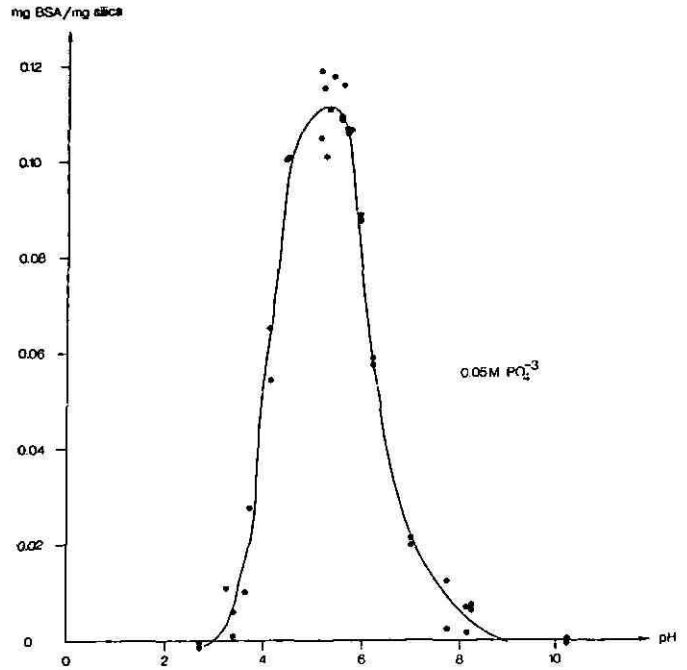

Fig. 2. The effect of pH on the adsorption of BSA to silica in 0.05 *M* phosphate buffer.

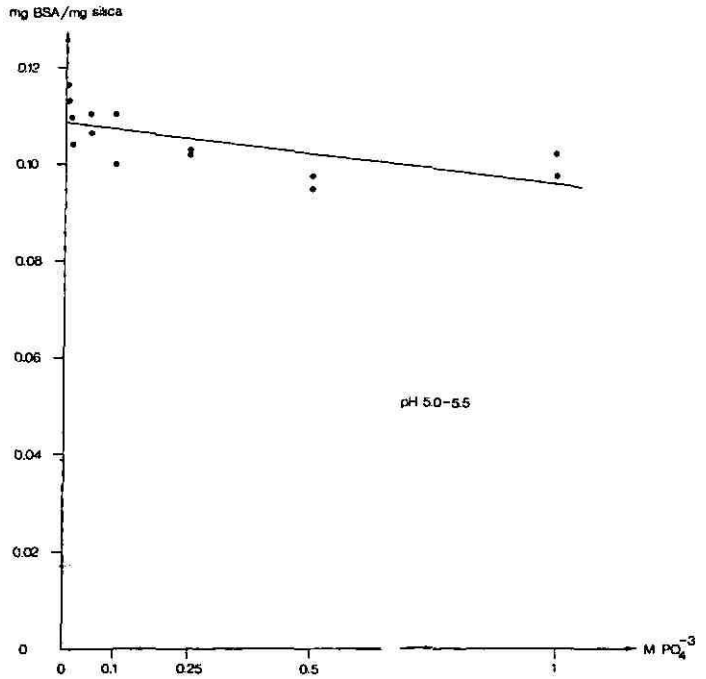

Fig. 3. The effect of the phosphate concentration on the adsorption of BSA to silica in phosphate buffer.

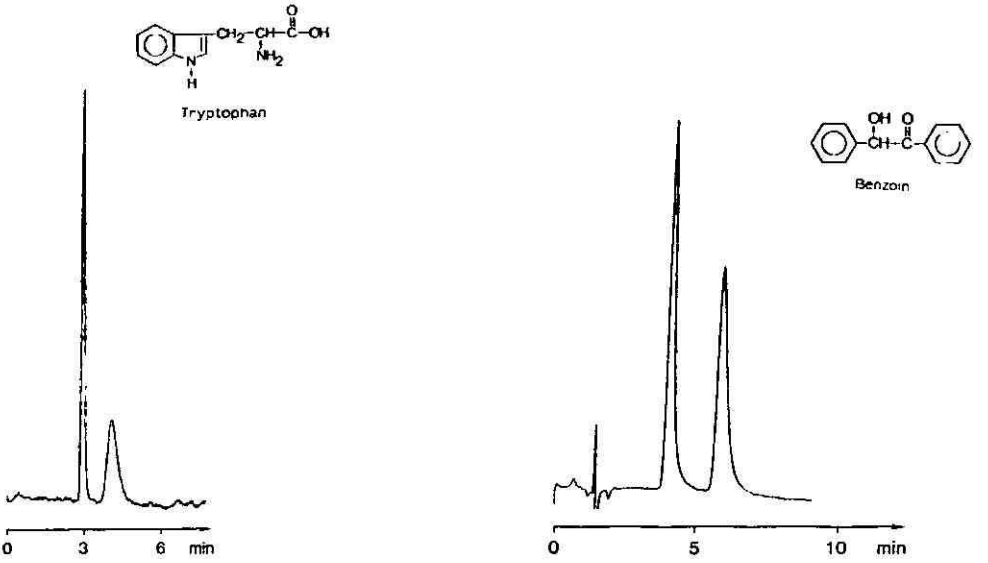

Fig. 4. Resolution of DL-tryptophan (10 μl, 0.37 mM injected) on a 200 mm × 4.6 mm column packed with 5-μm BSA–silica; mobile phase 0.05 M phosphate, pH 7.0; flow-rate 1.0 ml/min; UV detection at 278 nm. $k'_1 = 0.26$, $k'_2 = 0.78$, $\alpha = 3.0$, $N_1 = 2500$ and $N_2 = 460$.

Fig. 5. Resolution of DL-benzoin (10 μl, 0.01 mg/ml injected). Details as in Fig. 4, except 2% 1-propanol as modifier and UV detection at 250 nm. $k'_1 = 1.7$, $k'_2 = 3.0$, $\alpha = 1.7$, $N_1 = 2000$ and $N_2 = 1600$.

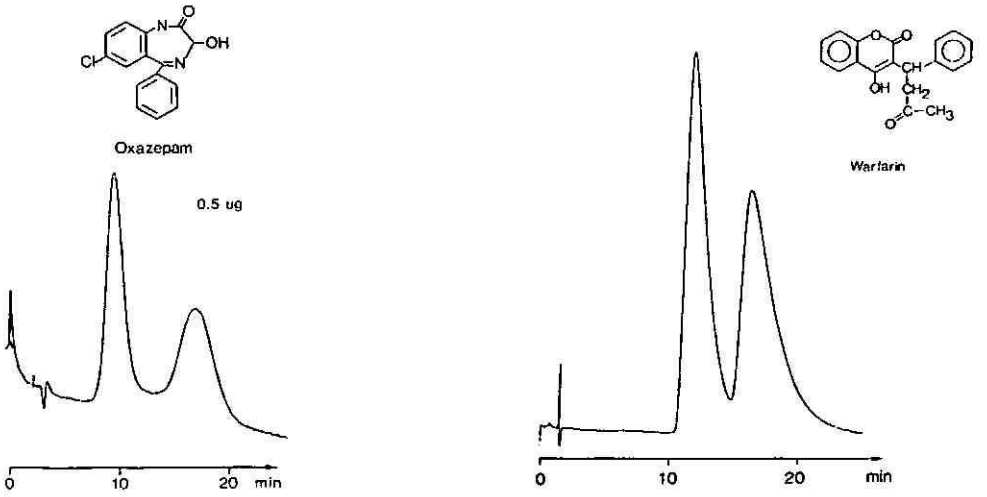

Fig. 6. Resolution of DL-Oxazepam (10 μl, 0.05 mg/ml injected) on a 200 mm × 4.6 mm column packed with 20–45 μm BSA–silica; mobile phase 0.1 M phosphate, pH 7.0; 2% 1-propanol as modifier; flow-rate 1.0 ml/min; UV detection at 230 nm. $k'_1 = 2.1$, $k'_2 = 4.5$, $\alpha = 2.1$, $N_1 = 170$ and $N_2 = 120$.

Fig. 7. Resolution of DL-Warfarin (10 μl saturated solution in water, (less than 0.1 mg/ml injected) on a 200 mm × 4.6 mm column packed with 5-μm BSA–silica; mobile phase 0.05 M phosphate, pH 7.0; 2% 1-propanol as modifier; flow-rate 1.0 ml/min; UV detection at 308 nm. $k'_1 = 7.0$, $k'_2 = 10.3$, $\alpha = 1.5$, $N_1 = 250$ and $N_2 = 200$.

TABLE I

SUMMARY OF CHROMATOGRAPHIC DATA

0.05 *M* phosphate buffer, pH 7.0 was used as the mobile phase and the column size was 200 mm × 4.6 mm.

Solute	*Silica (μm)*	*1-Propanol (%)*	k'_1	k'_2	α	N_1	N_2	*Fig.*
DL-Tryptophan	5	–	0.26	0.78	3.0	2500	460	3
DL-Benzoin	5	2	1.73	3.0	1.73	2000	1600	4
DL-Oxazepam	20–45	2	2.13	4.53	2.13	170	120	5
DL-Warfarin	5	2	7.0	10.3	1.48	250	200	6

BET nitrogen adsorption[11] and it seems reasonable that a monolayer of BSA is obtained.

Our results are in good agreement with those obtained for porous glass (particle size 10 μm, 240 Å, surface area 97 m^2/g) by Mizutani[12] where 136 mg albumin per g glass were adsorbed under optimum conditions, *i.e.*, in phosphate buffer pH 5. Mizutani deduced that albumin was adsorbed as a monolayer and that adsorption was caused by two factors; one is the amine–silanol ionic bonding and the other is a cooperative aggregative force between silica and proteins. It was also stated that both hydrogen bonding and hydrophobic interaction are of minor importance for protein adsorption.

Once the BSA is immobilized at pH 5 only a small fraction of BSA is lost from the column by changing the pH in the range 4–7.5.

The separations obtained for DL-tryptophan, DL-benzoin, DL-Oxazepam and DL-Warfarin (see Table I and Figs. 4–7) are in good agreement with results published by Allenmark *et al.*[13–16] from columns with covalently bonded BSA. Preliminary results show however differences in chiral selection between adsorbed and covalently bonded BSA. Chiral sulphoxides such as DL-Omeprazole and DL-2-methylsulphinylbenzoic acid could not be resolved on the adsorbed BSA–silica column. The reason for this behaviour is not yet known.

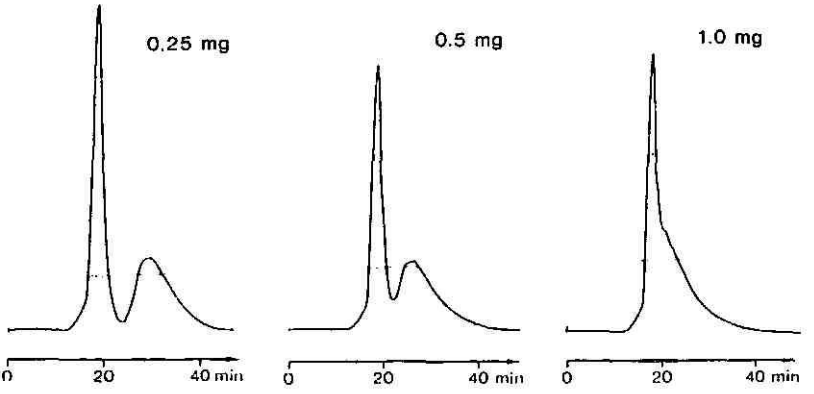

Fig. 8. Chromatograms showing the loadability of DL-tryptophan (0.25, 0.5 and 1.0 mg) on a 500 mm × 22 mm column packed with 20–45 μm BSA–silica; mobile phase 0.05 *M* phosphate, pH 7.5; flow-rate 11 ml/min; UV detection at 278 nm.

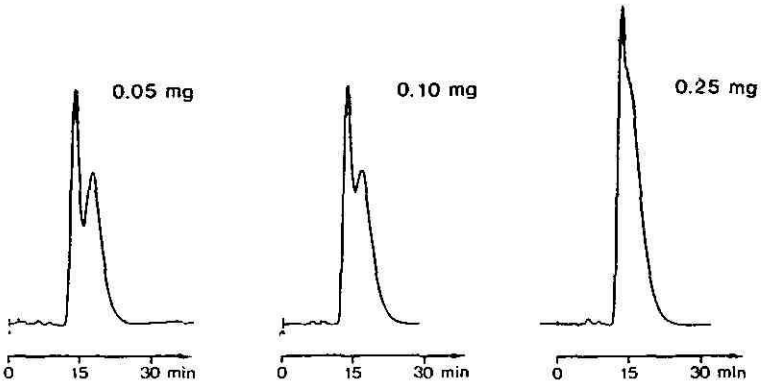

Fig. 9. Chromatograms showing the loadability of DL-benzoin (0.05, 0.10 and 0.25 mg). Details as in Fig. 8, except flow-rate 28 ml/min and *UV detection at 250 nm*.

The preparative use of columns with chiral discriminators of high molecular weight is limited because of the intrinsically low loadabilities of such columns[17]. In spite of this, the use of these columns in preparative work is of interest in studies, of, *e.g.*, the biological activity of potent drugs where milligram quantities are sufficient. In such cases, the stationary phase must be accessible in large quantities or easily made in the laboratory from commercially available materials.

To evaluate the adsorbed BSA–silica stationary phase for preparative purposes, a preparative column was prepared and the loadability of DL-tryptophan (see Fig. 8) and DL-benzoin (see Fig. 9) was investigated. The amount of adsorbed BSA on

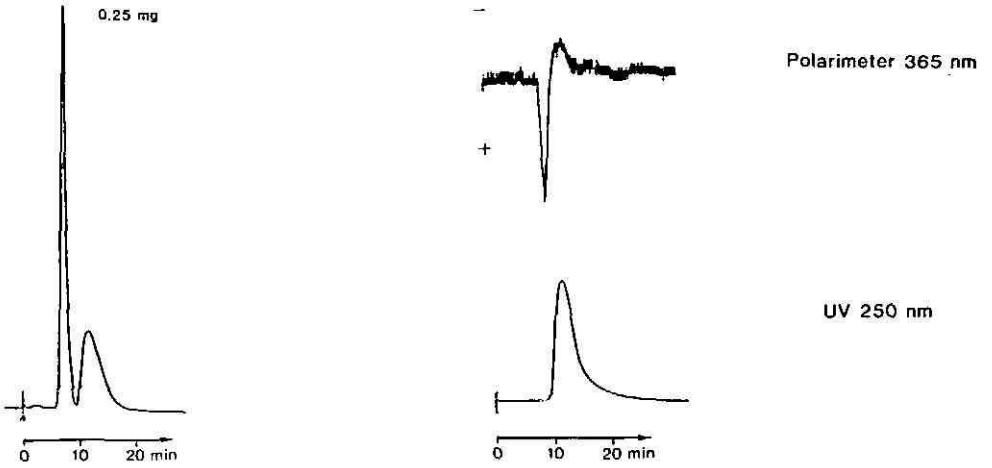

Fig. 10. Resolution of 0.25 mg DL-tryptophan in 15 min with baseline separation. Column: 500 mm × 22 mm packed with 20–45 μm BSA–silica. Mobile phase: 0.05 *M* phosphate, pH 7.5; flow-rate 28 ml/min. UV detection at 278 nm.

Fig. 11. Polarimetric detection at 365 nm and simultaneous UV detection at 250 nm of 5 mg DL-benzoin eluted from a 500 mm × 22 mm column packed with 20–45 μm BSA–silica. Mobile phase: 0.05 *M* phosphate, pH 7.5; flow-rate 28 ml/min.

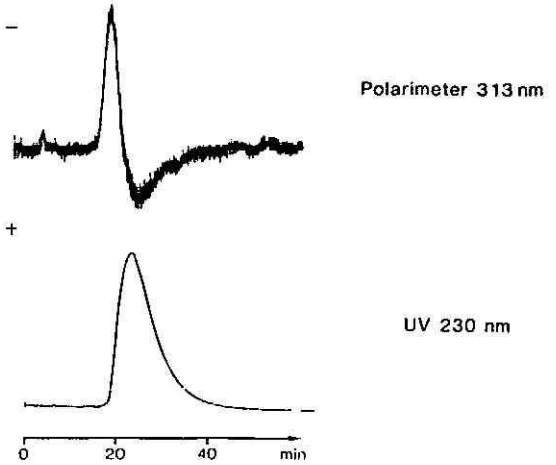

Fig. 12. Polarimetric detection at 313 nm and simultaneous UV detection at 230 nm of 2.5 mg DL-Oxazepam. Details as in Fig. 11.

the 500-Å silica was approximately 0.1 g per 50 m^2 (1 g), which gives a surface density of BSA of twice that for 300-Å silica (surface area values according to the supplier). The reason for this may be that a larger portion of the pores of the 500-Å silica is accessible to the BSA. The total amount of BSA in the preparative column was approximately 8 g. In favourable cases, a throughput of approximately 1 mg/h of racemic compounds could be obtained with baseline separation (see Fig. 10). It was also possible to use a polarimeter as a detector to determine the elution order of enantiomers (see Figs. 11 and 12) which facilitates, *e.g.*, recycling techniques. Because of the low sensitivity of the polarimeter and the low specific rotations of benzoin and Oxazepam, overloading of the column was necessary for these compounds.

Leaching of BSA from the equilibrated column was found to be below the detection limit of the assay, 0.01 mg/ml. Changes in the pH of the mobile phase and injection of solutes in organic solvents such as methanol, ethanol and 1-propanol displaces small amounts of BSA from the column. The displaced BSA is unretained and causes no interference with the retained solutes. Of the above mentioned alcohols, methanol causes the smallest amount of BSA to be displaced.

The lifetime of the columns is more than 6 months if they are stored properly, *i.e.*, at +4°C, pH 5–7 when not in use. The pH stability under alkaline conditions is primarily limited by the silica. At pH 8, some BSA is lost and exposes the silica surface onto which BSA can be recoated. After two to four recoatings the columns do not show acceptable performance and must be discarded.

REFERENCES

1 S. Allenmark, *J. Biochem. Biophys. Methods*, 9 (1984) 1–25.
2 G. Hesse and R. Hagel, *Liebigs Ann. Chem.*, (1976) 996–1008.
3 J. Hermansson, *J. Chromatogr.*, 269 (1983) 71–80.
4 S. Allenmark, B. Bomgren and H. Borén, *J. Chromatogr.*, 264 (1983) 63–68.
5 K. K. Stewart and R. F. Doherty, *Proc. Natl. Acad. Sci. U.S.A.*, 70 (1973) 2850–2852.

6 C. Pettersson, T. Arvidsson, A.-L. Karlsson and I. Marle, in C. Pettersson, *Dissertation*, University of Uppsala, 1984.
7 P. A. Bristow, P. N. Brittain, C. M. Riley and B. F. Williamson, *J. Chromatogr.*, 131 (1977) 57–64.
8 L. R. Snyder and J. J. Kirkland, *Introduction to Modern Liquid Chromatography*, Wiley, New York, 2nd ed., 1979, p. 31.
9 A. L. Lehninger, *Biochemistry*, Worth, New York, 2nd ed., 1978, p. 162.
10 P. G. Squire, P. Moser and C. T. O'Konski, *Biochemistry*, 7 (1968) 4261–4272.
11 B. H. Kaye, in F. J. Welcher (Editor), *Standard Methods of Chemical Analysis*, Vol. 3, Van Nostrand, New York, 6th ed., 1966, pp. 829–831.
12 T. Mizutani, *J. Liq. Chromatogr.*, 8 (1985) 925–983.
13 S. Allenmark, B. Bomgren and H. Borén, *J. Chromatogr.*, 237 (1982) 473–477.
14 S. Allenmark, B. Bomgren and H. Borén, *J. Chromatogr.*, 316 (1984) 617–624.
15 S. Allenmark, *LC, Liq. Chromatogr. HPLC Mag.*, 3 (1985) 348–353.
16 S. Allenmark, *J. Liq. Chromatogr.*, 9 (1986) 425–442.
17 W. Lindner and C. Pettersson, in I. W. Wainer (Editor), *Liquid Chromatography in Pharmaceutical Development*, Aster Publishing Corp., Springfield, OR, 1985, p. 99.

Journal of Chromatography, 370 (1986) 485–493
Elsevier Science Publishers B.V., Amsterdam — Printed in The Netherlands

CHROM. 19 024

THIN-LAYER ELECTROPHORETIC BEHAVIOUR OF OLIGO- AND MONOSACCHARIDES, URONIC ACIDS AND POLYHYDROXY COMPOUNDS OBTAINED AS BIOMASS DEGRADATION PRODUCTS

GÜNTHER BONN* and MICHAEL GRÜNWALD
Institute of Radiochemistry, University of Innsbruck, Innrain 52a, A-6020 Innsbruck (Austria)
HEIMO SCHERZ
Deutsche Forschungsanstalt für Lebensmittelchemie, Lichtenbergstrasse 4, D-8046 Garching (F.R.G.)
and
ORTWIN BOBLETER
Institute of Radiochemistry, University of Innsbruck, Innrain 52a, A-6020 Innsbruck (Austria)
(First received July 31st, 1986; revised manuscript received August 19th, 1986)

SUMMARY

A recently developed thin-layer electrophoretic method has been applied to the determination of biomass degradation products comprising mono-, oligo- and polysaccharides and their derivatives as well as phenolic compounds. The separation was carried out using 0.3 *M* aqueous borate solution as the buffer and silanized silica gel as the support, the surface of the latter being covered with a thin film of octanol-1. For visualization of the carbohydrates, specific sulphuric acid-containing naphthoresorcinol and orcinol reagents were applied. The mobility of hydrolyzed products is determined by the number and position of their reactive sites and, to a less extent, by the size of their molecule. The good separations obtained confirm this method as an alternative to the commonly utilized chromatographic procedures.

INTRODUCTION

Zone electrophoresis is a method frequently applied in carbohydrate analysis[1–3]. Ionic compounds, such as uronic acids or sugar phosphates, migrate even at neutral pH, but electrically neutral substances (mono-, oligo- and polysaccharides) have to be converted into an ionic form. Borate ions have proved to be suitable for this purpose, as they react with vicinal hydroxyl groups forming negatively charged complexes[2–5]. Steric hindrance by large side-chains and interaction with other ligands may promote or block the formation of complexes[3]; therefore a wide variety of mobilities can be found. A special advantage of using borate complexes is their high mobility under the influence of an electric field, up to ten times higher than the mobilities of other charged carbohydrate systems[1].

The choice of the carrier materials is a central problem. Good separations of mono- and oligosaccharides were obtained by high-voltage electrophoresis on chro-

0021-9673/86/$03.50

matography paper[6]. For the analysis of polysaccharides, foils of cellulose acetate[7] and glass fibre paper[8] are suitable. The use of gel materials (acrylamide, agarose, starch), frequently utilized in protein and nucleic acid chemistry, is not possible here because of the molecular sieve effect and the polydispersity of the polysaccharides[9].

The following factors have additionally reduced the applicability of electrophoresis to this case: (a) the limited possibilities for visualization (for chromatography paper and cellulose acetate); (b) the adsorption and electroendoosmosis effects (for glass fibre paper)[8,10]. The first limitation is especially relevant to non-reducing oligo- and polysaccharides, as the specific reagents containing sulphuric or phosphoric acids cannot be used because of simultaneous side-reactions with the carrier materials, such as chromatography paper, cellulose acetate or gels. These reagents may be applied on glass fibre paper, but adsorption and endoosmosis effects cause distortion of zones and complex conditions for migration. When silanized glass fibre paper is used, these phenomena can be suppressed and good results are obtained for polysaccharides, but this carrier material is mechanically unstable and difficult to handle[8].

To overcome these disadvantages, silanized silica gel, which has been used in thin-layer chromatography (TLC)[11], can be used as a support. Its surface is covered with a thin film of an organic fluid not miscible with water[12]. With this system, stable thin layers are obtained, adsorption and endoosmosis effects are low and chemically aggressive reagents can be employed. The carbohydrate-containing zones are detected by using special phenol–sulphuric acid reagents. Sulphuric acid degrades carbohydrates to furfural derivatives, which form coloured compounds with phenols[13].

The present work describes the evaluation of this technique and its application to the special problem of analyzing degradation products obtained by hydrothermolysis of biomass. In this procedure, the biomass components are solubilized in pure water under pressure at temperatures of 170 to > 300°C. Hemicellulose, cellulose and lignin can be dissolved step by step[14,15]. This treatment leads to aqueous solutions containing a complex mixture of poly-, oligo- and monosaccharides as well as other polyhydroxy compounds, furan derivatives and phenolcarboxylic acids. For the determination of these substances, high-performance liquid chromatography (HPLC)[16], ion-exchange and gas chromatography[17], TLC[18] and isotachophoresis (for phenolic components of the lignin)[19] have been employed. Electrophoresis could therefore be a suitable supplement to these commonly utilized methods.

MATERIALS AND METHODS

Instrumentation

In all experiments a Bio-Rad horizontal electrophoresis cell (for 15 cm × 10 cm plates) with a power supply and Desaga equipment for the manufacture of TLC plates (with variable adjustment for thickness of the layer) were used.

Chemicals

Special chemicals employed in the experimental procedures were silica gel 60 H, silanized (Merck Art. No. 7761), octanol-1 (p.a.), glass fibre paper (Whatman GF/C), 1,3-dihydroxynaphthalene (naphthoresorcinol), 3,5-dihydroxytoluene (orcinol), polyvinylpyrrolidone K 90 (molecular weight 340000; Fluka, Buchs, Switzer-

land) and xylan (mol.wt. about 25000; Serva Feinbiochemica, Heidelberg, F.R.G.).

The following chemicals were used as reference substances for the determination of the migration distances: DL-glyceraldehyde, methylglyoxal, 1,3-dihydroxyacetone and cellobiose (Fluka, Buchs, Switzerland); glycolaldehyde, furfural, 5-hydroxymethylfurfural, D-glucose, D-fructose, D-xylose (Merck, Darmstadt, F.R.G.); maltotriose (EGA-Chemie, Steinheim, F.R.G.); 1,6-anhydro-β-D-glucose (Sigma, St. Louis, MO, U.S.A.).

Buffer solution

Crystallized boric acid 18.54 g (0.3 mol) and Titriplex III (7.44 g, 0.02 mol) were dissolved in 200 ml of distilled water and 2 *M* sodium hydroxide solution was added until the pH was 10; then the solution was made up to 1000 ml with distilled water.

Thin-layer plates

A 15-g amount of silanized silica gel was suspended in 100 ml dichloromethane containing 4 g octanol-1. After stirring for 30 min the solvent was vacuum-evaporated. The remaining dry powder, which should be free from lumps, was mixed with 10 ml of a 2% solution of polyvinylpyrrolidone in the buffer and 35 ml pure buffer solution. Then the plates were coated to a thickness of 0.3 mm and placed in a desiccator. They were kept in an humid atmosphere (over the buffer solution) for 12 h.

Preparation of the solutions to be analyzed

Samples of wheat straw and poplar wood were chopped and ground, then degraded in the hydrothermolysis apparatus at 200 and 270°C (see refs. 14 and 15). The eluates were concentrated and dissolved in buffer solution (one to three times the quantity of the concentrate). Alternatively, standard solutions of pure substances and mixtures were prepared (0.5–3% solutions).

Electrophoretic procedure

The plates were taken from the desiccator and put immediately onto cooling block of the electrophoresis apparatus. The connection to the electrolyte vessels was made through strips of glass fibre paper, soaked with buffer. The plates were equilibrated for 30 min at the chosen voltage, then the samples (dissolved in buffer solution) were spread in small grooves (1 cm long) scratched into the layer with a needle. Electrophoretic conditions: 200–400 V for 60–120 min.

Preparation of visualization reagents

Naphthoresorcinol reagent (for carbohydrates). Immediately before use, 2.5 ml concentrated sulphuric acid were carefully added dropwise to 50 ml pure ethanol, then 1.5 ml octanol-1 were added. In this mixture, 0.4 g naphthoresorcinol were dissolved.

Orcinol reagent (for carbohydrates). Solution a (6% orcinol in pure ethanol containing 3–5% octanol-1) and solution b [1% iron(III) chloride in 10% sulphuric acid] were mixed in the ratio a:b = 1:10 before use.

Iron(III) chloride reagent (for phenolic compounds). 5% Iron(III) chloride solution in 0.5 *M* hydrochloric acid.

Visualization and preservation

After electrophoresis the plates were dried at 110°C for 15–30 min. The cool plates were sprayed with one of the reagents. In the case of carbohydrates, the plates were kept at room temperature (30 min) for prehydrolysis of the polysaccharides. They were then heated to 110°C until the coloured zones developed. The phenolic compounds appear immediately after spraying. The plates were then covered with a second glass plate of the same size and kept airtight by putting adhesive tape around them. They were stored in the dark (at 4°C); for documentation the electropherograms were photographed.

RESULTS AND DISCUSSION

Separation of standard mixtures

Fig. 1a shows an electropherogram of standard substances: oligo- and monosaccharides, uronic acids, anhydro sugars and fragments of sugars such as polycarbonyl and polyhydroxy compounds. Their migration distances are spread over a wide range according to their borate complexes. The line electropherogram in Fig. 1b

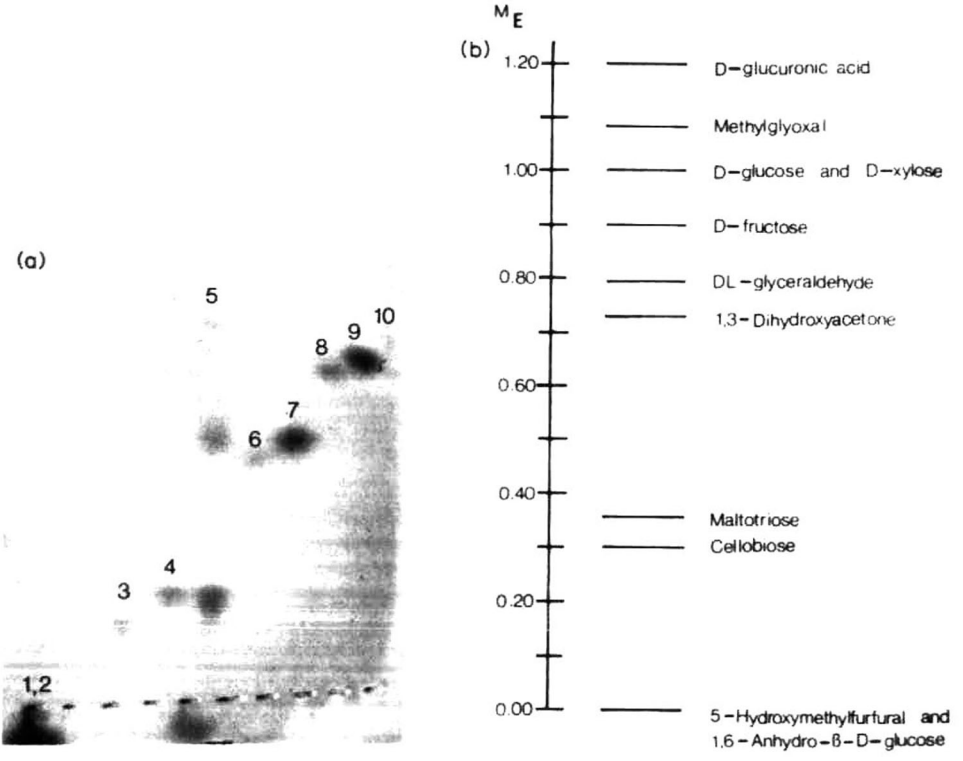

Fig. 1. (a) Electropherogram of standard substances occurring after hydrothermolytic degradation (350 V, 60 min; borate buffer pH 10). Detection with orcinol reagent. Substances: 1 = 5-hydroxymethylfurfural; 2 = 1,6-anhydro-β-D-glucose; 3 = cellobiose; 4 = maltotriose; 5 = mixture of all substances; 6 = 1,3-dihydroxyacetone; 7 = glyceraldehyde; 8 = glucose; 9 = methylglyoxal; 10 = glucuronic acid. (b) Line electropherogram showing the mobilities of the standard substances in M_E units (reference substance, D-glucose, M_E = 1.00). The lines mark the centres of the electrophoretic zones obtained.

TABLE I

RELATIVE MOBILITIES, M_E, OF BIOMASS DEGRADATION PRODUCTS

Reference substance: D-glucose, M_E = 1.00.

Zone	*Compound*	M_E	*Colour reactions*	
			With naphthoresorcinol	*With orcinol*
1	5-Hydroxymethylfurfural	0.00	Red*, blue-green	Yellow-dark brown
2	1,6-Anhydro-β-D-glucose	0.00	Blue	Dark brown
3	Cellobiose	0.30	Dark blue	Green-blue
4	Maltotriose**	0.35	Blue (weak)	Green-blue
5	1,3-Dihydroxyacetone	0.73	Blue-gray, brown	Yellow-light brown
6	DL-Glyceraldehyde	0.78	Red*, blue-gray	Dark brown
7	D-Fructose	0.90	Gray-blue	Reddish brown
8	D-Glucose	1.00	Blue	Green-blue
9	D-Xylose	1.00	Blue	Green blue
10	Methylglyoxal	1.08	Gray-green	Blue-violet
11	D-Glucuronic acid	1.20	Blue	Blue-green
	Furfural	–	Not detected	
	Glycolaldehyde	–	Not detected	

* Colour of zone before heating.

** Reference substance, since cellotriose was not available, and maltose has a similar M_E to that of cellobiose.

enables a comparison of all the determined components; the corresponding values of the relative mobilities (reproducibility 5–7%) are given in Table I. In this table the colour reactions obtained by application of the naphthoresorcinol and orcinol reagents are also specified. Some compounds, *e.g.*, hydroxymethylfurfural and glyceraldehyde, can be identified even by their characteristic colour changes.

When lignocellulose-containing materials are degraded at temperatures higher

TABLE II

RELATIVE MOBILITIES, M_E, OF PHENOLS AND PHENOLCARBOXYLIC ACIDS

Reference substance: 3,4-dihydroxybenzoic acid, M_E = 1.00.

Compound	*Fluorescence*	*Colour of the iron complexes*	M_E
2,6-Dimethoxyphenol 1st fraction	–	Brown	0.0
2nd fraction	+	–	0.4
Sinapic acid 2st fraction	+	–	0.0
2nd fraction	+	Brown-gray	0.5
Ferulic acid 1st fraction	+	–	0.1
2nd fraction	+	Light brown	0.6
Acetovanillone	+	–	0.6
Homovanillic acid	–	Violet	0.6
4-Hydroxyphenylacetic acid	–	Reddish brown	0.7
4-Hydroxycinnamic acid	–	Orange	0.8
trans-3,4-Dihydroxycinnamic acid	+	Gray	1.0
3,4-Dihydroxybenzoic acid	–	Gray	1.0

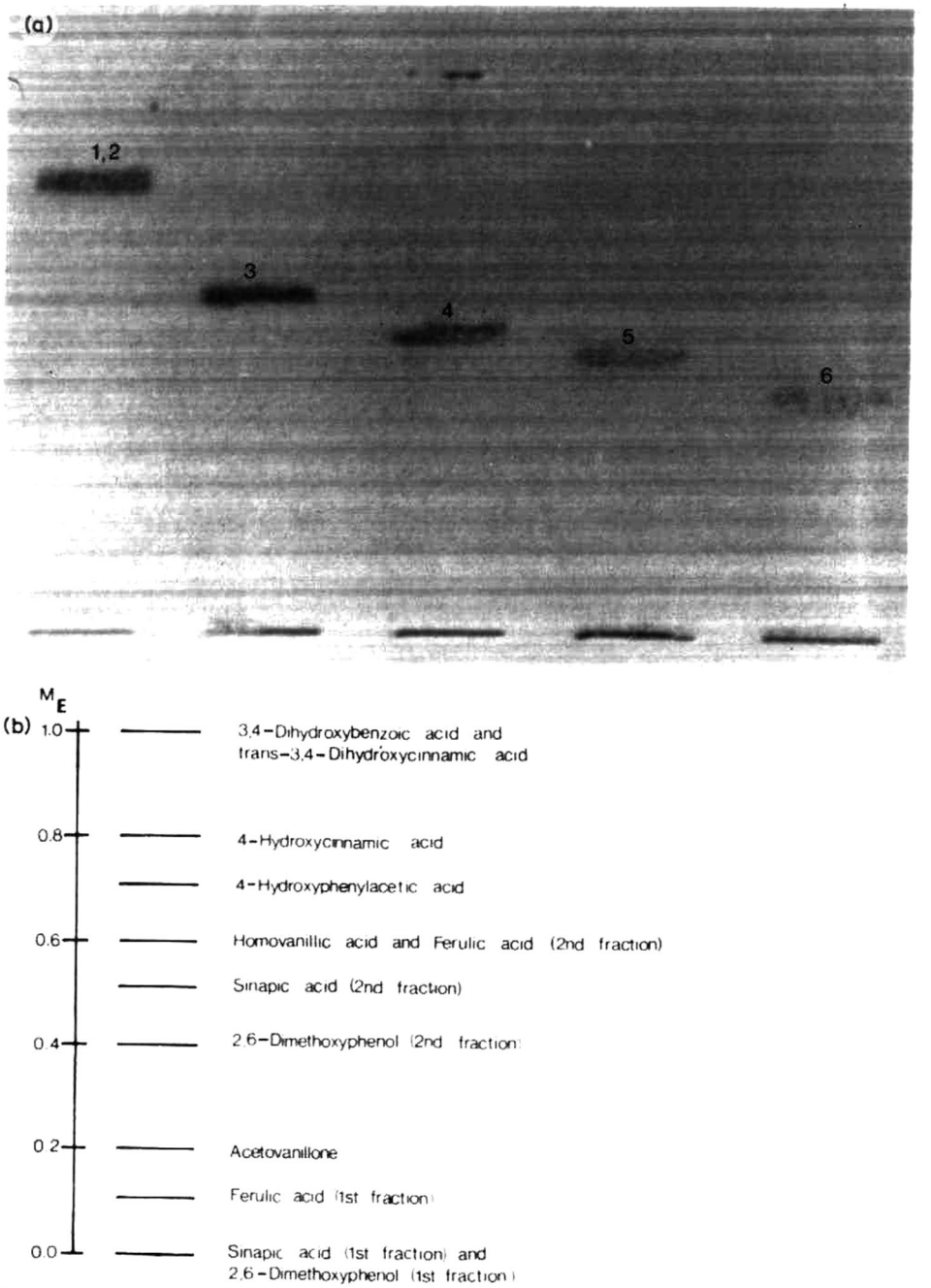

Fig. 2. (a) Electropherogram of phenolcarboxylic acids (200 V, 120 min; borate buffer pH 10). Detection with iron(III) chloride reagent. Substances: 1 = 3,4-dihydroxybenzoic acid; 2 = *trans*-3,4-dihydroxycinnamic acid; 3 = 4-hydroxycinnamic acid; 4 = 4-hydroxyphenylacetic acid; 5 = homovanillic acid; 6 = sinapic acid. (b) Line electropherogram showing the mobilities of phenols and phenolcarboxylic acids in M_E units (reference substance, 3,4-dihydroxybenzoic acid, M_E = 1.00). The lines mark the centres of the electrophoretic zones obtained.

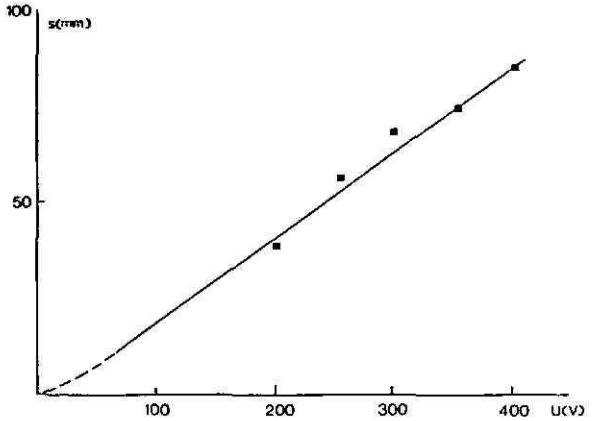

Fig. 3. Migration distance of D-glucose, *s*, *versus* the voltage between the electrodes, *U*, for constant electrophoresis time (60 min).

than 200°C; fragments of lignin will be dissolved, especially phenols and phenolcarboxylic acids. These compounds also form borate complexes, as shown in Fig. 2a. A wide variety of mobilities is found (see line electropherogram in Fig. 2b, Table II); some substances also form two complexes with different charges. Phenolic compounds are detected by application of the iron(III) chloride reagent and by their fluorescence in the UV range (254 nm).

It has been further shown that the basic relationship describing electrophoretic migration[20], namely the linear increase of the migration velocity with electric field strength (or voltage, when the distance between the electrodes is constant), is valid. Fig. 3 shows the mobility of D-glucose as a function of the voltage applied.

Separation of degraded biomass components

In Fig. 4 the electrophoretic behaviour of samples obtained by different decomposition procedures is shown. Fig. 4a shows hemicellulose from an alkaline degradation process, as compared to xylan (molecular weight *ca.* 25 000, Fig. 4b). Both components form zones with two maxima. This is very similar to the behaviour of a sample of wheat straw degraded by the hydrothermolysis process at 180–200°C, and indicates the heterogeneity of the polysaccharides (inhomogeneous fragments). In the electropherogram of a poplar wood sample (degraded at 270°C), products of lower molecular weight derived from the hemicellulose and cellulose parts of the biomass can be identified (Fig. 4c), such as hydroxymethylfurfural, oligosaccharides, glucose, xylose and fructose, and small amounts of undetermined byproducts (Table III).

Contrary to the chromatographic methods, the separation principle of this technique is based on the tendency of the compounds to form charged borate complexes, which depends on the positions of the hydroxyl groups. Their mobility is mainly determined by the relationship between the charge and the Stokes radius of the molecule, whereas their absolute size has no influence, *e.g.*, high-molecular-weight xylan has approximately the same mobility as cellobiose or maltotriose. Also the

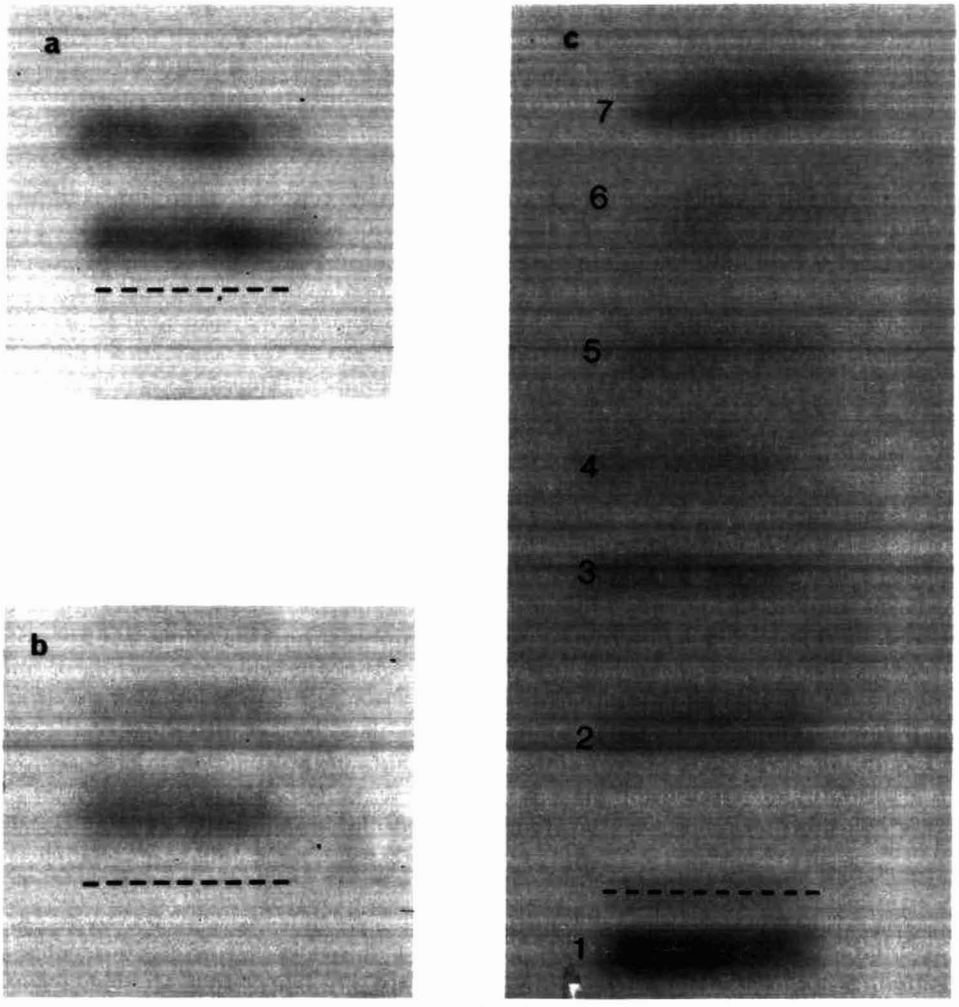

Fig. 4. Electropherograms of alkaline degraded hemicellulose (a) and xylan (b) (170 V, 120 min) and of poplar wood degraded hydrothermally at 270°C (c) (350 V, 60 min). Borate buffer pH 10; detection with naphthoresorcinol reagent.

TABLE III

RELATIVE MOBILITIES, M_E, OF THE ELECTROPHORETIC ZONES OF A POPLAR WOOD SAMPLE DEGRADED AT 270°C

Reference substance: D-glucose, M_E = 1.00.

Zone	M_E	*Corresponding compounds*
1	0.00	5-Hydroxymethylfurfural and 1,6-anhydro-β-D-glucose
2	0.2–0.35*	Cellobiose and oligosaccharides
3	0.50	Not identified
4	0.59	Not identified
5	0.71	1,3-Dihydroxyacetone
6	0.85	D-Fructose
7	1.00	D-Glucose and D-xylose

* Intensity maxima at 0.20 and 0.30.

steric positions of the hydroxyl groups are important, and compounds of comparable size having the same number of sterically suitable binding sites show similar mobilities, *e.g.*, glucose and xylose; glyceraldehyde and dihydroxyacetone.

After evaporation of the organic liquid covering the surface, the inactive support is suitable for the application of chemically aggressive detection reagents. This is a great advantage over previous supports. It enables visualization of the reducing as well as the non-reducing carbohydrates. Coverage of the surface of the support diminishes the adsorption effects and the electroendoosmosis[12].

A further advantage of this technique is the utilization of humid plates. This prevents concentration of the sample at the site of application and therefore possible chemical side-reactions.

ACKNOWLEDGEMENTS

We thank the "Österreichisches Forschungszentrum Seibersdorf GesmbH" for financial support in the form of a scholarship.

REFERENCES

1 J. L. Frahn and J. L. Mills, *Chem. Ind. (London)*, (1956) 578.
2 H. Weigel, *Adv. Carbohydr. Chem.*, 18 (1963) 61.
3 A. B. Foster, *Adv. Carbohydr. Chem.*, 12 (1957) 81.
4 R. Consden and W. M. Stanier, *Nature (London)*, 169 (1952) 783.
5 J. Böeseken, *Adv. Carbohydr. Chem.*, 4 (1949)189.
6 E. J. Bourne, P. M. Foster and J. Grant, *J. Chem. Soc.*, (1956) 4311.
7 U. Pechanek, G. Blaicher, W. Pfannhauser and H. Woidich, *J. Assoc. Off. Anal. Chem.*, 65 (1982) 745.
8 H. Schaefer and H. Scherz, *Z. Lebensm.-Unters.-Forsch.*, 177 (1983) 193.
9 M. C. Jarvis, D. R. Threlfall and J. Friend, *Phytochemistry*, 16 (1977) 849.
10 B. Bettler, R. Amado and H. Neukom, *Mitt. Gebiete Lebensm. Hyg.*, 76 (1985) 69.
11 E. von Arx, J. Faupel, *J. Chromatogr.*, 154 (1978) 68.
12 H. Scherz, *Z. Lebensm.-Unters.-Forsch.*, 181 (1985) 40.
13 G. Pastuska, Fresenius, *Z. Anal. Chem.*, 179 (1961) 427.
14 H. Binder and O. Bobleter, *Holzforschung*, 34 (1980) 48.
15 G. Bonn, R. Concin and O. Bobleter, *Wood Sci. Technol.*, 17 (1983) 195.
16 G. Bonn, *J. Chromatogr.*, 322 (1985) 411.
17 O. Bobleter and G. Bonn, *Identification and Nature of Inhibitory Substances Formed During Pretreatment*, IEA/FE Project CPD-2, 1986, in press.
18 G. Bonn and O. Bobleter, *J. Radioanal. Chem.*, 79 (1983) 171.
19 P. A. Pfeifer, G. Bonn and O. Bobleter, in C. J. Holloway (Editor), *Analytical and Preparative Isotachophoresis*, Walter de Gruyter, Berlin, New York, 1984, p. 89.
20 F. M. Everaerts, F. E. P. Mikkers, Th. P. E. M. Verheggen and J. Vacik, in E. Heftmann (Editor), *Chromatography (Journal of Chromatography Library*, Vol. 22A), Elsevier, Amsterdam, 1983, Ch. 9, p. A334.

Journal of Chromatography, 370 (1986) 495–500
Elsevier Science Publishers B.V., Amsterdam — Printed in The Netherlands

CHROM. 19 020

CORRELATION OF UROKINASE ACTIVITY FROM BIOPOTENCY AND HIGH-PERFORMANCE LIQUID CHROMATOGRAPHIC ASSAYS

RAYMOND A. COX, KATHRYN N. McFARLAND, PATRICIA HOLT SACKETT* and MICHAEL T. SHORT
Abbott Laboratories, 14th and Sheridan Road, North Chicago, IL 60064 (U.S.A.)
(First received June 4th, 1986; revised manuscript received August 13th, 1986)

SUMMARY

A simpler, less expensive, and faster high-performance liquid chromatographic method was shown to be an alternative to urokinase potency determinations by the Ploug method. Post-elution recovery of the low-molecular-weight form was 104 ± 2.4% as determined by the Ploug method. Two analysts reported relative standard deviations of 1.6% and 1.1% based on peak height determination of eight replicate injections of a single sample of low-molecular-weight material. Linearity at the same wavelength for low- and high-molecular-weight forms was 0.9999 and 0.9992, respectively, for peak height *versus* potency.

INTRODUCTION

The proteolytic enzyme urokinase, which catalyzes the conversion of plasminogen to plasmin, appears in two active forms with molecular weights of approximately 54 000 (S_2) and 32 000 (S_1). The current testing procedures for the bulk material are labor- and capital-intensive, and do not discriminate between the two components.

The use of a TSK G3000SW column has been suggested for the separation of the high- and low-molecular-weight forms of urokinase[1]. This paper describes a detailed investigation of the separation, particularly regarding correlation with activity determinations made by the Ploug falling ball assay method[2].

MATERIALS AND METHODS

Materials

Sodium chloride, sodium azide, and potassium phosphate monobasic were reagent grade and used as received. Standard low-molecular-weight urokinase was obtained as a lyophilized powder (Abbott Labs., North Chicago, IL, U.S.A.) and reconstituted with distilled water. High-molecular-weight urokinase was purified by repetitive gel filtration chromatography on Sephadex G75 (Pharmacia, Piscataway, NJ, U.S.A.). Fractions containing purified high-molecular-weight urokinase, ob-

0021-9673/86/$03.50

tained by cation-exchange chromatography, were repetitively chromatographed to increase their purity and confirmed by chromatography of the final product. Blue dextran, ovalbumin, bovine serum albumin and α-chymotrypsinogen A molecular weight standards (Sigma, St. Louis, MO, U.S.A.) were used as received.

Measurement of urokinase activity

Urokinase activity was determined by a modified Ploug falling ball method[2] using urokinase standard (Abbott Labs.) verified against a WHO standard. In the modified method used here, thrombin, plasma and excess plasminogen are mixed at 0°C until clotting is complete. Urokinase is added and the sample incubated at 37°C. The time required for a small ball to drop through the dissolving clot is monitored and urokinase potency calculated via comparison with standard material of known potency.

High-performance liquid chromatography (HPLC)

A TSK G3000SW column (30 cm × 7.5 mm I.D.) was used (Alltech Assoc., Deerfield, IL, U.S.A.). The mobile phase consisted of 0.1 *M* potassium dihydrogen phosphate adjusted to pH 6.0 with 10 *M* sodium hydroxide, 0.1 *M* sodium chloride, and 0.005 *M* sodium azide to prevent microbial growth. The flow-rate at ambient column temperature was 0.5 ml/min with typical column pressures of 200–300 p.s.i. The chromatographic system consisted of a Beckman 112 pump, 210 injector, and 165 variable-wavelength detector set at 280 nm. A Shimadzu C-R3A integrator was used to obtain peak area data; height measurements were made by the integrator or manually. All potency values were calculated on an external standard basis from replicate injections of a single standard of known potency.

Post-column recovery of urokinase

Better resolution of the two forms is obtained with smaller injection volumes. To give enhanced sensitivity for Ploug determinations, however, 200-μl injections were made when fractions were collected. To calculate the percent potency recovered, 200-μl aliquots of the samples were diluted to 5 ml in mobile phase and submitted for the Ploug potency assay. These values were compared with the potency values obtained after injection of 200 μl of material, collection of the appropriate peak (approximately 0.5–1 ml), and dilution of the eluate to 5 ml prior to submission for the Ploug assay.

RESULTS AND DISCUSSION

Although superior results have been reported with relatively acidic mobile phases for urokinase separation[1], optimum resolution was found in this laboratory at a pH of 6.0. A typical chromatogram of material containing both low- and high-molecular-weight forms is seen in Fig. 1.

Molecular weight determinations were made using as calibration standards dextran blue (void volume marker), bovine serum albumin, ovalbumin, and α-chymotrypsinogen A. Good precision was found for this measurement based on eight replicate injections of a single sample (molecular weight 30 600 ± 1.3%). G3000SW columns which had been calibrated using this mixture, however, gave broad, mis-

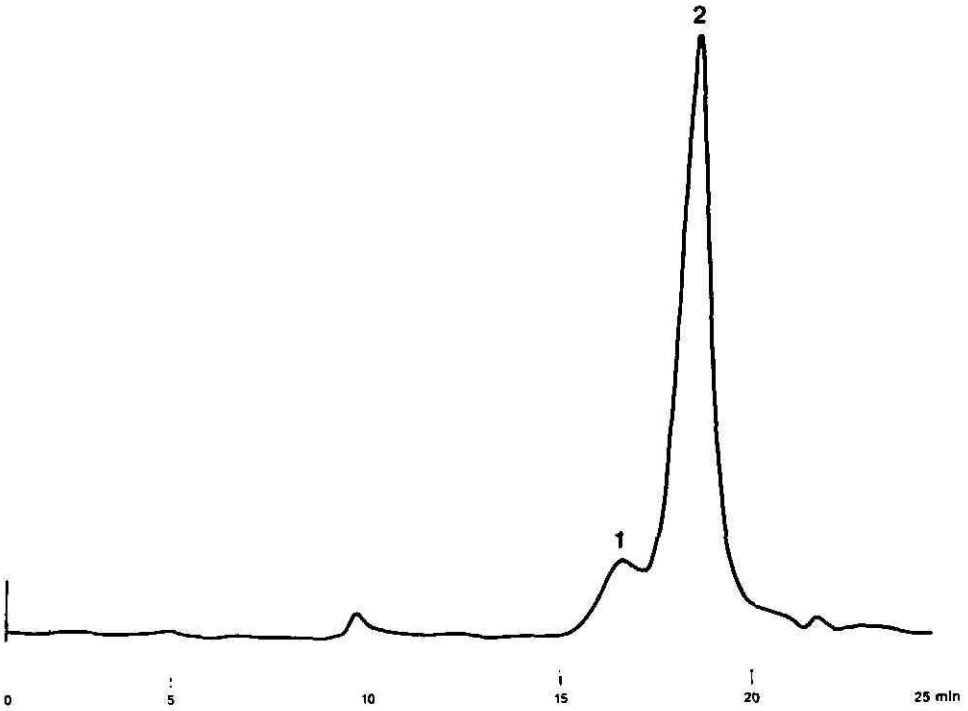

Fig. 1. Typical chromatogram of low- and high-molecular-weight urokinase; approximately 125 000 IU/ml S_1 (2) and 21 000 IU/ml S_2 (1).

shapen peaks for injections of pure S_2 material. Suspecting adsorption of α-chymotrypsinogen A which might degrade the S_2 as it passed through the column[3], a calibration solution without the suspect component was injected onto a fresh column. No S_2 degradation was seen thereafter. A suitable substitute for the α-chymotrypsinogen A could not be found, leaving only two points for subsequent molecular weight calibration curves.

The linearity of potency recovery was demonstrated by injecting solutions containing from 0 to 120 000 IU/ml S_1 urokinase and comparing pre- and post-elution potency values measured by a Ploug U-5 assay. Correlation coefficients of experimental *versus* theoretical potencies were 0.9987 and 0.9972, respectively, indicating little difference is seen before and after chromatography. Two analysts also tested the precision of urokinase recovery by making replicate injections of a single sample of material containing approximately 45 000 IU/mL S_1. The results of these precision studies are shown in Table I, along with mean recovery values for eight lots of material containing 30 000–50 000 IU/mL S_1. Biological activity was also maintained in samples of material purified by HPLC, lyophilized, and then reconstituted.

The effect of variations in the mobile phase was examined by systematically changing pH, buffer strength, ionic strength and column temperature while maintaining other variables constant. Ionic strength and column temperature had essentially no effect on peak resolution or assay results, while optimal resolution was seen at pH 6.0 and a buffer strength of 0.1 *M*.

TABLE I

PRECISION OF POST-ELUTION POTENCY RECOVERY

	Analyst 1		*Analyst 2*	
	Single lot	*8 lots*	*Single lot*	*8 lots*
Mean (% recovery)	104	96	110	104
Rel. std. dev. (%)	2.4	6.9	1.2	4.0

The linearity of the UV detector response at 280 nm to low-molecular-weight urokinase from 0 to 200 000 IU/ml was determined. A correlation of 0.9984 was seen for peak area measurements, and 0.9999 for peak height determinations. The response from 0 to 300 000 IU/ml was examined for the S_2 form. Peak area *versus* potency gave a correlation of 0.9976, while peak height measurements yielded a value of 0.9992.

Two analysts made eight replicate injections of the same material and calculated the potency based on injection of an external standard of known potency. The data are shown in Table II for both peak area and peak height calculations. Similarly, precision data for S_2 in a sample containing approximately 300 000 IU/ml S_1 are given. Linearity and precision data justify the use of peak heights for external standard calculations.

HPLC and Ploug U-4 assays were performed on eleven samples of material containing 50 000–300 000 IU/ml S_1. A paired t-test calculated with peak height assay values yielded $t = 0.78$ ($t_{0.1} = 1.363$), indicating essentially no difference in the results obtained by the two methods.

Recovery of S_2 from spiked samples of S_1 (125 000 IU/ml) was demonstrated by comparison with an external standard of pure S_2. Table III contains experimental and calculated results. The limit of detection for S_2 is approximately 1% of S_1 on a potency–potency basis. The slightly high recovery values can be explained in several ways: (i) incomplete resolution of the S_1 and S_2 forms results in some over-estimation of peak heights, (ii) because only small quantities of purified S_2 were available, spikes were prepared by adding a few microliters of solution to S_1 standard, with less than optimal measurement of volumes, and (iii) the precision of measurement of S_2 was 7.2% at the highest level spiked (see Table II), thus all values reported are within the error of measurement.

TABLE II

PRECISION OF POTENCY DETERMINATIONS FOR S_1 AND S_2 BY HPLC

	S_1				S_2
	Analyst 1		*Analyst 2*		*Peak height*
	Peak area	*Peak height*	*Peak area*	*Peak height*	
Mean (IU/ml)	251 800	217 675	244 000	212 000	20 067
Rel. std. dev. (%)	2.2	1.6	1.8	1.1	7.2

TABLE III

RECOVERY OF S_2 FROM S_1 (125 000 IU/ml)

IU/ml spiked	*IU/ml found*	*IU/ml recovered*	*% recovered*
0	3570	–	–
3914	7932	4362	111
7874	11 898	8328	106
11 590	16 460	12 890	111
15 214	21 021	17 451	115
		Mean	111

To test whether the method was stability-indicating, samples of S_1 material were subjected to refluxing for 3 h in acid, base and neutral aqueous solutions, 105°C for 1 week, and exposure to short-wavelength UV for 3 h. Quantitative recovery was found only for the sample exposed to UV light; in the other conditions, aggregate formation and low-molecular-weight fragments were observed with at best 2–3% recovery of intact S_1. Under refrigeration the sample solutions were stable for several months.

CONCLUSIONS

Besides the immediate consideration of providing a fast, simple assay for urokinase potency determinations, the method has potential value in other areas of biological testing. Post-chromatographic recovery of biological activity has long been a problem in enzyme purification[4]. Normal- and reversed-phase HPLC separations can require harsh conditions such as high pressures and high concentrations of organic modifiers which can induce degradation of the analyte. The conditions encountered in gravity-flow systems are less severe but these methods are expensive in terms of material and time. Long on-column residence times might also affect sensitive proteins. The system described here generates fairly low pressures (200–300 p.s.i. for a 30-cm analytical column) and uses a mobile phase containing no organic constituents. Residence time is under 20 min regardless of temperature, thus cold room conditions can be used with no penalty in throughput time if higher stability is achieved below ambient temperatures.

Compared to classical bioassays, more information can be obtained from an HPLC method since active constituents can be isolated and estimates of their relative amounts made through the use of standards. Although the initial cost of HPLC instrumentation is higher than that for bioassay equipment, long-term cost savings are typical of those seen for HPLC methods with their shorter analysis and hands-on time. The use of autosamplers can significantly reduce analyst time, further increasing the cost savings of this method over other means of activity determinations.

ACKNOWLEDGEMENTS

The authors would like to thank Mary Cipriano and Raj Bhatt for support and providing samples, Linda Bogue for technical assistance, and Jeanene Nering for manuscript preparation.

REFERENCES

1 T. Someno, K. Katoh, K. Niijima and H. Miyazaki, *J. Chromatogr.*, 188 (1980) 185–192.
2 J. Ploug, *Biochim. Biophys. Acta*, 13 (1957) 278.
3 W. A. Gunzler, G. J. Steffens, F. Otting, G. Buse and L. Flohe, *Hoppe-Seyler's Z. Physiol. Chem.*, 363 (1982) 133–141.
4 F. Regnier, *Anal. Chem.*, 55 (1983) 1298A–1306A.

Journal of Chromatography, 370 (1986) 501–507
Elsevier Science Publishers B.V., Amsterdam — Printed in The Netherlands

CHROM. 19 034

PURIFICATION OF COPPER-ZINC-SUPEROXIDE DISMUTASE AND CATALASE FROM HUMAN ERYTHROCYTES BY COPPER-CHELATE AFFINITY CHROMATOGRAPHY

MISAKO MIYATA-ASANO, KEIZO ITO, HISAMI IKEDA and SADAYOSHI SEKIGUCHI
Hokkaido Red Cross Blood Center, Sapporo 064 (Japan)
and
KATSURA ARAI and NAOYUKI TANIGUCHI*
Department of Biochemistry, Osaka University Medical School, Kitaku, Osaka 530 (Japan)
(First received July 18th, 1986; revised manuscript received August 23rd, 1986)

SUMMARY

A relatively simple and reproducible procedure involving copper-chelate affinity chromatography for the isolation of copper-zinc-superoxide dismutase (E.C. 1.15.1.1) and catalase (E.C. 1.11.1.6) from human erythrocytes has been developed. Using this method, the two enzymes were easily and highly purified and appeared to be homogeneous as judged by polyacrylamide gel electrophoresis.

INTRODUCTION

Copper-zinc-superoxide dismutase (SOD) and catalase are considered to be of major importance in protecting living cells against toxic oxygen derivatives. SOD catalyzes the dismutation of the superoxide anion to hydrogen peroxide, and catalase converts hydrogen peroxide into water and oxygen (see ref. 1 for a review). These two enzymes have been used experimentally or clinically as anti-inflammatory drugs. They are usually purified by a conventional technique involving precipitation by ammonium sulphate, ion-exchange chromatographies and gel filtration[2]. However, the yields and extents of purification are relatively low. By using copper-chelate affinity chromatography, preparations of the two enzymes have been highly purified. The simple isolation procedure described in this paper will make the enzymes more readily available for a variety of investigations.

EXPERIMENTAL

Materials

Xanthine oxidase was obtained from Boehringer Mannheim, xanthine from Sigma, nitroblue tetrazolium (NBT) from Nakarai Chemicals (Japan), Tonein-TP from Otsuka Assay Laboratories (Japan) and DE-52 from Whatman. Sephadex G-150 and chelating Sepharose 6B, which is basically an iminodiacetic acid agarose gel first introduced by Porath *et al.*[3], were obtained from Pharmacia Fine Chemicals.

0021-9673/86/$03.50

Enzyme assays

SOD activity was assayed using xanthine and xanthine oxidase according to Beauchamp and Fridovich[4], using a Beckman DU-50 spectrophotometer at 25°C. One unit of activity is defined as the colour intensity corresponding to half-inhibition of the development of blue formazan in 0.5 ml of the assay mixture at 25°C. The specific activity is expressed in units per mg protein. Catalase activity was assayed by the method described by Sinha[5], and the enzyme activity is expressed as $K(0)$. The specific activity is expressed as $K(0)$ per mg protein.

Protein was determined from the absorbances at 280 and 590 nm, as well as by a dye-binding method[6] using Tonein-TP. The haem concentration was determined from the absorbance at 405 nm.

Electrophoresis and isoelectric focusing

Polyacrylamide gel electrophoresis on 7.5% gels for SOD, 5% gels for catalase, was performed according to Davis[7]. The SOD preparation was applied on duplicate gels. One was stained for protein with Coomassie Brilliant Blue G-250 and the other was assayed for SOD activity with *o*-dianisidine and riboflavin[8]. The molecular weights of SOD and catalase were estimated by disc gel electrophoresis on 12% gels and slab electrophoresis on 5–15% gels, respectively, in the presence of sodium dodecyl sulphate and 1% 2-mercaptoethanol, according to Laemmli[9].

The molecular weight of SOD was also determined by high-performance liquid chromatography (HPLC) (UV-8000, Toyo Soda) on a TSK G3000SW column. Isoelectric focusing (range pH 3–10) was carried out as described[10].

Purification of SOD and catalase

All procedures were carried out at 4°C. Human blood which had been stored for 10–15 days at 4°C in a citrate–phosphate–dextrose solution was used. The erythrocytes were washed with a 0.9% sodium chloride solution by low speed centrifugation at 1500 *g* for 15 min and then haemolyzed by adding an equal volume of water to the packed red cells. The haemolysates were dialyzed against 1.5 m*M* phosphate buffer (pH 6.8) and then centrifuged at 11 600 *g* for 20 min. The supernatant was adsorbed in a batchwise manner on DE-52, which had been equilibrated with the above phosphate buffer. The DE-52 was then washed thoroughly with the same buffer and packed in the column. SOD and catalase were eluted with 1.5 volumes of 20 m*M* phosphate buffer (pH 6.8). The eluted fractions of both enzymes were applied to a column (6 cm × 1 cm) of chelating Sepharose 6B primed with a copper(II) sulphate solution, which had been equilibrated with 50 m*M* phosphate buffer containing 500 m*M* sodium chloride (pH 7.0). After the column had been washed with the same buffer, SOD was eluted with 50 m*M* Tris–HCl buffer containing 500 m*M* sodium chloride (pH 8.0) and the eluted fractions were pooled (fraction 1). Further elution was carried out with a linear gradient between 20 ml of 50 m*M* Tris–HCl buffer containing 500 m*M* sodium chloride (pH 6.0) and 20 ml of the same buffer containing 200 m*M* histidine. The eluted fractions were pooled (fraction 2).

RESULTS AND DISCUSSION

Purification of SOD and catalase

Fig. 1 shows a typical elution profile for the two enzymes in copper-chelate chromatography. After sample application the column was washed with the buffer to remove non-adsorbed proteins. Most of the SOD were recovered in fraction 1 and all the catalase activity was recovered in fraction 2. Since the catalase was eluted at the start of the gradient, a better separation might be possible by use of a shallower gradient or a solution, containing histidine or immidazole at pH 6.0. However, on Sephadex, G-150, other contaminants could be separated. Fractions 1 and 2 were dialyzed against 20 m*M* phosphate buffer (pH 6.8) in order to remove Cu^{2+} and histidine. Fraction 2 was also loaded on a column (86 cm × 2.7 cm) of Sephadex G-150 which had been equilibrated with 20 m*M* phosphate buffer (pH 6.8) (Fig. 2).

The purification steps for SOD and catalase are summarized in Table I. The specific activity of purified SOD was of the same order of magnitude as that obtained in immunoaffinity chromatography using goat-anti-SOD[11]. The specific activity of the purified catalase was also of the same order as that obtained by Mörikofer-Zwez *et al.*[12].

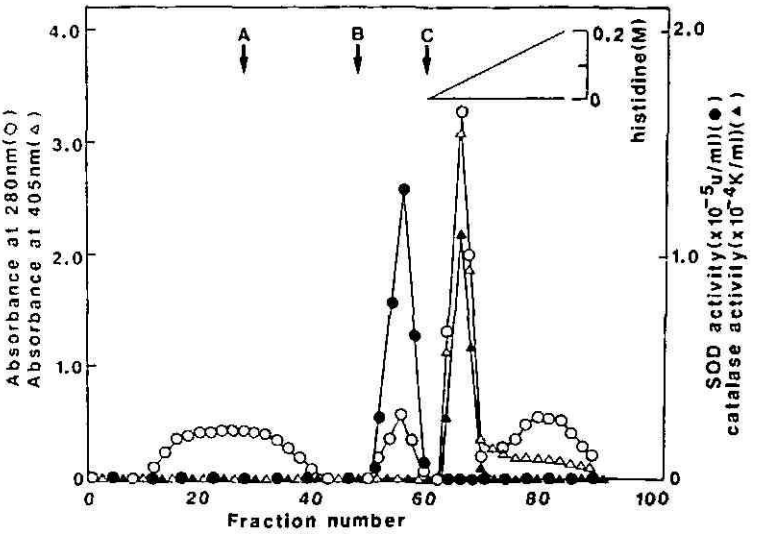

Fig. 1. Copper-chelate affinity chromatography. The fractions eluted from the DE-52 column were applied on a column (6 cm × 1 cm) of copper-chelating Sepharose 6B which had been equilibrated with 50 m*M* phosphate buffer containing 500 m*M* sodium chloride (pH 7.0). At A, the column was washed with 30 ml of the above buffer. At B, fraction 1 was eluted with 20 ml of 50 m*M* Tris–HCl buffer containing 500 m*M* sodium chloride (pH 8.0). At C, the active enzyme fraction was eluted with a linear gradient between 20 ml of 50 m*M* Tris–HCl buffer containing 500 m*M* sodium chloride (pH 6.0) and 20 ml of the same buffer containing 200 m*M* histidine (fraction 2) at a flow-rate of 10 ml/h. Fractions of 2 ml were collected. The protein concentration (○) was determined from the absorbance at 280 nm, and the haem concentration (△) from the absorbance at 405 nm. The SOD (●) and catalase (▲) activities were assayed as described in Experimental.

TABLE I

PURIFICATION OF SOD AND CATALASE

Step	*Total protein (mg)*	*SOD*				*Catalase*			
		Total activity (· 10^{-4} units)	*Specific activity (units/mg)*	*Yield (%)*	*Purification fold*	*Total activity [· 10^{-3} K(0)]*	*Specific activity [K(0)/mg]*	*Yield (%)*	*Purification fold*
Red blood cells	34 900	177	51	100	1	184	3.82	100	1
DE-52	218	98	4480	55	89	107	531	58.4	139
Copper-chelate column									
Fraction-1	5.40	60	110 500	35	2190	0			
Fraction-2	25.3					43.1	1700	23.4	445
Sephadex G-150	9.8					21.3	2160	11.6	565

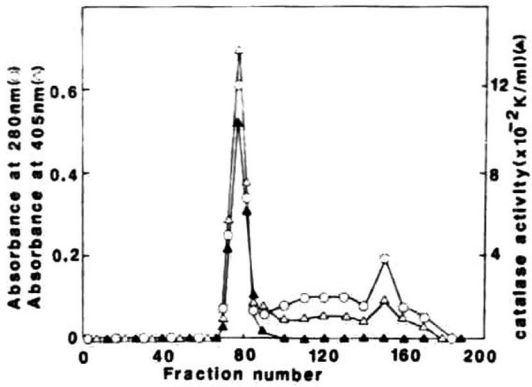

Fig. 2. Chromatography on Sephadex G-150. The pooled fractions showing catalase activity obtained from copper-chelate affinity chromatography were dialyzed against 20 m*M* phosphate buffer (pH 6.8) and then applied to a columnn (86 cm × 2.7 cm) of Sephadex G-150 which had been equilibrated with the above buffer. The column was washed with the same buffer at a flow-rate of 9 ml/h. Fractions of 3 ml were collected. ○—○, Protein concentration; △—△, haem concentration; ▲—▲, catalase activity.

Properties of the purified SOD and catalase

Figs. 3 and 4 show the electrophoretic patterns of the purified SOD and catalase. In disc electrophoresis, the SOD preparation gave two bands (Fig. 3A), which corresponded to the areas where the enzymatic activity was stained (Fig. 3B). The

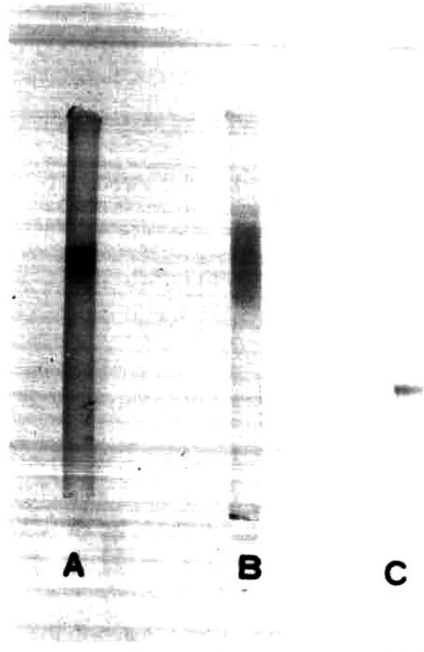

Fig. 3. Disc gel electrophoresis of the purified SOD. For lanes A and B, 7.5% gels were used. For lane C, a 12% gel in the presence of 1% sodium dodecyl sulphate was used. Lanes: A and C, protein staining with Coomassie Brilliant Blue G-250; B, SOD activity staining with *o*-dianisidine and riboflavin.

Fig. 4. Disc and slab gel electrophoresis of the purified catalase. For lane A, a 5% gel was used. For lanes B and C, 5–15% gradient gels in the presence of 1% sodium dodecyl sulphate were used. Lanes: A and B, protein staining of the purified catalase with Coomassie Brilliant Blue G-250; C, protein staining with Coomassie Brilliant Blue G-250 of the following molecular weight standards, ferritin (450000), bovine catalase (240000), aldolase (150000), bovine serum albumin (68000), ovalbumin (45000), chymotrypsinogen (25000) and cytochrome *c* (12500).

molecular weight of SOD was estimated to be 17000 ± 1000 (Fig. 3C). In HPLC the purified SOD gave a single peak with a molecular weight of 32000 (data not shown). The catalase preparation also gave a single protein band (Fig. 4A). The molecular weight of catalase was estimated to be 240000 by polyacrylamide gel electrophoresis in the presence of sodium dodecyl sulphate and 1% 2-mercaptoethanol (Fig. 4B). In isoelectric focusing the SOD preparation gave three sharp bands corresponding to p*I* 4.7, 4.8 and 4.9. Therefore SOD seemed to exhibit charge heterogeneity. This result is consistent with our previous finding that SOD is antigenically cross-reactive with molecular species which have the same molecular weight[11]. In isoelectric focusing of the catalase preparation, a duplicate gel was used to locate the enzyme activity. For the detection of the catalase activity, 5-mm slices of the gel were incubated in the assay mixture. The gel showing catalase activity corresponded to the area stained for protein. The catalase preparation was also found to be heterogeneous as to p*I* 5.8 to 6.5, as reported by Mörikofer-Zwez *et al.*[13].

In the present study we used metal-chelate affinity chromatography to purify catalase as well as SOD. The affinity of a metalloenzyme to a metal-chelate column has been reported by Ohkubo *et al.*[14]. They purified nucleoside diphosphatase using

a zinc-chelate column and histidine as eluent. The binding of a metalloenzyme to a metal-chelate column is mediated by surface-located histidine residues of the metalloenzymes[15,16]. However, the affinity is dependent on the type of metalloenzyme. SOD did not bind to a zinc-chelate column, whereas catalase did (data not shown). This may also indicate that selective usage of such a column will be useful for preparing various metalloenzymes. Special care may be necessary, for metalloenzymes from which the metals, under certain conditions, can be effectively removed. In such cases, activity may be restored by the addition of the relevant metal ion. In the present study, however, such a treatment was not necessasry.

Erythrocytes contain large amounts of catalase and SOD. In contrast to the reported purification methods for enzymes, the present method involves only two or three purification steps with higher recoveries of the enzymes and no other time-consuming procedure is required. This method with a metal-chelate column will be useful for preparing metalloenzymes from human erythrocytes on a large scale. Very recently Waselake *et al.*[17] reported that SOD had been purified by use of a copper-chelate column and the result is almost consistent with our results.

ACKNOWLEDGEMENTS

We thank Professor Akira Makita, Hokkaido University School of Medicine and Dr. Shigeru Sasakawa, Japanese Red Cross Central Blood Center, for their valuable suggestions and criticism during this work.

REFERENCES

1 D. A. Lewis, *Biochem. Pharmacol.*, 33 (1984) 1705.
2 M. J. Stansell and H. F. Deutsch, *J. Biol. Chem.*, 240 (1965) 4299.
3 J. Porath, J. Carlsson, I. Olsson and G. Belfrage, *Nature (London)*, 258 (1975) 598.
4 C. Beauchamp and I. Fridovich, *Anal. Biochem.*, 44 (1971) 276.
5 A. K. Sinha, *Anal. Biochem.*, 47 (1972) 389.
6 M. M. Bradford, *Anal. Biochem.*, 72 (1976) 248.
7 B. J. Davis, *Ann. NY Acad. Sci.*, 121 (1964) 404.
8 H. P. Misra and I. Fridovich, *Arch. Biochem. Biophys.*, 183 (1977) 511.
9 U. K. Laemmli, *Nature (London)*, 227 (1970) 680.
10 M. C. Hoyle, *Int. Lab.*, 25 (1980).
11 K. Arai, S. Iizuuka, A. Makita, K. Oikawa and N. Taniguchi, *J. Immunol. Methods*, 91 (1986) 139.
12 S. Mörikofer-Zwez, M. Cantz, H. Kaufmann, J. P. Wartburg and H. Aebi, *Eur. J. Biochem.*, 11 (1969) 49.
13 S. Mörikofer-Zwez, J. P. Wartburg and H. Aebi, *Experientia*, 26 (1970) 945.
14 I. Ohkubo, T. Kondo and N. Taniguchi, *Biochim. Biophys. Acta*, 616 (1980) 89.
15 J. Porath and B. Olin, *Biochemistry*, 22 (1983) 1621.
16 E. Sulkowski, *Trends Biotechol.*, 3 (1985) 1.
17 R. J. Waselake, S. L. Chesney, A. Pethau and A. D. Friesen, *Anal. Biochem.*, 155 (1986) 193.

Journal of Chromatography, 370 (1986) 508–512
Elsevier Science Publishers B.V., Amsterdam — Printed in The Netherlands

CHROM. 19 086

Note

Simple device for high-performance liquid chromatographic separation on microbore columns

AJIT S. BHOWN*, JAMES WAYLAND and J. CLAUDE BENNETT
Division of Clinical Immunology and Rheumatology, Department of Medicine, University of Alabama at Birmingham, Birmingham, AL 35294 (U.S.A.)
(Received August 5th, 1986)

High-performance liquid chromatography (HPLC) has played a very significant role in isolation, purification and structural studies and more so for compounds of biological importance, such as proteins, peptides and amino acids. The technological advancement of HPLC has paralleled the need for analyzing compounds available in low amounts. One such advancement is the miniaturization of HPLC columns to achieve higher sensitivity. The most commonly employed columns in the past have been 4–30 cm long with internal diameter (I.D.) of 0.4 to 0.6 cm. In recent years[1], however, there has been a considerable interest in columns of smaller diameter (1–2 mm I.D.), commonly known as "microbore" columns. The efficiency of these columns is generally higher, thus improving the separation of complex mixtures or hard to resolve molecules. Although various factors influence the effeciency of microbore columns, the pumping system has often been the limiting factor, particularly if the separation is achieved by gradient mode. For microbore column chromatography the most desired aspects of HPLC are its capability of (i) pumping mobile phase at a slower flow-rate (50–200 μl/min), (ii) generating accurate gradients at low flow-rates and (iii) spectrophotometric detection in small volumes of eluent. Commonly available HPLC systems are not designed to meet these requirements with reasonable precision and accuracy. In this communication, a very simple and economical device is described to modify a conventional HPLC system (single- or dual-pump) for microbore column chromatography. The modification requires minimum plumbing, can be used with or without autoinjector, and can be installed within a short period of time. The device has been used extensively in this laboratory in conjunction with protein studies, and the results are presented in this communication.

MATERIALS AND METHODS

Chemicals

Chemicals for HPLC were purchased from EM Science (Cherry Hill, NJ U.S.A.) and for amino acid sequence anlysis from Spinco Division of Beckman Instruments (Palo Alto, CA, U.S.A.), and Pierce (Rockford, IL, U.S.A.).

0021-9673/86/$03.50

Instrumentation

Sequence analyses were performed on a Beckman 890M sequencer as described earlier[2], and phenylthiohydantoin (PTH) derivatives of the cleaved amino acids were identified by HPLC with a macrobore (4.5 mm I.D.) column as described previously[3] and with a microbore (2.0 mm I.D.) column as described in this communication. To examine the efficiency of the device three different HPLC systems were employed: Perkin-Elmer Series 4 microprocessor-controlled solvent delivery system (single-pump); Waters HPLC (dual-pump) equipped with two 6000A solvent delivery pumps and a System controller (Model 720); Beckman HPLC (dual-pump) equipped with a 421A controller, two 110B solvent delivery modules and a system organizer. All three HPLC systems were equipped with Waters autoinjector WISP 710B and a dual-channel absorbance detector containing a micro cell (1-μl capacity, Waters Assoc., Cat. No. 97379).

Ultrasphere 5-μm ODS macrobore and microbore columns (150 × 4.6 mm I.D. and 150 × 2.0 mm I.D., respectively) manufactured by Altex and marketed by Beckman Instruments (parts No. 235330 and 237390) were employed to separate the PTH derivatives.

Modification

In order to adopt the conventional HPLC system to microbore column chromatography the solvent delivery systems were modified, as shown in Figs. 1 and 2. Irrespective of the HPLC system used (one pump or two pumps) the tube from the mixing chamber/solvent delivery system was connected to a "T" ("C" in Fig. 1 and 2) with a minimum dead volume. One outlet of the "T" was connected in series to a fine metering valve (Cat. No. 55-22RF2; "D" in Fig. 1 and 2) manufactured by Whitey Co. (Highland Hts., OH, U.S.A.) and to a pulse damper (Water Assoc., Millford, MA, U.S.A.; Cat. No. 98060; "E" in Fig. 1 and 2). The second outlet from the "T" joint was connected to the autoinjector ("F" in Fig. 2) through a stainless-steel tube of minimum length and 0.007 in. I.D. The solvent delivery tube (0.007 in. I.D.) from the injector to the column ("G" in Fig. 2) and from column to the detector

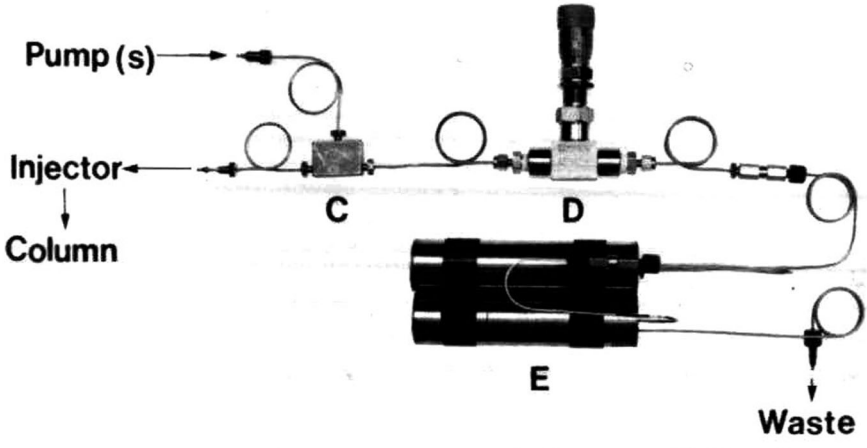

Fig. 1. Arrangement of "T", fine metering valve and pulse damper. C = "T"; D = fine metering valve; E = pulse damper.

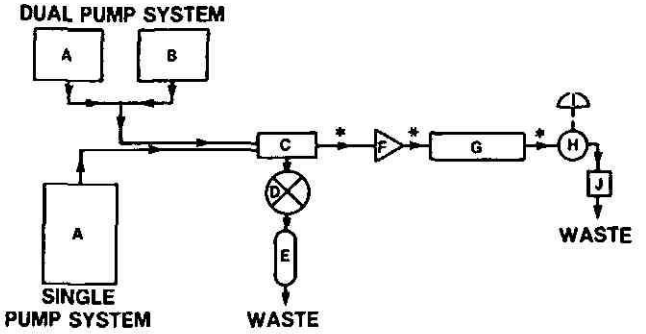

Fig. 2. Schematics of the plumbing for fine metering valve in one pump or two pumps conventional HPLC. A and B = HPLC pumps; C = "T"; D = fine metering valve; E = pulse damper; F = autoinjector; *G = microbore column; H = detector; I = recorder; J = back pressure restrictor;* * = 0.007 *in* I.D. stainles-steel tubing.

("H" in Fig. 2) was also of shortest possible length. Tube length and 0.007 in. I.D. for plumbing is critical. Because of the slow flow-rate and small volume (1.0 μl) detector cell (Waters Assoc.; Cat. N. 97379) it was necessary to create a back pressure inside the detector cell to avoid the possibility of air bubble formation. This was achieved by introducing a back pressure restrictor (manufactured by Upchurch, Oak Harbor, WA, U.S.A.; Cat. No. U4462; "J" in Fig. 2) at the outlet side of the detector cell ("H" in Fig. 2). The only plumbing change in the autoinjector was to disconnect the 2.0-ml loop of the injector assembly.

Separation of standard PTH-amino acids and residue from the sequencer run was achieved by the procedure described previously[3]. The flow-rate was 1.5 ml/min for both macrobore and microbore columns; however, for the microbore column the metering valve was adjusted to maintain the column back pressure (which can be read on the controller screen) at the same level as with the microbore system (*ca.* 2000 p.s.i.). This corresponds to flow of 0.320 μl/min through the macrobore column. The excess solvent was directed to the waste through the "T" joint and pulse damper. Injection volumes for the microbore column were kept to a minimum, never to exceed 25 μl.

RESULTS AND DISCUSSION

Fig. 1 shows the arrangement of "T" (C), fine metering valve (D) and pulse damper (E) while the schematics is shown in Fig. 2. The separation of different amounts (50–100 pmol) of standard PTH amino acid mixture on a microbore and macrobore column at two different sensitivities is compared in Fig. 3 (see figure legends for details). It is evident from Fig. 3 that by introducing split streaming and metering valve (Figs. 1 and 2) it is possible to reduce to flow to a desired rate without adversely effecting the gradient to obtain resolution of the peaks. Fig. 4 shows the PTH-amino acid analysis results on microbore column of cycles No. 5 and No. 9 from two different tryptic peptides. This further suggests that the system described here can be effectively used for the analysis of the samples obtained from the amino acid sequencer run.

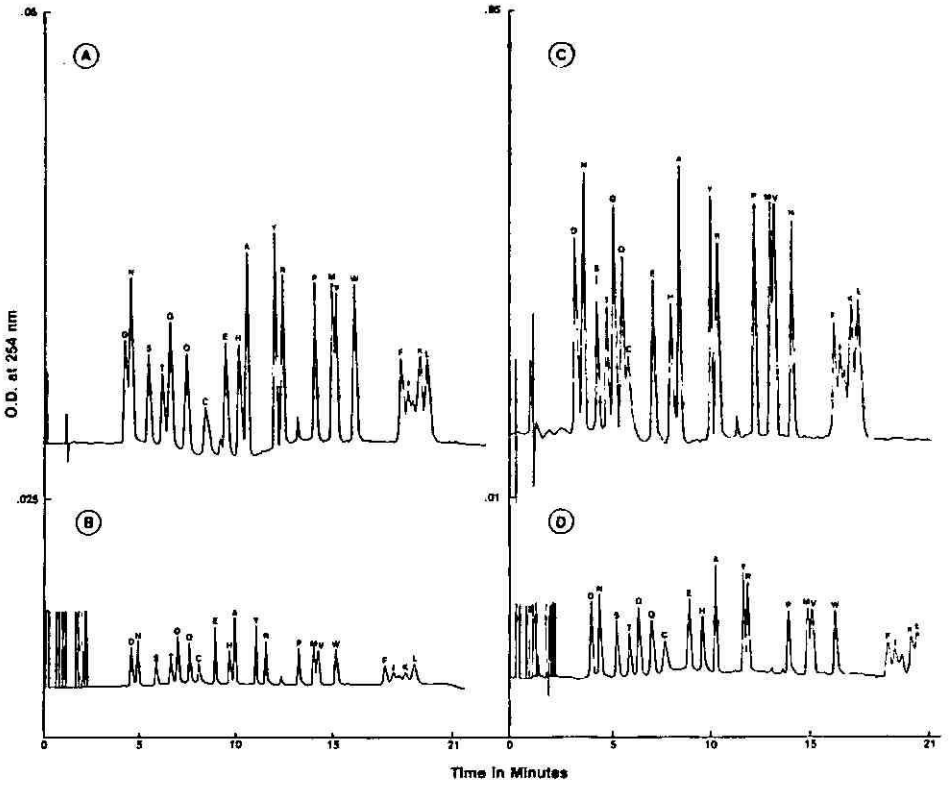

Fig. 3. Separation of standard PTH-amino acid mixture. (A) 100 pmol on microbore column using dual-pump system; (B) same as in A on macrobore column; (C) 50 pmol on microbore column using single-pump system; D = same as in C on macrobore column. Single-letter symbols are used for amino acids.

Most of the available HPLC units are capable of performing gradient elution on macrobore columns; however, they are not at their best performance at a lower flow-rate, which is a prerequisite for gradient elution on microbore columns. In order to surmount this problem a number of approaches have been taken[4–8]. One such approach has been flow splitting, described by Van der Wal and Yang[5] on a single-pump system without the use of autoinjector. Moreover, they have reported a gradient system for fused-silica columns and not a high-pressure system. Alternatively a gradient storage procedure has been described by a number of investigators[6–7], and more recently by Schachterle and Alfredson[9]. This procedure, although it allows gradients to be run at slower flow-rates, needs sophisticated programming because of the system hydraulics. Furthermore, efficiency of both these systems has not been described in conjunction with autoinjector and/or dual-pump system. An autoinjector is essential when continuous unattended runs are performed, particularly in the structural studies of proteins and in industrial laboratories.

The split stream system described in this paper gives reproducible results and can be adapted to a single- or dual-pump conventional HPLC system with or without the autoinjector. In addition, by closing the metering valve completely, macrobore

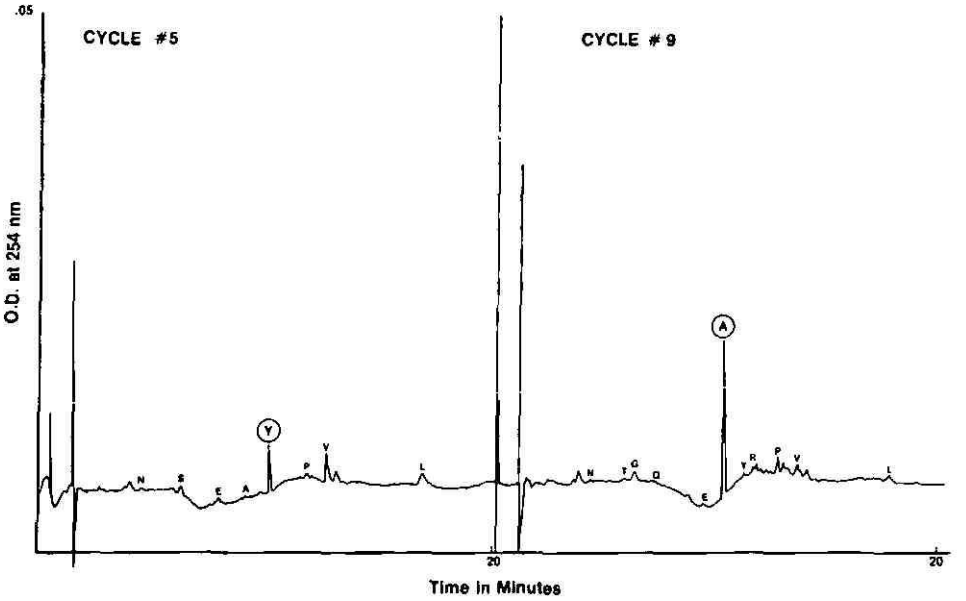

Fig. 4. PTH-amino acid analysis results on microbore column from two different tryptic peptides. Actual residue is circled. Single-letters symbols are used for amino acids.

column HPLC can be performed, thus avoiding any plumbing changes. It is interesting to note that since the separation is achieved at a pressure equivalent to that used with the macrobore column, the gradient forming program is the same for both types of column, as evident from Fig. 3. Because of the fine metering valve, virtually any flow-rate can be achieved, without any major plumbing changes. Currently we are in the process of automation of the metering valve, by linking it to the HPLC controller to read the pressure values through an added microprocessor, and thus regulate the metering valve to keep the flow constant during the run.

ACKNOWLEDGEMENTS

We thank Lisa Kallman for her expert assistance, Sandra Reid for typing this manuscript and Robert W. Herrick for sciencewriting. The work was supported by Grants AM-03555 and AM-20614.

REFERENCES

1 H. E. Schwartz and V. V. Berry, *Mag. Liquid Gas Chromatogr.*, 3(1985) 110.
2 A. S. Bhown, J. Wayland and J. C. Bennett, *J. Biochem. Biophys. Methods*, submitted for publication.
3 A. S. Bhown and J. C. *Anal. Biochem.*, 150(1985) 457.
4 R. P. W. Scott and P. Kucera, *J. Chromatogr.*, 185(1979) 27.
5 S. van der Wal and F. J. Yang, *J. High Resolut. Chromatogr. Chromatogr. Commun.*, 6(1983) 216.
6 D. Ishii, K. Asai, K. Hibi, T. Jonokuchi and M. Nagaya, *J. Chromatogr.*, 144(1977) 157.
7 E. Katz and R. P. W.Scott, *J. Chromatogr.*, 253(1982) 159.
8 K. J. Bombaugh, *Am. Lab.*, 5(1973) 69.
9 S. Schachterle and T. Alfredson, *Anal. Chem.*, 58(1986) 1368.

Journal of Chromatography, 370 (1986) 513–519
Elsevier Science Publishers B.V., Amsterdam — Printed in The Netherlands

CHROM. 19 003

Note

One-step chromatographic isolation of collagen cross-links

PATRICIA A. RYAN and PAUL F. DAVIS*
Malaghan Institute of Medical Research, Wellington Clinical School of Medicine, Wellington Hospital, Wellington 2 (New Zealand)
(First received May 1st, 1986; revised manuscript received August 5th, 1986)

One of the unusual features of the connective tissue proteins collagen and elastin is the extensive post-translational modification that occurs after synthesis of the polypeptide chains. These include hydroxylations of prolines and lysines, glycosylations of hydroxylysines, Schiff base condensations between aldoses and lysyl residues and cross-link formation based on lysine and hydroxylysine residues[1–4]. These cross-links link the polypeptide chains but only comprise a small proportion of the total composition of the protein[5–7]. This paucity makes their isolation and characterization somewhat difficult.

Cellulose media have been used for the chromatography of the pyridinium cross-links desmosine and isodesmosine, found in elastin[8–10]. In acid hydrolyzates of collagen that have been reduced with tritiated sodium borohydride there are the pyridinium cross-links, pyridinoline (Pyr) and 3-hydroxypyridinoline (Hypyr)[6,11] as well as the radioactively labelled monohydroxylysinonorleucine (MLNL), dihydroxylysinonorleucine (DLNL), lysinonorleucine (LNL) and histidinohydroxymerodesmosine (HHMD)[12]. In this paper we describe a method for the quantitative isolation of these cross-links by cellulose chromatography.

EXPERIMENTAL

Collagens were purified from rat tail tendon[13], sheep periodontal ligament[14], sheep blood vessels[15], bovine achilles tendon[16] and calf skin[17]. The preparations were reduced with tritiated sodium borohydride (The Radiochemical Centre, Amersham, U.K., 9.1 Ci/mmole) that had been diluted to 10 mCi/mmole according to the procedure of Light and Bailey[12]. LNL was purchased from Elastin Products (Pacific, MO, U.S.A.) and histidinohydroxymerodesmosine was kindly provided by Kathleen Smolenski. Cellulose powder was from Riedel de Haen and *n*-butanol and acetic acid were from May and Baker.

The collagen preparations were hydrolysed *in vacuo* for 24 h at 110°C in 6 *M* hydrochloric acid. Amino acid analysis was used to check the purity of the collagens.

For the isolation of the cross-links, hydrolyzates were mixed with glacial acetic acid, cellulose slurry and *n*-butanol, loaded on to a column of celulose (10 × 1 cm) and chromatographed firstly with at least 25 ml of *n*-butanol–acetic acid–water (4:1:1)

0021-9673/86/$03.50

and then with 5 ml of water according to the method of Skinner[9]. The two eluates were dried before redissolving in 0.01 *M* hydrochloric acid for further analysis.

Amino acid analyses were performed on a Beckman 119CL amino acid analyzer. For radioactivity profiles, 1-min fractions were collected after elution through the photometer and 0.5-ml aliquots were taken for counting.

High-voltage paper electrophoresis was performed at either pH 6.4 or pH 2.1 in a Savant electrophoresis enclosure on either Whatman No. 1 paper for analytical separations or on Whatman 3MM paper for preparative separations. Analytical electropherograms were stained with ninhydrin–cadmium acetate reagent[18]. For radio-

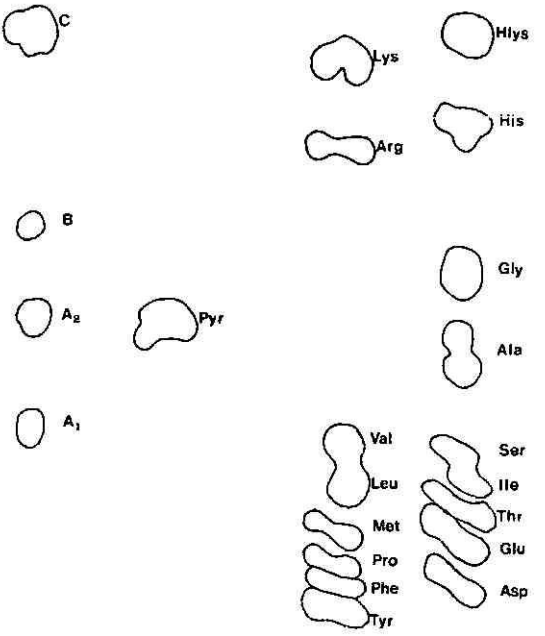

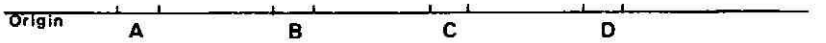

Fig. 1. Electrophoresis of water eluate of cellulose chromatography of bovine achilles tendon collagen hydrolyzate (lane A), pyridinoline (lane B), amino acid markers (lanes C and D). Electrophoresis was at pH 1.9 for 40 min. The paper was stained with ninhydrin–cadmium acetate reagent[18]. See Table II for identification of components in Lane A.

activity detection, 1-cm squares were cut from the paper and placed in scintillation counting vials. Compounds of interest were eluted from paper strips in an elution chamber using 2% acetic acid. Measurement of radioactivity was performed by adding 4.5 ml of ACSII (The Radiochemical Centre) to the sample in the vial and counting in a Philips PW4700 beta counter.

RESULTS

When 40 mg of an acid hydrolyzate of collagen is chromatographed on a cellulose mini-column as described under Experimental, Pyr is eluted in the water phase. Its identity was confirmed by high-voltage electrophoresis at pH 1.9 (Fig. 1), an ultraviolet absorption peak at 295 nm, a fluorescence emission at 395 nm after excitation at 295 nm and amino acid analysis. Pyr was not detected by any of these methods in the butanol–acetic acid eluate. Pyr was isolated by this method from hydrolyzates of collagen from sheep blood vessels, rat tail tendon, periodontal ligament and bovine achilles tendon but was not detected in calf skin collagen.

When 40 mg of an acid hydrolyzate of sodium borohydride-treated collagen was chromatographed, the higher specific radioacitivity (cpm of tritium per nmol of amino acid) was in the water eluate (Table I).

When this water phase was electrophoresed at pH 6.5 (Fig. 2A) and at pH 1.9 (Fig. 2B), several ninhydrin-positive components are detected. Details of their radioactivity and electrophoretic behaviour and ultraviolet properties are listed in Table II. As expected, Pyr was detected and confirmed in these hydrolyzates. It was not radioactive and had the same properties as mentioned above for the unreduced hydrolyzates.

TABLE I

PARTITIONING OF TRITIUM AND AMINO ACIDS DURING CELLULOSE CHROMATOGRAPHY OF HYDROLYZATES OF NaB^3H_4-TREATED COLLAGENS

Tissue	*Radioactivity (cpm/100 µl)*	*Amino acids [nanomoles (leucine equiv.)/100 µl]*	*Specific radioactivity (cpm/nmol)*
Rat tail tendon			
Mobile phase	62780	349.0	179.9
Water phase	7030	5.0	1406.0
Sheep periodontal ligament			
Mobile phase	25750	269.0	95.7
Water phase	74040	75.0	987.2
Sheep blood vessel			
Mobile phase	9090	659.0	13.8
Water phase	3300	92.0	35.9
Bovine achilles tendon			
Mobile phase	8420	335.9	25.1
Water phase	7755	28.6	271.2

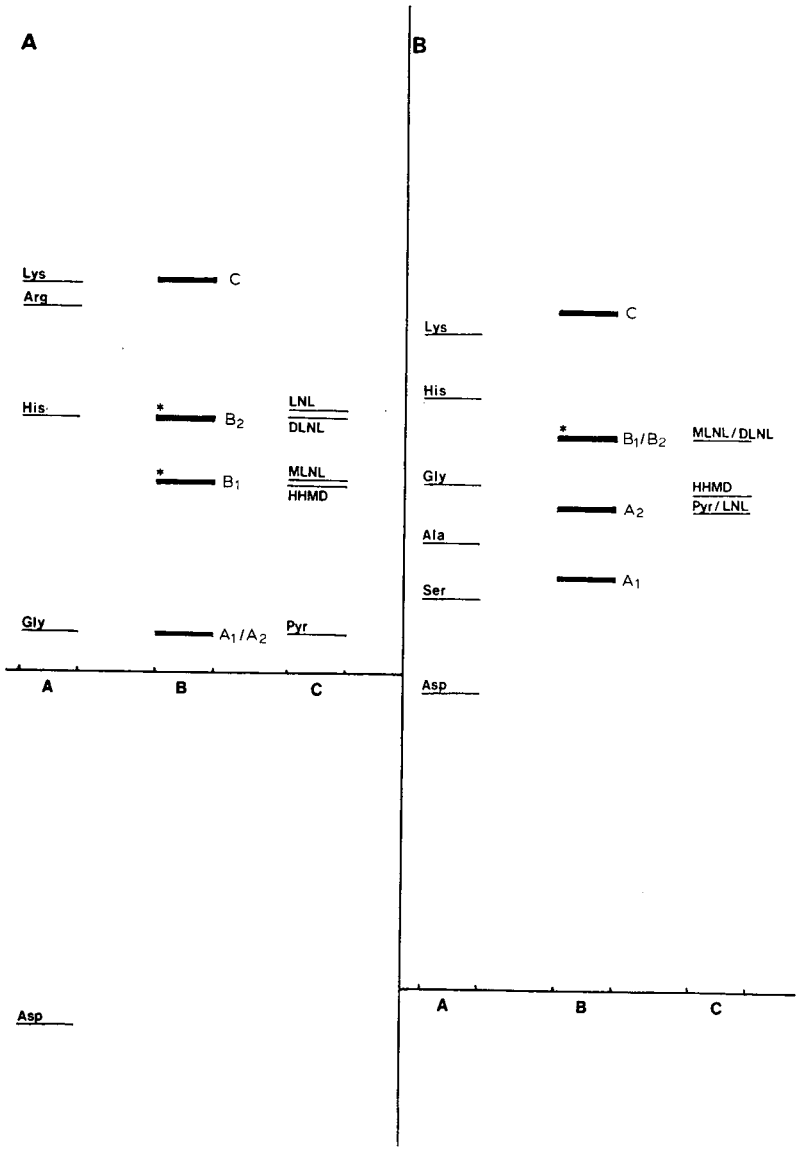

Fig. 2. Electrophoresis of water eluate of cellulose chromatography of ^{3}H-labelled bovine achilles tendon collagen hydrolyzate (lane B), amino acid markers (lane A) and cross-link markers (lane C). See Table II for identification of components in lane B. The paper was stained with ninhydrin–cadmium acetate reagent. An asterisk (*) indicates the position of elution of the tritium label. (A) Electrophoresis was at pH 6.4 for 40 min. (B) Electrophoresis was at pH 1.9 for 40 min.

There were two radioactive species detected, both of which were basic at pH 6.5 with B2 being more basic than B1. However, at pH 1.9, both B1 and B2 had similar mobilities. When these species were electrophoresed preparatively, eluted and chromatographed on the amino acid analyzer, they were identified as MLNL (B1) and DLNL (B2).

TABLE II

CHARACTERIZATION OF WATER ELUATE FROM CELLULOSE CHROMATOGRAPHY OF HYDROLYZATES OF NaB^3H_4-TREATED COLLAGEN

See Fig. 2 for electrophoresis.

	*Mobility at pH 6.5**	*Mobility at pH 1.9***	*Radioactivity*	*UV Absorbance*	*Fluorescence*	*Identity*
A1	0	1.05	–	–	–	Serine
A2	0	1.25	–	+ (295 nm)	+	Pyr
B1	−0.39	1.40	+	–	–	MLNL
B2	−0.55	1.40	+	–	–	DLNL
C	−0.90	1.73	–	–	–	Hydroxylysine

* Mobile relative to aspartic acid. A negative value indicates migration is in the opposite direction to aspartic acid.

** Mobility relative to serine.

In separate experiments, ^3H-labelled HHMD and unreduced LNL were added to 40 mg of non-reduced tendon collagen hydrolyzates. Most of the HHMD was insoluble in butanol–acetic acid but over 80% LNL was eluted in the mobile phase (Table III).

When hydrolyzed radioactive collagens were chromatographed on the cellulose column and both the organic eluate and the water eluate were analyzed on the amino acid analyzer for the distribution of radioactivity, peaks appeared in the water phase at the positions expected for the mjaor cross-links (Fig. 3). As expected there was very little radioactivity in the mobile organic phase. The majority of the radioactivity in this solvent was in the vicinity of the hexitol–lysyl and hexitol–hydroxylysyl residues. But as there were labelled species in the same position in the water phase, the partitioning of these derivatives did not seem to be quantitative.

DISCUSSION

In elastin, there are unique interchain cross-links of which the principal ones are the pyridinium-based desmosine and isodesmosine. These structures can be separated from the other constituents in hydrolyzates by cellulose chromatography[8–10]. Most amino acids are soluble in butanol–acetic acid–water mixtures but these compounds are not[19]. For collagen, most of the characterized cross-links are acid-labile, aliphatic compounds that precursors of the more complex non-reducible mature

TABLE III

PARTITIONING OF RADIOACTIVITY IN CELLULOSE CHROMATOGRAPHY OF COLLAGEN SUPPLEMENTED WITH ^3H-LABELLED HHMD OR LNL

	Collagen + HHMD (%)	*Collagen + LNL (%)*
Mobile phase	23.7	82.7
Water phase	76.3	17.3

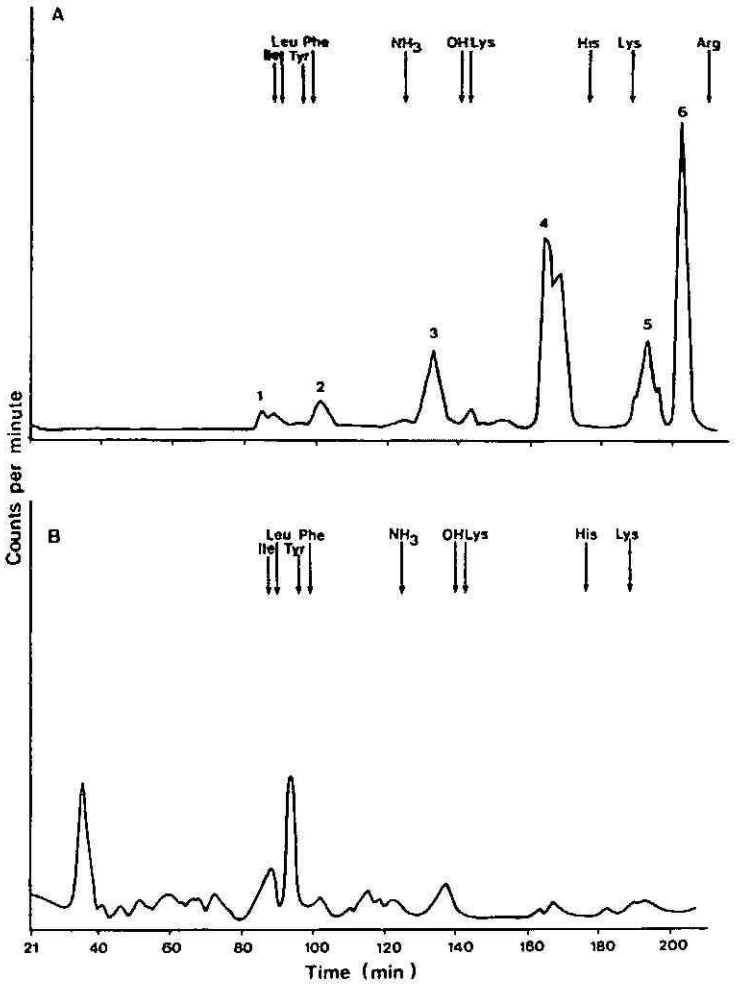

Fig. 3. Ion-exchange chromatography on amino acid analyzer of water phase (A) and mobile phase (B) of ^{3}H-labelled acid hydrolyzate of bovine achilles tendon collagen. Peaks: 1 = hexitol-hydroxylysines, 2 = hexitol-lysines, 3 = MLNL, 4 = DLNL, 5 = LNL, 6 = HHMD.

cross-links[12]. Recently a stable, non-reducible pyridinium compound, pyridinoline, has been identified in a number of collagen hydrolyzates[6,11].

If the insolubility of the desmosines in butanol–acetic acid mixtures is due to the pyridinium nucleus, Pyr might be expected to behave similarly when collagen hydrolyzates are chromatographed. This paper shows that this is indeed so and that the subsequent recovery in the water phase is quantitative. However there are several other components present in this water phase. As well as hydroxylysine and serine, the major cross-links of immature collagen (MLNL, DLNL and HHMD) are present in this eluate. The exception is LNL which is not present in all collagen samples.

The occurrence of the amino acids serine and hydroxylysine in the water eluate is interesting. These, as well as the reducible cross-links, are aliphatic compounds

and are structurally distinct from the pyridinium cross-links. This suggests that there may be two mechanisms of chromatography occurring. One is based on the insolubility of pyridinium compounds in butanol–acetic acid and the second is for hydroxylated aliphatic amino compounds. The presence of most of the LNL in the mobile phase is consistent with this interpretation. This will need further evaluation so as to understand the mechanisms that are of importance in this system.

ACKNOWLEDGEMENTS

The authors acknowledge the financial assistance of the Medical Research Council of New Zealand, the New Zealand Lottery Board and the War Pensions Medical Research Trust Board. They thank Kathleen Smolenski for the gift of histidinohydroxymerodesmosine.

REFERENCES

1 K. I. Kivirikko and R. Myllyla, *Methods Enzymol.*, 82 (1982) 245.
2 D. J. Prockop and L. Tuderman, *Methods Enzymol.*, 82 (1982) 305.
3 J. A. Foster, *Methods Enzymol.*, 82 (1982) 559.
4 J. H. Fessler, K. J. Doege, K. G. Duncan and L. I. Fessler, *J. Cell. Biochem.*, 28 (1985) 31.
5 R. J. Boucek, N. L. Noble and Z. Gunja-Smith, *Biochem. J.*, 177 (1979) 853.
6 D. R. Eyre, T. J. Koob and K. P. van Ness, *Anal. Biochem.*, 137 (1984) 380.
7 M. A. Paz, D. A. Keith and P. M. Gallop, *Methods Enzymol.*, 82 (1982) 571.
8 B. C. Starcher and M. J. Galione, *Prep. Biochem.*, 5 (1975) 455.
9 S. J. M. Skinner, *J. Chromatogr.*, 229 (1982) 200.
10 B. C. Starcher, *Anal. Biochem.*, 79 (1977) 11.
11 M. Barber, R. S. Bordoli, G. J. Elliott, D. Fujimoto and J. E. Scott, *Biochem. Biophys. Res. Commun.*, 109 (1982) 1041.
12 N. D. Light and A. J. Bailey, *Methods Enzymol.*, 82 (1982) 360.
13 A. J. Bailey, C. M. Peach and L. J. Fowler, *Biochem. J.*, 117 (1970) 819.
14 J. Sodek and H. F. Limeback, *J. Biol. Chem.*, 254 (1979) 10496.
15 P. F. Davis and Z. M. Mackle, *Anal. Biochem.*, 115 (1981) 11.
16 J. Einbinder and M. Schubert, *J. Biol. Chem.*, 188 (1951) 335.
17 P. M. Gallop and S. Seifter, *Methods Enzymol.*, 6 (1963) 635.
18 J. G. Heathcote and C. Haworth, *J. Chromatogr.*, 43 (1969) 84.
19 S. M. Partridge, D. F. Elsden and J. Thomas, *Nature (London)*, 197 (1963) 1297.

Journal of Chromatography, 370 (1986) 520–527
Elsevier Science Publishers B.V., Amsterdam — Printed in The Netherlands

CHROM. 19 120

Note

Chemische Unterscheidungsmerkmale der Samen von *Trifolium repens* L. und *Trifolium repens* L. var. *giganteum*

J. SACHSE

Eidgenössische Forschungsanstalt für landwirtschaftlichen Pflanzenbau, Reckenholzstrasse 191/211, CH-8046 Zürich (Schweiz)

(Eingegangen am 26. September 1986)

Trifolium repens L. und *Trifolium repens* L. var. *giganteum* sind wertvolle Futterpflanzen, die sich in ihren agronomischen Eigenschaften deutlich unterscheiden[1].

In der Liste der empfohlenen Gräser und Kleesorten waren in der Schweiz seit 1976 die Sorten Ladino und Milkanova aufgeführt[2,3]. Milkanova entspricht *T. repens* L. und Ladino *T. repens* L. var. *giganteum*. Seitdem wurde die Liste um einige Weisskleesorten erweitert, die ihrem Habitus nach zu dem einen oder anderen Typ gehören. Ein weiteres Unterscheidungsmerkmal bietet der Blausäuregehalt in der Weisskleepflanze, der bei *T. repens* L. ein mittlerer, hingegen bei *T. repens* L. var. *giganteum* niedrig ist (siehe Tabelle I).

Obgleich Weisskleesamen verschiedene Farben aufweisen, können diese nicht als Sortenmerkmal gewertet werden, weil sie von der Reife und der Lagerzeit der Samen abhängen. Ebensowenig charakteristisch ist ihr Tausendkorngewicht und ihr sehr geringer Blausäuregehalt. Aus diesen Gründen kommt es gelegentlich zu Verwechslungen von Saatgut. Bisher ist eine Identifizierung nach Aussaat der Samen erst in einigen Wochen an Hand der grünen Pflanze möglich gewesen. Da in der Literatur von Unterscheidungsmerkmalen in Weisskleesamen bis jetzt noch nichts berichtet wurde, soll versucht werden, individuelle Kennzeichen im Saatgut dieser Futterpflanzen zu finden.

EXPERIMENTELLES

Reagentien

Petroläther (Kp. 40–70°C), Seesand feinkörnig, Natriumsulfat rein, wasserfrei, Hexan p.a., 2 *N* methanolische Kalilauge, Ölsäure-, Linolsäure- und Linolensäuremethylester, Stickstoff 99,99%, Pressluft, Wasserstoff.

Geräte

Elektrische Kaffeemühle, Heizkalotten, Kühler, Rundkolben 250 ml mit Schliff, Soxhletapparatur und -hülsen, Vakuumtrockenschrank, Tischzentrifuge, Zentrifugenrohre 10 ml mit Plastikstopfen, Tablettenröhrchen 5 ml mit Plastikstopfen, Gaschromatograph Hewlett-Packard 5830 A mit Flammenionisationsdetector, GC-Terminal Hewlett-Packard 18 850 A, GC-Säule, 1,8 m × 2 mm I.D., Chromosorb W AW 100–200 mesh, belegt mit 6% SP-2300.

0021-9673/86/$03.50

TABELLE I

UNTERSCHEIDUNGSMERKMALE AM SPROSS VON *TRIFOLIUM REPENS* L. UND *TRIFOLIUM REPENS* L. VAR. *GIGANTEUM*

Botanische Bezeichnung	*Wuchs*	*Blätter*	*Kleekrebs-anfälligkeit*	*Landwirtschaftl. Ertrag*	*Blausäure-gehalt*	*Sorten*
Trifolium repens L.	Niedrig bis mittelhoch	Mittelgross bis klein	Gering bis mittel	Mittel	Mittel bis hoch	Milkanova Sandra Nesta Alban Sonja
Trifolium repens L. var. *giganteum*	Hoch	Gross	Hoch	Hoch	Gering	Ladino Regal Merit Sacramento Titan

Extraktion

Gemahlene Kleesamen (10–15 g) in einer Soxhlet-Apparatur mit Petroläther 48 h extrahieren. Den Soxhlethülsen etwa 3 g wasserfreies Natriumsulfat beigeben, um den Petroläther während der Extraktion zu trocknen. Den Rundkolben gegen einen eventuellen Siedeverzug einige Seesand-Körnchen beifügen. Vom erhaltenen Extrakt den Petroläther schonend abdestillieren, einen kleinen Rest mit Stickstoff ausblasen und das Öl im Vakuumtrockenschrank 2 h bei 85°C trocknen.

Umesterung

Das getrocknete Fett (200 mg) in kleine Zentrifugenrohre einwägen, das Öl in 5 ml Hexan lösen und mit 0,6 ml 2 *N* methanolischer Kalilauge versetzen. Das Zentrifugenrohr verschliessen, sofort 20 s kräftig schütteln, genau 40 s stehen lassen und sofort 2 min zentrifugieren. Einen Teil der oberen Phase in kleine Tablettenröhrchen dekantieren, mit wenig wasserfreiem Natriumsulfat versetzen und bis zur gaschromatographischen Untersuchung im Kühlschrank aufbewahren. Die Proben für das vollständige Chromatogramm unverdünnt verwenden, für das Teilchromatogramm 1:30 vor der Injektion verdünnen.

Gaschromatographische Bedingungen

Injizierte Probenmenge für unverdünnte Proben 0,5 µl, für verdünnte 0,3 µl. Für das Teilchromatogramm 30 ml Stickstoff/min, Injektortemperatur 230°C, Detektortemperatur 250°C, Ofentemperatur 200°C, Dämpfung 6, Peakschwellenwert 0,3, Papiervorschub 1 cm/min, Integrationsunterdrückung 3 min am Anfang des Laufs, Stopp nach 7 min. Für das vollständige Chromatogramm 60 ml Stickstoff/min, Ofentemperatur 4 min 175°C, Anstieg auf 200°C in Raten von 2°C/min, 10 min, bei 200°C belassen, Integrationsunterdrückung 0,4 min nach dem Start, Stopp nach 25 min. Die übrigen Bedingungen sind die gleichen wie für das Teilchromatogramm.

ERGEBNISSE UND DISKUSSION

Auf der Suche nach einem Unterscheidungsmerkmal zwischen den Weisskleetypen *T. repens* L. und *T. repens* L. var. *giganteum* bot sich die Extraktion der Samen mit verschiedenen Lösungsmitteln und die Untersuchung der Extrakte mit Hilfe der Dünnschichtchromatographie an.

Zur Extraktion wurden polare bis apolare Lösungsmittel, nämlich je 50 ml Wasser, Äthanol, Essigsäureäthylester, Chloroform und Petroläther für 1 g Kleesamen verwendet. Eine Extraktion wurde mit Aceton vorgenommen, nachdem das Material 1 h mit 2 *N* Salzsäure hydrolysiert worden war.

Die Dünnschichtchromatographie wurde sowohl auf Kieselgel Merck Typ 60 ohne Aktivierung als auch auf Polyamid Woelm Eschwege durchgeführt. Als Fliessmittel dienten *n*-Butanol–Eissesig–Wasser (100:10:30) für den wässrigen, Petroläther–Aceton (50:50) für den äthanolischen bzw. Essigesterextrakt, dasselbe Fliesmittel im Verhältnis 40:30 für den Chloroformextrakt und für den Petrolätherextrakt im Verhältnis 40:20. Die Extrakte wurden im Vakuum eingedampft und der Rückstand in 1 ml entsprechendem Lösungsmittel gelöst. Die Auftragsmenge betrug 100 µl. Neben der Flüssigextraktion wurde noch der gepulverte Samen im TAS-Ofen nach E. Stahl bei verschiedenen Temperaturen erhitzt und flüchtige Substanzen direkt auf der Dünnschichtplatte aufgefangen. Als Sprühmittel wurden folgende nach Stahl[4] ausgewählt: Ninhydrin No. 176, Schwefelsäure–Methanol No. 217, Naturstoffreagens nach Neu No. 80 sowie 10%ige Ammoniaklösung. Die Dünnschichtplatten wurden vor und nach dem Besprühen bei Tages- und UV-Licht betrachtet. Von all den Versuchen, einschliesslich des hydrolysierten Acetonextraktes, ergaben der Chloroformextrakt und das Naturstoffreagens die eindrücklichsten Dünnschichtplatten. Gelbe, orangefarbene, rote, grüne und blaue Flecken waren unter der UV-Lampe sichtbar, die ersten auch bei Tageslicht, die wohl auf Flavonoide vor allem aus der Samenschale zurückzuführen sind. Vergleiche zwischen den Sorten Milkanova und Ladino zeigten zwar quantitative aber keine qualitativen Unterschiede. Da das ungleiche Aussehen der Samen schon durch die Samenreife und ihre Lagerzeit bedingt ist, dürften die quantitativen dünnschichtchromatographischen Unterschiede ebenfalls diesen Einflüssen zuzuschreiben sein. Auch das TAS-Verfahren liess keine Differenzen zwischen den untersuchten Sorten erkennen.

Elektrophorese der Samenproteine

Eine weitere Möglichkeit, verschiedene Wesensmerkmale zwischen hoch- und niedrigwachsenden Weisskleesorten zu finden, bot die Elektrophorese der Samenproteine. Drei Verfahren wurden getestet:

(1) Die Auftrennung wasserlöslicher Proteine bei pH 7,9 in Polyacrylamid nach Stegemann und Loeschcke[5]. Hier bestand bei Haupt- und Nebenbanden kein Unterschied zwischen den Sorten.

(2) Die Trennung von Proteinen, die in 70%igen Äthanol löslich sind, bei pH 3,1 auf Polyacrylamid[6]. Bei diesem Versuch waren überhaupt keine Banden sichtbar, d.h. es sind keine alkohollöslichen Proteine vorhanden.

(3) Die Elektrophorese pufferlöslicher Proteine bei pH 6,8 mit Natriumdodecylsulfatzusatz in Polyacrylamidgel[7] bei pH 8,3 ergab viele Banden, aber keine Abweichungen im Proteinmuster.

Fettsäuremuster

Da Samen meist Fett enthalten, Kleesamen etwa 6%, lag es nahe, das Fettsäuremuster der Sorten zu prüfen. Wie im experimentellen Teil ersichtlich, wurde das Rohfett nach Soxhlet gewonnen, und die Fettsäuren wurden zu Methylestern umgeestert. Ein Vergleich der Ergebnisse, die mit der beschriebenen Umesterungsmethode und mit dem Bortrifluorid-Verfahren nach van Wijngaarden[8] erzielt wurden, zeigten Übereinstimmung. Die Reproduzierbarkeit der Umesterung liegt für die interessierenden Fettsäuren bei *T. repens* L. und *T. repens* L. var. *giganteum* über 99%.

Wie das Gaschromatogramm (Fig. 1) zeigt, sind mindestens 15 Fettsäuren im Kleesamen enthalten, die nahezu in allen untersuchten Sorten vertreten sind. Hauptkomponenten sind die Palmitinsäure (11–13%), die Stearinsäure (etwa 3%), die Ölsäure (6–15%), die Linolsäure (54–67%) und Linolensäure (4–8%) bezogen auf die Gesamtfettsäuremenge. Die Ansprechbarkeit des Flammenionisationsdetektors auf die verschiedenen Fettsäuren wurde in diesem Versuch nicht berücksichtigt. Neben den genannten Fettsäuren wurden noch die Arachinsäure und die Erucasäure nach ihren Retionszeiten identifiziert.

Die Unterscheidung der Weisskleesorten an ihrem Samenfett ist durch die Untersuchung des Fettsäuremusters nicht qualitativ, wohl aber quantitativ am Prozentgehalt zweier Fettsäuren, der Öl- und Linolsäure, innerhalb der gesamten Fettsäuremenge möglich. Wir konnten feststellen, dass hochwüchsige Sorten im Samen

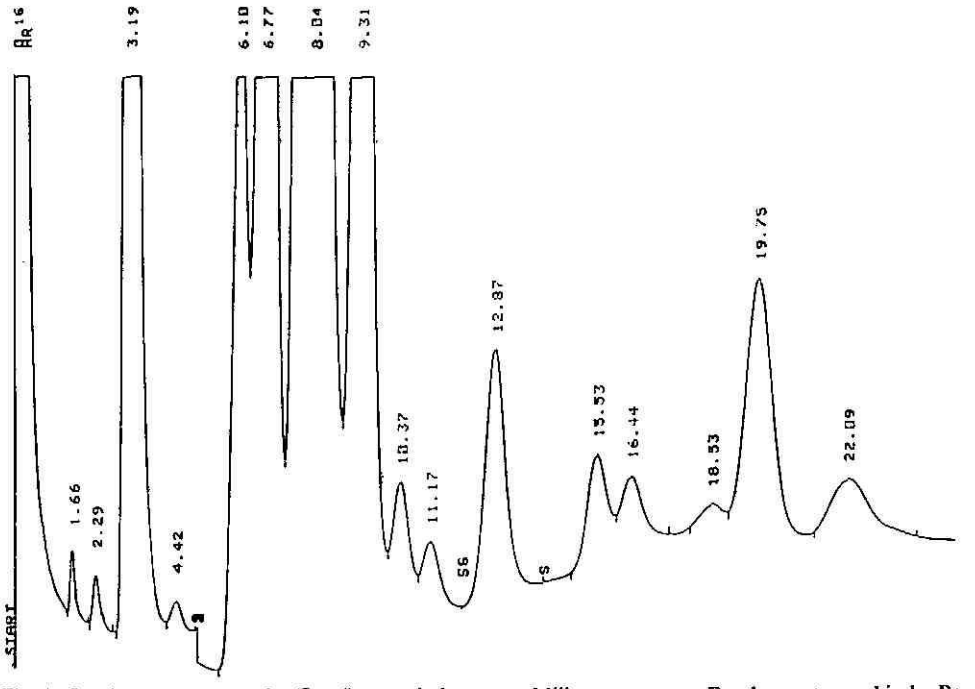

Fig. 1. Gaschromatogramm der Fettsäuremethylester aus Milkanovasamen. Gaschromatographische Bedingungen siehe experimentellen Teil. Palmitinsäure (t_R = 3,19 min); Stearinsäure (6,10 min); Ölsäure (6,77 min); Linolsäure (8,04 min); Linolensäure (9,31 min); Arachinsäure (10,37 min); Heneicosansäure (zugesetzt) (12,87 min); Erucasäure (16,44 min).

TABELLE II

RELATIVER GEHALT AN AUSGEWAHLTEN FETTSÄUREN IN WEISSKLEESAMEN VERSCHIEDENER SORTEN

Relativer Gehalt bezogen auf die gesamte Fettsäuremenge. $\bar{x}$ = Mittelwert aus zwei Einzelwerten, Einzelwerte aus einer Fettextraktion, einer Veresterung und zwei Einspritzungen in den Gaschromatographen. d = Prozentuale Abweichung der Einzelwerte vom Mittelwert $\bar{x}$; $\bar{d}$ = mittlere prozentuale Abweichung.

Weisskleesorte	*Ernte-jahr*	*Züchter*	*Ölsäure (%)*	$\bar{x}$	d
Trifolium repens L.					
Milkanova	1983	Dansk Plante-foraedling (Dänemark)	11,20 11,18	11,19	0,1
	1984	Dansk Plante-foraedling (Dänemark)	7,48 7,82	7,65	2,2
	1985	Dansk Plante-foraedling (Dänemark)	8,85 8,95	8,90	0,6
Milo	1982	Dansk Plante-foraedling (Dänemark)	10,95 11,40	11,23	1,5
DP 79-S-6	1983	Dansk Plante-foraedling (Dänemark)	11,01 10,96	10,99	0,2
WW V 14	1979	Weibullsholm (Schweden)	9,08 8,96	9,02	0,7
	1982	Weibullsholm (Schweden)	11,29 11,42	11,36	0,5
	1983	Weibullsholm (Schweden)	11,14 10,91	11,03	1,0
Sandra	?	Svalöf (Schweden)	12,31 12,08	12,20	0,9
Sv 0437	1984	Svalöf (Schweden)	9,57 9,41	9,49	0,8
Nesta	1983	Nat. Seed Develop. Organisation (Grossbritannien)	10,08 10,34	10,21	1,3
	1984	Nat. Seed Develop. Organisation (Grossbritannien)	10,52 10,51	10,52	0,05
Alban	1984	Daehnfeldt (Dänemark)	7,16 7,02	7,09	1,0
Sonja	1984	Weibullsholm (Schweden)	10.38 10,77	10,58	1,8
Trifolium repens L. var. giganteum					
Ladino	1983	Cal/West Seeds (U.S.A.)	17,90 17,85	17,88	0,1
Regal	1982	Cal/West Seeds (U.S.A.)	17,28 17,56	17,42	0,8
	1983	Cal/West Seeds (U.S.A.)	15,83 15,97	15,90	0,4
	1984	Cal/West Seeds (U.S.A.)	15,80 16,50	16,15	2,1
	1985	Cal/West Seeds (U.S.A.)	17,34 16,24	16,79	3,2
Merit	1983	Sacramento Milling (U.S.A.)	14,42 14,50	14,46	0,3
Sacramento	1983	Sacramento Milling (U.S.A.)	17,71 17,68	17,70	0,1
Titan	1983	Northrup King (U.S.A.)	16,53 16,48	16,51	0,1
					$\bar{d}$ = 0,9

Linolsäure (%)	$\bar{x}$	*d*	*Linolensäure (%)*	$\bar{x}$	*d*	*Öl- u. Linolens. (%)*	*Linolsäure/-Öls. u. Linolens.*
78,84 78,88	78,86	0,03	6,77 6,75	6,76	0,1	17,95	4,39
80,77 80,23	80,50	0,3	9,24 9,40	9,32	0,9	16,97	4,74
79,45 79,51	79,48	0,04	8,88 8,81	8,85	0,3	17,75	4,47
78,83 80,07	79,45	0,8	6,34 6,06	6,20	2,2	17,43	4,55
78,47 78,55	78,51	0,05	7,86 7,86	7,86	0	17,85	4,40
79,55 79,73	79,64	0,1	8,74 8,79	8,77	0,2	17,79	4,48
79,08 78,60	78,84	0,3	6,30 6,47	6,39	1,2	17,75	4,41
77,91 79,16	78,54	0,8	7,98 7,16	7,52	5,2	18,60	4,22
77,36 78,15	77,76	0,5	7,03 6,51	6,77	3,7	18,97	4,10
79,76 79,72	79,74	0,03	7,91 8,08	8,00	1,0	17,49	4,56
79,32 78,89	79,11	0,3	7,33 7,52	7,43	1,2	17,64	4,48
79,19 79,10	79,15	0,05	7,34 7,41	7,38	0,4	17,90	4,42
80,53 80,13	80,33	0,2	10,05 10,65	10,35	2,8	17,44	4,61
79,83 79,42	79,63	0,3	7,35 7,15	7,25	1,4	17,83	4,47
71,40 71,74	71,57	0,03	7,37 7,42	7,40	0,3	25,28	2,83
73,74 74,00	73,87	0,2	5,32 4,90	5,11	4,0	22,53	3,28
74,65 75,21	74,93	0,4	5,46 5,94	5,70	4,0	21,60	3,47
75,03 75,50	75,27	0,3	5,01 5,51	5,26	4,5	21,41	3,52
74,31 73,77	74,04	0,4	5,58 5,90	5,74	2,8	22,53	3,29
74,85 74,76	74,81	0,05	8,15 8,13	8,14	0,1	22,60	3,31
72,24 72,84	72,54	0,4	6,86 6,39	6,63	3,4	24,33	2,98
73,25 73,64	73,58	0,1	6,91 6,84	6,88	0,4	23,39	3,15
		$\bar{d} = 0,3$			$\bar{d} = 1,8$		

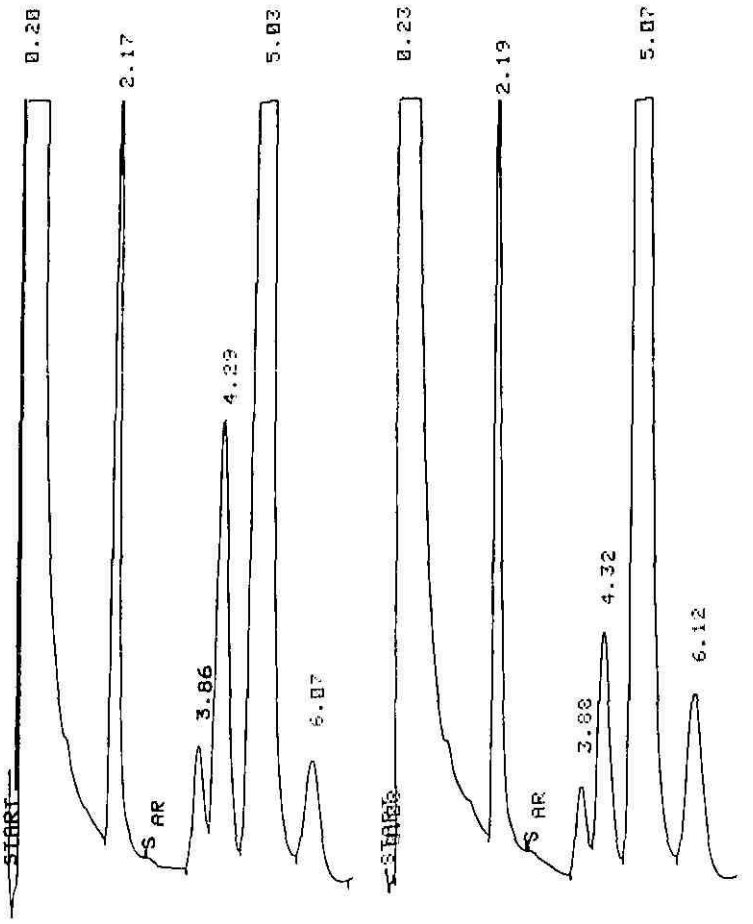

Fig. 2. Gekürztes Gaschromatogramm der Fettsäuremethylester aus Samen von *Trifolium repens* L. var. *giganteum* (links) und *Trifolium repens* L. (rechts). Gaschromatographische Bedingungen siehe experimentellen Teil. Palmitinsäure (t_R = 2,17/2,19 min); Stearinsäure (3,86/3,88 min); Ölsäure (4,29/4,32 min); Linolsäure (5,03/5,07 min); Linolensäure (6,07/6,12 min).

einen höheren Ölsäuregehalt (etwa 13–16%) und einen tieferen Linolsäuregehalt (etwa 54–63%) aufweisen als niedrig wachsende Weisskleesorten (7–10 bzw. 64–67%). Zwischen den Gehalten an Palmitinsäure besteht in den zwei Weisskleetypen kein Unterschied. Wohl aber ein geringer im Linolensäurevorkommen, der bei *T. repens* L. zwischen 5 und 8%, bei *T. repens* L. var *giganteum* zwischen 4 und 6% liegt. Allerdings ist die Schwankungsbreite der Messergebnisse bei diesen geringen Saureanteilen höher als bei Öl- und Linolsäure.

Um die Untersuchung zu vereinfachen, haben wir uns auf die quantitative Erfassung der Fettsäuren beschränkt, die in den zwei Weisskleetypen in unterschiedlicher Menge vorkommen, das sind die Öl- und Linolsäure. Da die erwähnten Fettsäuren sehr ähnliche Retentionszeiten haben, konnten wir am Anfang des Chromatogramms die Peakintegration 3 min unterdrücken und nach 7 min auf die später

eluierten Fettsäuren verzichten (Fig. 2). Ausserdem mussten die gewonnenen Methylester 30-fach verdünnt werden, da die für uns wesentlichen Fettsäuren in sehr hoher Konzentration vorliegen. Aus dem veränderten Chromatographieverfahren resultieren andere Prozentgehalte der gesuchten Fettsäuren, die in Tabelle II von den untersuchten Sorten aufgeführt sind. Um die Schwankungen der Ergebnisse gering zu halten, wurde der Gehalt von Öl- und Linolensäure addiert und diese Summe in Beziehung zum Gehalt an Linolsäure gesetzt. Der sich daraus ergebende Quotient kann zur Unterscheidungen von Sorten aus *T. repens* L. und *T. repens* L. var. *giganteum* dienen Allerdings ist zu prüfen, ob sich dieser Quotient tatsächlich aus den in Tabelle II erhaltenen Werten ergeben hat. Die Unterschiede im Öl- und Linolsäuregehalt der beiden Kleetypen sind nach dem *t*-Test zu mehr als 99% gesichert, der im Linolensäuregehalt zu mehr als 95%. Werden die Prozente an Öl- und Linolensäure für jede Sorte addiert, so unterscheiden sich die Summen von *T. repens* L. und *T. repens* L. var. *giganteum* ebenfallt mit 99%iger Sicherheit. Dasselbe gilt für die jeweiligen Quotienten aus dem Verhältnis der Summe Öl- und Linolensäure zu Linolsäure.

Für die Sorten, deren Ölsäure- und Linolsäuregehalt zwischen den angegebenen Richtwerten liegt, z.B. für Menna, Luclair, Astra, Rena, Aran, Ross und Lune de Mai, dürften keine Zuordnungen möglich sein. Durch das freundliche Entgegenkommen einiger Saatzuchtfirmen waren wir in der Lage, das gefundene Unterscheidungsmerkmal für die zwei Weisskleetypen an weiteren Sorten verschiedener Herkunft und Anbaujahre zu testen. Ihr Einfluss auf das Fettsäuremuster war sehr gering, weshalb geschlossen werden kann, dass dieser deutliche Gehaltsunterschied an Öl- und Linolsäure genetisch bedingt ist und in Zukunft für die Unterscheidung von niedrig- und hochwüchsigen Weisskleesorten an Hand ihrer Samen in der Regel benutzt werden kann.

LITERATUR

1 J. Lehmann und U. Zihlmann, *Mitt. Schweiz. Landwirtsch.*, 28 (1980) 130.
2 J. Lehmann und J. P. Charles, *Mitt. Schweiz. Landwirtsch.*, 25 (1977) 103.
3 J. Lehmann, H. U. Briner, E. Meister und D. Joggi, *Mitt. Schweiz. Landwirtsch.*, 32 (1984) 96.
4 E. Stahl, *Dünnschichtchromatographie*, Springer, Berlin, Heidelberg, New York, 1967, S. 815.
5 H. Stegemann und V. Loeschcke, *Mitt. Biol. Bundesanst. Land- Forstwirtsch., Berlin-Dahlem*, 168 (1967).
6 R. Tkachuk und V. J. Methlish, *Ann. Technol. Agric.*, 29 (1980) 207.
7 P. T. Payne, K. G. Corfield und J. A. Blackman, *Theor. Appl. Genet.*, 55 (1979) 153.
8 D. van Wijngaarden, *Anal. Chem.*, 39 (1967) 848.

Author Index

Akiyama, K., see Kamata, K. 344
Arai, K., see Miyata-Asano, M. 501
Bahsitta, H.-P., see Stehle, P. 131
Bártů, V.
——, Wičar, S., Scherpenzeel, G.-J. and Leclercq, P. A.
Optimization of temperature programming in gas chromatography with respect to separation time. I. Temperature programme optimization fundamentals 219
——, Wičar, S., Scherpenzeel, G.-J. and Leclercq, P. A.
Optimization of temperature programming in gas chromatography with respect to separation time. II. Optimization of the individual temperature programme substrategies 235
Beldman, G. see Voragen, A. G. J. 113
Bellander, T., see Skarping, G. 245
Bennett, J. C., see Bhown, A. S. 508
Berman, S. S., see Quinn, A. M. 203
Bhown, A. S.
——, Wayland, J. and Bennett, J. C.
Simple device for high-performance liquid chromatographic separation on microbore columns 508
Bieganowska, M. L., see Glowniak, K. 281
Bijloo, G. J., see Rekker, R. F. 355
Bobleter, O., see Bonn, G. 485
Bonn, G.
——, Grünwald, M., Schèrz, H. and Bobleter, O.
Thin-layer electrophoretic behaviour of oligo- and mono-saccharides, uronic acids and polyhydroxy compounds obtained as biomass degradation products 485
Brieva, A.
—— and Rubio, N.
Rapid purification of the main allergen of *Lolium perenne* by high-performance liquid chromatography 165
Brinckmann, F. E., see Parks, E. J. 206
Brinkman, U. A. Th., see Irth, H. 439
Bryn, K.
—— and Jantzen, E.
Quantification of 2-keto-3-deoxyoctonate in (lipo)polysaccharides by methanolytic release, trifluoroacetylation and capillary gas chromatography 103
Burger, B. V.
—— and Munro, Z.
Headspace gas analysis. Quantitative trapping and thermal desorption of volatiles using fused-silica open tubular capillary traps 449
Carson, D. L., see Curley, Jr., R. W. 188
Cartoni, G. P.
——, Coccioli, F., Ronchetti, M., Simonetti, L. and Zoccolillo, L.
Determination of polycyclic aromatic hydrocarbons in natural waters by thin-layer chromatography and high-performance liquid chromatography 157
——, Goretti, G., Monticelli, B. and Russo, M. V.
Evaluation of capillary gas chromatographic columns in series. Analytical application to lemon oil 93
Checchini, L., see Desideri, P. G. 75
Churáček, J., see Herrmann, F. 49
Coccioli, F., see Cartoni, G. P. 157
Cox, R. A.
——, McFarland, K. N., Holt Sackett, P. and Short, M. T.
Correlation of urokinase activity from biopotency and high-performance liquid chromatographic assays 495
Curley, Jr., R. W.
——, Carson, D. L. and Ryzewski, C. N.
Effect of end-capping of reversed-phase high-performance liquid chromatographic matrices on the analysis of vitamin A and its metabolites 188
Darzhalieva, M. M., see Nikolov, R. N. 377
Davis, P. F., see Ryan, P. A. 513
De Jong, G. J., see Irth, H. 439
Derks, H. J. G. M.
——, Van Twillert, K., Pereboom-de Fauw, D. P. K. H., Zomer, G. and Loeber, J. G.
Determination of the heroin metabolite 6-acetylmorphine by high-performance liquid chromatography using automated pre-column derivatization and fluorescence detection 173
Desideri, P. G.
——, Lepri, L., Merlini, L. and Checchini, L.
High-performance liquid chromatography of amino acids and peptides on silica coated with ammonium tungstophosphate. I. Characteristics of the stationary phase 75
De Vries, G., see Rekker, R. F. 355
Dufka, O., see Herrmann, F. 49
Erlandsson, P.
——, Hansson, L. and Isaksson, R.
Direct analytical and preparative resolution of enantiomers using albumin adsorbed to silica as a stationary phase 475

Fonck, C.
——, Frutiger, S. and Hughes, G. J.
Solvent system for the rapid identification of phenylthiohydantoin derivatives of amino acids by high-performance liquid chromatography 339
Frei, R. W., see Irth, H. 439
Frutiger, S., see Fonck, C. 339
Fürst, P., see Stehle, P. 131
Gardner, G. J., see Quinn, A. M. 203
Gill, R., see Stevens, H. M. 39
Glowniak, K.
—— and Bieganowska, M. L.
Effects of modifier and molecular structure of some coumarins on retention in reversed-phase high-performance thin-layer and column chromatography 281
Goretti, G., see Cartoni, G. P. 93
Gray, D. O., see Hayman, A. R. 194
Grob, Jr., K.
Static coating methods for glass capillary columns at elevated temperatures 352
Grünwald, M., see Bonn, G. 485
Hansson, L., see Erlandsson, P. 475
Hayakawa, T., see Nishikawa, H. 327
Hayman, A. R.
—— and Gray, D. O.
Paper electrophoresis of the dansyl derivatives of amino acids and amines 194
Herrmann, F.
——, Matoušek, P., Dufka, O. and Churáček, J.
Fused-silica capillary gas chromatography–mass spectrometry of some dicarboxylic acids present in condensation-type polymers. II. Bis(trimethylsilyl) esters 49
Hill, E.
——, Humphreys, E. and Malcolme-Lawes, D. J.
Electrochemiluminescence as a detection technique for reversed-phase high-performance liquid chromatography. III. A high-performance flow cell 427
Holt Sackett, P., see Cox, R. A. 495
Hoogmartens, J., see Van Schepdael, A. 149
Hughes, G. J., see Fonck, C. 339
Humphreys, E., see Hill, E. 427
Ikeda, H., see Miyata-Asano, M. 501
Ikeda, H., see Tanaka, M. 293
Inoue, T., see Ishiwata, H. 275
Irth, H.
——, De Jong, G. J., Brinkman, U. A. Th. and Frei, R. W.
Metallic copper-containing post-column reactor for the detection of thiram and disulfiram in liquid chromatography 439
Isaksson, R., see Erlandsson, P. 475
Ishiwata, H.
——, Inoue, T. and Yoshihira, K.
Gas chromatographic determination of tetramethylsuccinonitrile in poly(vinyl chloride) products in contact with food 275
Ito, K., see Miyata-Asano, M. 501
Jantzen, E., see Bryn, K. 103
Jee, M. H.
—— and Ritchie, A. S.
Separation of certain triglyceride isomers by argentation thin-layer chromatography with flame ionisation detection by the Iatroscan TH 10 214
Jenke, D. R.
Column poisoning by multivalent cations in ion chromatographic analysis for alkali metals 419
Jong, G. J. de, see Irth, H. 439
Kalant, H., see Kim, C. 303
Kamata, K.
—— and Akiyama, K.
Determination of bufexamac in cream and ointment by high-performance liquid chromatography 344
Kanda, M., see Yamamoto, S. 179
Ketola, M., see Lehtonen, K. 465
Kim, C.
——, Speisky, M. B. and Kalant, H.
Simultaneous determination of biogenic amines and morphine in discrete rat brain regions by high-performance liquid chromatography with electrochemical detection 303
Kobatake, N., see Onodera, S. 259
Kool, L. B., see Parks, E. J. 206
Krishnan, S.
—— and Vijayalakshmi, M. A.
Purification and some properties of three serine carboxy-peptidases from *Aspergillus niger* 315
Kuwata, K., see Nishikawa, Y. 121
Lau-Cam, C. A., see Roos, R. W. 403
Leclercq, P. A., see Bártů, V. 219, 235
Lehtonen, K.
—— and Ketola, M.
Derivatization of phenolic acids for capillary gas chromatography with hydrogen flame ionization and electron-capture detection 465
Lepri, L., see Desideri, P. G. 75
Loeber, J. G., see Derks, H. J. G. M. 173
McFarland, K. N., see Cox, R. A. 495
Malcolme-Lawes, D. J., see Hill, E. 427
Markowski, W., see Soczewiński, E. 63
Massart, D. L., see Musch, G. 1
Mathiasson, L., see Skarping, G. 245
Matoušek, P., see Herrmann, F. 49

Mattiasson, B., see Olsson, U. 29
—— and Olsson, U.
General chromatographic purification procedure based on the use of heterobifunctional affinity ligands 21
Merlini, L., see Desideri, P. G. 75
Miyata-Asano, M.
——, Ito, K., Ikeda, H., Sekiguchi, S., Arai, K. and Taniguchi, N.
Purification of copper-zinc-superoxide dismutase and catalase from human erythrocytes by copper-chelate affinity chromatography 501
Monticelli, B., see Cartoni, G. P. 93
Munro, Z., see Burger, B. V. 449
Muralidharan, D.
——, Sundara Rao, V. S. and Thyagarajan, G.
Thin-layer chromatographic identification of leather dyes. II. Studies of mixtures of leather dyes 348
Muratani, T., see Onodera, S. 259
Musch, G.
—— and Massart, D. L.
Expert system for pharmaceutical analysis. II. Relative contribution of and rule validation for amperometric detection (oxidation mode) 1
Nikolov, R. N.
—— and Darzhalieva, M. M.
Hydrophobic-dispersive partition coefficient in alkyl-bonded reversed-phase systems with water–methanol mobile phases 377
Nishikawa, H.
——, Hayakawa, T. and Sakai, T.
Determination of micro amounts of acrolein in air by gas chromatography 327
Nishikawa, Y.
——, Taguchi, K., Tsujino, Y. and Kuwata, K.
Ion chromatographic determination of nitrogen dioxide in the atmosphere by using a triethanolamine-coated cartridge 121
Okazaki, J., see Tanaka, M. 293
Olsson, U., see Mattiasson, B. 21
—— and Mattiasson, B.
Theoretical and experimental evaluation of the use of heterobifunctional affinity ligands in general chromatographic purification systems 29
Onodera, S.
——, Muratani, T., Kobatake, N. and Suzuki, S.
Chemical changes of organic compounds in chlorinated water. XII. Gas chromatographic–mass spectrometric studies of the reactions of methylnaphthalenes with hypochlorite in dilute aqueous solution 259
Oya, S.
—— and Snyder, J. K.
Chiral resolution of a carboxylic acid using droplet counter-current chromatography 333
Parkin, J. E.
Assay of phenylmercuric acetate and nitrate in pharmaceutical products by high-performance liquid chromatography with indirect photometric detection 210
Parks, E. J.
——, Brinckman, F. E. and Kool, L. B.
Characterization of organolead polymers in trace amounts by element-specific size-exclusion chromatography 206
Pereboom-De Fauw, D. P. K. H., see Derks, H. J. G. M. 173
Quinn, A. M.
——, Siu, K. W. M., Gardner, G. J. and Berman, S. S.
Determination of heteroatoms in organic compounds by ion chromatography after Schöniger flask decomposition 203
Rao, V. S. Sundara, see Muralidharan, D. 348
Rekker, R. F.
——, De Vries, G. and Bijloo, G. J.
Retention studies of alkyl- and halogen-substituted aromatics on normal-phase silica and alumina columns. I. Alkylbenzenes and halogenoalkylbenzenes 355
Ritchie, A. S., see Jee, M. H. 214
Roets, E., see Van Schepdael, A. 149
Rombouts, F. M., see Voragen, A. G. J. 113
Ronchetti, M., see Cartoni, G. P. 157
Roos, R. W.
—— and Lau-Cam, C. A.
General reversed-phase high-performance liquid chromatographic method for the separation of drugs using triethylamine as a competing base 403
Rubio, N., see Brieva, A. 165
Russo, M. V., see Cartoni, G. P. 93
Ryan, P. A.
—— and Davis, P. F.
One-step chromatographic isolation of collagen cross-links 513
Ryzewski, C. N., see Curley, Jr., R. W. 188
Sachse, J.
Chemische Unterscheidungsmerkmale der Samen von *Trifolium repens* L. und *Trifolium repens* L. var. *giganteum* 520
Sackett, P. Holt, see Cox, R. A. 495
Sakai, T., see Nishikawa, H. 327
Schepdael, A., Van, see Van Schepdael, A. 149
Scherpenzeel, G.-J., see Bártů, V. 219, 235
Scherz, H., see Bonn, G. 485
Schols, H. A., see Voragen, A. G. J. 113

Searle-van Leeuwen, M. F., see Voragen, A. G. J. 113
Sekiguchi, S., see Miyata-Asano, M. 501
Shono, T., see Tanaka, M. 293
Short, M. T., see Cox, R. A. 495
Simonetti, L., see Cartoni, G. P. 157
Siu, K. W. M., see Quinn, A. M. 203
Skarping, G.
——, Bellander, T. and Mathiasson, L.
Determination of piperazine in working atmosphere and in human urine using derivatization and capillary gas chromatography with nitrogen- and mass-selective detection 245
Snyder, J. K., see Oya, S. 333
Soczewiński, E.
—— and Markowski, W.
Stepwise gradient development in thin-layer chromatography. III. A computer program for the simulation of stepwise gradient elution 63
Speisky, M. B., see Kim, C. 303
Stehle, P.
——, Bahsitta, H.-P. and Fürst, P.
Analytical control of enzyme-catalyzed peptide synthesis using capillary isotachophoresis 131
Stevens, H. M.
—— and Gill, R.
High-performance liquid chromatography systems for the analysis of analgesic and non-steroidal anti-inflammatory drugs in forensic toxicology 39
Sundara Rao, V. S., see Muralidharan, D. 348
Suzuki, S., see Onodera, S 259
Taguchi, K., see Nishikawa, Y. 121
Tahara, S., see Yamamoto, S. 179
Takeuchi, T.
—— and Yeung, E. S.
High-performance liquid chromatographic separation of inorganic anions on a silica gel column modified with a quaternary ammonium salt 83
Tanaka, M.
— —, Okazaki, J., Ikeda, H. and Shono, T.
Methylated cyclodextrin-bonded stationary phases for liquid chromatography 293
Taniguchi, N., see Miyata-Asano, M. 501
Thyagarajan, G., see Muralidharan, D. 348
Treiber, L. R.
Quantitative thin-layer chromatography in accelerated stability studies for prediction of inherent sensitivity of drugs toward oxygen 139
Tsujino, Y., see Nishikawa, Y. 121
Twillert, K., van, see Derks, H. J. G. M. 173
Wayland, J., see Bhown, A. S. 508
Wičar, S., see Bártů, V. 219, 235
Vanderhaege, H., see Van Schepdael, A. 149
Van Schepdael, A.
——, Roets, E., Hoogmartens, J. and Vanderhaeghe, H.
Separation of ampicillin esters and their diastereoisomers by reversed-phase liquid chromatography 149
Van Twillert, K., see Derks, H. J. G. M. 173
Vijayalakshmi, M. A., see Krishnan, S. 315
Voragen, A. G. J.
——, Schols, H. A., Searle-van Leeuwen, M. F., Beldman, G. and Rombouts, F. M.
Analysis of oligomeric and monomeric saccharides from enzymatically degraded polysaccharides by high-performance liquid chromatography 113
Vries, G. de, see Rekker, R. F. 355
Yamamoto, S.
——, Kanda, M., Yokouchi, M. and Tahara, S.
Simultaneous determination of multiple additives in cosmetics by high-performance liquid chromatography 179
Yeung, E. S., see Takeuchi, T. 83
Yokouchi, M., see Yamamoto, S 179
Yoshihira, K., see Ishiwata, H. 275
Zoccolillo, L., see Cartoni, G. P. 157
Zomer, G., see Derks, H. J. G. M. 173

Erratum

J. Chromatogr., 358 (1986) 453

Page 453, second line: "$A 198.00" should read "$A 19.00".

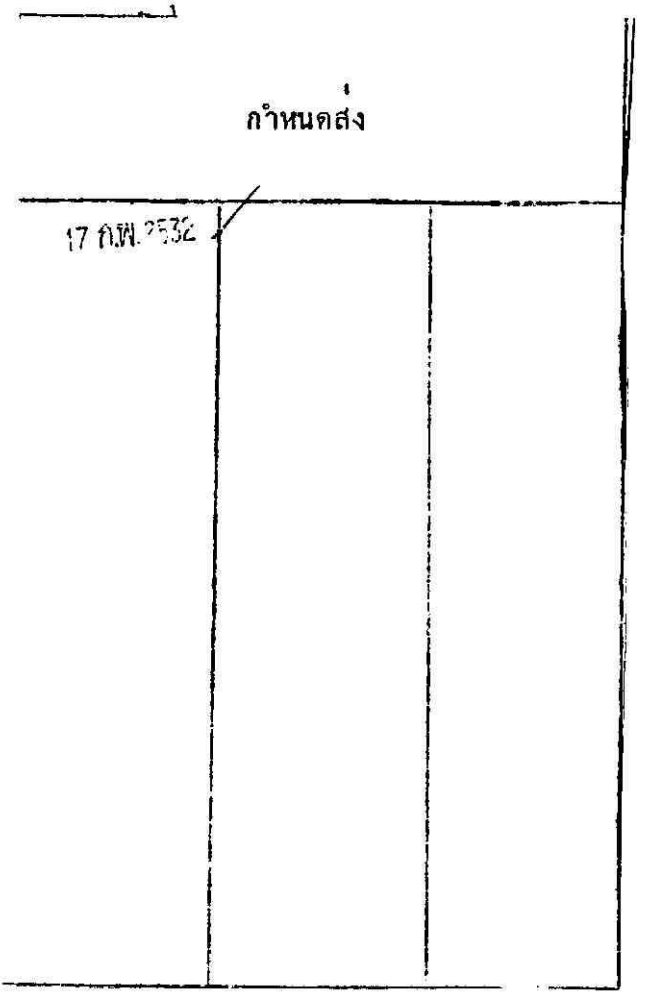

PUBLICATION SCHEDULE FOR 1986

Journal of Chromatography (incorporating *Chromatographic Reviews*) and *Journal of Chromatography, Biomedical Applications*

MONTH	1985	J 1986	F	M	A	M	J	J	A	S	O	N	D
Journal of Chromatography	346–350	351/1 351/2 351/3	352 353 354	355/1 355/2 356/1	356/2 356/3 357/1	357/2 357/3 358/1 358/2 359	360/1 360/2 361	362/1 362/2 362/3	363/1 363/2	364 365 366 367/1	367/2 368/1 368/2	369/1 369/2 370/1	370/2 370/3 371
Chromatographic Reviews						373/1						373/2	
Bibliography Section			372/1		372/2		372/3		372/4		372/5		372/6
Biomedical Applications		374/1 374/2	375/1	375/2	376 377	378/1	378/2 379	380/1	380/2 381/1	381/2	382	383/1	383/2

INFORMATION FOR AUTHORS

(Detailed *Instructions to Authors* were published in Vol. 362, No. 3, pp. 461–464. A free reprint can be obtained by application to the publisher.)

Types of Contributions. The following types of papers are published in the *Journal of Chromatography* and the section on *Biomedical Applications:* Regular research papers (Full-length papers), Short communications and Notes. Short communications are preliminary announcements of important new developments and will, whenever possible, be published with maximum speed. Notes are usually descriptions of short investigations and reflect the same quality of research as Full-length papers, but should preferably not exceed four printed pages. For review articles, see page 2 of cover under Submission of Papers.

Submission. Every paper must be accompanied by a letter from the senior author, stating that he is submitting the paper for publication in the *Journal of Chromatography*. Please do not send a letter signed by the director of the institute or the professor unless he is one of the authors.

Manuscripts. Manuscripts should be typed in double spacing on consecutively numbered pages of uniform size. The manuscript should be preceded by a sheet of manuscript paper carrying the title of the paper and the name and full postal address of the person to whom the proofs are to be sent. Authors of papers in French or German are requested to supply an English translation of the title of the paper. As a rule, papers should be divided into sections, headed by a caption (*e.g.*, Summary, Introduction, Experimental, Results, Discussion, etc.). All illustrations, photographs, tables, etc., should be on separate sheets.

Introduction. Every paper must have a concise introduction mentioning what has been done before on the topic described, and stating clearly what is new in the paper now submitted.

Summary. Full-length papers and Review articles should have a summary of 50–100 words which clearly and briefly indicates what is new, different and significant. In the case of French or German articles an additional summary in English, headed by an English translation of the title, should also be provided. (Short communications and Notes are published without a summary.)

Illustrations. The figures should be submitted in a form suitable for reproduction, drawn in Indian ink on drawing or tracing paper. Each illustration should have a legend, all the *legends* being typed (with double spacing) together on a *separate sheet.* If structures are given in the text, the original drawings should be supplied. Coloured illustrations are reproduced at the author's expense, the cost being determined by the number of pages and by the number of colours needed. The written permission of the author and publisher must be obtained for the use of any figure already published. Its source must be indicated in the legend.

References. References should be numbered in the order in which they are cited in the text, and listed in numerical sequence on a separate sheet at the end of the article. Please check a recent issue for the layout of the reference list. Abbreviations for the titles of journals should follow the system used by *Chemical Abstracts.* Articles not yet published should be given as "in press", "submitted for publication", "in preparation" or "personal communication".

Dispatch. Before sending the manuscript to the Editor please check that the envelope contains three copies of the paper complete with references, legends and figures. One of the sets of figures must be the originals suitable for direct reproduction. Please also ensure that permission to publish has been obtained from your institute.

Proofs. One set of proofs will be sent to the author to be carefully checked for printer's errors. Corrections must be restricted to instances in which the proof is at variance with the manuscript. "Extra corrections" will be inserted at the author's expense.

Reprints. Fifty reprints of Full-length papers, Short communications and Notes will be supplied free of charge. Additional reprints can be ordered by the authors. An order form containing price quotations will be sent to the authors together with the proofs of their article.

Advertisements. Advertisement rates are available from the publisher on request. The Editors of the journal accept no responsibility for the contents of the advertisements.

A New International Journal CHEMOMETRICS AND INTELLIGENT LABORATORY SYSTEMS

(With the CHEMOMETRIC NEWSLETTER, official bulletin of the CHEMOMETRICS SOCIETY)

This international journal publishes articles about new developments on laboratory techniques in chemistry and related disciplines which are characterized by the application of statistical and computer methods. Special attention is given to emerging new technologies and techniques for the building of intelligent laboratory systems, i.e. artificial intelligence and robotics.

The journal aims to be interdisciplinary; more particularly it intends to bridge the gap between chemists and scientists from related fields, statisticians, and designers of laboratory systems.

The journal deals with the following topics:

- ★ **chemometrics:** the chemical discipline that uses mathematical and statistical methods
  - — to design or select optimal procedures and experiments
  - — to provide maximum chemical information by analyzing chemical data
- ★ **computerized acquisition, processing and evaluation of data:** processing of instrumental data storage and retrieval systems computerized and automated analysis for industrial processes and quality control
- ★ **robotics**
- ★ **developments in statistical theory and mathematics with application to chemistry**
- ★ **intelligent laboratory systems** including self-optimizing instruments, planned organic synthesis, data banks with interpretative facilities, and in general applications of expert systems and knowledge representation systems in analytical chemistry
- ★ **application (case studies) of statistical and computational methods** to chemical or related data obtained from natural (medical, geochemical, environmental, food science, pharmacological, toxicological, etc.) and industrial systems (including modelling of processes and quality control)
- ★ **new software** to implement the methods described above and problems associated with the use of software (validation of software for instance)
- ★ **imaging techniques and graphical software applied in chemistry**

The journal is of interest to chemists and other natural scientists, as well as statisticians and information specialists working in a variety of fields of chemistry including analytical chemistry, organic chemistry and synthesis, environmental chemistry, food chemistry, industrial chemistry, pharmaceutical chemistry and pharmacy.

Both original research papers and tutorial articles/reviews are published. The journal also participates actively in software dissemination through articles on software developments, software descriptions, and reviews of software.

There are no page charges. Fifty reprints of original papers and short communications will be supplied free of charge. Instructions for the preparation of manuscripts can be obtained from the publisher.

1986/1987: Volume 1 (4 issues)
US $ 89.75 / Dfl. 242.00 (including postage)
ISSN 0169-7439

ELSEVIER SCIENCE PUBLISHERS

P.O. Box 211, 1000 AE Amsterdam, The Netherlands